UNIVERSIDADE FEDERAL DO PARÁ
INSTITUTO DE GEOCIÊNCIAS
PROGRAMA DE PÓS-GRADUAÇÃO EM GEOLOGIA E GEOQUÍMICA

TESE DE DOUTORADO

PETROGÊNESE E EVOLUÇÃO MAGMÁTICA DA SUÍTE SANUKITÓIDE RIO MARIA, TERRENO GRANITO-*GREENSTONE* DE RIO MARIA, CRÁTON AMAZÔNICO

Tese apresentada por:

MARCELO AUGUSTO DE OLIVEIRA

BELÉM
2009

Universidade Federal do Pará
Instituto de Geociências
Programa de Pós-Graduação em Geologia e Geoquímica

PETROGÊNESE E EVOLUÇÃO MAGMÁTICA DA SUÍTE SANUKITÓIDE RIO MARIA, TERRENO GRANITO-*GREENSTONE* DE RIO MARIA, CRÁTON AMAZÔNICO

TESE APRESENTADA POR

MARCELO AUGUSTO DE OLIVEIRA

Como requisito parcial à obtenção do Grau de Doutor em Ciências na Área de GEOQUÍMICA E PETROLOGIA.

Data de Aprovação: **25 /08 /2009**

Comitê de Tese:

ROBERTO DALL'AGNOL (Orientador)

BRUNO SCAILLET

CLÁUDIO NERY LAMARÃO

LAURO VALENTIM STOLL NARDI

VALDECIR DE ASSIS JANASI

Belém

Dados Internacionais de Catalogação-na-Publicação(CIP)
Biblioteca Geól. Rdº Montenegro G. de Montalvão

Oliveira, Marcelo Augusto de

O48c Petrogênese e evolução magmática da Suíte Sanukitóide Rio Maria, Terreno Granito – *Greenstone* de Rio Maria, Cráton Amazônico / Marcelo Augusto de Oliveira – 2009

176 f. : il.

Tese (Doutorado em Geoquímica e Petrologia) – Programa de Pós-Graduação em Geologia e Geoquímica, Instituto de Geociências, Universidade Federal do Pará, Belém, 2009.

Orientador; Roberto Dall'Agnol.

1. Arqueano. 2. Séries sanukitóides. 3. Cráton Amazônico. 4. Condições de cristalização. 5. Granitóides Alto-Mg. 6. Química mineral. 7. Petrogênese. 8. Modelamento geoquímico. 9. Manto Metassomatizado. I. Universidade Federal do Pará. II. Dall'Agnol, Roberto, Orient. III. Título.

CDD 20. ed.: 551.712

Este trabalho é dedicado principalmente a minha mãe Vânia, exemplo de mulher, guerreira e maravilhosa. Serei sempre grato por todo amor, por sempre ter confiado em mim e ter proporcionado tudo que eu poderia desejar e sonhar na vida. Ao meu irmão Marcus, pela amizade, amor, lealdade e companheirismo de todos os dias. Ao meu pai Ângelo pelo amor e incentivo.

À Laura, por todo amor, amizade, carinho e sinceridade que trouxe à minha vida.

AGRADECIMENTOS

Neste espaço o autor gostaria de expressar seus sinceros agradecimentos a algumas pessoas e instituições que, por diferentes razões, deram a sua contribuição para que este trabalho fosse realizado.

- Em primeiro lugar a Deus, por esta oportunidade única em minha vida;

- Aos meus familiares, em especial meus pais e meu irmão pelo amor e por tudo o que já vencemos juntos;

- À Universidade Federal do Pará por toda infra-estrutura e ajuda financeira fornecida;

- Ao Conselho Nacional de Desenvolvimento Científico e Tecnológico (CNPq) pela concessão da bolsa de pesquisa durante a realização deste trabalho;

- Ao professor Roberto Dall'Agnol pela orientação, dedicação, amizade, por sempre ter acreditado e confiado em mim, e pelas tantas oportunidades durante minha ainda breve vida científica;

-Ao professor Bruno Scaillet pelo apoio, acolhida e pelas ótimas discussões petrológicas durante estada em Orléans-França;

- Ao professor, colega de período de tese e, principalmente, amigo José de Arimatéia Costa de Almeida, por inúmeros momentos de reflexão, por muitos dias cansativos, mas valiosos, de campo, pelos ensinamentos, discussões e pela lealdade profissional;

- Ao professor Fernando Jacques Althoff pela amizade e indispensável apoio durante a primeira etapa de campo nas rochas da Suíte Rio Maria;

- Ao professor Cláudio Nery Lamarão pela amizade, diversas conversas e sugestões no decorrer do trabalho;

- Aos geólogos Marco Aurélio Benevides Maia Figueiredo e Albano Antônio da Silva Leite por muitos ensinamentos durante a época que fomos companheiros no Grupo de Pesquisa Petrologia de Granitóides (GPPG);

- Aos amigos geólogos Carlos Marcello Dias Fernandes e Davis Carvalho de Oliveira pelo companheirismo, momentos de descontração e, principalmente, pelas valorosas conversas sobre rochas magmáticas;

- Aos colegas do GPPG (Alex, Maryelle, Alan, Fernanda, Luciene, Erimar, Régis, Samantha, Fabriciana, Antônio, Sabrina, Luís, Mike, Cléber, Gilmara, Manoel, Tayla, Patrick, Nathan e Adriel) pelas discussões e sugestões, bem como pelo companheirismo e momentos de descontração proporcionados;

- Aos demais amigos, agradeço pelo excelente clima que sempre teve o nosso ambiente de estudo e trabalho. Obrigado pela amizade!;

- Ao grupo de professores e funcionários do Centro de Geociências, especialmente Cleida Freitas, José Esteves, Carlos Alberto Dias e Walter Pompeu.

- Ao Bibliotecário Hélio Braga Martins (Biblioteca Raimundo Montalvão – IG) pela revisão bibliográfica e de norma.

Não é possível refazer este país, democratizá-lo, humanizá-lo, torná-lo sério, com adolescentes brincando de matar gente, ofendendo a vida, destruindo o sonho, inviabilizando o amor. Se a educação sozinha não transforma a sociedade, sem ela tampouco a sociedade muda.

PAULO FREIRE

SUMÁRIO

LISTA DE ILUSTRAÇÕES

FIGURAS

1 – INTRODUÇÃO

2 - MESOARCHEAN SANUKITOID ROCKS OF THE RIO MARIA GRANITE-GREENSTONE TERRANE, AMAZONIAN CRATON, BRAZIL

3 - PETROLOGICAL CONSTRAINTS ON CRYSTALLIZATION CONDITIONS OF MESOARCHEAN SANUKITOID ROCKS, SOUTHEASTERN AMAZONIAN CRATON, BRAZIL

4 - PETROLOGY OF THE MESOARCHEAN RIO MARIA SUITE: IMPLICATIONS FOR THE GENESIS OF SANUKITOID ROCKS

TABELAS

1 – INTRODUÇÃO

2 - MESOARCHEAN SANUKITOID ROCKS OF THE RIO MARIA GRANITE-GREENSTONE TERRANE, AMAZONIAN CRATON, BRAZIL

3 - PETROLOGICAL CONSTRAINTS ON CRYSTALLIZATION CONDITIONS OF MESOARCHEAN SANUKITOID ROCKS, SOUTHEASTERN AMAZONIAN CRATON, BRAZIL

4 - PETROLOGY OF THE MESOARCHEAN RIO MARIA SUITE: IMPLICATIONS FOR THE GENESIS OF SANUKITOID ROCKS

RESUMO

Rochas que compõem a Suíte Sanukitóide arqueana Rio Maria (2,87 Ga) estão expostas em vários domínios do Terreno Granito-*Greenstone* de Rio Maria, sudeste do Cráton Amazônico. As rochas da suíte são intrusivas em *greenstone-belts* do Supergrupo Andorinhas, nos tonalitos Arco Verde, Mariazinha e Caracol, e no Trondhjemito Mogno, enquanto que leucogranitos potássicos de afinidade cálcico-alcalina, o Trondhjemito Água Fria e granitos paleoproterozóicos da Suíte Jamon são intrusivos nas rochas da Suíte Rio Maria. As rochas dominantes da suíte têm composições granodioríticas com monzogranitos subordinados, e menores proporções de quartzo-dioritos ou quartzo-monzodioritos (rochas intermediárias), além de rochas acamadadas e enclaves máficos. Rochas da Suíte Rio Maria apresentam claramente características de séries sanukitóides (alto #Mg, elevados conteúdos de Cr e Ni, enriquecimento em elementos terras raras leves e altos conteúdos de Ba e Sr, comparados as típicas séries cálcico-alcalinas). Os contrastes geoquímicos significativos entre as diferentes ocorrências de granodioritos que compõem a suíte sugerem que a unidade anteriormente denominada Granodiorito Rio Maria, corresponde realmente a uma suíte de rochas predominantemente granodioríticas, as quais derivaram a partir de magmas similares, porém distintos.

Apesar das amplas similaridades geoquímicas, granodioritos, rochas intermediárias e enclaves máficos mostram algumas diferenças significantes em seus padrões de elementos terras raras e no comportamento de Rb, Ba, Sr e Y. Os granodioritos e rochas intermediárias não são relacionados por processos de cristalização fracionada e a evolução interna das rochas intermediárias foi comandada pelo fracionamento de anfibólio + biotita ± apatita, enquanto que os granodioritos evoluíram pelo fracionamento de plagioclásio + anfibólio ± biotita. As rochas acamadadas devem ter sido derivadas a partir do magma granodiorítico pela acumulação de 50% de anfibólio, no caso dos níveis mais ricos em material cúmulus, e 30% de anfibólio ± plagioclásio, no caso dos níveis ricos em material intercúmulus.

Dados geoquímicos e testes de modelamento sugerem que os magmas granodiorítico e do enclave máfico foram originados em diferentes profundidades e devem ter sofrido processo de "mingling" durante a ascensão e final da colocação, pois só uma interação limitada poderia explicar o comportamento geoquímico relativamente uniforme desses dois grupos de rochas e os *trends* distintos mostrados por cada grupo em diferentes diagramas modais e geoquímicos. Esses contrastes entre granodioritos e enclaves máficos são refletidos no comportamento de Sr e Y, os

quais são geralmente admitidos como bons indicadores das condições de pressão reinantes quando da formação dos magmas. O comportamento desses elementos, observados em rochas sanukitóides de diferentes terrenos arqueanos do mundo, indica que os contrastes observados entre as séries sanukitóides granodioríticas (granodioritos) e monzoníticas (enclaves máficos) são características gerais dessas rochas e suas origens dependem fortemente da condição de pressão quando da geração dos magmas e, como conseqüência, que a natureza das séries pode indicar a profundidade aproximada de geração de seu magma.

A petrogênese da Suíte Rio Maria requer a fusão de um manto, previamente metassomatizado pela adição de ~30% de líquido TTG para gerar os magmas granodiorítico (21% de fusão) e intermediário (24% de fusão), e ~20% de líquido TTG no caso do magma do enclavo máfico (9% de fusão). Os testes de modelamento geoquímico indicam que um ambiente de subducção ativo esteve presente no Terreno Granito-*Greenstone* de Rio Maria entre 2,98 e 2,92 Ga para gerar, ao menos em parte, os magmas TTGs e produzir o metassomatismo do manto por esses magmas, antes do processo responsável pela origem dos magmas sanukitóides. Um evento tectonotermal em 2,87 Ga, possivelmente relacionado à pluma do manto, causaria a fusão parcial do manto metassomatizado e geraria os magmas sanukitóides Rio Maria.

Nas rochas da Suíte Rio Maria, a assembléia mineral é dominada por anfibólio, plagioclásio, biotita e epidoto, todos de provável origem magmática, sendo que piroxênio nunca foi identificado. Critérios texturais e composicionais indicaram que o anfibólio foi a fase *liquidus* durante a cristalização dos magmas Rio Maria. Esses magmas foram ricos em água (H_2O > 7%), com temperaturas de cristalização entre 950 e 680° C. As razões Mg/(Mg+Fe) de anfibólios e biotitas indicaram condições oxidantes, entre NNO + 0,5 e NNO + 2,5, similares as indicadas pelos teores de pistacita em cristais de epidotos magmáticos. Análises de conteúdos de alumínio em anfibólios, indicaram pressões entre 700 e 1000 MPa para o início da cristalização e, de aproximadamente 200 Mpa para o final da colocação dos magmas Rio Maria. Os magmas sanukitóides do Terreno Granito-*Greenstone* de Rio Maria são oxidantes e ricos em água, características de magmas de arcos modernos, o que sugerem, assim como resultados de modelamento geoquímico, bem como aspectos geológicos e petrográficos, que eles podem ter sido formados em um ambiente geodinâmico similar as zonas de subducção modernas.

ABSTRACT

The Archean sanukitoid Rio Maria suite yielded zircon ages of ~2.87 Ga and is exposed in large domains of the Rio Maria Granite-Greenstone Terrane, southeastern Amazonian craton. It is intrusive in the greenstone belts of the Andorinhas Supergroup, in the Arco Verde, Mariazinha, and Caracol tonalite, and Mogno trondhjemite. Archean potassic leucogranites, Água Fria trondhjemite, and the Paleoproterozoic granites of Jamon Suite are intrusive in the rocks of the Rio Maria suite. The dominant rocks have granodiorite to subordinate monzogranitic compositions, with minor proportions of intermediate quartz-diorites or quartz-monzodiorites rocks, in addition to mafic end members occurring as layered rocks or as enclaves. The Rio Maria suite has clear geochemical characteristics of Sanukitoids rocks (high Mg#, elevated Cr and Ni contents, LREE enrichment, and high Ba and Sr contents relative to typical calc-alkaline series). The significant geochemical contrasts between the occurrences of the granodiorites in different areas suggest that this unit corresponds in fact to a granodioritic suite of rocks derived from similar but distinct magmas.

In spite of their broad geochemical similarities, granodiorites, intermediate rocks, and mafic enclaves show some significant differences in their REE patterns and in the behavior of Rb, Ba, Sr, and Y. The granodiorites and intermediate rocks are not related by fractional crystallization and the internal evolution of intermediate rocks were leaded by fractionation of amphibole + biotite ± apatite, whereas granodiorites evolved by fractionation of plagioclase + amphibole ± biotite. The layered rocks should have been derived from the granodiorite magma by accumulation of 50% of amphibole (dark layer) and 30% of amphibole ± plagioclase accumulation (gray layer).

Modeling and geochemical data suggest that mafic enclave and granodiorite magmas were originated at different depths and should have mingled during their ascent and final emplacement and a limited interaction would explain the relatively uniform geochemical behavior of each rock variety and the distinct trends displayed by their rocks in different modal and geochemical diagrams. These contrasts between granodiorites and mafic enclaves are reflected in the behavior of the Sr and Y, which are generally seen as good indicators of the pressure of melt formation. The behavior of these elements, observed in different sanukitoid rocks from Archean terranes worldwide, indicates that the geochemical and modal contrasts observed between the

granodioritic (granodiorites) and monzonitic (mafic enclaves) sanukitoid series are a general feature of these rocks and their origin is strongly dependent of the pressure of magma generation and, as a consequence, that the nature of the series could indicate the approximate depth of formation of its magma.

The petrogenesis of the Rio Maria suite requires melting of a modified mantle extensively metasomatized by addition of about 30% TTG-like melt to generate the granodiorite (21% of melt) and intermediate magmas (24% of melt), and ~20% TTG-like melt in the case of mafic enclave magma (9% of melt). Our modeling results indicate that an active subduction tectonic setting was present in the Rio Maria terrane in between 2.98 to 2.92 Ga to generate the TTG magmas and the proposed metasomatism of the mantle by these magmas, before the melting process responsible for the origin of the sanukitoid magmas. A tectonothermal event at ~2.87 Ga, possibly related to a mantle plume, causing the partial melting of the metasomatized mantle and generating the Rio Maria sanukitoid magmas.

In the rocks of the Rio Maria suite, the mineral assemblage is dominated by amphibole-plagioclase-biotite and epidote minerals, all of inferred magmatic origin, pyroxenes being notably absent. Textural and compositional criteria indicate that amphibole is a principal mineral on the liquidus of all the Rio Maria rocks. To derive crystallisation conditions, the phase assemblages, proportions and compositions of the natural rocks were compared with experimental works carried out on similar magma compositions. The comparison shows that the parental magmas were water-rich, with more than 7 wt% dissolved H_2O near liquidus, with crystallisation temperature in the range 950-680°C. The Mg/(Mg+Fe) ratios of both amphibole and biotite indicate fO_2 conditions in the range NNO + 0.5 up to NNO + 2.5, therefore pointing to both water-rich and oxidizing conditions for sanukitoid magmas. Analyses of amphibole aluminium content in cumulate rocks, indicate in addition a high pressure crystallisation stage, around 700-1000 MPa, prior to emplacement in the upper crust at around 200 MPa. Sanukitoid magmas share therefore two of the principal characteristics of modern arc magmas, elevated redox sate and volatile contents, which suggest that they may have formed in a geodynamic environment broadly similar to present-day subduction zones.

CAPÍTULO – 1

INTRODUÇÃO

1 - INTRODUÇÃO

1.1 - APRESENTAÇÃO

Os terrenos granito-*greenstone* arqueanos de diferentes crátons são constituídos fundamentalmente por associações granitóides dominadas por rochas que formam as clássicas associações TTGs e por *greenstone belts* (Condie & Hunter 1976, Dall'Agnol et al. 2006). Entretanto, maciços formados por dioritos a granodioritos com altos teores de Mg, denominados sanukitóides, geralmente intrusivos nas associações TTGs, possuem uma importante distribuição areal em alguns destes terrenos. Granitos stricto sensu também podem ocupar áreas expressivas de terrenos arqueanos (Sylvester 1994).

As suítes sanukitóides foram descritas originalmente no Canadá (Província Superior; Shirey & Hanson 1984, Stern & Hanson 1991, Stevenson et al. 1999), porém têm sido identificadas em vários locais do mundo como Austrália (Cráton Pilbara; Smithies and Champion 2000), países bálticos e Rússia (Escudo Báltico: Lobach-Zhuchenko et al. 2000, Kovalenko et al. 2005, Lobach-Zhuchenko et al. 2005, Bibikova et al. 2005), África do Sul (Cráton Zimbábue; Bagai et al. 2002), Índia (Cráton Dharwar; Moyen et al. 2001, Moyen et al. 2003) e Brasil (Terreno Granito-*Greenstone* de Rio Maria; Althoff 1996, Leite 2001, Oliveira et al. 2006, Oliveira et al. submetido). Estas rochas são fundamentais para o entendimento da evolução tectônica e geológica dos terrenos arqueanos em que ocorrem. Os estudos desenvolvidos em diferentes terrenos resultaram em propostas para explicar a gênese destas rochas que convergem no sentido de que os magmas formadores das séries sanukitóides seriam produtos de um manto enriquecido por fluídos e/ou líquidos crustais em um ambiente de subducção.

Assim como nos demais terrenos arqueanos típicos, o magmatismo ocorrido no Terreno Granito-*Greenstone* de Rio Maria (TGGRM) foi bastante expressivo, tendo originado rochas com idades variando de 2,98 Ga a 2,86 Ga. Uma das unidades relacionadas a este magmatismo é Suíte sanukitóide arqueana Rio Maria, que foi estudada e caracterizada a sul de Rio Maria (Medeiros 1987, Medeiros & Dall'Agnol 1988, Huhn et al. 1988, DOCEGEO 1988), na área de Xinguara (Souza 1994, Leite 2001, Leite et al. 2004), na área de Marajoara (Althoff 1996, Althoff et al. 2000) e a leste da cidade de Bannach (Oliveira 2005, Oliveira et al. 2006, Oliveira et al. 2009, Oliveira et al., submetido a, b). A importância do magmatismo sanukitóide no Terreno Granito-*Greenstone* de Rio Maria é ressaltada pela sua vasta distribuição areal (Figura

1) e pelo fato de suas variedades menos evoluídas serem prováveis fontes para a formação dos granitos paleoproterozóicos da Suíte Jamon (Dall'Agnol et al. 1999a, b).

Os objetivos principais desta tese são, além de aprimorar a caracterização da associação sanukitóide de Rio Maria, buscar definir os processos de geração e a fonte dos magmas formadores do Granodiorito Rio Maria e rochas máficas, incluindo os enclaves, esclarecer os processos de cristalização e diferenciação desses magmas e as relações entre eles, bem como estimar os parâmetros de cristalização (T, P, fO_2, XH_2O) prevalecentes durante sua evolução. Para atingir tais objetivos, pretende-se partir de um refinamento e integração dos dados petrográficos, mineralógicos, geoquímicos, geocronológicos e isotópicos já existentes sobre o Granodiorito Rio Maria e rochas máficas associadas, nas suas diversas áreas de ocorrência, aos quais foram somados estudos adicionais de geoquímica, química mineral, geocronologia e comparações com estudos experimentais em rochas de composições similares.

A presente tese de doutorado, intitulada "Petrogênese e Evolução Magmática da Suíte Sanukitóide Rio Maria, Terreno Granito-*Greenstone* de Rio Maria, Cráton Amazônico", foi estruturada na forma de integração de artigos científicos de acordo com as normas gerais definidas pela Comissão da Pós-Graduação em Geologia e Geoquímica da Universidade Federal do Pará. Este trabalho inclui um capítulo introdutório, onde é feita apresentação, a área de estudo é localizada, e onde é abordado o contexto geológico regional, destacando-se os principais aspectos geológicos e geocronológicos da Província Mineral de Carajás e a caracterização do magmatismo sanukitóide arqueano. Em seguida, são definidos os principais problemas geológicos que motivaram esta proposta de trabalho, a partir dos quais foram definidos os objetivos da pesquisa. As atividades e procedimentos metodológicos que viabilizaram alcançar os objetivos propostos serão descritos e discutidos nos capítulos subseqüentes. Os resultados alcançados neste trabalho são apresentados e discutidos na forma de três artigos científicos (Capítulos 2, 3 e 4), e abordados de forma integrada no capítulo final (Capítulo 5).

Capítulo 2 – *Artigo 1* - **MESOARCHEAN SANUKITOID ROCKS OF THE RIO MARIA GRANITE-GREENSTONE TERRANE, AMAZONIAN CRATON, BRAZIL.** Publicado na

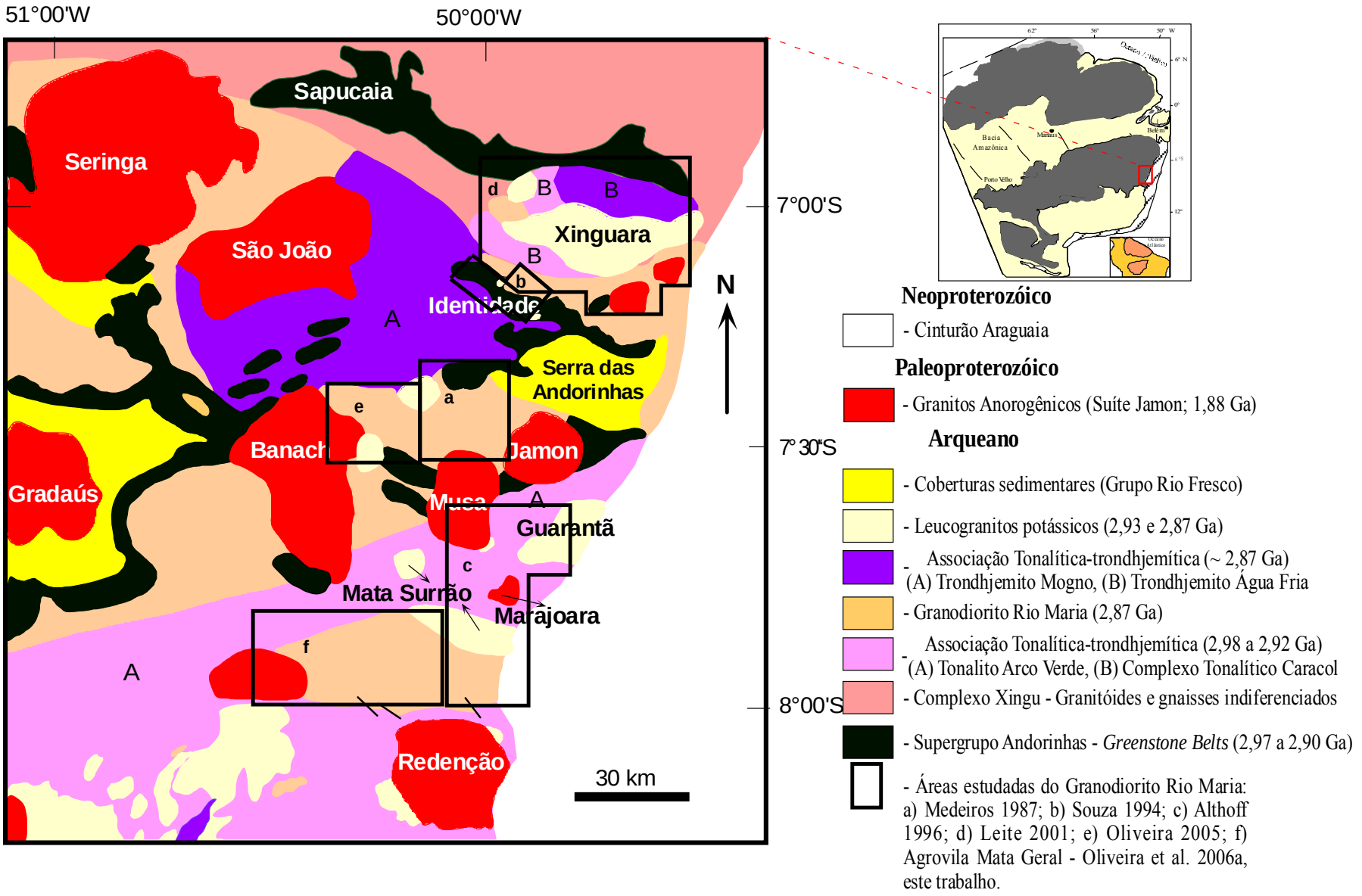

Figura 1 - Mapa geológico do Terreno Granito-*Greenstone* de Rio Maria, modificado de Leite (2001).

revista *JOURNAL OF SOUTH AMERICAN EARTH SCIENCES*. Apresenta os dados de campo, petrográficos, geoquímicos e isotópicos dos granodioritos e rochas intermediárias das diferentes áreas de ocorrência das rochas da Suíte Rio Maria. Os dados químicos foram utilizados para discutir a caracterização da série magmática e para fazer considerações sobre a evolução magmática e geoquímica das rochas estudadas. Neste mesmo trabalho, baseado nas observações petrográficas e na literatura, foi feita uma discussão sobre o papel do anfibólio como fase máfica principal e do epidoto como fase magmática, nas rochas da Suíte Rio Maria.

Capítulo 3 – *Artigo 2* - **PETROLOGICAL CONSTRAINTS ON CRYSTALLIZATION CONDITIONS OF MESOARCHEAN SANUKITOID ROCKS, SOUTHEASTERN AMAZONIAN CRATON, BRAZIL.** Submetido para publicação à revista *JOURNAL OF PETROLOGY*. Apresenta os dados de campo, petrográficos, geoquímicos e de química mineral dos granodioritos, rochas intermediárias, rochas acamadadas e enclaves máficos que compõem a Suíte Rio Maria. O trabalho é baseado nos dados das ocorrências da área de Bannach, onde há as melhores exposições das amostras citadas. Os dados são discutidos com intuito de estimar os parâmetros, como conteúdo de água, fugacidade de oxigênio, pressão e temperatura, reinnantes durante a cristalização dos magmas formadores das rochas em questão. Para tanto, são avaliados os dados de química mineral de epidoto, bitotita e anfibólio, bem como são feitas comparações com rochas de composições similares e nas quais tenham sido realizados estudos experimentais.

Capítulo 4 – *Artigo 3* - **PETROLOGY OF THE MESOARCHEAN RIO MARIA SUITE: IMPLICATIONS FOR THE GENESIS OF SANUKITOID ROCKS.** Submetido para publicação à revista *LITHOS*. Discute com base no comportamento geoquímico e em trabalhos de modelamento, as relações genéticas entre as rochas que compõem a Suíte Rio Maria. São avaliados modelos de origem das rochas sanukitóides de Rio Maria e ambém são discutidos os processos que comandaram a evolução desses magmas, como cristalização fracionada e assimilação. Neste trabalho, é feita uma avaliação das duas principais séries, granodiorítica e monzonítica, que compõem as principais Suítes Sanukitóides do mundo, buscando-se uma relação entre suas petrogêneses e suas características petrográficas e geoquímicas.

1.2 – LOCALIZAÇÃO DA ÁREA

O Terreno Granito-*Greenstone* de Rio Maria está situado no sudeste do Estado do Pará (Figuras 1 e 2), e as áreas de ocorrências de rochas da Suíte Rio Maria estão inseridas nas Folhas SB-22-Z-C-II, Rio Maria, SB-22-Z-C-III. Xinguara, e SB-22-Z-C-V, Vila Marajoara. O acesso à área pode ser feito por via aérea até as cidades de Carajás, Marabá ou Redenção, seguindo-se por via terrestre pela rodovia PA-150. Por via terrestre, o acesso a partir de Belém é pela rodovia PA-150, passando por várias cidades da área, como Xingura, Rio Maria, Pau D'Arco e Redenção.

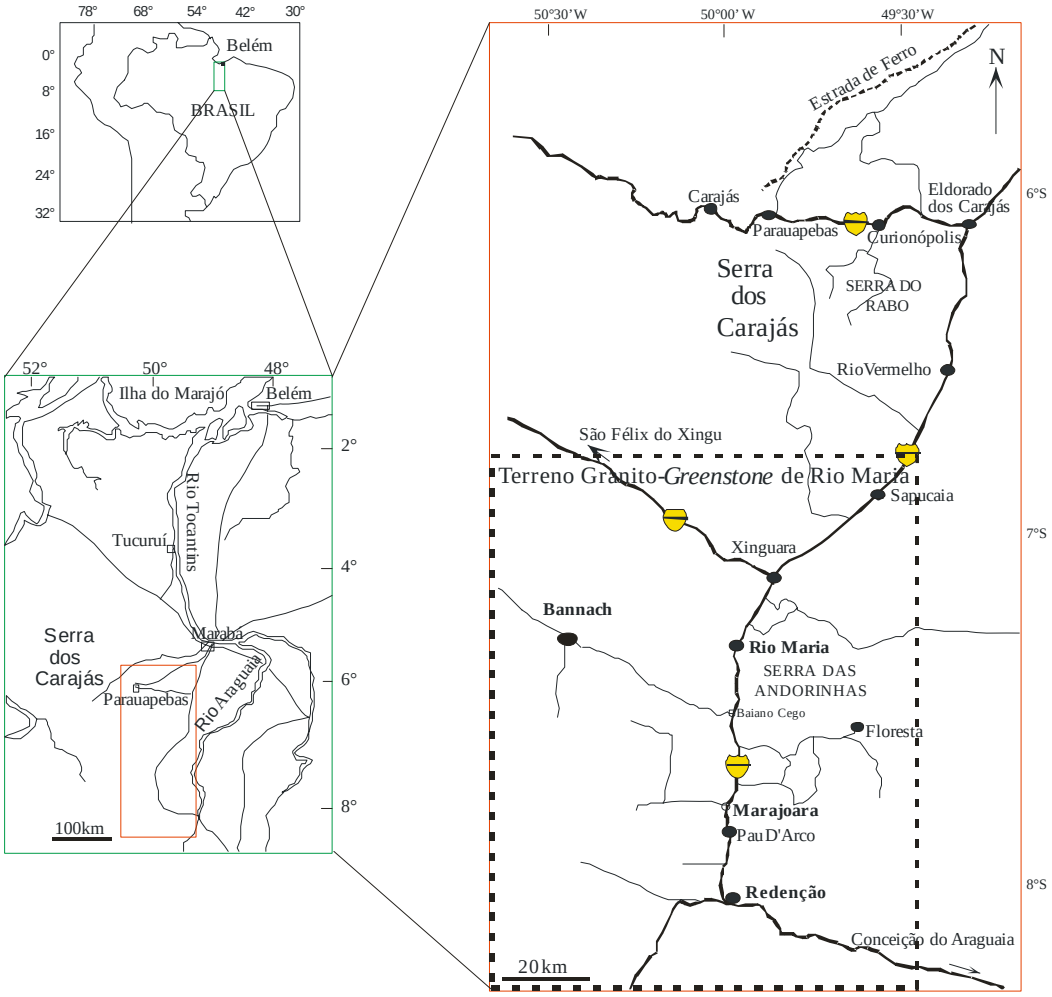

Figura 2 - Mapa de localização do Terreno Granito-*Greenstone* de Rio Maria.

1.3 – CONTEXTO GEOLÓGICO REGIONAL

A Suíte Rio Maria está localizada no Terreno Granito-*Greenstone* de Rio Maria, porção sul da Província Carajás. A Província Carajás está inclusa dentro da Província Amazônia Central

(Tassinari & Macambira 2004; Figura 3), porção leste do Cráton Amazônico, e compreende principalmente rochas arqueanas intrudidas por granitos anorogênicos paleoproterozóicos. Esta província é limitada a oeste por um terreno dominado por granitóides proterozóicos e assembléias vulcânico-piroclásticas do Supergrupo Uatumã, com idades próximas de 1,88 Ga (Teixeira et al. 2002; Figura 3); a leste, é bordejada pelo Cinturão Araguaia do Neoproterozóico, relacionado ao Ciclo Brasiliano (Pan-Africano), o qual não afetou significativamente o Cráton Amazônico; a norte e a sul, pela Província Maroni-Itacaiúnas e pelo domínio Santana do Araguaia (Vasquez et al. 2008), respectivamente, ambos formados durante o Evento Trans-Amazônico (2,20 - 2,10 Ga).

A Província Carajás é subdividida atualmente em Terreno Granito-*Greenstone* de Rio Maria, com idade de 3,00 - 2,86 Ga (Macambira & Lafon 1995, Dall`Agnol et al. 2006), e a Bacia tipo *rift* de Carajás, composta dominantemente de rochas metavulcânicas, formações ferríferas bandadas e granitóidescom idades de 2,76 – 2,55 Ga (Machado et al. 1991, Macambira & Lafon 1995, Barros et al. 2001). A Suíte Rio Maria está situada no Terreno Granito-*Greenstone* de Rio Maria o qual é formado por *greenstone belts* e granitóides arqueanos, recobertos por sedimentos do Grupo Rio Fresco, provavelmente também de idade arqueana, e são cortados por granitos tipo-A paleoproterozóicos da Suíte Jamon (Dall'Agnol et al. 2005, 2006).

No Terreno Granito-*Greenstone* de Rio Maria o evento que produziu os *greenstone belts* foi dominantemente vulcânico máfico-ultramáfico, gerando maior abundância de komatiítos e basaltos toleíticos com idades que variam de 2,97 a 2,9 Ga (Macambira 1992, Pimentel & Machado 1994, Souza 1994). Contribuições vulcânicas ácidas e rochas sedimentares ocorrem subordinadamente.

Os Granitóides arqueanos do Terreno Granito-*Greenstone* de Rio Maria foram divididos por Dall'Agnol et al. (1997a, 2006), com base em aspectos petrográficos, geoquímicos e geocronológicos, em quatro grupos com idades arqueanas de 3,0 a 2,86 Ga (Tabela 1). Um quinto

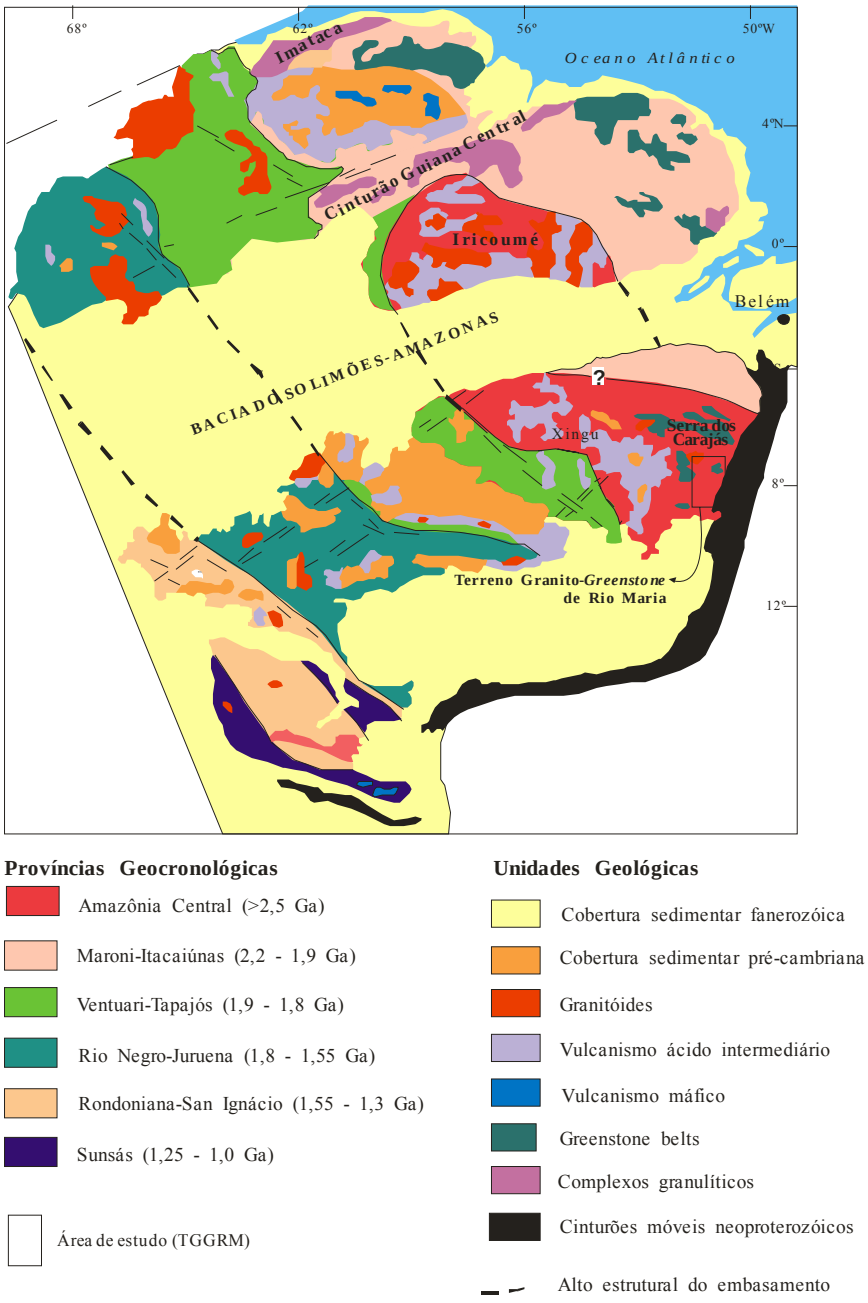

Figura 3 - Províncias geocronológicas do Cráton Amazônico, de acordo com Tassinari & Macambira (2004).

grupo reuniria os granitos paleoproterozóicos (1,88 Ga). Os quatro grupos de granitóides arqueanos foram assim definidos: 1) séries tonalito-trondhjemito-granodioritos do tipo TTG mostrando idades entre 2,98 e 2,92 Ga e representadas pelo Tonalito Arco Verde, Tonalito Caracol, Tonalito Mariazinha e Trondhjemito Mogno (Althoff et al. 2000, Leite et al. 2004, Almeida et al. submetido, Guimarães et al., submetido); 2) granitóides sanukitóides com alto Mg

(Althoff 1996, Leite 2001, Oliveira 2005), representados pelas diferentes ocorrências de rochas da Suíte Rio Maria, com idades em torno de 2,87 Ga (Medeiros 1987, Macambira & Lancelot 1996, Althoff et al. 2000, Leite et al. 2004, Oliveira et al. 2009, Oliveira et al. submetido a, b); 3) granitóides das séries TTGs jovens representados pelo Trondhjemito Água Fria (2,86 Ga; Huhn et al. 1988, Pimentel & Machado 1994, Leite et al. 2004); 4 – leucogranitos potássicos de afinidade cálcico-alcalina. No que diz respeito aos leucogranitos potássicos, o evento mais expressivo de sua formação foi datado em torno de 2,87 Ga (Lafon et al. 1994, Leite et al. 2004).

Durante o Paleoproterozóico, mais precisamente em torno de 1,88 Ga, a região de Rio Maria foi palco de magmatismo granítico anorogênico (Dall'Agnol et al. 2005, 2006, Dall'Agnol & Oliveira 2007), representado na região por Granitos da suíte Jamon (Jamon, Musa, Redenção, Marajoara e Bannach) e por diques félsicos a máficos, por vezes compostos, que são contemporâneos dos granitos proterozóicos, e que seccionam tanto as unidades arqueanas quanto os granitos paleoproterozóicos.

O quadro litoestratigráfico do Terreno Granito-*Greenstone* de Rio Maria pode ser melhor visualizado no mapa geológico da Figura 1 e os dados geocronológicos disponíveis estão na Tabela 1.

1.4 – SUÍTES SANUKITÓIDES

O termo suite sanukitóide (ou suíte diorítica-granodiorítica alto Mg) foi introduzido por Shirey & Hanson (1984) para rochas vulcânicas e plutônicas félsicas arqueanas, na Província Superior do Canadá, geoquimicamente distintas das suítes TTGs. Em diversos crátons do mundo, as rochas sanukitóides formaram-se no final do Arqueano (2,95 - 2,54Ga) como intrusões comumente tardi a pós-cinemática, as quais não são, necessariamente, temporalmente relacionadas a um magmatismo TTG, mas quase sempre são precedidas por intrusões dessas rochas que, em geral, ocorrem entre 50 e 150 Ma antes (Tabela 2). As principais características geocronológicas, petrográficas e geoquímicas dessas associações, são sumarizadas na tabela 2.

Os sanukitóides apresentam altos teores de Mg, Cr, Ni e também Sr, Ba, P e elementos terras raras leves. Suas assinaturas isotópicas, assim como as químicas, são contrastantes, pois os isótopos de Nd e Sr indicam origem mantélica, enquanto os isótopos de Pb mostram que há um importante componente crustal nessas rochas.

Tabela 1 – Dados geocronológicos das rochas arqueanas do Terreno Granito-*Greenstone* de Rio Maria

Unidades Estratigráficas	Tipo de Rocha	Método	Material Analisado	Idade/Referência
Granito tipo Xinguara	Leucogranito (Serra do Inajá)	Pb-Pb Pb-Pb	Zircão Zircão	2875 ± 11 Ma (8) 2881 ± 2 Ma (11)
Granito Xinguara	Leucogranito (área tipo)	Pb-Pb	Zircão	2865 ± 1 Ma (10)
Granito tipo Mata Surrão	Leucogranito (Pau D'Arco)	Pb-Pb	Zircão	2868 ± 5 Ma (12)
Granito tipo Mata Surrão	Leucogranito (Marajoara)	Pb-Pb	Zircão	2871 ± 7 Ma (6)
Granito Mata Surrão	Leucogranito (área tipo)	Pb-Pb	Rocha total	2872 ± 10 Ma (5)
Granodiorito Cumaru	Granitóide	Pb-Pb	Zircão	2817 ± 4 Ma (4)
Tonalito Parazônia	Granitóide	U-Pb	Titanita	2858 Ma (2)
Trondhjemito Água Fria	Trondhjemito	Pb-Pb	Zircão	2864 ± 21 Ma (9, 10)
Suíte Rio Maria	Granodiorito Granodiorito Quartzo-diorito Granodiorito (S. Inajá) Granodiorito (S. Inajá) Diorito (S. Inajá) Granodiorito (S. Inajá)	U-Pb U-Pb Pb-Pb Pb-Pb Pb-Pb Pb-Pb Pb-Pb	Zircão Zircão,Tit. Zircão Zircão Zircão Zircão Zircão	2874 + 9/-10 Ma (1) 2872 ± 5 Ma (2) 2878 ± 4 Ma (3) 2879 ± 4 Ma (8) 2877 ± 6 Ma (11) 2880 ± 4 Ma (11) 2881 ± 8 Ma (11)
Granito Guarantã	Leucogranito	Pb-Pb	Zircão	2930 Ma (7)
Tonalito Mariazinha	Tonalito	Pb-Pb	Zircão	2925 ± 3 (13)
Trondhjemito Mogno	Granitóide Trondhjemito Trondhjemito Trondhjemito	U-Pb Pb-Pb Pb-Pb Pb-Pb	Titanita Zircão Zircão Zircão	2871 ± ? Ma (2) 2963 ± 6 Ma (13) 2968 ± 2 (13) 2959 ± 5 (13)
Complexo Tonalítico Caracol	Tonalito Tonalito Tonalito	Pb-Pb Pb-Pb Pb-Pb	Zircão Zircão Zircão	2948 ± 5 Ma (10) 2936 ± 3 Ma (10) 2924 ± 2 Ma (10)
Tonalito Arco Verde	Tonalito Tonalito Tonalito Saprólito Tonalito Tonalito	U-Pb Pb-Pb Pb-Pb Pb-Pb Pb-Pb Pb-Pb	Zircão Zircão Zircão Zircão Zircão Zircão	2957+25/-21 Ma (1) 2948 ± 7 Ma (8) 2981 ± 8 Ma (11) 2965 ± 1 Ma (11) 2988 ± 5 Ma (11) 2936 ± 4 Ma (12)
Supergrupo Andorinhas /Lagoa Seca	Metagrauvacas Metavulcânica Félsica Metavulcânica Félsica	U-Pb U-Pb U-Pb	Zircão Zircão Zircão	2971 ± 18 Ma (1) 2904+29/-22Ma(1) 2972 ± 5 Ma (2)

Fontes dos dados: (1) - Macambira (1992); (2) - Pimentel & Machado (1994); (3) - Dall'Agnol et al. (1999a); (4) - Lafon & Scheller (1994); (5) - Lafon et al. (1994); (6) - Althoff et al. (1998); (7) - Althoff et al. (2000); (8) - Rolando & Macambira (2002); (9) Macambira et al. (2000); (10) Leite et al. (2004); (11) Rolando & Macambira (2003); (12) Almeida et al. (2008); (13) Almeida et al. submetido.

Em resposta aos comportamentos geoquímicos e isotópicos que apontam para características mantélicas e crustais, a maioria dos modelos propostos para explicar a gênese dos sanukitóides arqueanos considera a fusão de um manto peridotítico metassomatizado, ou por fluídos ou por líquidos gerados a partir de uma zona de subducção, como processo mais provável para a formação dessas rochas. Apesar disso, a origem de granodioritos arqueanos ricos em Mg é ainda motivo de discussão entre pesquisadores que trabalham nos principais terrenos arqueanos do mundo, e duas principais hipóteses tem sido propostas para sua petrogênese: I - fusão do manto, enriquecido através da adição de fluidos e/ou líquidos em um ambiente de subducção. Neste modelo, a fusão e o enriquecimento do manto, aconteceriam em dois estágios temporalmente distintos: 1° Metassomatismo da cunha do manto; 2° Posteriormente, evento tectonotermal gerou os magmas sanukitóides através da fusão parcial do manto enriquecido (Stern et al. 1989, Stern & Hanson 1991, Smithies & Champion 2000, Halla 2005, Kovalenko et al. 2005); II – durante a ascensão através da cunha do manto, fusões oriundas da lasca subductada assimilariam porções do manto peridotítico em um processo de *mixing* (Rapp et al. 1999, Moyen et al. 2003).

Em relação ao papel da crosta arqueana na formação dos sanukitóides, levando em consideração as características, principalmente as químicas, dessas rochas, Stern et al. (1989) aventou a possibilidade de contaminação de magma komatiítico ou basáltico por uma crosta rica em elementos litófilos. Após estudos envolvendo modelamento geoquímico, ele concluiu que a interação entre fusões máficas ou ultramáficas e material crustal não pode produzir, ao mesmo tempo, os altos teores de Ni e Cr e altos conteúdos de SiO_2 e elementos litófilos encontrados em sanukitóides. Kovalenko et al. (2005) ressaltaram que os altos teores de LREE, Ba, Sr e P encontrados nos sanukitóides não poderiam ser causados por contaminação crustal porque as médias das concentrações desses elementos na crosta arqueana são mais baixas do que as dos sanukitóides (Taylor & McLennan 1985).

Conclusão similar foi obtida por Smithies & Champion (1999a), embora Moyen et al. (1997) e Stevenson et al. (1999) tenham mostrado que a assimilação de material crustal pode ser muito importante para explicar a origem dos membros mais félsicos das suítes. Baseados em dados de ε_{Nd}, Stevenson et al. (1999) consideram que os dioritos seriam derivados de uma fonte mantélica capaz de produzir rochas com, ao mesmo tempo, altos conteúdos de Mg, Cr e Ni, e também SiO_2, Ba, Sr, P e ETRL, enquanto os membros mais félsicos seriam produtos de

assimilação crustal. Também com base em estudos isotópicos, porém em dados de Pb, Halla (2005) admite como fonte para os sanukitóides do cráton Kareliano, o manto enriquecido. Porém, destaca que material crustal reciclado, colocado em profundidades mantélicas em zonas de subducção, pode ter tido um papel importante para o enriquecimento do manto e consequente geração no Arqueano de granitóides sanukitóides com importantes conteúdos de Pb crustal.

A busca do mecanismo petrogenético mais favorável a geração de rochas sanukitóides, bem como o papel de processos de cristalização fracionada e assimilação crustal na evolução dos magmas gerados, e ainda a relação entre os processos que geraram associações TTGs e aqueles que causaram o metassomatismo e fusão do manto, são questões fundamentais na procura do melhor entendimento da gênese e evolução das suítes sanukitóides as quais certamente ainda serão muito discutidas na literatura mundial.

1.5 – SUÍTE SANUKITÓIDE RIO MARIA

Dall'Agnol et al. (1986) denominaram informalmente de Granodiorito Rio Maria, os domos de granitóides arrasados identificados por Cordeiro (1982), truncando biotita gnaisses, migmatitos e seqüências do tipo *greenstone-belts*. Medeiros et al. (1987) formalizaram a denominação de Granodiorito Rio Maria. O Granodiorito Rio Maria ocorre em grandes áreas do Terreno Granito-*Greenstone* de Rio Maria (Figura 1). Sua área-tipo está localizada nas proximidades da cidade de Rio Maria, mas também está exposto a sul e noroeste de Xinguara, a norte de Redenção, a leste da cidade de Bannach e nas proximidades da Agrovila Mata Geral (noroeste de Redenção). Alguns granitóides descritos nas regiões de Carajás, Xingu e Serra do Inajá são também correlacionados ao Granodiorito Rio Maria (Docegeo 1988, Costa et al. 1995, Rolando & Macambira 2002, 2003).

Em sua área tipo, o Granodiorito Rio Maria forneceu idades de cristalização de 2874 +9/-10 Ma (U/Pb em zircão, Macambira 1992, Macambira & Lancelot 1996) e 2872 ± 5 Ma (U/Pb em zircão e titanita, Pimentel & Machado 1994). Idade similar foi obtida em quartzo-diorito aflorante na região de Xinguara (2878 ± 4 Ma, método Pb-Pb em zircão por evaporação, Dall'Agnol et al. 1999a). Rolando & Macambira (2002, 2003) também obtiveram idades similares (Tabela 3, método Pb-Pb em zircão por evaporação) para rochas do Granodiorito Rio Maria e afins, aflorantes na região da Serra do Inajá, a aproximadamente 100 km ao sul da cidade

Tabela 2 - Características geocronológicas, químicas e petrográficas principais de suítes sanukitóides de diferentes crátons do mundo.

LOCALIZAÇÃO	IDADES DE CRISTALIZAÇÃO /COLOCAÇÃO	IDADES T_{DM}	IDADES DE EVENTOS TTG	PETROGRAFIA				GEOQUÍMICA							
				Tipos de Rochas	Minerais Fe-Mg	Minerais Acessórios	Outras Características Comuns	#Mg	A/CNK	K/Na	ETR	HFSE	Rb	LILE	Elementos de Transição
Província Superior do Canadá [1]	2,67 - 2,70 Ga	X	2,83-2,74 Ga	Dioritos a Granodioritos	Hornblenda e biotita, raramente clinopiroxênio	Apatita Titanita Zircão Alanita	Enclaves dioríticos a monzodioríticos e aglomerados máficos compostos por Hb ± Bt ± Plg	40-68	0,6-1,1	0,2-0,7	$(La/Yb)_n$ = 24-90 Anomalia de Eu = fracamente negativa a ausente	Nb = 3-14 Zr = 50-290 Y = 8-35	28-111	Sr = 300-2200 Ba = 800-3200	Ni = 10-100 Cr = 20-170
Cráton Dharwar[2]	2,55 Ga	X	3,0-2,7 Ga 2,55-2,53 Ga	Monzodioritos a Granodioritos	Hornblenda e biotita, raramente clinopiroxênio	Magnetita Ilmenita Apatita Titanita Zircão Alanita	Enclaves dioríticos a monzodioríticos e aglomerados máficos compostos por Hb ± Bt ± Plg	45-75	0,8-1,2	0,4-0,7	$(La/Yb)_n$ = 23-70 Anomalia de Eu = fracamente negativa a ausente	Nb = 5-10 Zr = 100-200 Y = 5-20	50-150	Sr = 400-1000 Ba = 500-2000	Ni = 20-60 Cr = 20-150
Cráton Pilbara[3]	2,95 Ga	X	>3,44Ga 3,2-2,99Ga	Dioritos a Granodioritos	Hornblenda e biotita. Nos granodioritos há núcleos de clinopiroxênio na hornblenda	Magnetita Apatita Titanita Zircão	Enclaves dioríticos	41-62	0,7-1,1	0,3-0,7	$(La/Yb)_n$ = 14-53 Anomalia de Eu = fracamente negativa a ausente	Nb = 4-10 Zr = 100-190 Y = 8-20	36-136	Sr = 350-750 Ba = 450-1600	Ni = 14-120 Cr = 22-224
Escudo Báltico[4]	2,74-2,71 Ga	Domínio Central < 2,80 Ga Domínio Oeste e Vodlozero 2,90-2,85 Ga	3,20-3,10 Ga 2,90-2,85 Ga 2,80-2,75 Ga	Monzodioritos a Granodioritos	Hornblenda e biotita	(Magnetita) Apatita Titanita Zircão Epidoto	X	45-52	0,8-1,0	0,4-0,8	$(La/Yb)_n$ = 19-65 Anomalia de Eu = negativa	Nb = 3-10 Zr = 120-290 Y = 10-27	42-98	Sr = 610-850 Ba = 1200-2300	Ni = 20-30 Cr = 40-80
Terreno Granito-*Greenstone* de Rio Maria[5]	2,87 Ga	2,92 Ga 2,95 Ga 3,00 Ga	2,98-2,92 Ga 2,87 Ga	Dioritos a Granodioritos	Hornblenda e biotita, raramente clinopiroxênio	(Magnetita) Apatita Titanita Zircão Alanita Epidoto	Enclaves dioríticos a monzodioríticos e aglomerados máficos compostos por Hb ± Bt ± Plg	48-63	0,8-1,1	0,3-0,7	(La/Yb)n = 11-73 Anomalia de Eu = fracamente negativa a ausente	Nb = 4-13 Zr = 79-161 Y = 5-21	67-183	Sr = 300-900 Ba = 600-1600	Ni = 25-120 Cr = 40-310

Fontes dos Dados: [1]Stern et al. (1989), Stern & Hanson (1991), Stevenson et al. (1999); [2]Smithies & Champion (2000); [3]Jayananda et al. (1995), Moyen et al. (2003); [4]Halla (2005, Kovalenko (2005); [5]Medeiros (1987), Medeiros & Dall'Agnol (1988), Althoff (1996), Leite (2001, Rämö et al. (2002), Oliveira et al. (2006b).

de Redenção. Rochas correlacionadas ao Granodiorito Rio Maria que ocorrem na região do Xingu mostraram, por sua vez, idade de 2850 ± 17 Ma (método Pb-Pb em zircão por evaporação; Avelar 1996, Avelar et al. 1999). Relações de campo indicam que rochas da Suíte Rio Maria são intrusivas no Supergrupo Andorinhas (Docegeo 1988, Souza 1994). Além disto, na área de Xinguara, granodioritos são intrusivos no Complexo Tonalítico Caracol, ao passo que são cortados pelo Trondhjemito Água Fria e Granito Xinguara (Leite 2001).

Tabela 3 – Dados geocronológicos da Suíte Rio Maria.

Localização	**Tipo de Rocha**	**Método**	**Material Analisado**	**Idade/Referência**
Área tipo	Granodiorito	U-Pb	Zircão	2874 + 9/-10 Ma (1)
Área tipo	Granodiorito	U-Pb	Zircão, Titanita	2872 ± 5 Ma (2)
Norte de Xinguara	Quartzo-diorito	Pb-Pb	Zircão	2878 ± 4 Ma (3)
Serra do Inajá	Granodiorito	Pb-Pb	Zircão	2879 ± 4 Ma (4)
	Granodiorito	Pb-Pb	Zircão	2877 ± 6 Ma (5)
	Granodiorito	Pb-Pb	Zircão	2881 ± 8 Ma (6)
	Diorito	Pb-Pb	Zircão	2880 ± 4 Ma (6)

Fonte dos dados: (1) - Macambira (1992); (2) - Pimentel & Machado (1994); (3) - Dall'Agnol et al. (1999b); (4) Rolando & Macambira (2002); (5) Rolando & Macambira (2003).

Rochas máficas e intermediárias são encontradas associadas ao aos granodioritos, mais raramente que os enclaves, estando presentes nas áreas de Xinguara (Leite 2001) e Bannach (Oliveira et al. Submetido a), Na área de Bannach, as ocorrências de rochas máficas e intermediárias são mais expressivas e concentram-se em dois domínios: no domínio principal, localizado próximo à cidade de Bannach, ocorre um stock composto principalmente por quartzo-dioritos e quartzo-monzodioritos.

As rochas da Suíte Rio Maria são, em grande maioria, classificadas como epidoto-biotita-hornblenda-granodiorito e as rochas intermediárias mostram composições dominantemente quartzo-dioríticas com variações, no limite entre os campos, para quartzo-monzodioríticas. A presença de enclaves máficos de tendência monzonítica englobados pelos granodioritos é uma feição marcante. Segundo evidências de estudos anteriores (Medeiros 1987, Souza 1994, Leite 2001, Oliveira 2005, Oliveira et al. submetido a), os enclaves podem estar ligados geneticamente

às rochas máficas e intermediárias e aos granodioritos. É importante destacar, também, a intensidade e penetratividade do processo de saussuritização do plagioclásio, que pode estar ligado a transformações pós-magmáticas ou a um possível evento de metamorfismo regional que teria afetado as rochas arqueanas do Terreno Granito-*Greenstone* de Rio Maria (Medeiros 1987, Souza 1994, Althoff 1996, Leite 2001). A hipótese de a saussuritização e reequilíbrio do plagioclásio e outras transformações serem devidas a metamorfismo de baixo grau, ocorrido na região, ou reflexo dos processos deformacionais merece consideração. Porém, mesmo as rochas da Suíte que parecem isotrópicas mostram saussuritização do plagioclásio e transformações em biotita e hornblenda, levando a pensar que não há uma ligação direta entre tais transformações e os processos deformacionais atuantes na região. Isso implica admitir que, caso tenha ocorrido um processo de metamorfismo regional, ele seria devido essencialmente a efeitos de temperatura e fluídos ricos em H_2O. Outra hipótese seria associar tais transformações a processos hidrotermais que teriam afetado o granodiorito e rochas associadas em condições subsolidus (Souza 1994).

Rochas da Suíte Rio Maria são metaluminosas e mostram outras características afins com as das séries cálcico-alcalinas em certos diagramas, porém mostram conteúdos mais baixos de Al_2O_3 e CaO e mais altos de MgO, Cr e Ni do que estas séries, assemelhando-se geoquimicamente às suítes sanukitóides.

Os dados apresentados mostram que as rochas que compõem a Suíte Rio Maria possuem todas as características petrográficas e geoquímicas típicas de rochas sanukitóides (Stern et al. 1989, Stern & Hanson 1991, Smithies & Champion 2000, Moyen et al. 2003, Halla 2005): 1) Eles são compostos de rochas ígneas félsicas a intermediárias metaluminosas com granodioritos, geralmente incluindo aglomerados ou enclaves máficos, como rochas granitóides dominantes; 2) Eles possuem alto #Mg, Cr, e Ni, junto com altos conteúdos de LILE, especialmente Ba e Sr; 3) Conteúdos moderados de K_2O, refletidos nas razões K/Na que variam de 0,35 a 0,74; 4) Conteúdos relativamente altos de ETRL e forte fracionamento de ETRP, associados com fraca ou ausente anomalia de Eu.

1.6 - APRESENTAÇÃO DO PROBLEMA

No Terreno Granito-*Greenstone* de Rio Maria tem-se uma situação similar à descrita nos principais terrenos arqueanos do mundo (Província Superior do Canadá: Stern et al. 1999, Stern & Hanson 1991, Stevenson et al. 1999; Cráton Pilbara: Smithies & Champion 2000, Smithies et

al. 2003, 2004; Terreno Granito-*Greenstone* Kareliano: Lobach-Zuchenko et al. 2000, 2005, Halla 2005) com rochas da Suíte sanukitóide Rio Maria intrudindo segmentos crustais constituídos por *greenstone*-belts e granitóides de associações TTGs (Medeiros & Dall'Agnol 1988, Althoff et al. 2000, Leite et al. 2004, Oliveira et al. 2006b, Oliveira et al. 2009, Oliveira et al. submetido a, b).

A Suíte Rio Maria foi estudada em diferentes áreas de ocorrência por diversos autores, sendo definida sua idade de colocação, suas características mineralógicas e assumida sua afinidade sanukitóide (Medeiros & Dall'Agnol 1988, Althoff et al. 2000, Leite et al. 2004, Oliveira et al. 2009). As informações disponíveis sobre as rochas da Suíte são relativamente abundantes e mostram que os estudos desenvolvidos até então geraram dados consistentes e de boa qualidade. Entretanto, a ausência de integração de dados das diferentes áreas e de comparações a nível local e com ocorrências internacionais, limita o entendimento das variações mineralógicas e químicas dessas rochas em cada área estudada. Também são indispensáveis estudos mais dirigidos, voltados para o preenchimento de lacunas no conhecimento dessas rochas. Além disto, não há na literatura discussões mais aprofundadas quanto à gênese, processos de formação e evolução dos magmas que geraram as rochas da Suíte Rio Maria, sendo esta uma das principais limitações no conhecimento desta associação magmática.

Alguns modelos para origem dos granodioritos da Suíte foram sugeridos, na maioria das vezes baseados em dados geológicos, petrográficos, geoquímicos e geocronológicos. Para Medeiros (1987), a origem mais plausível dessas rochas seria a de fusão parcial na base da crosta, podendo envolver contribuições de material de origem mantélica ou com baixo tempo de residência crustal. Outra possibilidade seria a de um modelo genético que envolveria anatexia de rochas máficas dos *greenstone-belts* (crosta oceânica) na zona de subducção, com o magma inicial tendo uma interação com o manto enriquecido e a crosta siálica para explicar o enriquecimento em elementos incompatíveis e de transição que ocorrem nos granodioritos (Dall'Agnol et al. 1997). Leite (2001), baseado na afinidade geoquímica entre os granodioritos e as séries sanukitóides, aventa que o magma gerador dos granodioritos seria derivado de um manto enriquecido situado acima de uma zona de subducção.

As expressivas ocorrências de rochas máficas (acamadadas) e intermediárias (quartzo-dioritos e quartzo-monzodioritos) associadas aos granodioritos, identificadas na área a leste da cidade de Bannach (Oliveira 2005), têm um papel fundamental na busca do entendimento das

questões apresentadas. Características petrográficas e geoquímicas indicam que os granodioritos e as rochas intermediárias derivaram de líquidos distintos, evoluindo independentemente, sendo ambos cogenéticos, mas não comagmáticos (Oliveira 2005, Oliveira et al. 2009). As rochas intermediárias seriam originadas a partir de fontes similares às dos granodioritos, mas resultariam possivelmente de um maior grau de fusão. As rochas acamadadas que ocorrem nesta associação, embora geneticamente vinculadas à associação sanukitóide, têm uma evolução magmática particular envolvendo a participação de processos de acúmulo de cristais. As relevantes ocorrências das rochas máficas e intermediárias, bem como de enclaves máficos, aliadas aos resultados preliminares que apontam para ligação genética com o granodiorito, confere às mesmas um papel fundamental no entendimento da gênese e evolução das rochas sanukitóides do Terreno Granito-*Greenstone* de Rio Maria.

Uma importante característica da associação é a presença marcante de enclaves máficos nas ocorrências dos granodioritos. Um processo capaz de explicar a presença constante desses enclaves, aventado por Souza (1994) e abordado por Oliveira (2005), seria o de *magma mingling* (Didier & Barbarin 1991). Isso implicaria a presença de outro magma, mais máfico que o gerador dos granodioritos, dando-se a interação entre eles. Dentro dessa hipótese, há carência de estudos mais detalhados dos aspectos mineralógicos e químicos dos enclaves que possam colaborar no entendimento de sua gênese e do seu papel dentro da evolução do magma que originou os granodioritos.

O aumento do conhecimento sobre as rochas sanukitóides de Rio Maria é um passo indispensável no atual estágio. Os novos estudos, realizados durante esta tese, foram necessários para que seja possível a construção de modelos mais sólidos para a petrogênese e evolução magmática dessas rochas.

Dentre as inúmeras perguntas a serem respondidas destacamos as seguintes:

Em que ambiente tectônico foi gerado o Granodiorito Rio Maria?

Qual a relação entre a formação das rochas sanukitóides e a dos TTGs e leucogranitos calcico-alcalinos?

Qual(is) magma(s) foi(ram) determinante(s) na formação das rochas sanukitóides?

Qual(is) foi(ram) a(s) fonte(s) desse(s) magma(s)?

Qual o papel da crosta na formação e evolução do magma granodiorítico?

Quais foram os parâmetros de cristalização (T, P, fO_2, XH_2O) reinantes durante a cristalização das principais rochas da associação?

Qual o significado das rochas acamadadas e como explicar os prováveis processos cumuláticos envolvidos em sua formação?

Que papel desempenharam anfibólio e epidoto na evolução magmática da suíte sanukitóide?

Qual a relação entre o magma formador dos enclaves e aqueles responsáveis pela geração de rochas intermediárias e acamadadas?

1.7 - OBJETIVOS

O objetivo principal deste trabalho é definir a fonte dos magmas e processos geradores das rochas que formam a Suíte Rio Maria, bem como das condições reinantes e processos magmáticos envolvidos em suas evoluções. Como objetivos específicos destacam-se:

- Melhor caracterização em termos petrográficos e geoquímicos, de ocorrências de rochas associadas de áreas de maior interesse petrológico;
- Reavaliar os dados existentes, comparando as características mineralógicas e químicas das diversas ocorrências dos granodioritos e rochas associadas no Terreno Granito-*Greenstone* de Rio Maria;
- Determinar a idade das rochas intermediárias associadas aos granodioritos;
- Aprofundar a caracterização geoquímica e mineralógica das rochas em questão, procurando estimar os parâmetros (fO_2, XH_2O, P, T) reinantes durante as suas respectivas cristalizações;
- Definir modelos para explicar os processos de formação e as fontes dos magmas geradores dos granodioritos, rochas máficas e intermediárias associadas e enclaves máficos;
- Comparar as características da Suíte Rio Maria com as principais associações sanukitóides descritas na literatura.

CAPÍTULO – 2

MESOARCHEAN SANUKITOID ROCKS OF THE RIO MARIA GRANITE-GREENSTONE TERRANE, AMAZONIAN CRATON, BRAZIL

Marcelo Augusto de Oliveira
Roberto Dall'Agnol
Fernando Jacques Althoff
Albano Antônio da Silva Leite

Publicado: *JOURNAL OF SOUTH AMERICAN EARTH SCIENCES* special issue of Magmatism, Crustal Evolution, and Metallogenesis of Carajás and adjacent provinces.

Journal of South American Earth Sciences 27 (2009) 146–160

Contents lists available at ScienceDirect

Journal of South American Earth Sciences

journal homepage: www.elsevier.com/locate/jsames

Mesoarchean sanukitoid rocks of the Rio Maria Granite-Greenstone Terrane, Amazonian craton, Brazil

Marcelo Augusto de Oliveira [a,b,*], Roberto Dall'Agnol [a,b,*], Fernando Jacques Althoff [a,c], Albano Antonio da Silva Leite [a,d]

[a] Group of Research on Granite Petrology, Instituto de Geociências (IG), Universidade Federal do Pará (UFPA), Caixa Postal 8608, CEP 66075-900, Belém, Pará, Brazil
[b] Programa de Pós-Graduação em Geologia e Geoquímica (PPGG), IG, UFPA, Brazil
[c] Programa de Pós-Graduação em Geologia, Universidade do Vale do Rio dos Sinos, Caixa Postal 275, CEP 93022-000, São Leopoldo, RS, Brazil
[d] CDM – Centro de Desenvolvimento MineralBR 381 Km 450, CEP 33040 900, Companhia Vale, Brazil

ARTICLE INFO

Article history:
Received 6 August 2007
Accepted 27 July 2008

Keywords:
Archean
Sanukitoid series
Granodiorite
Intermediate rocks
Amazonian craton

ABSTRACT

The Archean sanukitoid Rio Maria Granodiorite yielded zircon ages of ~2.87 Ga and is exposed in large domains of the Rio Maria Granite-Greenstone Terrane, southeastern Amazonian craton. It is intrusive in the greenstone belts of the Andorinhas Supergroup, in the Arco Verde Tonalite and Caracol Tonalitic Complex (older TTGs). Archean potassic leucogranites, younger TTGs and the Paleoproterozoic granites of Jamon Suite are intrusive in the Rio Maria Granodiorite.

The more abundant rocks of the Rio Maria Granodiorite have granodioritic composition and display medium to coarse even-grained textures. These rocks show generally a gray color with greenish shades due to strongly saussuritized plagioclase, and weak WNW-ESE striking foliation. The significant geochemical contrasts between the occurrences of Rio Maria Granodiorite in different areas suggest that this unit corresponds in fact to a granodioritic suite of rocks derived from similar but distinct magmas. Mingling processes involving the Rio Maria Granodiorite and similar mafic to intermediate magmas are able to explain the constant occurrence of mafic enclaves in the granodiorite.

The associated intermediate rocks occur mainly near Bannach, where mostly quartz diorite and quartz monzodiorite are exposed. The dominant rocks are mesocratic, dark-green rocks, with fine to coarse even-grained texture. The Rio Maria Granodiorite and associated intermediate rocks show similar textural and mineralogical aspects. They follow the calc-alkaline series trend in some diagrams. However, they have high-Mg#, Cr, and Ni conjugate with high contents of large ion lithophile elements (LILEs), typical of sanukitoids series. The patterns of rare earth elements of different rocks are similar, with pronounced enrichment in light rare earth elements (LREEs) and strong to moderate fractionation of heavy rare earth elements (HREEs).

Field aspects and petrographic and geochemical characteristics denote that the granodiorites and intermediate rocks have sanukitoid affinity. However, geochemical data suggest that the intermediate rocks and the granodiorites are not related by a fractional crystallization process. It is concluded that the intermediate rocks derived from similar sources to the granodiorites, but probably result from a higher degree of melting, being both cogenetic, but not comagmatic rocks.

Mineralogical aspects associated with experimental evidence suggest that the Rio Maria Granodiorite magma was relatively water-enriched (>4 wt.%), explaining the presence of hornblende at the liquidus and the absence of clinopyroxene and orthopyroxene in the studied rocks. The occurrence of well-preserved magmatic epidote crystals, admitting that the Rio Maria Granodiorite was emplaced at shallow crustal levels, points to a rapid ascent of the Rio Maria Granodiorite magma.

1. Introduction

Archean sanukitoid suites have been described over the last 20 years in the Canadian Shield (Shirey and Hanson, 1984; Stern and Hanson, 1991; Stevenson et al., 1999), Pilbara craton (Smithies and Champion, 2000), Karelian craton of the Fennoscandian Shield (Chekulaev, 1999; Lobach-Zhuchenko et al., 2000a,b, 2005;

* Corresponding authors. Address: Group of Research on Granite Petrology, Instituto de Geociências (IG), Universidade Federal do Pará (UFPA), Caixa Postal 8608, CEP 66075-900, Belém, Pará, Brazil. Tel.: +55 91 3201 7123; fax: +55 91 3201 7537.
E-mail addresses: mao@ufpa.br (M.A. de Oliveira), robdal@ufpa.br (R. Dall'Agnol), fjalthoff@gmail.com (F.J. Althoff), albano.leite@vale.com.br (A.A. da Silva Leite).

0895-9811/$ - see front matter © 2008 Elsevier Ltd. All rights reserved.
doi:10.1016/j.jsames.2008.07.003

Kovalenko et al., 2005; Bibikova et al., 2005), Zimbabwe craton (Bagai et al., 2002; Kampunzu et al., 2003), Dharwar craton (Moyen et al.,2001, 2003) and Amazonian craton (Althoff et al., 2000; Souza et al., 2001; Leite et al., 2004; Oliveira et al., 2006a,b; Dall'Agnol et al., 2006). The term sanukitoid suite (or high-Mg diorite suite), first introduced by Shirey and Hanson (1984) for Late Archean felsic intrusive and volcanic rocks from the Superior Province geochemically distinct of the TTG suites, refers to a series of associated high-magnesium rocks (diorites through granodiorites) that have similar geochemical characteristics. Halla (2005) used the term sanukitoid series for an assemblage of granitoids having relatively high-Mg numbers and high Cr, Ni, P, LILE (Sr, Ba) and LREE abundances at any given silica content.

The main geochemical characteristics of these rocks have been attributed to their origin by melting an enriched mantle source (Stern et al., 1989; Stern and Hanson, 1991; Stevenson et al., 1999; Smithies and Champion, 2000; Moyen et al., 2001). This origin contrasts with that generally accepted for TTG formation involving melting a basaltic slab (Barker, 1979; Condie, 1981; Martin, 1999). On the other hand, the isotope and geochemical characteristics of sanukitoid suites are ambiguous, indicating both mantle and crustal influences (Stern and Hanson, 1991; Stevenson et al., 1999; Halla, 2005). To explain these characteristics, it was suggested that the sanukitoid suites formed from an enriched mantle wedge contaminated either by fluids (Stern and Hanson, 1991; Stevenson et al., 1999), or by adakitic melts (Martin, 1999; Rapp et al., 1999), both released from the slab in a subduction zone.

Large domains of sanukitoid rocks have been identified in the Archean Rio Maria Granite-Greenstone Terrane (RMGGT) in the southeastern domain of the Amazonian craton (Althoff et al., 2000; Souza et al., 2001; Leite et al., 2004; Oliveira et al., 2006a,b; Dall'Agnol et al., 2006). The sanukitoid suites are composed of the Rio Maria Granodiorite and associated mafic and intermediate rocks. The Rio Maria Granodiorite occurs in different areas of the Rio Maria Granite-Greenstone Terrane (Fig. 1; Redenção Althoff et al., 2000; Xinguara Souza et al., 2001; Leite et al., 2004; and Bannach Oliveira et al., 2006a,b), while the associated mafic and intermediate rocks, originally restricted to a local occurrence in the Xinguara Area (Souza et al., 2001; Leite et al., 2004), were mapped recently in the Bannach Area (Fig. 1; Oliveira, 2005).

The aim of this paper is to discuss the geochemical signature and magmatic evolution of the sanukitoid rocks of the southeastern Amazonian craton, and the significance of the intermediate rocks in their evolution. To achieve this goal, the geological, petrographic and geochemical characteristics of the Archean sanukitoid rocks of the Rio Maria Granite-Greenstone Terrane will be summarized. Although the available data on the sanukitoid rocks from different areas of the Rio Maria Granite-Greenstone Terrane will be considered, emphasis will be put in the granodiorites and associated intermediate rocks from the Bannach area.

2. Geologic setting

The Rio Maria Granite-Greenstone terrane is situated in the southeastern part of the Amazonian craton inside the Archean Carajás Province (Docegeo, 1988; Dall'Agnol et al., 2006). The Amazonian craton is composed of Archean and Proterozoic terranes and remained tectonically stable since the Neoproterozoic. The craton has been subdivided into several geochronological provinces (Tassinari and Macambira, 2004; Santos et al., 2000). The Carajás Province is the oldest and best preserved Archean province of the craton (Dall'Agnol et al., 2006). It has been included into the Central Amazonian Province by Tassinari and Macambira (1999) or considered an independent tectonic province (Santos et al., 2000). It is divided in two major tectonic domains, the 3.0–2.86 Ga Rio Maria Granite-Greenstone Terrane and the rift-related Carajás Basin dominantly composed of 2.76–2.55 Ga metavolcanic rocks, banded iron formations, and granitoids (Machado et al., 1991; Macambira and Lafon, 1995; Barros et al., 2001; Dall'Agnol et al., 2006). Geophysical evidence suggests that the limit between both domains coincides with a regional ~EW trending discontinuity situated to the north of Sapucaia and south of Canaã dos Carajás. The Archean crust of both domains was intruded by ~1.88 Ga rapakivi-type granites of the Jamon and Serra dos Carajás suites (Dall'Agnol et al., 1999a, 2005; Dall'Agnol and Oliveira 2007).

The Mesoarchean magmatism of the Rio Maria Granite-Greenstone Terrane is similar to that recorded in classical granite-greenstone terranes. It is composed of greenstone belts of the Andorinhas Supergroup (Souza and Dall'Agnol, 1995; Souza et al., 2001) and several groups of Archean granitoids (Dall'Agnol et al., 2006). The greenstone belts are composed dominantly of komatiites and tholeiitic basalts. The Archean granitoids of the Rio Maria Granite-Greenstone Terrane are similar to those found in classical Archean terranes and yielded ages between 2.98 and 2.86 Ga. Four groups of granitoids have been distinguished (Dall'Agnol et al., 2006 and references therein): (1) older TTG series (2.98–2.93 Ga); (2) sanukitoid Rio Maria Granodiorite and associated rocks (~2.87 Ga); (3) younger TTG series (~2.86 Ga); (4) Potassic leucogranites of calc-alkaline affinity mostly (~2.86 Ga). The Archean units of the terrane are intruded by ~1.88 Ga A-type granites and associated dikes (Jamon Suite; Dall'Agnol et al., 2005; Dall'Agnol and Oliveira, 2007).

3. Archean sanukitoid series: Rio Maria Granodiorite and associated intermediate rocks

3.1. Geochronologic and geologic aspects

The Rio Maria Granodiorite and associated rocks yielded in different areas of occurrence remarkably uniform U–Pb and Pb–Pb evaporation zircon ages of ~2.87 Ga (Table 1). These granitoids are intrusive in the Andorinhas Supergroup (greenstone sequences; Souza et al., 2001), Arco Verde Tonalite (Althoff et al., 2000) and in the Caracol tonalitic complex and are intruded by the Água Fria Trondhjemite (younger TTG series; Leite et al., 2004), Archean potassic leucogranites (Mata Surrão Granite (Duarte, 1992); Xinguara Granite (Leite et al., 2004); Rancho de Deus Granite (Oliveira et al., 2006a,b)) and Paleoproterozoic granites of the Jamon Suite (Dall'Agnol et al., 2006).

The Rio Maria Granodiorite covers a large area of the Rio Maria Granite-Greenstone Terrane (Fig. 1), being exposed, besides the type-area, south of Rio Maria (Fig. 2a), to the south and NE of Xinguara, to the north of Redenção and to the east of Bannach. Some granitoids described in the Xingu and Carajás regions have been correlated to the Rio Maria Granodiorite (Docegeo, 1988; Costa et al., 1995; Avelar, 1996), but more detailed studies are necessary to confirm these assumptions. Although younger than the Rio Maria Granodiorite, the Cumaru Granodiorite (~2.82 Ga; Santos and Leonardos, 1994) is also similar to it.

The dominant rocks in the Rio Maria Granodiorite include systematically centimetric to decimetric mafic enclaves (Fig. 2b and c), and display generally a gray color with greenish shades due to strongly saussuritized plagioclase. They show a weak (Fig. 2) or more rarely striking WNW-ESE to E-W subvertical foliation, which was formed from magmatic to subsolidus high-temperature conditions and is outlined by the preferred mineral orientation of mafic minerals and, locally, enclaves. The mafic enclaves have flattened or rounded form, being stretched only along shear zones (Souza, 1994; Althoff et al., 2000; Leite, 2001). The enclaves display evidence of interaction with the granodiorite and both rocks show

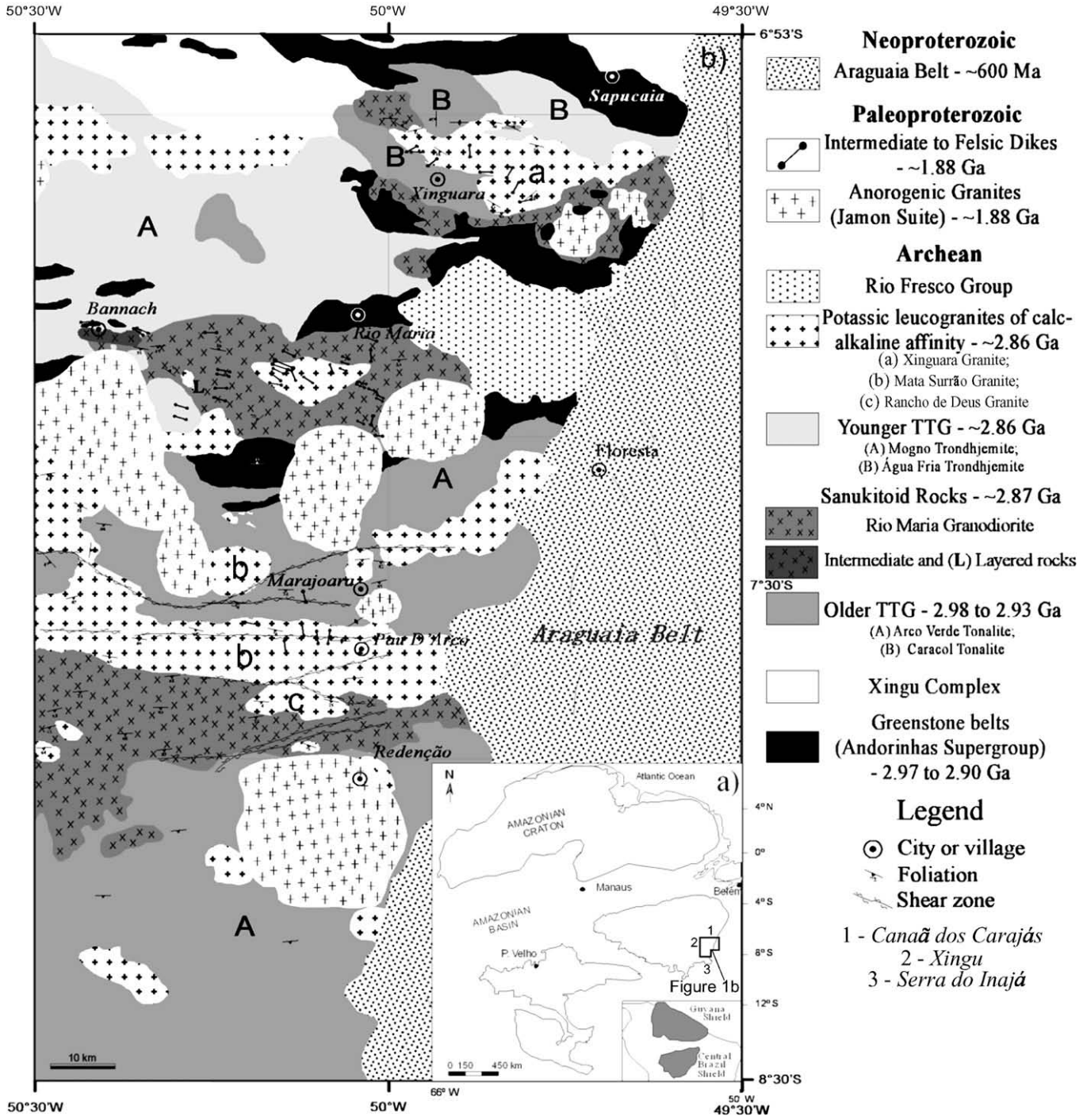

Fig. 1. (a) Location of the studied area in the Amazonian craton. (b) Geological map of the Rio Maria Granite-Greenstone Terrane (modified from Leite (2001)).

Table 1
Geochronology of the Rio Maria Granodiorite and associated rocks

Area	Rock	Method	Analyzed material	Age
Rio Maria	Granodiorite	U–Pb	Zircon	2874 + 9/−10 Ma (1)
Rio Maria	Granodiorite	U–Pb	Zircon, Titanite	2872 ± 5 Ma (2)
Xinguara	Quartz-diorite	Pb–Pb	Zircon	2878 ± 4 Ma (3)
Serra do Inajá	Granodiorite	Pb–Pb	Zircon	2879 ± 4 Ma (4)
Serra do Inajá	Granodiorite	Pb–Pb	Zircon	2877 ± 6 Ma (4)
Serra do Inajá	Granodiorite	Pb–Pb	Zircon	2888 ± 8 Ma (5)
Serra do Inajá	Granodiorite	Pb–Pb	Zircon	2880 ± 4 Ma (5)
Serra do Inajá	Granodiorite	Pb–Pb	Zircon	2875 ± 7 Ma (5)

Data source: (1) Macambira (1992), (2) Pimentel and Machado (1994), (3) Dall'Agnol et al. (1999a), (4) Rolando and Macambira (2002), (5) Rolando and Macambira (2003).

Fig. 2. (a) Outcrop of the Rio Maria Granodiorite of type-area. (b) Field aspects of the Rio Maria Granodiorite, showing elongated mafic enclaves and weak foliation. (c) Polished sample of the Rio Maria Granodiorite displaying a gray color with greenish shades due to the strongly saussuritized plagioclase and mafic clusters. (d) Hand sample of an associated intermediate rock displaying dark-green color and well-preserved igneous texture.

similar high-temperature structures, suggesting that they were deformed simultaneously. The mentioned features indicate a low viscosity contrast between the enclaves and the Rio Maria Granodiorite, and suggest their coexistence in the magmatic stage (Souza and Dall'Agnol, 1995; Althoff, 1996; Leite, 2001).

Other structures identified in the Rio Maria Granodiorite are folded veins, shear bands and tension cracks. Low angle shear zones were described in the Redenção (Althoff et al., 2000) and Xinguara (Leite, 2001) areas.

Mafic and intermediate rocks are found, more rarely, forming small bodies (Xinguara area, Leite, 2001) or stocks (Bannach area, Oliveira et al., 2006a,b) associated with the Rio Maria Granodiorite. In the Bannach area, the mafic and intermediate rocks occur in two domains (Fig. 1): In the main domain, located near Bannach, a stock composed mostly of quartz diorites and quartz monzodiorites is exposed; in the second domain, situated along the road between Rio Maria and Bannach, an occurrence of layered rocks was described. The dominant intermediate rocks are mesocratic, dark-green rocks, with fine to coarse even-grained texture (Fig. 2d). The layered rocks are inequigranular with a remarkable concentration of generally quadratic or short prismatic coarse amphibole crystals, enveloped by leucocratic intercumulus material. These layered rocks were interpreted as cumulate rocks, cogenetic with the Rio Maria sanukitoid granodiorite (Oliveira, 2005). They will not be further discussed in this paper that is devoted to the Rio Maria Granodiorite and associated intermediate rocks.

3.2. Petrography

In all occurrences of the Rio Maria Granodiorite, the dominant rocks have granodioritic to subordinate monzogranitic composition and display equigranular, medium to coarse even-grained textures. The intermediate rocks are quartz diorites and quartz monzodiorites, with equigranular, medium- to fine-grained textures. The rocks are in general not intensely deformed, and original igneous textures are well-preserved (Fig. 2c and d). The Rio Maria Granodiorite and intermediate rocks contain amphibole ± biotite ± magmatic epidote as their principal mafic minerals, and present strongly saussuritized plagioclase (Fig. 3). Primary accessory minerals include zircon, apatite, magnetite, titanite, and allanite.

The modal compositions (Table 2) of 52 representative samples of the sanukitoid rocks of the RMGGT are strongly concentrated in the granodiorite field in the Q–A–P diagram (Fig. 4), with the more evolved rocks occupying the monzogranite field, and the intermediate rocks occupying the quartz monzodiorite and quartz diorite fields. The diagram shows that *M* values (% volume of mafic minerals) vary generally from 10 to 25 in the granodiorites, attaining higher values in the intermediate rocks (Fig. 4).

In the dominant epidote-biotite-hornblende sanukitoid granodiorite, apatite, zircon, magnetite and allanite are early crystallized phases. They are followed by magnesian hornblende and plagioclase. Amphibole forms euhedral, twinned crystals that are well-preserved or partially replaced by late magmatic biotite (Fig. 3c and d) and subordinate titanite and epidote. Plagioclase is euhedral

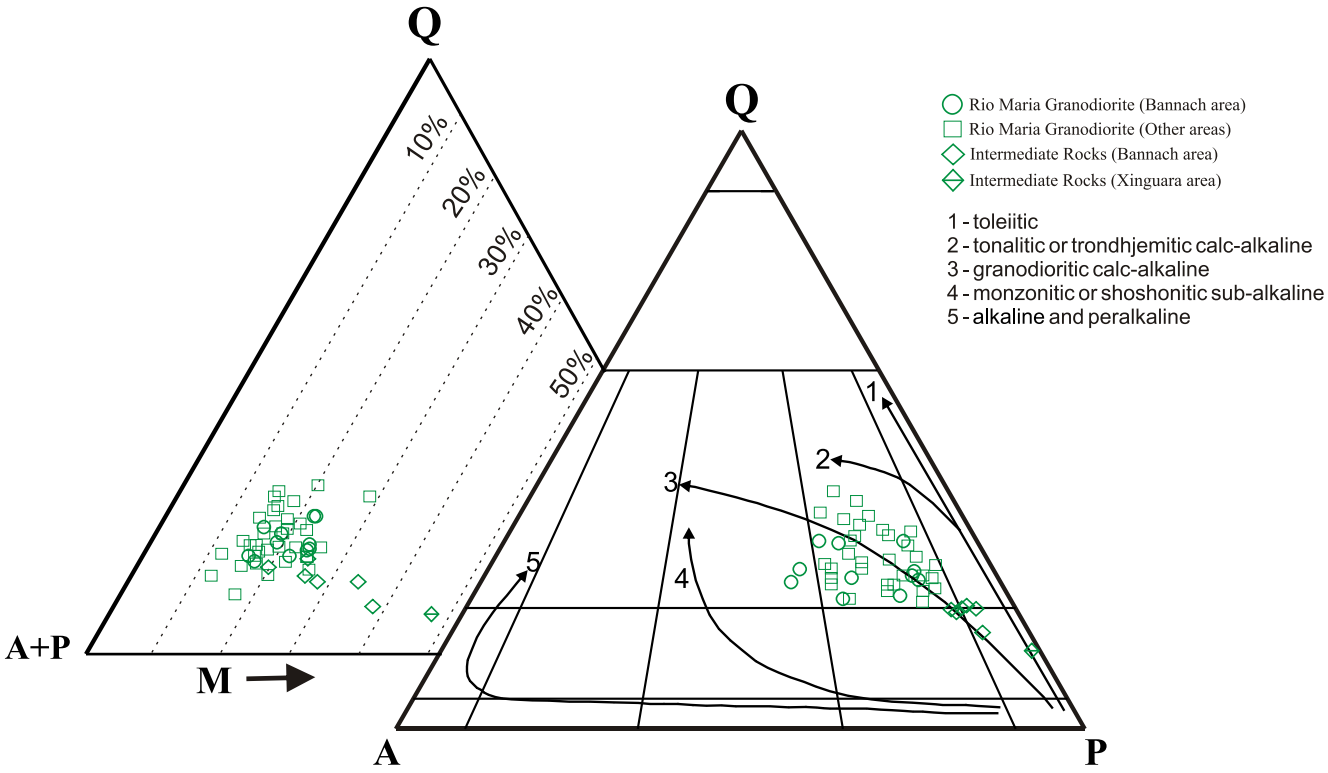

Fig. 3. QAP and Q–(A + P)–M plots for the Rio Maria Granodiorite and associated intermediate rocks. Data sources: Rio Maria Granodiorite and intermediate rocks – Bannach area (Oliveira, 2005); Rio Maria Granodiorite – Other areas (Medeiros, 1987; Souza, 1994; Althoff, 1996; Leite, 2001); Intermediate rocks – Xinguara area (Leite, 2001).

Table 2
Modal composition (point counting) of the Rio Maria Granodiorite and associated intermediate rocks (Bannach area)

Intermediate rocks							Rio Maria Granodiorite										
Facies	EBAQzD			EBAQzMD			EBAGD							EABGD		EBAMzG	
Sample	MFR-102	ADR-4B	ADR-4A	ADR-7	ADR-5	MFR-100D	MFR-32	MFR-80A	MFR-114	MFR-112	MFR-27A	MFR-26A	ADR-3A	MFR-62A	MFR-91A	MFR-29	MFR-111
Plagioclase	55.6	47.1	46.0	57.0	57	47.9	49.7	48.2	46.6	40.3	44.6	37.2	36.8	47.9	40.3	37.5	36.2
Alkali-feldspar	4.7	4.3	4.7	7.9	6.7	8.8	15.9	8.81	9.3	20.3	8.3	18,0	19.32	11.7	16.1	23.1	24 2
Quartz	14.7	13,0	9.3	15.7	13.7	18.6	23.21	20.5	22.2	17.6	24,0	25.6	23.2	17.5	18.9	22.2	19.6
Amphibole	17.8	28.7	25.1	16.6	20.3	28.1	9.8	8.2	12.7	8.18	11.8	8.2	11.1	7.6	10.2	8.1	8.7
Biotite	5,0	0.7	7.9	0.6	4.5	5.1	4.4	7.2	8.2	4.2	7.8	7.7	7.5	10.7	11.3	4.8	7.6
Epidote$^{(m)}$	0.5	1.5	1.30	0.2	0.6	0.2	1.2	1.9	1.1	1.1	0.7	0.6	1.8	1.3	0.3	0.7	0.8
Epidote$^{(S)}$	0.2	0.3	0.5	0.7	0.5	0.4	1.1	2.6	0.8	1.4	1,0	1.3	2,0	1.5	0.8	1.1	1.1
Opaques	0.1	1.1	2 2	0.5	0.8	0.7	–	n.d.	0.1	n.d.	0.2	–	n.d.	–	–	0.2	n.d.
Titanite	0.6	1.5	1.2	0.9	0.5	0.8	0.6	0.7	0.7	0.2	0.4	0.3	0.9	0.8	1.1	1.1	0.6
Apatite	0.4	0.7	1,0	0.2	0.2	0.6	0.2	0.8	0.2	0.2	0.7	0.4	0.2	0.3	0.1	0.3	0.1
Allanite	0.2	1.0	0.7	0.1	0.4	n.d.	0.3	n.d.	n.d.	0.1	0.1	0.5	0.1	0.2	n.d.	0.5	0.6
Carbonate	n.d.	n.d.	0.1	n.d.	n.d.	–	–	–	–	n.d.	0.1	–	–	n.d.	n.d.	–	0.1
Felsic	75,0	64.4	60.0	80.6	72.1	75.3	81.7	77.8	75.1	83.2	76.9	80.8	75.2	77.1	75.3	82.8	80.0
Mafic	24.8	35.5	39.6	19.8	27.8	22.9	17.6	21.4	23.8	16.0	22.7	19.0	23.6	22.9	23.8	16.8	19.5

Data source: (1) Oliveira (2005); E = epidote; B = biotite; A = amphibole; Qz = quartz; D = diorite; MzD = Monzodiorite; GD = granodiorite; MzG = Monzogranito$^{(m)}$, magmatic; $^{(s)}$secondary.

to subhedral, originally zoned but so intensely saussuritized (Fig. 3a and b) that its original composition cannot be determined. Biotite initiates its crystallization after amphibole and plagioclase, and displays textural evidence of equilibrium with euhedral epidote (Fig. 3e). In these rocks, excluding secondary epidote derived from plagioclase, two textural epidote types interpreted as magmatic are distinguished: Epidote with zoned allanite core (Fig. 3f) and epidote associated with and partially enclosed by biotite (Fig. 3e). Quartz forms subhedral to anhedral medium-grained crystals that are sometimes recrystallised, forming subgrains with undulatory extinction. K-feldspars crystallized late forming anhedral, sometimes poikilitical crystals, including quartz, plagioclase and euhedral amphibole. At the subsolidus stage, chlorite, epidote, sericite and carbonates were generated.

In the quartz diorites and quartz monzodiorites, the mineral assemblages and textural relationships between different minerals are very similar to those observed in the dominant granodiorite, but amphibole and plagioclase are more abundant and quartz and K-feldspars modal contents are lower than in the granodiorite, and these minerals begin to crystallize later.

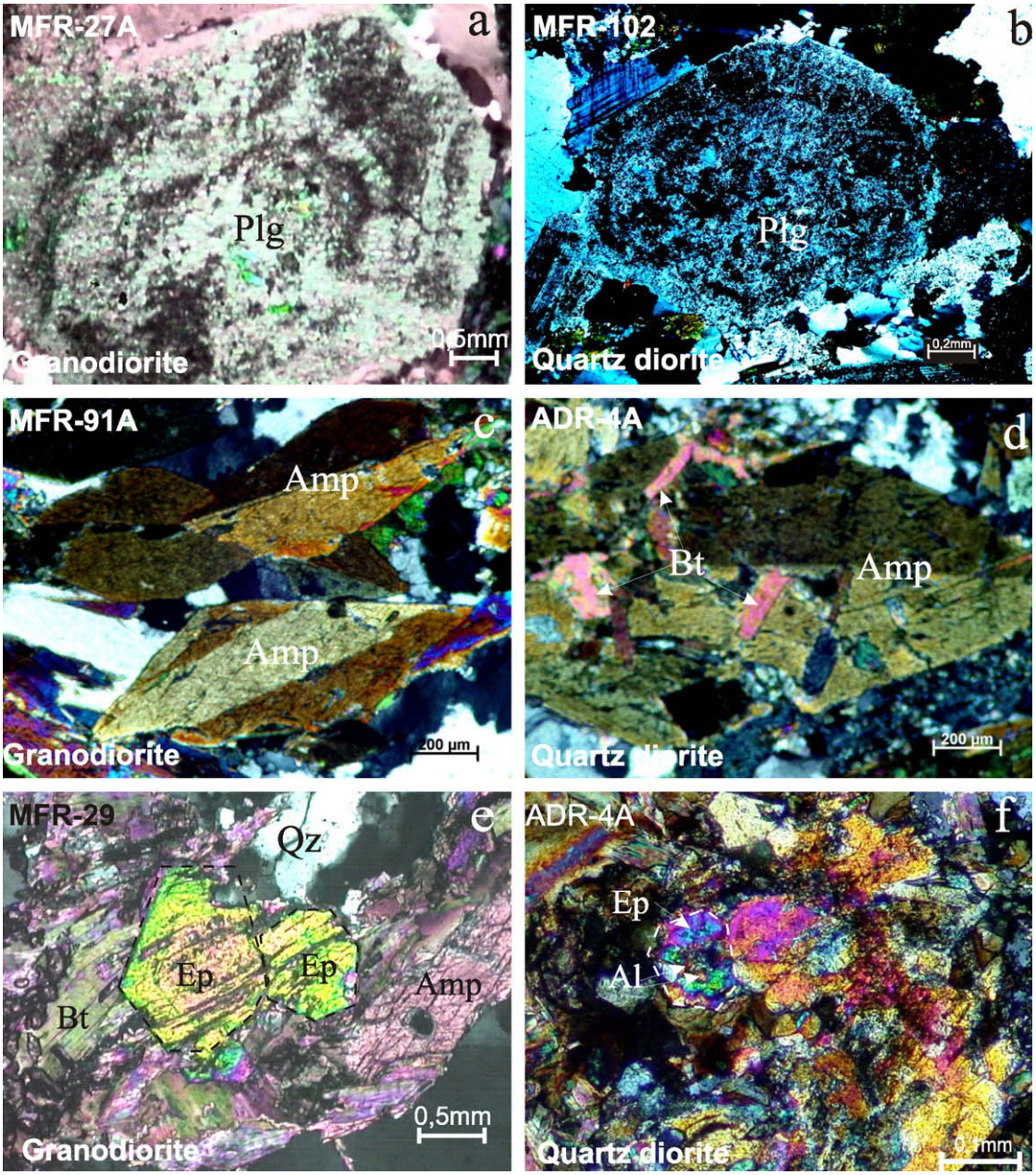

Fig. 4. Photomicrographs of Rio Maria Granodiorite (a, c, e) and associated intermediate rocks (b, d, f) showing preserved igneous texture. (a, b) Euhedral plagioclase, originally zoned but so intensely saussuritized. (c, d) Euhedral amphibole well-preserved or partially replaced by late magmatic biotite. (e) Euhedral magmatic epidote associated and partially enclosed by biotite. (f) Epidote with zoned allanite core.

3.3. Geochemistry

The chemical characteristics of the Rio Maria Granodiorite and associated intermediate rocks are discussed based mainly on a recent set of whole rock analyses of samples from the Bannach area (Table 3; Oliveira, 2005; Oliveira et al., 2006a,b). In that area comparatively larger domains of intermediate rocks have been found. The composition of the Rio Maria Granodiorite from other occurrences in the Rio Maria Granite-Greenstone Terrane is shown for comparison (Table 4).

The samples of the granodiorite and intermediate rocks from the Bannach area show little variation of silica contents (Table 3; respectively, 62.52–66.49 and 58.47–63.61 wt.%). Al_2O_3 contents are low (14.85 and 14.40 wt.% on average for granodiorite and intermediate rocks, respectively) compared to the values found in calc-alkaline series (Irvine and Baragar, 1971; Ringwood, 1975; Wilson, 1989). The granodiorites and intermediate rocks show high-MgO contents, resulting in the elevated values of Mg# (0.63–0.48, Table 3, Fig. 6a) that decrease from the intermediate rocks (>0.54, generally >0.60) to the granodiorite (0.50–0.48).

Consistent with the presence of hornblende as a major modal mafic phase, all analyzed rocks are metaluminous (Fig. 5a), implying excess of molecular CaO ($+Na_2O + K_2O$) in relation to Al_2O_3 in the norm. In the normative An–Ab–Or diagram (Fig. 5b), the intermediate rocks and granodiorite samples plot in the granodiorite field, very near to their limits with the tonalite (intermediate rocks) and granite (granodiorite) fields. The relatively low contents of Al_2O_3 of these rocks inhibited a more accentuated increase of the An-normative component in the intermediate rocks. However, a clear enrichment in Or-normative from the intermediate rocks to

Table 3
Chemical composition of the samples of the Rio Maria Granodiorite and associated intermediate rocks (Bannach area)

Area	Intermediate rocks						Bannach Rio Maria Granodiorite							
Facies	EBAQzD to EBAQzMD						EBAGD to EBAMzG							
Sample	ADR-4A	ADR-4B	ADR-5 M	MFR-102	MFR-100D	ADR-7	MFR-114	MFR-27	MFR-111	MFR-29	ADR-3A	MFR-112	MFR-91A	MFR-80A
SiO_2 (wt.%)	58.47	60.51	61.75	62.15	63.29	63.61	63.2	63.2963	64.726	64.726	63.9	64.58	64.72	66.49
TiO_2	0.47	0.4	0.3	0.39	0.38	0.37	0.46	0.49	0.42	0.45	0.3	0.42	0.39	0.33
Al_2O_3	14.02	14.03	13.96	14.5	14.97	14.9814	15.23	14.82	14.87	14.9814	14.82	14.55	14.98	14.55
Fe_2O_3	2.46	2.37	2.89	2.34	2.91	2.862	2.91	2.8	2.81	3,00	2.91	2.86	2.71	2.27
FeO	3.94	3.43	2.44	2.56	1.96	1.41	1.97	1.89	1.64	1.48	1.65	1.47	1.49	1.32
MnO	0.09	0.09	0.07	0.07	0.06	0.06	0.07	0.06	0.06	0.06	0.06	0.06	0.06	0.05
MgO	5.81	5.37	4.62	4.11	2.89	2.86	2.61	2.49	2.31	2.31	2.39	2.28	2.06	1.85
CaO	5.88	4.73	4.84	4.65	4.18	4.03	4.4	4.36	3.99	4.17	4.02	3.77	4.08	3.02
Na_2O	3.77	4.04	3.98	4.21	4.36	4.04	4.3	4.21	4.19	4.09	4.05	4.04	4.29	4.13
K_2O	2.21	2.16	2.31	2.24	2.57	2.66	2.983	3.01	3.2	3.22	3.21	3.44	2.98	3.75
P_2O_5	0.17	0.18	0.16	0.14	0.15	0.13	0.17	0.15	0.15	0.14	0.14	0.15	0.12	0.14
LOI	1.9	1.9	1.9	2,00	2,00	1.8	1.6	1.8	1.9	1.9	1.8	1.5	1.5	1.4
Total	99.19	99.25	99.35	99.36	99.32	99.39	99.17	99.31	99.32	99.32	99.38	99.22	99.38	99.3
Ba (ppm)	812	701	847	830	1008	1090	1139	1175	1052	1022	1098	1064	1044	1089
Rb	73	72	72	74	87	82	98	103	113	112	109	122	101	116
Sr	745	618	724	828	872	905	692	661	615	611	576	567	632	512
Zr	94	94	101	94	95	103	113	126	103	131	109	110	113	122
Nb	6	5	6	5	6	7	8	9	8	8	7	11	9	10
Y	11	10	11	10	10	12	16	13	11	15	11	12	17	12
Ga	18	18	19	20	20	20	20	20	19	20	20	19	20	19
Th	3	2	5	5	6	5	7	7	7	8	5	11	8	12
Ni	79	89	81	92	43	57	31	29	28	29	31	29	26	25
Cr	308	253	274	219	130	144	48	68	55	96	68	55	41	55
La	23.7	23.3	25.1	25.12	42.2	33.8	37.3	36.9	33.7	34.3	20.0	40.7	53.5	48.0
Ce	51.1	50.3	51.4	47.6	68.3	58.6	72.8	71.9	64.1	64.1	45.7	70.8	72.2	64.2
Pr	5.35	5.35	5.3	5.35	7.37	7.35	7.19	7.57	6.32	6.53	4.94	7.04	8.51	6.81
Nd	21.4	21.4	19.3	20.8	26.1	29.2	27.2	27.8	22.9	24.7	21.7	25.6	31.6	23.9
Sm	3.6	3.4	3.3	3.6	4.1	4.3	4.14	4.9	3.7	4.3	3.7	3.9	4.5	3.4
Eu	1.02	0.95	0.98	0.99	1.05	1.23	1.25	1.35	1.06	1.14	1.05	1.07	1.3	0.95
Gd	2.78	2.49	2.58	2.42	2.82	3.19	3.47	3.56	2.9	3.2	2.63	2.71	3.37	2.43
Tb	0.45	0.37	0.37	0.4	0.35	0.48	0.56	0.53	0.42	0.47	0.41	0.4	0.52	0.36
Dy	2.25	1.84	1.98	1.75	1.67	2. 2	2.41	2.19	1.92	2.19	1.86	1.9	2.31	1.56
Ho	0.38	0.34	0.33	0.34	0.31	0.42	0.48	0.42	0.34	0.42	0.41	0.4	0.49	0.32
Er	1.03	0.97	0.88	0.95	0.78	1.13	1.3	1.15	0.92	1.19	1.02	0.92	1.25	0.81
Tm	0.13	0.1	0.1	0.1	0.11	0.13	0.14	0.17	0.11	0.17	0.1	0.23	0.17	0.12
Yb	0.93	0.83	0.81	0.9	0.69	1,00	1,00	1.06	0.92	1.09	0.87	0.83	0.99	0.73
Lu	0.15	0.14	0.12	0.13	0.12	0.15	0.16	0.16	0.11	0.15	0.14	0.15	0.15	0.13
ΣREE	114.27	111.78	112.55	110.53	155.97	143.18	159.66	159.66	139.42	143.95	104.53	156.65	180.86	153.72
(La/Yb)n	17.20	18.95	2018.952	18.9520	41.28	22.81	218	23.50	24.72	218.904	15.52	33.10	36.48	44.38
(La/Sm)n	4.14	4.31	4.79	4.41	6.48	4.745	5.34	4.74	5.73	5.02	3.4	6.57	7.49	8.89
(Dy/Yb)n	1.57	1.44	1.59	1.26	1.57	1.3	1.57	1.34	1.36	1.391	1.39	1.49	1.52	1.39
Eu/Eu^*	0.99	1.00	1.03	1.03	0.94	1.02	0.98	0.99	0.99	0.94	1.03	1.01	1.02	1.01
Rb/Sr	0.1	0.12	0.1	0.09	0.1	0.09	0.14	0.16	0.18	0.18	0.19	0.22	0.16	0.23
Sr/Ba	0.92	0.88	0.85	1.00	0.86	0.83	0.61	0.56	0.58	0.6	0.53	0.53	0.61	0.47
K/Na	0.39	0.35	0.38	0.35	0.39	0.460	0.5	0.47	0.52	0.52	0.52	0.56	0.46	0.60
Mg#	0.62	0.63	0.62	0.61	0.5	0.4	0.5	0.5	0.5	0.49	0.49	0.5	0.48	0.49

Data source: [(1)]Oliveira (2005). Chemical ratios: Mg# molecular ratio Mg/(Mg + Fe); K/Na molecular ratio. $Eu/Eu^* = EuN/[0.5^*(SmN + GdN)]$. E = epidote; B = biotite; A = amphibole; Qz = quartz; D = diorite; MzD = monzodiorite; GD = granodiorite; MzG = monzogranite.

Table 4
Chemical composition of the representative samples of the Rio Maria Granodiorite and associated intermediate rocks of the other areas in the Rio Maria Granite-Greenstone Terrane

Area	Redenção (1)						Type-area (2)														Xinguara					
Facies	EBAQzD						EBAGD to EABGD														EBAGD	EBAGD to EABGD				
Sample	F-9A	92-20	F-66D	F-10	92-23	F-66A	220	152(5)	131(5)	284	158	239	119	16	207(5)	337	278	355	179	9	Z-509B(4)	AL-141(3)	AL-166A(3)	ZRM-45(5)	Z-192B(5)	ALF-233A(3)
SiO_2 (wt.%)	62.03	63.03	63.33	64.39	64.5	66.29	62.72	64.96	65.24	65.8	65.88	66.5	66.7	67.71	68.47	68.8	69.16	69.3	69.8	69.8	55.17	63.29	64.32	65.52	65.60	68.40
TiO_2	0.52	0.44	0.46	0.43	0.43	0.36	0.51	0.46	0.4	0.37	0.38	0.44	0.42	0.31	0.3	0.34	0.31	0.37	0.35	0.37	0.78	0.51	0.40	0.41	0.43	0.41
Al_2O_3	16.15	15.11	14.3	14.77	15.5	14.03	15.5	14.16	14.51	14.92	15.63	14.63	15.73	15.87	14.48	13.42	15.5	15.71	14.21	14.56	14.13	14.61	14.22	14.33	14.30	15.20
Fe_2O_3	6.28*	5.44*	5.73*	5.29*	3.97*	4.61*	2.9	5.15*	4.69*	2.05	2.57	2.34	2.01	1.99	3.58*	1.86	1.76	1.86	1.95	1.99	9.05*	2.57	1.98	4.83*	4.82*	1.67
FeO	n.d.	n.d.	n.d.	n.d.	n.d.	n.d.	2.81	n.d.	n.d.	1.94	1.83	2.23	2.16	1.37	n.d.	2.02	1.51	1.73	1.66	1.8	n.d.	2.36	2.65	n.d.	n.d.	1.56
MnO	0.06	0.08	0.07	0.07	0.08	0.06	n.d.	0.06	0.04	n.d.	n.d.	n.d.	n.d.	n.d.	0.04	n.d.	n.d.	n.d.	n.d.	n.d.	0.12	0.07	0.06	0.07	0.08	0.04
MgO	2.68	3.5	3.79	2.39	2.22	2.64	2.95	2.74	2.4	1.72	1.67	2.1	1.92	1.34	1.56	1.62	1.43	1.58	1.57	1.65	5.77	3.01	4.12	2.34	2.77	1.50
CaO	5.35	4.62	4.59	3.97	3.12	3.69	4.18	3.95	3.4	3,00	3.48	3.42	3.17	2.91	2.77	2.92	2.14	2.84	2.94	3.14	7.66	4.57	4.23	3.3	2.87	3.10
Na_2O	3.9	4.04	3.54	4.15	4.66	3.78	3.8	3.77	3.94	3.62	4.01	3.77	3.76	3.92	4.12	3.95	3.71	3.73	3.89	3.84	3.42	3.76	3.55	3.54	4.15	3.30
K_2O	2.16	2.97	3.28	2.94	2.87	3.28	2.96	2.99	3.37	3.7	3.25	3.41	3.7	3.43	3.84	3,00	4.19	3.7	3.45	3.58	1.79	3.31	3.70	3.97	2.45	3.30
P_2O_5	0.24	0.2	0.28	0.25	0.19	0.24	n.d.	0.25	0.26	n.d.	n.d.	n.d.	n.d.	n.d.	0.22	n.d.	n.d.	n.d.	n.d.	n.d.	0.38	0.34	0.27	0.27	0.24	0.10
LOI	n.d.	0.99	n.d.	n.d.	n.d.	n.d.	n.d.	0.74	1.2	n.d.	n.d.	n.d.	n.d.	n.d.	n.d.	n.d.	n.d.	n.d.	n.d.	n.d.	1.16	1.12	0.43	n.d.	n.d.	0.76
Total	99.38	100.42	99.37	98.64	97.52	98.98	98.33	99.23	99.45	97.12	98.70	98.84	99.57	98.85	99.38	97.93	99.71	100.82	99.82	100.73	99.43	99.52	99.93	98.58	97.71	99.34
Ba (ppm)	n.d.	966	n.d.	n.d.	859	n.d.	n.d.	832	1061	n.d.	n.d.	n.d.	n.d.	n.d.	996	n.d.	n.d.	n.d.	n.d.	n.d.	739	1586	928	1008	617	989
Rb	n.d.	130	n.d.	n.d.	112	n.d.	115	101	94	153	139	128	143	147	145	142	183	129	138	122	67	110	131	139	76	146
Sr	n.d.	564	n.d.	n.d.	719	n.d.	594	469	489	429	568	548	497	479	461	553	336	567	480	462	477	785	463	337	298	434
Zr	n.d.	115	n.d.	n.d.	161	n.d.	124	108	99	126	100	113	120	100	94	108	104	106	110	107	79	129	152	122	120	121
Nb	n.d.	8	n.d.	n.d.	13	n.d.	n.d.	5	5	n.d.	n.d.	n.d.	n.d.	n.d.	5	n.d.	n.d.	n.d.	n.d.	n.d.	6	4	5	8	5	5
Y	n.d.	17	n.d.	n.d.	21	n.d.	7	20	13	7	12	14	14	7	10	9	10	16	28	11	17	13	12	13	13	14
Ga	n.d.	21	n.d.	n.d.	23	n.d.	n.d.	22	9	n.d.	n.d.	n.d.	n.d.	n.d.	6	n.d.	n.d.	n.d.	n.d.	n.d.	24	11	10	24	5	27
Th	n.d.	5	n.d.	n.d.	11	n.d.	n.d.	5	5	n.d.	n.d.	n.d.	n.d.	n.d.	13	n.d.	n.d.	n.d.	n.d.	n.d.	5	7	8	18	27	5
Ni	n.d.	n.d.	n.d.	n.d.	n.d.	n.d.	n.d.	58	36	n.d.	n.d.	n.d.	n.d.	n.d.	26	n.d.	n.d.	n.d.	n.d.	n.d.	119	n.d.	n.d.	46	34	n.d.
Cr	n.d.	135	n.d.	n.d.	132	n.d.	n.d.	125	93	n.d.	n.d.	n.d.	n.d.	n.d.	73	n.d.	n.d.	n.d.	n.d.	n.d.	273	n.d.	n.d.	82	70	n.d.
La	n.d.	31.73	n.d.	n.d.	51.82	n.d.	n.d.	22.83	34.61	n.d.	n.d.	n.d.	n.d.	n.d.	27.67	n.d.	n.d.	n.d.	n.d.	n.d.	24.30	57.69	27.71	32.09	30.33	n.d.
Ce	n.d.	66.83	n.d.	n.d.	64.72	n.d.	n.d.	48.98	52.84	n.d.	n.d.	n.d.	n.d.	n.d.	44.73	n.d.	n.d.	n.d.	n.d.	n.d.	54.50	123.00	49.22	53.71	52.75	n.d.
Pr	n.d.	n.d.	n.d.	n.d.	9.2	n.d.	n.d.	n.d.	n.d.	n.d.	n.d.	n.d.	n.d.	n.d.	n.d.	n.d.	n.d.	n.d.	n.d.	n.d.	n.d.	n.d.	n.d.	n.d.	n.d.	n.d.
Nd	n.d.	26.42	n.d.	n.d.	33.92	n.d.	n.d.	19.87	24.76	n.d.	n.d.	n.d.	n.d.	n.d.	18.73	n.d.	n.d.	n.d.	n.d.	n.d.	26.6	54.2	8.48	21.91	21.78	n.d.
Sm	n.d.	3.99	n.d.	n.d.	6.07	n.d.	n.d.	4.49	4.71	n.d.	n.d.	n.d.	n.d.	n.d.	3.93	n.d.	n.d.	n.d.	n.d.	n.d.	5.90	8.6	4.21	4.82	4.19	n.d.
Eu	n.d.	1.01	n.d.	n.d.	1.52	n.d.	n.d.	1.03	1.05	n.d.	n.d.	n.d.	n.d.	n.d.	0.82	n.d.	n.d.	n.d.	n.d.	n.d.	1.60	1.55	0.82	1.04	0.99	n.d.
Gd	n.d.	3.15	n.d.	n.d.	5.07	n.d.	n.d.	5.27	4.29	n.d.	n.d.	n.d.	n.d.	n.d.	4.67	n.d.	n.d.	n.d.	n.d.	n.d.	5,00	4.48	2.59	6.23	3.18	n.d.
Tb	n.d.	n.d.	n.d.	n.d.	0.67	n.d.	n.d.	n.d.	n.d.	n.d.	n.d.	n.d.	n.d.	n.d.	n.d.	n.d.	n.d.	n.d.	n.d.	n.d.	n.d.	n.d.	n.d.	n.d.	n.d.	n.d.
Dy	n.d.	2.19	n.d.	n.d.	3.39	n.d.	n.d.	2.68	2.27	n.d.	n.d.	n.d.	n.d.	n.d.	1.84	n.d.	n.d.	n.d.	n.d.	n.d.	3.30	2.4	1.42	2.42	2.26	n.d.
Ho	n.d.	0.48	n.d.	n.d.	0.68	n.d.	n.d.	n.d.	n.d.	n.d.	n.d.	n.d.	n.d.	n.d.	n.d.	n.d.	n.d.	n.d.	n.d.	n.d.	n.d.	0.41	0.26	n.d.	n.d.	n.d.
Er	n.d.	1.21	n.d.	n.d.	1.51	n.d.	n.d.	1.55	1.19	n.d.	n.d.	n.d.	n.d.	n.d.	1.17	n.d.	n.d.	n.d.	n.d.	n.d.	1.80	0.84	0.72	1.42	1.30	n.d.
Tm	n.d.	n.d.	n.d.	n.d.	0.2	n.d.	n.d.	n.d.	n.d.	n.d.	n.d.	n.d.	n.d.	n.d.	n.d.	n.d.	n.d.	n.d.	n.d.	n.d.	n.d.	n.d.	n.d.	n.d.	n.d.	n.d.
Yb	n.d.	1.34	n.d.	n.d.	1.32	n.d.	n.d.	1.04	0.89	n.d.	n.d.	n.d.	n.d.	n.d.	0.83	n.d.	n.d.	n.d.	n.d.	n.d.	1.40	0.53	0.45	0.97	1.16	n.d.
Lu	n.d.	0.22	n.d.	n.d.	0.21	n.d.	n.d.	0.24	0.21	n.d.	n.d.	n.d.	n.d.	n.d.	0.16	n.d.	n.d.	n.d.	n.d.	n.d.	0.30	0.09	0.08	0.25	0.19	n.d.
ΣREE		138.57	n.d.	n.d.	180.3	n.d.	n.d.	107.98	126.82	n.d.	n.d.	n.d.	n.d.	n.d.	104.55	n.d.	n.d.	n.d.	n.d.	n.d.	124.7	253.79	105.96	124.86	118.13	n.d.
(La/Yb)n	n.d.	16.02	n.d.	n.d.	26.48	n.d.	n.d.	14.82	26.25	n.d.	n.d.	n.d.	n.d.	n.d.	22.50	n.d.	n.d.	n.d.	n.d.	n.d.	11.72	73.47	41.56	22.33	17.65	n.d.
(La/Sm)n	n.d.	5,00	n.d.	n.d.	5.37	n.d.	n.d.	3.2	4.63	n.d.	n.d.	n.d.	n.d.	n.d.	4.43	n.d.	n.d.	n.d.	n.d.	n.d.	2.59	4.22	4.14	4.19	4.58	n.d.
(Dy/Yb)n	n.d.	1.07	n.d.	n.d.	1.67	n.d.	n.d.	1.67	1.66	n.d.	n.d.	n.d.	n.d.	n.d.	1.44	n.d.	n.d.	n.d.	n.d.	n.d.	1.53	2.94	2.05	1.62	1.27	n.d.
Eu/Eu*	n.d.	0.87	n.d.	n.d.	0.84	n.d.	n.d.	0.65	0.71	n.d.	n.d.	n.d.	n.d.	n.d.	0.59	n.d.	n.d.	n.d.	n.d.	n.d.	0,90	0.69	0.76	0.58	0.83	n.d.
Rb/Sr	n.d.	0.23	n.d.	n.d.	0.16	n.d.	0.19	0,22	0,19	0.36	0.24	0.23	0.29	0.31	0.31	0.26	0.54	0.23	0.29	0.26	0,14	0.14	0,28	0.41	0.26	0.34
Sr/Ba	n.d.	0,58	n.d.	n.d.	0.84	n.d.	n.d.	0,56	0,46	n.d.	n.d.	n.d.	n.d.	n.d.	0.46	n.d.	n.d.	n.d.	n.d.	n.d.	0,65	0.49	0,50	0,33	0.48	0.44
K/Na	0.37	0.48	0.61	0.47	0.41	0.57	0.51	0.52	0.56	0.67	0.53	0.6	0.65	0.58	0.61	0.5	0.74	0.65	0.58	0.61	0.35	0.58	0.69	0.74	0.39	0.66
Mg#	0.45	0.56	0.56	0.47	0.52	0.53	0.49	0.51	0.5	0.45	0.42	0.46	0.46	0.43	0.46	0.44	0.45	0.45	0.45	0.45	0.55	0.53	0.62	0.49	0.53	0.46

Data source: (1) Althoff (1996), (2) Medeiros and Dall'Agnol (1988), (3) Leite (2001), (4) Dall'Agnol et al. (1999a, 1999b), (5) Dall Agnol (unpublished data). Chemical ratios: Mg# molecular ratio Mg/(Mg + Fe); K/Na molecular ratio. n.d. = not determined; * = Fe_2O_3 as total; Eu/Eu* = EuN/[0.5 * (SmN + GdN)]; E = epidote; B = biotite; A = amphibole; Qz = quartz; GD = granodiorite; D = diorite.

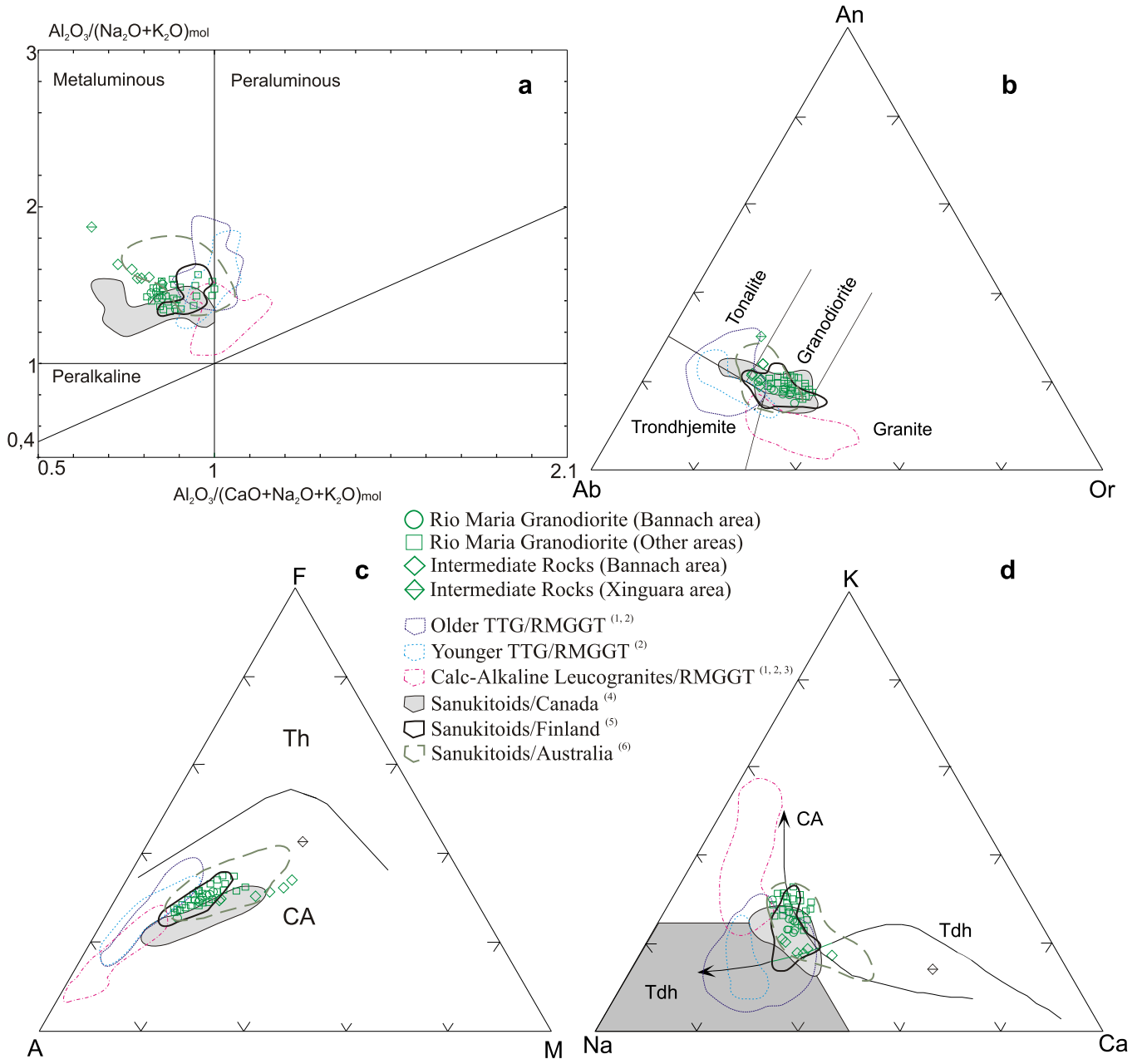

Fig. 5. Diagrams showing the distribution of samples of the Rio Maria Granodiorite and associated rocks and shields for rocks of Archean TTGs and Leucogranites of Rio Maria Granite-Greenstone Terrane (RMGGT) ([1]Althoff, 1996; [2]Leite, 2001; [3]Duarte, 1992) and sanukitoids of Superior Province of Canada ([4]Stern and Hanson, 1991), Karelian craton ([5]Halla, 2005) and Pilbara craton of Australia ([6]Smithies and Champion, 2000). (a) Rio Maria Granodiorite and associated rocks plot in the metaluminous field of the [Al_2O_3/($CaO + Na_2O + K_2O$)]mol vs. [Al_2O_3/($K_2O + Na_2O$)]mol diagram (Shand, 1950). (b) Ab–An–Or-normative diagram. Fields from Barker (1979). (c) AFM diagram (Irvine and Baragar, 1971). CA = calc-alkaline, Th = tholeiitic. (d) K–Na–Ca plots. Trends for calc-alkaline (CA) and trondhjemite (Tdh) series as defined by Nockolds and Allen (1953) and Barker and Arth (1976).

the granodiorites is observed. In the AFM diagram (Fig. 5c), all samples plot in the calc-alkaline field, showing increase of alkalis and decrease of MgO and FeO_t from the intermediate rocks to the granodiorites. A possible affinity of the studied rocks with the calc-alkaline series is also suggested by the K–Na–Ca diagram (Fig. 5d). In fact the AFM and K–Na–Ca diagrams only demonstrate that the studied rocks do not have the geochemical characteristics of tholeiitic or TTG series.

Cr and Ni contents (Table 3) are high in the granodiorite and intermediate rocks, and decrease markedly from the latter to the granodiorite (Fig. 6a and b). Both elements display similar behavior, consistent with the observed Mg# variation, with a compositional gap between the intermediate rocks and granodiorite. A similar compositional gap is also shown by Zr, Rb/Sr, and Sr/Ba in Harker diagrams (Fig. 6d–f), suggesting that the intermediate rocks follow a differentiation trend distinct from that of the granodiorite. Zr and Rb/Sr increase and Sr/Ba decreases parallel to SiO_2 increase, indicating the more evolved character of the granodiorite compared to the intermediate rocks.

Light rare earth elements (LREEs) and ∑REE are higher in the granodiorite compared to the intermediate rocks (Table 3). The patterns of rare earth elements of the granodiorite and intermediate rocks from the Bannach area are similar (Fig. 7), with weak or no Eu anomaly ($0.94 < Eu/Eu^* < 1.03$), pronounced enrichment in

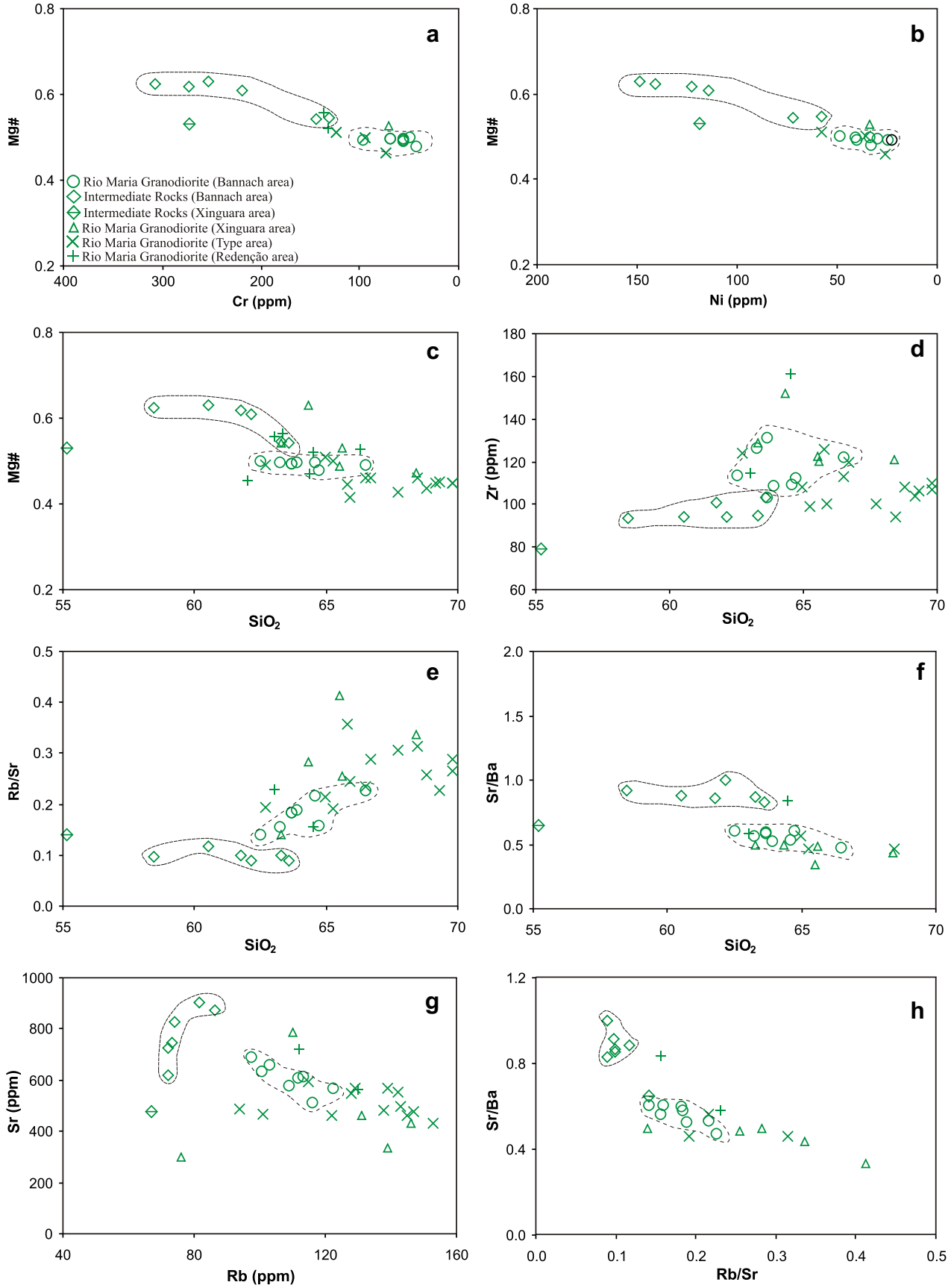

Fig. 6. (a) Mg# vs. Cr; (b) Mg# vs. Ni; (c, d, e, f) Harker diagrams; (g) Sr vs. Rb; (h) Sr/Ba vs. Rb/Sr diagrams comparing Rio Maria Granodiorite and associated rocks from Bannach and other areas.

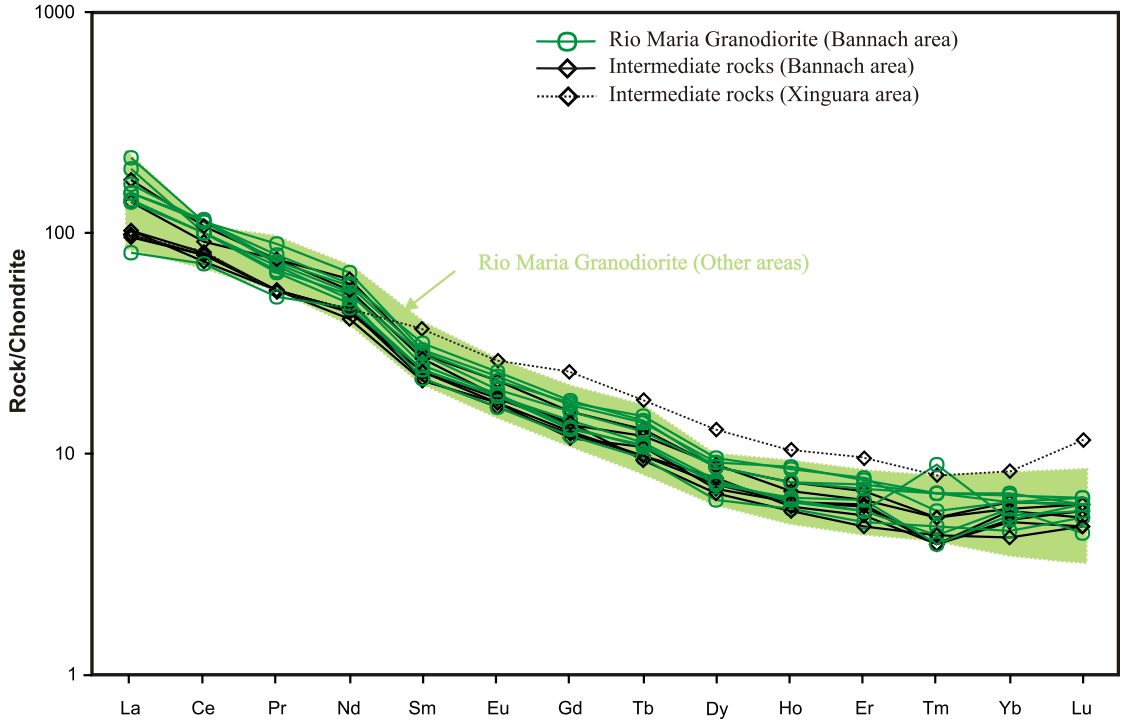

Fig. 7. Chondrite-normalized REE patterns for the Rio Maria Granodiorite and associated intermediate rocks of Rio Maria Granite-Greenstone Terrane (normalization values from Evensen et al. (1978)).

LREE and strong to moderate fractionation of heavy rare earth elements (HREE; $La/Yb_n = 15.52–44.38$). $(La/Yb)_n$ ratios are slightly lower in the intermediate rocks ($average_{La/Yb_n} = 23.34$), compared to the granodiorites ($average_{La/Yb_n} = 28.02$). Fractionation of amphibole, pyroxene and garnet could possibly explain the impoverishment in HREE. However, the absence of any petrographic evidence of crystallization of garnet or of its retention in the residue and the rare occurrence of clinopyroxene in the studied rocks, together with the constant and prominent presence of hornblende, indicate that the fractionation of the latter was probably dominant.

The compositions of the Rio Maria Granodiorite samples from other areas of the Rio Maria Granite-Greenstone Terrane (Table 4) are similar in their major characteristics to those obtained in the Bannach area. A/CNK, AFM, An–Ab–Or, and K–Na–Ca plots (Fig. 5) demonstrate that the Rio Maria Granodiorite samples from different areas are mostly superposed in those plots with the samples from Bannach. However, a closer examination of the available data indicates some significant contrasts between granodiorites from different areas. The Rio Maria Granodiorite from the type-area and those from Bannach follow similar trends in different geochemical plots (Fig. 6). However, the former tends to show higher silica and Rb/Sr together with lower Mg# and Sr compared to Bannach. This evidence and the fact that both areas are in physical continuity suggest that there is a general magmatic differentiation trend from Bannach to some domains of the Rio Maria Granodiorite in the type-area containing the more evolved rocks of the series. The rocks from Redenção and Xinguara areas tend to show higher Mg#, Zr, Rb/Sr values for similar SiO_2 contents compared to Bannach (Fig. 6). Sr and Sr/Ba are lower in the samples of Xinguara area (Fig. 6f and g), and the Sr/Ba vs. Rb/Sr plot (Fig. 6h) shows a clear discrimination between samples from Xinguara and Bannach.

A quartz diorite with a high modal content of mafic minerals from the Xinguara area (Dall'Agnol et al., 1999a,b) is the only analyzed sample of intermediate rock out of the Bannach area. It has the lowest silica content of all analyzed samples, but its Mg#, Sr/Ba, Sr, Cr and Ni are lower, and Rb/Sr is higher than those shown by the intermediate rocks from Bannach (Table 4).

Geochemical data (Tables 3 and 4; Figs. 5 and 6) put in evidence that the Rio Maria Granodiorite and associated rocks from different areas of the Rio Maria Granite-Greenstone Terrane have similar general characteristics and are consistent with their affiliation with the same magmatic series of rocks. On the other hand, the significant differences observed between rocks of distinct areas indicate that these rocks derived from magmas were cogenetic but certainly not identical.

3.4. Nd and Pb isotope data

Available Nd isotope data (Dall'Agnol et al., 2006; Leite, 2001; Souza et al., 2001; Ramö et al., 2002) on the Rio Maria Granodiorite and associated rocks demonstrate that these rocks show quite uniform positive ε_{Nd} values, varying from 0.2 to 1.2 and depleted-mantle ($T_{DM;}$ DePaolo, 1981) ages ranging from 2.92 to 3.01 Ga, just a little older than their crystallization age of 2.87 Ga. In a ε_{Nd} vs. age diagram, these Archean granitoids plot near and a little below the depleted-mantle evolution curve. These data are not conclusive, but associated with additional information on other Archean units of the RMGGT, they have been interpreted as indicating that it differentiated from the mantle c. 3.0 to 2.9 b. y. ago (Macambira and Lancelot, 1996; Souza et al., 2001; Ramö et al., 2002; Dall'Agnol et al., 2006).

Pb isotope data on representative alkali-feldspar fractions from two samples of the Rio Maria Granodiorite and associated quartz diorite ($\mu 2 \sim 12$; R. Dall'Agnol, unpublished data) indicate a very radiogenic lead signature for the Rio Maria rocks. The Pb isotope data are extremely limited but suggest a contribution of crustal components, possibly including subducted sediments in the evolution of the studied rocks.

4. Discussion

4.1. Characterization of the magmatic series

The Rio Maria Granodiorite and associated intermediate rocks display all the typical petrographic and geochemical characteristics of sanukitoid rocks (Stern et al., 1989; Stern and Hanson, 1991; Smithies and Champion, 2000; Moyen et al., 2003; Halla, 2005): (1) They are composed of metaluminous intermediate to acid igneous rocks (Fig. 5a; Tables 3 and 4) with granodiorite, generally including mafic enclaves or clusters, as dominant granitoid rocks (Fig. 2b and c). (2) They have high-Mg#, Cr, and Ni conjugate with high contents of large ion lithophile elements (LILEs), specially Ba and Sr. (3) Moderate contents of K_2O, reflected in K/Na varying from 0.35 to 0.74. (4) Relatively high content of LREE and strong fractionation of HREE, associated with small or absent Eu anomaly (Fig. 7).

In selected diagrams (Figs. 5 and 8), the studied rocks are compared with classical sanukitoid series of different Archean cratons (Superior Province of Canada, Stern and Hanson, 1991; Pilbara craton of Australia, Smithies and Champion, 2000; Karelian craton, Halla, 2005). The A/CNK, normative An–Ab–Or, AFM, and K–Na–Ca plots (Fig. 5) indicate that the geochemical characteristics of the Rio Maria Granodiorite and associated rocks are largely coincident with those of the Archean sanukitoid series selected for comparison. The A/CNK vs. K/Na or Mg#, Mg# vs. K/Na and TiO_2 vs. K/Na diagrams, employed by Moyen et al. (2003) to compare different series of Archean granitoids, also illustrate the geochemical similarities between the studied rocks and sanukitoid series of other Archean cratons (Fig. 8). The Rio Maria Granodiorite and associated rocks are disposed in all diagrams in the fields defined for sanukitoid series. This demonstrates the coincidence in Mg#, A/CNK, K/Na, and TiO_2 values of the former with the mentioned series, and is a strong indicative of a similar origin for this series of rocks.

The older and younger Archean tonalite-trondhjemite-granodiorite series (TTGs) and the potassic calc-alkaline leucogranites of Rio Maria are also plotted in the selected diagrams (Figs. 5 and 8). Althoff et al. (2000), Leite (2001) and Dall'Agnol et al. (2006) had stressed the geochemical contrast between the Rio Maria Granodiorite and the TTG suites of the RMGGT and emphasized that the former should correspond to sanukitoid rocks. In the selected plots (Figs. 5 and 8), the contrast in composition between the Rio Maria Granodiorite and associated rocks, on one hand, and the TTGs and leucogranites, on the other hand, is remarkable, demonstrating that the former are geochemically distinct from the latter series of rocks.

The available geochemical data on the Rio Maria Granodiorite and associated rocks demonstrate conclusively that these rocks appertain to the sanukitoid series, and are geochemically distinct of the TTGs and leucogranites of the Rio Maria Granite-Greenstone Terrane and by analogy also of other TTGs and leucogranites of Archean terranes.

4.2. Geochemical and magmatic evolution of the sanukitoid series of Rio Maria

SiO_2 contents of intermediate rocks and Rio Maria Granodiorite (Tables 3 and 4) are partially superposed, suggesting the possibility of the derivation of the latter from the intermediate magma by

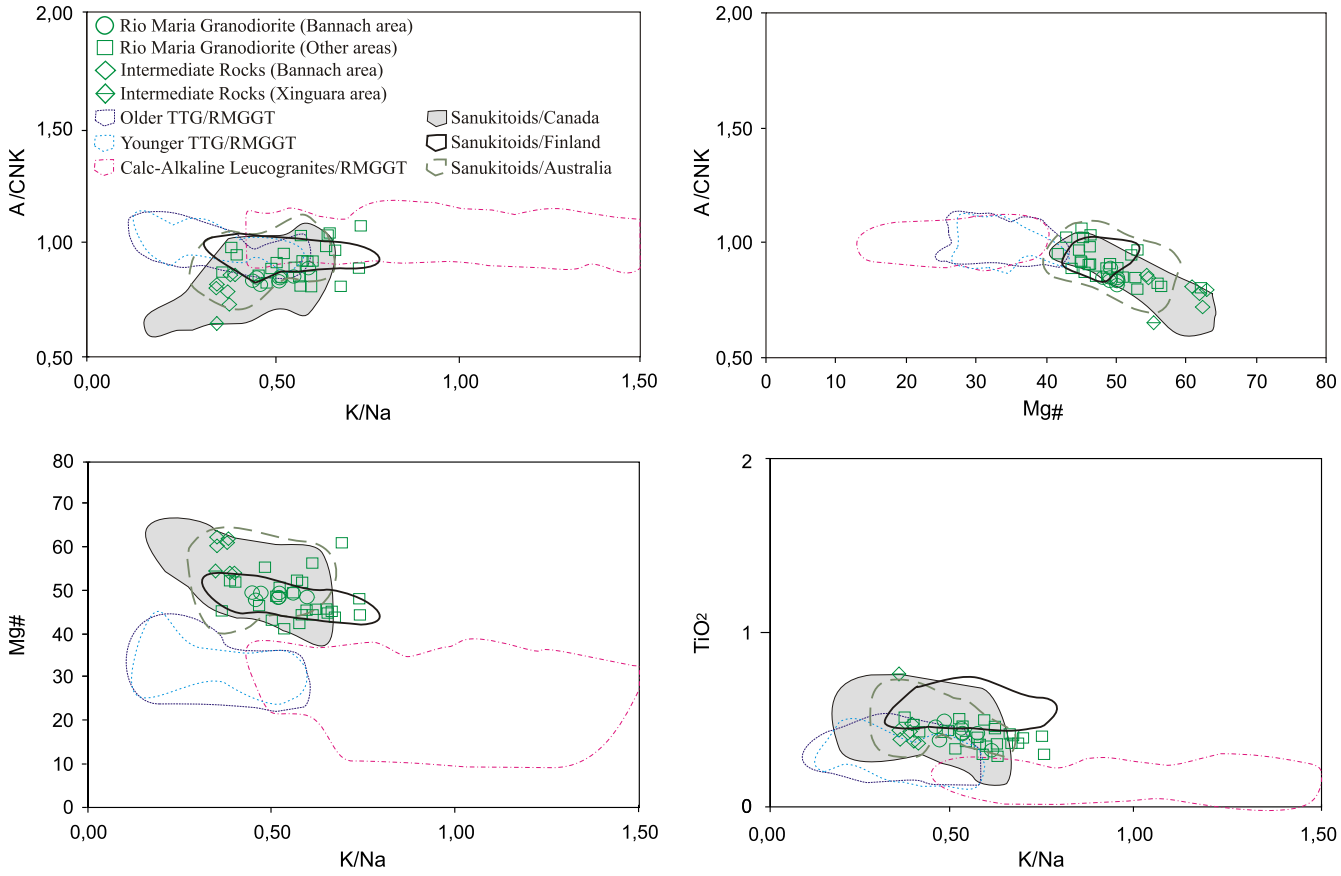

Fig. 8. Binary diagrams with major element and major element ratio for over 200 analysis of Late Archean granitoids of the Rio Maria Granite-Greenstone Terrane (RMGGT); 25 analysis of Canadian sanukitoid (Stern and Hanson, 1991); 11 analyses of sanukitoid of the Baltic Shield (Halla, 2005) and 27 analysis of sanukitoid of the Pilbara craton (Smithies and Champion, 2000). Mg# molecular ratio Mg/(Mg + Fe); A/CNK molecular ratio Al/(Ca+Na+K); K/Na molecular ratio. Same symbols and data source as Fig. 5.

fractional crystallization processes. However, the bulk of geochemical data, particularly the contrast in Mg#, Zr, Rb/Sr, Sr, Sr/Ba, in both groups of rocks (Fig. 6c–g), indicate that they follow two distinct trends. In the same way, the strong similarity of REE patterns of the intermediate rocks and the Rio Maria Granodiorite (Fig. 7) does not favor the hypothesis that they were linked by fractional crystallization. On the other hand, the strong mineralogical and textural similarities shown by intermediate rocks and the granodiorite, together with the fact that all these rocks appertain to the same magmatic series, point to a cogenetic origin for the studied sanukitoid rocks of Rio Maria.

Taking into account the large areas of exposure of the Rio Maria Granodiorite and associated rocks in the Rio Maria terrane, the derivation of the sanukitoid rocks of different areas from a unique magma looks improbable. Effectively, the available geochemical data suggest significant differences between assemblages from different areas (Bannach and type-area vs. Redenção and Xinguara; cf. Fig. 6). The data on the Bannach and type-area cover all the series and indicate that the intermediate rocks and the granodiorite from Rio Maria derived from two different cogenetic magmas. The granodioritic magma possibly mingled with the intermediate or similar mafic magmas to explain the constant occurrence of mafic enclaves in the granodiorite. The granodioritic magma evolved through fractional crystallization forming subordinate rocks relatively enriched in silica in the type-area. The small but significant differences in composition shown by the granodiorites of Bannach + type-area vs. those of Redenção and Xinguara areas (Fig. 6) suggest that the granodiorites from different areas are also cogenetic but not comagmatic.

A possible explanation for the contrast between intermediate rocks and granodiorites would be the origin of their magmas from different degrees of melting of a similar source. The small contrasts between the granodiorites of different areas could be due to differences in the source rocks, in particular the degree of metasomatism in a possible modified mantle source (Stern et al., 1989; Stevenson et al., 1999; Smithies and Champion, 2000; Moyen et al., 2001; Halla, 2005; Kovalenko et al., 2005).

4.3. The significance of amphibole and epidote in the Rio Maria Granodiorite

Amphibole is the main mafic mineral in all studied rocks, independent of their intermediate or acid composition. It occurs also as centimetric cumulate crystals in the layered mafic rocks associated with the Rio Maria Granodiorite (Oliveira, 2005; Dall'Agnol et al., 2006). The euhedral to subeuhedral shape of amphibole crystals and their textural relationships with plagioclase are strong evidence of its early crystallization in the magma. According to several experimental studies on granitic systems (Naney and Swanson, 1980; Naney, 1983; Wyllie, 1984; Dall'Agnol et al., 1999b; Klimm et al., 2003), hornblende could only crystallize in liquids containing appreciable contents of water (>4 wt.% of water). Admitting that this experimental evidence could be extrapolated to the Rio Maria granodiorite magma, it would imply that it was relatively enriched in water. The high water content should have inhibited orthopyroxene and clinopyroxene crystallization and favored the presence of amphibole as a liquidus or near-liquidus phase. Evidence favoring this hypothesis is given by experiments at 800 MPa on synthetic granodiorite at variable water contents (Naney, 1983). In those conditions, clinopyroxene did not crystallize from the liquid, orthopyroxene was stable only at high-temperatures (>850 °C) and for water contents lower than 4 wt.%, and amphibole was the liquidus phase for higher water contents. Pressure should also play a role, inhibiting clinopyroxene crystallization. This is indicated by experimental studies in a water-saturated granodiorite system, showing that clinopyroxene was stable only at a pressures higher than 1600 MPa (Schmidt and Thompson, 1996).

The distinction between magmatic and secondary epidote is based on textural evidence (Zen and Hammarstrom 1984) and chemical criteria, mostly the pistacite content of epidote (Tulloch, 1979; cf. Sial et al., 1999). In the Rio Maria Granodiorite textural features point to a magmatic origin for epidote. Preliminary chemical data (M.A. Oliveira, unpublished data) indicate that the values of pistacite component in epidote (28 to 33 mol%) are also consistent with a magmatic origin. According to Whitney (1975), Johnston and Wyllie (1988), Zen and Hammarstrom (1984) and Schmidt and Thompson (1996), the crystallization of epidote in magmas depends on temperature, pressure and fO_2. At magmatic temperatures, epidote crystallization occurs generally approaching the solidus and is favored by oxidizing conditions (in between FMQ and HM; cf. Sial et al., 1999). Magmatic epidote is stable at pressures higher than 600–800 MPa, corresponding to lower crust conditions, showing a tendency to dissolution at pressures of 450 MPa (Brandon et al., 1996). This is consistent with the absence of epidote in low pressure experiments in granodioritic systems (e.g., at 200 MPa, Naney, 1983). For intensely oxidizing conditions, near the hematite-magnetite buffer, the magmatic stability field of epidote is enlarged down to a pressure of ~300 MPa (Schmidt and Thompson, 1996). On the other hand, the preservation of magmatic epidote depends largely on magma transport rate, being favored by rapid ascent of the magma, followed by fast crystallization that could inhibit re-equilibrium of epidote at low pressure.

Magmatic epidote present in the Rio Maria Granodiorite could possibly result from a peritectic reaction involving amphibole + plagioclase + liquid giving epidote + biotite (cf. Schmidt and Thompson, 1996; Sial et al., 1999). This is suggested by the regular contacts between epidote and biotite, indicating that they are in equilibrium. The assemblage with amphibole and epidote indicates a relatively water-rich magma, crystallizing at oxidizing conditions for the Rio Maria Granodiorite. The hypothesis of high water content in the magma is also favored by the widespread pervasive subsolidus alteration that affected this rock, responsible for the saussuritization of its plagioclase and other associated reactions.

5. Summary and conclusions

Large occurrences of Archean sanukitoid rocks were identified in the Rio Maria Granite-Greenstone Terrane in the southeastern Amazonian craton. The dominant rocks are attributed to the Rio Maria Granodiorite, but significant exposures of associated intermediate rocks have been recently identified. These rocks have all mineralogical and geochemical characteristics of typical sanukitoid rocks from different Archean cratons. They differ in these same aspects from the TTGs and potassic leucogranites found in the Rio Maria Granite-Greenstone Terrane. It is concluded that the Rio Maria Granodiorite and associated intermediate rocks correspond to an expanded sanukitoid series formed at 2.87 Ga, as indicated by geochronological data (Macambira, 1992; Pimentel and Machado, 1994; Dall'Agnol et al., 1999a; Rolando and Macambira, 2002, 2003).

The Rio Maria Granodiorite and associated rocks of the Rio Maria terrane are cogenetic but not comagmatic. The intermediate rocks and the granodiorite of the Bannach area are not linked by fractional crystallization processes, and it is assumed that they derived from two distinct magmas, both with sanukitoid affinity, possibly originated from different degrees of melting a modified mantle source. There are also significant geochemical contrasts between the occurrences of Rio Maria Granodiorite in different

areas, suggesting that this unit corresponds in fact to a granodiorite suite of rocks derived from similar but distinct magmas. Mingling processes involving the Rio Maria Granodiorite magma and similar mafic to intermediate magmas are able to explain the common occurrence of mafic enclaves in the granodiorite.

Amphibole is the main mafic mineral in all studied sanukitoid rocks. It is an early crystallized phase, probably initiating its separation from the magma at or near the liquidus. This feature, associated with experimental evidence, suggests that the Rio Maria granodiorite magma was relatively water-enriched (>4 wt.%), explaining the presence of hornblende at the liquidus and the absence of clinopyroxene and orthopyroxene in these rocks.

Textural features and preliminary chemical data point to a magmatic origin for the epidote of the Rio Maria Granodiorite. The crystallization of epidote indicates relatively high pressures (>600–800 MPa) and oxidizing conditions for the magma, and reinforces the hypothesis of significant water contents in it. Epidote should crystallize at relatively low magmatic temperatures, approaching the solidus. It could result from a peritetic reaction involving liquid + amphibole + plagioclase forming epidote + biotite. Assuming that the Rio Maria Granodiorite was emplaced at shallow crustal levels (Souza, 1994), the well-preserved state of epidote crystals points to a rapid ascent of the Rio Maria Granodiorite magma.

Acknowledgements

J.A.C. Almeida, D.C. Oliveira, C.N. Lamarão, F.G.C. Nascimento, S.B. Dias and F.V. Guimarães are acknowledged for support in geological mapping and mineralogical and petrographical work. N.V. Siqueira contributed in the FeO chemical analyses. This research received financial support from CNPq (Roberto Dall'Agnol – PRONEX Grants 66.2103/1998, 0550739/2001-7, 476075/2003-3, 307469/2003-4; Marcelo Augusto de Oliveira – master and doctor scholarship), and Federal University of Pará (UFPA). Thorough and constructive reviews were provided by Jean-François Moyen and two anonymous reviewers.

Appendix A. Analytical methods

Chemical analyses of samples of the Bannach area were done at ACME-Lab laboratories. Major, minor and trace elements were analyzed by X-ray fluorescence, whereas REE analyses were done by ICP-MS (Inductively coupled plasma–mass spectrometry). Chemical analyses of samples of the Redenção area were done at the Centre de Recherches Petrographiques et Geochimiques (CRPG-CNRS, France); all elements were analyzed using inductively coupled plasma (ICP) atomic emission spectrometry, with two multielement spectrometers and one sequential spectrometer. All chemical analyses were done after a preliminary lithium metaborate fusion of the samples, followed by appropriate acid dissolution.

Chemical analyses of samples of the Xinguara area were done at GEOSOL laboratories. The major, minor and trace elements were analyzed by X-ray fluorescence, whereas the REE analyses were done by ICP. The chemical analyses of type-area (Rio Maria area) performed at the Geosciences Centre of the Federal University of Pará, SiO, TiO, Al_2O_3, total Fe_2O_3, CaO, K_2O, P_2O_5, Rb, Sr, Zr, Y, and Nb were analyzed by X-ray fluorescence; Na_2O, MgO and MnO were analyzed by atomic absorption and FeO by wet chemistry. The REE analyses were done at the CRPG-CNRS (France) by ICP-MS.

The geochronologic data of the Rio Maria area were obtained by U–Pb on zircon and titanite. The data of the Xinguara and Serra do Inajá areas were obtained in the Pará Isotope Laboratory (Pará-Iso) by the Pb evaporation method on zircon, as described by Gaudette et al. (1998).

References

Althoff, F.J., 1996. Étude pétrologique et structurale des granitoïdes de Marajoara (Pará, Brésil): leur rôle dans l'évolution archéenne du craton Amazonien (2.7–3.2 Ga). Doctoral Thesis. Université Henri Poincaré, Nancy I, France, 296p. (in French).

Althoff, F.J., Barbey, P., Boullier, A.M., 2000. 2.8–3.0 Ga plutonism and deformation in the SE Amazonian craton: the Archean granitoids of Marajoara (Carajás Mineral province, Brazil). Precambrian Research 104, 187–206.

Avelar, V.G. 1996. Geocronologia Pb–Pb por evaporação em monocristal de zircão, do magmatismo da região de Tucumã, SE do Estado do Pará, Amazônia Oriental. Belém, Centro de Geociências, M.Sc. Thesis. Universidade Federal do Pará. CG, 199p. (in Portuguese).

Bagai, Z., Armstrong, R., Kampunzu, A.B., 2002. U–Pb single zircon geochronology of granitoids in the Vamba granite-greenstone terrane (NE Botswana): implications for the evolution of the Archaean Zimbabwe craton. Precambrian Research 118, 149–168.

Barker, F., 1979. Trondhjemites: definition, environment and hypotheses of origin. In: Barker, F. (Ed.), Trondhjemites, dacites and related rocks. Elsevier, Amsterdam, pp. 1–12.

Barker, F., Arth, J.G., 1976. Generation of trondhjemitic-tonalitic liquids and Archaean bimodal trondhjemite-basalt suites. Geology 4, 596–600.

Barros, E.M., Sardinha, A.S., Barbosa, J.P.O., Krimski, R., Macambira, M.J.B., 2001. Pb–Pb and U–Pb zircon ages of Archean syntectonic granites of the Carajás Metallogenic Province, northern Brazil. In: Simposio Sudamericano de Geologia Isotopica, 3. Pucon, Chile. Sociedade Geologica de Chile (CD ROM).

Bibikova, E.V. et al., 2005. The temporal evolution of sanukitóides in the Karelian craton, Baltic shield: an ion microprobe U–Th–Pb isotopic study of zircons. Lithos 79, 129–145.

Brandon, A.D., Creaser, R.A., Chacko, T., 1996. Constraints on rates of granitic magma transport from epidote dissolution kinetics. Science 271, 1845–1848.

Chekulaev, V.P., 1999. Archean sanukitoids of the Baltic shield. Dokl. RAS 368, 676–678 (translated in English).

Condie, K.C., 1981. Archaean Greenstone Belts. Elsevier, Amsterdam. 434p.

Costa, J.B.S., Araújo, O.J.B., Santos, A., Jorge João, X.S., Macambira, M.J.B., Lafon, J.M., 1995. A Província Mineral de Carajás: Aspectos Tectono-Estruturais, Estratigráficos e Geocronológicos. Boletim do Museu Paraense Emílio Goeldi, Série Ciências da Terra 7, 199–235.

Dall'Agnol, R., Oliveira, D.C., 2007. Oxidized, magnetite-series, rapakivi-type granites of Carajás, Brazil: implications for classification and petrogenesis of A-type granites. Lithos 93, 215–233.

Dall'Agnol, R., Ramö, O.T., Magalhães, M.S., Macambira, M.J.B., 1999a. Petrology of the anorogenic, oxidised Jamon and Musa granites, Amazonian Craton: implications for the genesis of Proterozoic, A-type Granites. Lithos 46, 431–462.

Dall'Agnol, R., Scaillet, B., Pichavant, M., 1999b. Evolution of A-type granite magmas: an experimental study of the Lower Proterozoic Jamon Granite, eastern Amazonian craton, Brazil. Journal of Petrology 40 (11), 1673–1698.

Dall'Agnol, R., Teixeira, N.P., Ramö, O.T., Moura, C.A.V., Macambira, M.J.B., Oliveira, D.C., 2005. Petrogenesis of the Paleoproterozoic rapakivi A-type granites of the Archean Carajás metallogenic province, Brazil. Lithos 80, 101–129.

Dall'Agnol, R., Oliveira, M.A., Almeida, J.A.C., Althoff, F.J., Leite, A.A.S., Oliveira, D.C., Barros, C.E.M., 2006. Archean and Paleoproterozoic granitoids of the Carajás metallogenetic province, eastern Amazonian craton. In: Dall'Agnol, R., Rosa-Costa, L.T., Klein, E.L. (Eds.), Symposium on Magmatism, Crustal Evolution, and Metallogenesis of the Amazonian Craton. Abstracts Volume and Field Trips Guide. Belém, PRONEX-UFPA/SBG-NO, pp. 99–150.

DePaolo, D.J., 1981. Neodymium isotopes in the Colorado Front Range and crust–mantle evolution in the Proterozoic. Nature 291, 193–196.

Docegeo, 1988. Revisão litoestratigráfica da Província Mineral de Carajás. In: Congresso Brasileiro de Geologia, 35, Belém. Anais do Congresso Brasileiro de Geologia, Belém, SBG, pp. 11–54.

Duarte, K.D., 1992. Geologia e geoquímica do Granito Mata Surrão (SW de Rio Maria – Pa): um exemplo de granito "stricto sensu" Arqueano. Belém, Centro de Geociências, Universidade Federal do Pará. M.Sc. Thesis. Programa de Pós-Graduação em Geologia e Geoquímica, Centro de Geociências, UFPA, 217p. (in Portuguese).

Evensen, N.M., Hamilton, P.T., O'Nions, R.K., 1978. Rare earth abundances in chondritic meteorites. Geochemical of Cosmochemical Acta 39, 55–64.

Gaudette, H.E., Lafon, J.M., Macambira, M.J.B., Moura, C.A.V., Scheller, T., 1998. Comparasion of single filament Pb evaporation/ionization zircon ages with conventional U–Pb results: exemples from Precambrian of Brazil. Journal of South American Earth Sciences 11, 351–363.

Halla, J., 2005. Late Archean high-Mg granitoids (sanukitoids) in the southern Karelian domain, eastern Finland: Pb and Nd isotopic constraints on crust–_mantle interactions. Lithos 79, 161–178.

Irvine, T.N., Baragar, W.R.A., 1971. A guide to the chemical classification of the common volcanic rocks. Canadian Journal of the Earth Science 8, 523–547.

Johnston, A.D., Wyllie, P.J., 1988. Constraints on the origin of Archean trondhjemites based on phase relationships of Nuk Gneiss with H_2O at 15 kbar. Contributions Minerals Petrology 100, 35–46.

Kampunzu, A.B., Tombale, A.R., Zhai, M., Bagai, Z., Majaule, T., Modisi, M.P., 2003. Major and trace element geochemistry of plutonic rocks from Francistown, NE Botswana: evidence for a Neoarchaean continental active margin in the Zimbabwe craton. Lithos 71, 431–460.

Klimm, K., Holtz, F., Johannes, W., King, P.L., 2003. Fractionation of metaluminous A-type granites: an experimental study of the Wangrah Suite, Lachlan Fold Belt, Australia. Precambrian Research 124, 327–341.

Kovalenko, A.V., Clemens, J.D., Savatenkov, V.M., 2005. Petrogenetic constraints for the genesis of Archaean sanukitoid suites: geochemistry and isotopic evidence from Karelia, Baltic Shield. Lithos 79, 147–160.

Leite, A.A.S., 2001. Geoquímica, petrogênese e evolução estrutural dos granitóides arqueanos da região de Xinguara, SE do Cráton Amazônico. Belém, Universidade Federal do Pará, Centro de Geociências. Doctoral Thesis. Programa de Pós-Graduação em Geologia e Geoquímica, Centro de Geociências, UFPA, 130p. (in Portuguese).

Leite, A.A.S., Dall'Agnol, R., Macambira, M.J.B., Althoff, F.J., 2004. Geologia e geocronologia dos granitóides arqueanos da região de Xinguara (PA) e suas implicações na evolução do Terreno Granito-Greenstone de Rio Maria. Revista Brasileira de Geociências. 34, 447–458.

Lobach-Zhuchenko, S.B., Chekulaev, V.P., Ivanikov, V.V., Kovalenko, A.V., Bogomolov, E.S., 2000a. Late Archaean high-Mg and subalkaline granitoids and lamprophyres indicators of gold mineralization in Karelia (Baltic shield), Russia. In: Kremenetsky, A.A., Lehman, B., Seltman, R. (Eds.), Ore-Bearing Granites of Russia and Adjacent Countries. IMGRE, Moscow, pp. 193–211.

Lobach-Zhuchenko, S.B., Chekulaev, V.P., Arestova, N.A., Levskii, L.K., Kovalenko, A.V., 2000b. Archean Terranes in Karelia: geological and isotopic-geochemical evidence. Geotectonics 34, 452–466.

Lobach-Zhuchenko, S.B., Rollinson, H., Chekulaev, V.P., Arestova, N.A., Kovalenko, A.V., Ivanikov, V.V., Guseva, N.S., Sergeev, S.A., Matukov, D.I., Jarvis, K.E., 2005. The Archaean sanukitoid series of the Baltic shield—geological setting, geochemical characteristics and implications for their origin. Lithos 79, 107–128.

Macambira, M.J.B., 1992. Chronologie U/Pb, Rb/Sr, K/Ar et croissance de la croûte continentale dans L'Amazonie du sud-est; exemple de la région de Rio Maria, Province de Carajas, Brésil. Doctoral Thesis. Montpellier, Université Montpellier II-France. 212p. (in French).

Macambira, M.J.B., Lafon, J.M., 1995. Geocronologia da Província Mineral de Carajás; Síntese dos dados e novos desafios. Boletim do Museu Paraense Emílio Goeldi, série Ciências da Terra, Belém (7), 263–287.

Macambira, M.J.B., Lancelot, J., 1996. Time constraints for the formation of the Archean Rio Maria crust, southeastern Amazonian Craton, Brazil. International Geology Review 38 (12), 1134–1142.

Machado, N., Lindenmayer, Z.G., Krogh, T.E., Lindenmayer, D., 1991. U–Pb geochronology of Archean magmatism and basement reactivation in the Carajás area, Amazon shield, Brazil. Precambrian Research 49, 329–354.

Martin, H., 1999. The adakitic magmas: modern analogues of Archaean granitoids. Lithos 46 (3), 411–429.

Medeiros, H., 1987. Petrologia da porção leste do maciço granodiorítico Rio Maria, Sudeste do Pará. M.Sc. Thesis. Programa de Pós-Graduação em Geologia e Geoquímica, Centro de Geociências, UFPA, 166p. (in Portuguese).

Medeiros, H., Dall'Agnol, R., 1988. Petrologia da porção leste do Batólito Granodiorítico Rio Maria, sudeste do Pará. In: Congresso Brasileiro de Geologia, 35, Belém. Anais de Congresso Brasileiro de Geologia. SBG. v 3, pp. 1488–1499.

Moyen, J.-F., Martin, H., Jayananda, M., 2001. Multi-element geochemical modelling of crust–mantle interactions during late- Archaean crustal growth: the Closepet granite (South India). Precambrian Research 112, 87–105.

Moyen, J.F., Martin, H., Jayananda, M., Auvray, B., 2003. Late-Archaean granites: a typology based on the Dharwar Craton (India). Precambrian Research 2375, 1–21.

Naney, M.T., 1983. Phase equilibria of rock-forming ferromagnesian silicates in granitic systems. American Journal of Science 283, 993–1033.

Naney, M.T., Swanson, S.E., 1980. The effect of Fe and Mg on crystallization in granitic systems. American Mineralogist 65, 639–653.

Nockolds, S.R., Allen, R., 1953. The geochemistry of some igneous rocks series. Geochimica et Cosmochimica Acta 4, 105–142.

Oliveira, M.A., 2005. Geologia, Petrografia e Geoquímica do Granodiorito Sanukitóide Arqueano Rio Maria e Rochas Máficas Associadas, Leste de Bannach-PA. Universidade Federal do Pará. M.Sc. Thesis. Programa de Pós-Graduação em Geologia e Geoquímica, Centro de Geociências, UFPA, 141p. (in Portuguese).

Oliveira, M.A., Dall'Agnol, R., Althoff, F.J., 2006a. Petrografia e Geoquímica do Granodiorito Rio Maria da região de Bannach e comparações com as demais ocorrências no terreno Granito-*Greenstone* de Rio Maria-Pará. Revista Brasileira de Geociências 36 (2), 313–326.

Oliveira, M.A., Dall'Agnol, R., Almeida, J.A.C., Althoff, F.J., Borges, R.M.K., 2006b. Relatório de Mapeamento Geológico na escala 1:100.000 da Folha Marajoara (SB-22-Z-C V). Programa GeoBrasil, CPRM – Serviço Geológico do Brasil, 147p.

Pimentel, M.M., Machado, N., 1994. Geocronologia U-Pb dos Terrenos granito-greenstone de Rio Maria, Pará. In: Congresso Brasileiro de Geologia, 38. Camboriú, 1988. Boletim de Resumos Expandidos. Camboriú, SBG, pp. 390–391.

Ramö, O.T., Dall'Agnol, R., Macambira, M.J.B., Leite, A.A.S., de Oliveira, D.C., 2002. 1.88 Ga oxidized A-type granites of the Rio Maria region, eastern Amazonian craton, Brazil: positively anorogenic! Journal of Geology 110, 603–610.

Rapp, R.P., Shimizu, N., Norman, M.D., Applegate, G.S., 1999. Reaction between slab-derived melts and peridotite in the mantle wedge: experimental constraints at 3.8 GPa. Chemical Geology 160, 335–356.

Ringwood, A.E., 1975. Composition and Petrology os the earth's mantle. McGraw-Hill. 618p.

Rolando, A.P., Macambira, M.J.B., 2002. Geocronologia dos granitóides arqueanos da região da Serra do Inajá, novas evidências sobre a formação da crosta continental no sudeste do Cráton Amazônico, SSE Pará. In: Congresso Brasileiro de Geologia, 41. Anais do Congresso Brasileiro de Geologia. João Pessoa, 2002. SBG. p. 525.

Rolando, A.P., Macambira, M.J.B., 2003. Archean crust formation in Inajá range area, SSE of Amazonian Craton, Brazil, basead on zircon ages and Nd isotopes. In: South American Symposium on Isotope Geology, 4, Salvador. Expanded Abstracts. Salvador: CD-ROM.

Santos, M.D., Leonardos, O.H., 1994. Granodiorito Cumaru: um pluton calcio-alcalino arqueano com mineralizações mesotermais de Au-Cu, Se do Pará. In: Congresso Brasileiro de Geologia, 38, Camboriú, 1994. Boletim de resumos expandidos. Camboriú, SBG, vol. 1, pp. 158–160.

Santos, J.O.S., Hartmann, L.A., Gaudette, H.E., Groves, D.I., McNaughton, N.J., Fletcher, I.R., 2000. A new understanding of the Provinces of the Amazon Craton based on integration of field and U–Pb and Sm–Nd geochronology. Gondwana Research 3, 453–488.

Schmidt, M.W., Thompson, A.B., 1996. Epidote in calc-alkaline magmas: An experimental study of stability, phase relationships, and the role of epidote in magmatic evolution. American Mineralogist 81, 462–474.

Shand, S.J., 1950. Eruptive rocks their genesis, composition, classification e their relation to ore deposit. fourth ed., London, 488p.

Shirey, S.B., Hanson, G.N., 1984. Mantle-derived Archean monzodiorites and trachyandesites. Nature 310, 222–224.

Sial, A.N., Toselli, A.J., Saavedra, J., Parada, M.A., Ferreira, V.P., 1999. Emplacement, petrological and magnetic susceptibility characteristics of diverse magmatic epidote-bearing granitoid rocks in Brazil, Argentina and Chile. Lithos 46, 367–392.

Smithies, R.H., Champion, D.C., 2000. The Archaean high-Mg diorite suite: links to tonalite–trondhjemite–granodiorite magmatism and implications for early Archaean crustal growth. Journal of Petrology 41 (12), 1653–1671.

Souza, Z.S., 1994. Geologia e petrogênese do "Greenstone Belt" Identidade: implicações sobre a evolução geodinâmica do terreno granito-"greenstone" de Rio Maria, SE do Pará. v-1 e 2. Doctoral Thesis. Programa de Pós-Graduação em Geologia e Geoquímica, Centro de Geociências, UFPA, 624p. (in Portuguese).

Souza, Z.S., Dall'Agnol, R., 1995. Geochemistry of metavolcanic rocks in the Archean Greenstone Belt of Identidade, SE Pará, Brazil. An Academia Brasileira de Ciências 67 (2), 217–233.

Souza, Z.S., Potrel, H., Lafon, J.M., Althoff, F.J., Pimentel, M.M., Dall'Agnol, R., Oliveira, C.G., 2001. Nd, pb and sr isotopes of the identidade belt, na archaean greenstone belt of the Rio Maria region (Carajas Province, Brazil): implications for the archaean geodynamic evolution of the Amazonian craton. Precambrian research 109 (2001), 293–315.

Stern, A.L., Hanson, G., 1991. Archean high-Mg granodiorite: a derivate of light rare earth element-enriched monzodiorite of mantle origin. Journal of Petrology 32, 201–238.

Stern, R.A., Hanson, G.N., Shirey, S.B., 1989. Petrogenesis of mantle-derived, LILE-enriched Archean monzodiorites and trachyandesites (sanukitoids) in southwestern Superior Province. Canadian Journal of Earth Sciences 26, 1688–1712.

Stevenson, R., Henry, P., Gariépy, C., 1999. Assimilation– fractional crystallization origin of Archaean sanukitoid suites: Western Superior Province, Canada. Precambrian Research 96, 83–99.

Tassinari, C.C.G., Macambira, M.J.B., 1999. Geochronological Provinces of the Amazonian Craton. Episodes 22, 174–182.

Tassinari, C.C.G., Macambira, M.J.B., 2004. Evolução tectônica do Cráton Amazônico. In: Mantesso-Neto, V., Bartorelli, A., Carneiro, C.D.R., Brito Neves, B.B. de (Org.). Geologia do Continente Sul Americano: Evolução da obra de F.F.M. de Almeida. BECA, São Paulo, 2004, v., pp. 471–486.

Tulloch, A., 1979. Secondary Ca–Al silicates as low-grade alteration products of granitoid biotite. Contribution Minerals Petrology 69, 105–117.

Whitney, J.A., 1975. The effects of pressure, temperature and XH_2 O on phase assemblage in four synthetic rock compositions. Journal of Geology 83, 1–31.

Wilson, M., 1989. Igneous Petrogenesis. Academic Press, London. 466p.

Wyllie, P.J., 1984. Sources of granitoid magmas at convergent plate boundaries. Physics of the Earth and Planetary Interiors 35, 12–18.

Zen, E., Hammarstrom, J.M., 1984. Magmatic epidote and its petrologic significance. Geology 12, 515–518.

CAPÍTULO – 3

PETROLOGICAL CONSTRAINTS ON CRYSTALLIZATION CONDITIONS OF MESOARCHEAN SANUKITOID ROCKS, SOUTHEASTERN AMAZONIAN CRATON, BRAZIL

Marcelo Augusto de Oliveira
Roberto Dall'Agnol
Bruno Scaillet
Submetido: *JOURNAL OF PETROLOGY*

02-Jul-2009

Dear Dr. Oliveira:

Your manuscript entitled "Petrological constraints on crystallization conditions of Mesoarchean Sanukitoid rocks, southeastern Amazonian craton, Brazil" has been successfully submitted online and is presently being given full consideration for publication in the Journal of Petrology.

Your manuscript ID is JPET-Jun-09-0082.

Please mention the above manuscript ID in all future correspondence or when calling the office for questions. If there are any changes in your street address or e-mail address, please log in to Manuscript Central at http://mc.manuscriptcentral.com/jpet and edit your user information as appropriate.

You can also view the status of your manuscript at any time by checking your Author Center after logging in to http://mc.manuscriptcentral.com/jpet .

Thank you for submitting your manuscript to the Journal of Petrology.

Regards,

Alastair Lumsden
Editorial Office Journal of Petrology

PETROLOGICAL CONSTRAINTS ON CRYSTALLIZATION CONDITIONS OF MESOARCHEAN SANUKITOID ROCKS, SOUTHEASTERN AMAZONIAN CRATON, BRAZIL

Marcelo Augusto de Oliveira[1,2,*] (mao@ufpa.br), Roberto Dall'Agnol[1,2] (robdal@ufpa.br), Bruno Scaillet[3] (bscaille@cnrs-orleans.fr)

[1]Group of Research on Granite Petrology – Instituto de Geociências (IG) – Universidade Federal do Pará (UFPA). Caixa Postal 8608. 66075-900, Belém, Pará.

[2]Programa de Pós-Graduação em Geologia e Geoquímica (PPGG) – IG – UFPA

[3]CNRS/INSU, Université d'Orléans, Université François Rabelais Tours, Institut des Sciences de la Terre d'Orléans, 1a rue de la Férollerie, 45071 Orléans cedex 2, France**.**

*Corresponding author. Tel.: +55 91 3201 7477; fax +55 91 3201 7474. E-mail address: mao@ufpa.br

ABSTRACT

We report petrological and geochemical data on the 2.87 Ga Rio Maria granodiorite and associated rocks from Mesoarchean granite-greenstone terranes of the eastern Amazonian craton, Brazil. The Rio Maria suite has clear geochemical characteristics of Sanukitoids rocks (high Mg#, elevated Cr and Ni contents, LREE enrichment, and high Ba and Sr contents relative to typical calc-alkaline series), and thus our study allows us to infer for the first time crystallisation conditions of sanukitoid magmas. The dominant rocks have granodiorite to subordinate monzogranitic compositions, with minor proportions of intermediate quartz-diorites or quartz-monzodiorites rocks, in addition to mafic endmembers occurring as layered rocks or as enclaves. The mineral assemblage is dominated by amphibole-plagioclase-biotite and epidote minerals, all of inferred magmatic origin, pyroxenes being notably absent. Textural and compositional criteria indicate that amphibole is a principal mineral on the liquidus of all the Rio Maria rocks. To derive crystallisation conditions, the phase assemblages, proportions and compositions of the natural rocks have been compared with experimental works carried out on similar magma compositions. The comparison shows that the parental magmas were water-rich, with more than 7 wt% dissolved H_2O near liquidus, with crystallisation temperature in the range 950-680°C. The Mg/(Mg+Fe) ratios of both amphibole and biotite indicate fO_2 conditions in the range NNO+0.5

up to NNO+2.5, therefore pointing to both water-rich and oxidizing conditions for sanukitoid magmas. Analyses of amphibole aluminium content in cumulate rocks, indicate in addition a high pressure crystallisation stage, around 700-1000 MPa, prior to emplacement in the upper crust at around 200 MPa. Sanukitoid magmas share therefore two of the principal characteristics of modern arc magmas, elevated redox sate and volatile contents, which suggest that they may have formed in a geodynamic environment broadly similar to present-day subduction zones.

keywords: Amazonian craton; Crystallization conditions; High-Mg granitoids; Mineral chemistry; Sanukitoid.

1 – INTRODUCTION

Sanukitoid suites have been reported in several cratons (Stern & Hanson, 1991; Smithies & Champion, 2000; Bagai *et al*., 2002; Moyen *et al*., 2003; Kovalenko *et al*., 2005; Halla, 2005) and are now recognized as an important component of Archean terranes (Martin *et al*., 2005, Condie, 2005). Sanukitoids were formed during the late Archean (2.95-2.54 Ga) and are high-Mg rocks which display geochemical characteristics similar to both mantle- and crust-derived magmatic rocks. Large occurrences of sanukitoid rocks were recently identified in the Mesoarchean Rio Maria granite-greenstone terrane of the eastern Amazonian craton (Althoff *et al*., 2000; Souza *et al*., 2001; Leite, 2001; Oliveira *et al*., 2009). This terrane consists predominantly of greenstone belts, TTG suites and sanukitoid rocks, with subordinate calc-alkaline leucogranites (Dall'Agnol *et al*., 2006, Oliveira *et al*., 2009). The sanukitoid rocks belong to the ~2.87 Ga old Rio Maria suite that is intrusive in the greenstone belts and older TTG series. Granodiorite is the dominant rock in the Rio Maria suite. It carries amphibole-rich clots and abundant mafic enclaves and, in the Bannach area, selected for the present study, has associated intermediate and layered mafic rocks.

The petrogenesis of sanukitoids is currently the subject of intense debate (Smithies & Champion, 2000; Kovalenko *et al*., 2005). Their high Mg#, associated to elevated Cr and Ni contents indicate a mantle influence and suggest a peridotitic, rather than basaltic, source. On the other hand, the relative LREE enrichment, and high Ba and Sr contents of sanukitoid magmas compared to typical calc-alkaline series could be interpreted as an evidence of their crustal origin or, alternatively, of crustal contamination during their evolution. However, the low contents of

those elements in the Archean crust do not favor these hypotheses as indicated by geochemical modeling (Taylor & McLennan, 1985; Stern *et al*., 1989). The isotopic composition of the sanukitoid rocks is also paradoxical, with Nd and Sr isotopes pointing to a mantle origin (Stern & Hanson, 1991; Kovalenko *et al*., 2005), whereas Pb isotope compositions of K-feldspars argue for a crustal source (Stevenson *et al*., 1999; Halla, 2005). At present, most authors agree that both mantle and arc-related components must play an important role in the petrogenesis of sanukitoid series and two main hypotheses have been proposed: (1) a two-stage process: during the first stage, the mantle is metasomatised by melts (Smithies & Champion, 2000) or by fluid-mobile elements (Kamber, *et al*. 2002), both slab-derived. In the second stage, melting of the enriched mantle produces sanukitoid magmas (Stern & Hanson, 1991); (2) a one-stage process, involving continuous assimilation of mantle peridotite by slab melts ascending through the mantle wedge (Rapp *et al*., 1999).

In addition to the uncertainties about the origin of sanukitoid rocks, their crystallization conditions, including oxidation state, H_2O content and pressure of crystallization, remain also poorly constrained. Over the last years, a number of experimental studies have been done so as to set quantitative constraints on the magmatic evolution of granitoids (Naney & Swanson, 1980; Naney, 1983; Wyllie *et al*., 1984; Clemens *et al*., 1986; Dall'Agnol *et al*., 1999; Scaillet & Evans, 1999; Klimm *et al*., 2003; Pichavant *et al*., 2007). In particular, Scaillet & Evans (1999), Prouteau & Scaillet (2003) and Bogaerts *et al*. (2006) have performed experimental studies on rocks having compositions similar to the dominant rocks of Rio Maria suite, which is the focus of the present study. Compared to early experimental work, in addition to phase equilibrium constraints, recent studies provide detailed information on the mineral compositions and their variations with intensive parameters. Such studies have shown to be of great help in the elucidation of the storage conditions of volcanic rocks (e.g., Martel *et al*., 1999; Scaillet & Evans, 1999), but also for the unravelling of the evolution of granitoids plutons (e.g., Clemens *et al*., 1986; Dall'Agnol *et al*., 1999).

The aim of this paper is to present a geochemical, mineralogical, and petrological study of the Rio Maria suite from the Bannach area in order to constrain the crystallization conditions, mainly H_2O content, pressure, temperature and fO_2, using available experimental data on related rocks. This is done with the purpose of clarifying the petrogenesis of sanukitoid rock series.

2 – GEOLOGIC SETTING AND FIELD RELATIONSHIPS

The Archean Rio Maria suite occurs in different areas of the Rio Maria granite-greenstone terrane, which corresponds to the southern part of the Archean Carajás province in the eastern domain of the Amazonian craton (Dall'Agnol *et al*., 2006; Oliveira *et al*., 2009). The Carajás province belongs to the Central Amazonian province (Tassinari & Macambira, 2004) and is divided into two Archean tectonic domains (Fig. 1, inset), the 2.98-2.86 Ga Rio Maria granite-greenstone terrane (Macambira and Lafon, 1995; Dall'Agnol *et al*., 2006) and the rift-related Carajás basin, mainly composed of 2.76-2.55 Ga metavolcanic rocks, banded iron formations, and granitoids (Machado *et al*., 1991; Macambira & Lafon, 1995; Barros *et al*., 2001). The two domains were cratonised at the end of the Archean and intruded by Paleoproterozoic A-type granites of the Serra dos Carajás and Jamon suite (Dall'Agnol *et al*., 2005). The Archean Rio Maria granite-greenstone terrane (Fig. 1) consists of greenstone belts (Andorinhas supergroup, Hunh *et al*., 1988; Souza *et al*., 2001) and different granitoids (Dall'Agnol *et al*., 2006). The greenstone belts have ages of 2.97-2.90 Ga and are composed dominantly of metamorphosed tholeiitic basalts and komatiites (Huhn *et al*., 1988; Souza *et al*., 2001). The granitoids yielded ages between 2.98-2.86 Ga and are broadly similar to those found in other Archean terranes. Four groups of granitoids can be distinguished: (1) an older TTG series represented by the Arco Verde and Caracol tonalite (~2.98-2.93 Ga; Althoff *et al*., 2000; Leite *et al*., 2004); (2) the 2.87 Ga Rio Maria sanukitoid suite formed by various occurrences of Rio Maria granodiorite and associated rocks (Medeiros, 1987; Macambira & Lancelot, 1996; Althoff *et al*., 2000; Leite *et al*., 2004; Oliveira *et al*., 2009); (3) a younger TTG series represented by the Mogno and Água Fria trondhjemites (2.87 Ga; Huhn *et al*., 1988; Pimentel & Machado, 1994; Leite *et al*., 2004); and (4) ~2.86 Ga potassic leucogranites of calc-alkaline affinity such as the Xinguara and Mata Surrão plutons (Lafon *et al*., 1994; Leite *et al*., 1999, 2004). The principal shearing deformational event identified in this area occurred at around 2.87 Ga (Althoff *et al*., 2000; Souza *et al*., 2001; Leite, 2001). The Archean granitoids and greenstone belts are intruded by ~1.88 Ga A-type granite plutons of the Jamon suite and associated dikes (Dall'Agnol *et al*., 2005; Dall'Agnol & Oliveira, 2007).

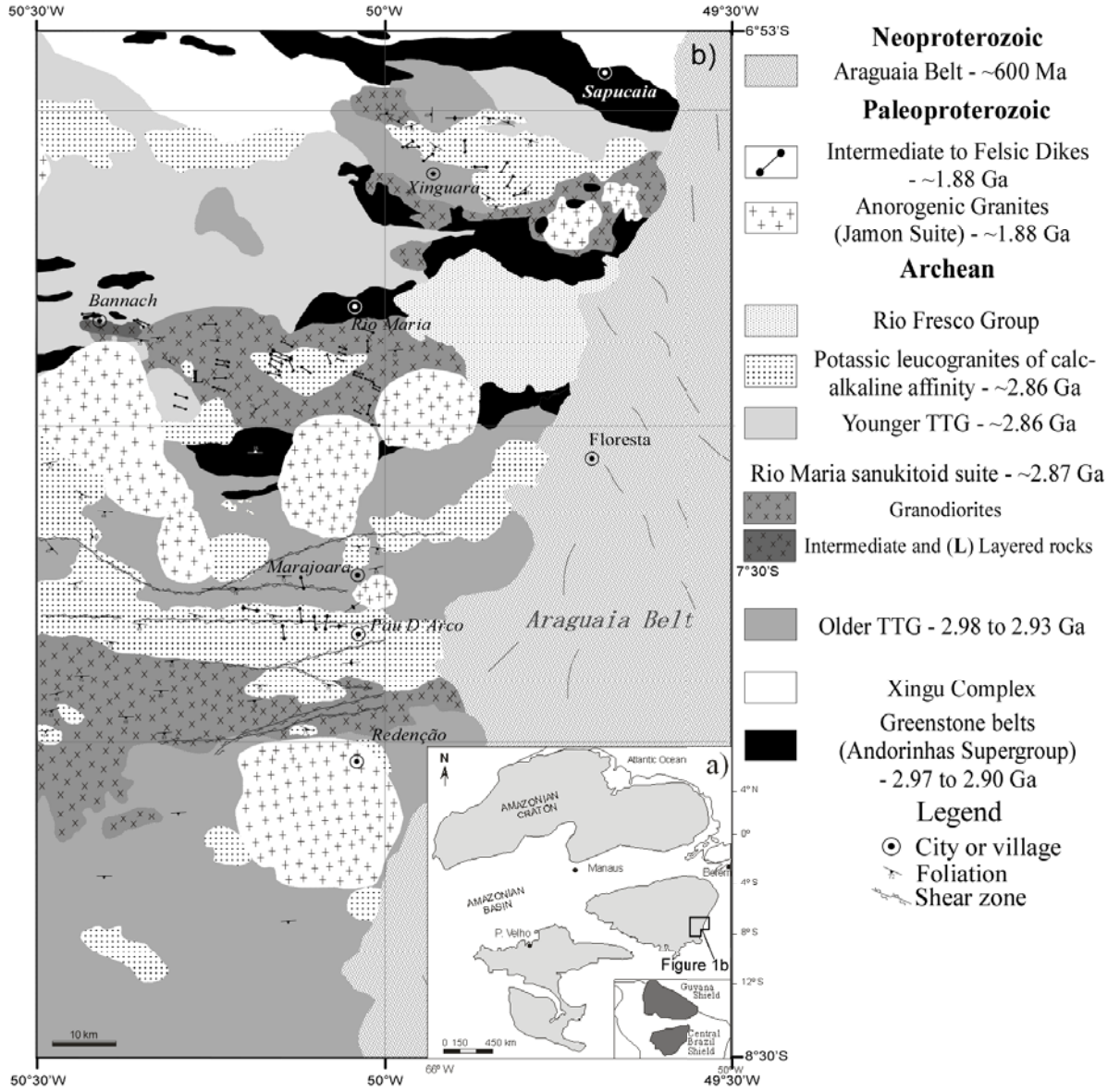

Fig. 1 - (a) Location of the studied area in the Amazonian craton; (b) Geological map of the Rio Maria Granite-Greenstone Terrane (modified from Leite, 2001).

The Rio Maria granodiorite is the dominant variety of rock of the sanukitoid suite, covering large areas of the Rio Maria granite-greenstone terrane (Fig 1). It is exposed south of Rio Maria (type-area; Medeiros, 1987), to the south and NE of Xinguara (Leite, 2001), to the north of Redenção (Althoff *et al*., 2000) and to the east of Bannach (Oliveira *et al*., 2009). Mafic and intermediate sanukitoid rocks are scarce, forming local occurrences (Xinguara area, Souza, 1994; Leite, 2001) or stocks (Fig. 2, Bannach area, Oliveira *et al*., 2006). Field relationships show that the Rio Maria suite is intrusive in the greenstone sequences (Souza *et al*., 2001) and Arco Verde and Caracol tonalites (Althoff *et al*., 2000; Leite *et al*., 2004) and is intruded by the Água Fria trondhjemite (Leite *et al*., 2004), potassic leucogranites (Mata Surrão granite, Duarte,

1992; Xinguara granite, Leite *et al*., 2004) and by the Paleoproterozoic granites of Jamon suite (Dall'Agnol *et al*., 2005).

The Rio Maria granodiorite bears systematically centimetric to decimetric mafic enclaves and displays generally a gray color with greenish shades due to strongly saussuritized plagioclase. It shows a weak subvertical foliation striking WNW-ESE to E-W acquired during late magmatic to high-temperature subsolidus conditions. This foliation is outlined by the preferred orientation of mafic minerals and, locally, enclaves (Althoff *et al*., 2000; Souza *et al*. 2001; Leite, 2001). The mafic enclaves have flattened or rounded shapes (Fig. 3a, b), being stretched only when located near or along shear zones (Souza, 1994; Althoff *et al*., 2000; Leite, 2001).

The enclaves display evidence of interaction with the granodiorite, both rocks sharing the same finite strain pattern. These features point to a low viscosity contrast between enclaves and the Rio Maria granodiorite at the time of enclave incorporation, which suggests coexistence of the two magmas while both were still partly molten (Souza & Dall'Agnol, 1995; Althoff *et al*., 2000; Leite, 2001). The Bannach area was selected for this study because of the abundance of mafic and intermediate rocks associated to the Rio Maria granodiorite (Oliveira *et al*., 2009). The mafic to intermediate rocks occur in two domains (Fig. 2). In the main domain, located near Bannach, it is exposed as a stock composed mostly of quartz diorites and quartz monzodiorites; in the second domain, situated along the road between Rio Maria and Bannach, various outcrops of layered rocks can be seen. The dominant intermediate variety is made of mesocratic, dark-green rocks, with medium to coarse grained texture. The layered rocks, of inferred cumulate origin (Oliveira, 2005), are characterized by a remarkable concentration of generally quadratic or short prismatic coarse amphibole crystals, set in a matrix of leucocratic intercumulus material. The igneous layering is drawn by the alternation of darker layers of coarse rocks enriched in centimeter sized amphibole crystals (Fig. 3c, d), with gray colored, and medium-grained layers. The layering is sub-horizontal, gently deeping eastward with no evidence of significant superimposed solid state deformation.

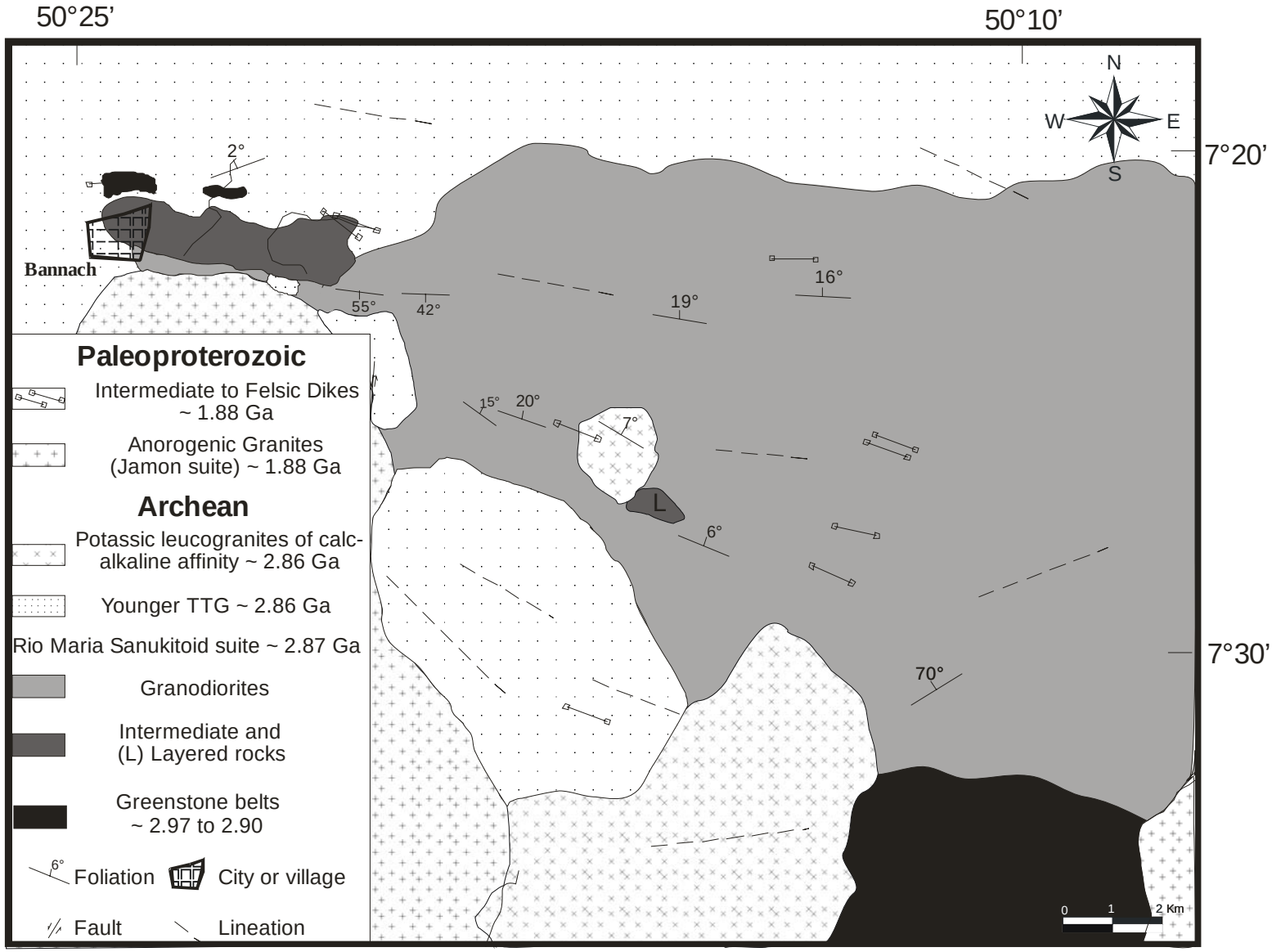

Fig.2 - Geological map of Bannach area.

Fig. 3 - (a, b) Field aspects of the Rio Maria Granodiorite, showing elongated (a) and rounded (b) mafic enclaves; (c, d) Outcrop of the layered rocks of Bannach area; (e, f) Hand samples of an layered rock displaying dark color and well-preserved centimeter sized euhedral amphibole crystals.

3 – PETROGRAPHY

In the Rio Maria suite the dominant rocks have granodioritic to subordinate monzogranitic (Table 1) composition and display equigranular, medium or coarse even-grained textures (Oliveira, 2005; Oliveira *et al*., 2009). The associated intermediate rocks are quartz-diorites and quartz-monzodiorites. All facies of the Rio Maria suite have strongly saussuritized plagioclase and contain amphibole ± biotite ± magmatic epidote as their principal mafic minerals. M (modal % in volume of mafic minerals) values normally vary between 10 to 25% in the granodiorites, attaining higher values (generally 20 to ~40%) in the intermediate rocks

(Oliveira *et al*., 2009). The assemblage of primary accessory minerals includes zircon, apatite, magnetite, titanite, and allanite.

In the dominant epidote-biotite-hornblende granodiorite, microscopic textural criteria indicate that apatite, zircon, magnetite and allanite are early crystallized phases followed by magnesian hornblende and plagioclase (Oliveira, 2005; Oliveira *et al*., 2009). Amphibole forms euhedral, twinned crystals, which are well preserved or only partially replaced by late magmatic

Table 1
Modal composition (Point counting) of the rocks of Rio Maria suite (Bannach area)

	Mafic enclaves [1]								Intermediate rocks [2]		Granodiorites [2]			
Facies	EBAD	EBAMzD		EBAQMzD		EBAQMz			EBAQD	EBAQMzD	EBAGD			
Sample	MFR-27C	ADR-2	MD-2D	MD-2C	MD-3A	MD-2F	MD-2A	MD-2B	ADR-4B	ADR-5	MFR-32	MFR-80A	MFR-114	ADR-3A
Plagioclase	48.4	44.9	39.1	31.5	34.0	24.9	23.8	23.4	47.1	51.7	49.7	48.2	46.6	36.8
Alkali-feldspar	0.6	14.6	13.0	12.3	9.6	14.9	18.7	22.1	4.3	6.7	15.9	9.1	9.3	15.2
Quartz	2.5	0.7	1.8	2.8	7.5	2.9	5.2	5.3	13,0	13.7	16.1	20.5	19.2	23.2
Amphibole	37.6	33.4	34.2	41.3	37.4	47.0	46.7	40.1	28.7	20.3	9.8	8.2	12.7	11.1
Biotite	7.9	3.3	7.1	5.5	7.0	5.3	3.1	4.5	0.7	4.5	4.4	7.2	8.2	7.5
Epidote[(m)]	1.5	0.6	2.4	1.6	0.6	1.3	1.5	1.5	1.5	0.6	1.2	1.9	1.1	1.8
Epidote[(S)]	0.9	0.5	0.3	0.2	0.2	0.3	0.1	0.2	0.3	0.5	1.1	2.6	0.8	2,0
Opaques	-	0.3	1.6	4.0	3.5	3.3	0.6	2.3	1.1	0.8	-	n.d.	0.1	n.d.
Titanite	0.2	0.3	0.2	0.4	0.2	0.1	0.1	0.6	1.5	0.5	0.6	0.7	0.7	0.9
Apatite	0.3	0.1	-	-	-	-	-	-	0.7	0.2	0.2	0.8	0.2	0.2
Allanite	0.2	-	-	-	-	-	-	-	1.0	0.4	0.3	n.d.	n.d.	0.1
Carbonate	-	-	-	-	-	-	-	-	n.d.	n.d.	-	-	-	-
Felsic	51.5	60.2	53.9	46.6	51.1	42.7	47.7	50.8	64.4	72.1	81.7	77.8	75.1	75.2
Mafic	48.6	38.5	45.8	53.0	48.9	57.3	52.1	49.2	35.5	27.8	17.6	21.4	23.8	23.6

Data Source: (1) This paper; (2) Oliveira (2005); E = epidote; B = biotite; A = amphibole; Q = quartz; D = diorite; MzD = monzodiorite; Mz= monzonite; GD = granodiorite; [(m)] magmatic; [(s)] secondary.

biotite and subordinate titanite and epidote. Plagioclase is euhedral to subeuhedral and originally zoned but the intense saussuritization prevents the determination of its original composition. Biotite crystallizes after both amphibole and plagioclase and displays regular contacts with euhedral epidote suggesting equilibrium between these two minerals. Such epidotes show, however, highly embayed, irregular contacts with quartz and plagioclase. Besides secondary epidote derived from plagioclase, two textural epidote types interpreted as magmatic in origin can be distinguished: (1) epidote with allanite core and (2) zoned epidote associated with, and partially enclosed by, biotite. In all rocks of the Rio Maria suite, modal abundances of magmatic epidote are as high as 5 vol. %. Quartz forms subhedral to anhedral medium-grained crystals that are sometimes recrystallised, forming subgrains with undulatory extinction. K-feldspars crystallized late forming anhedral, sometimes poikilitical crystals, with inclusions of quartz, plagioclase and euhedral amphibole. At the subsolidus stage, chlorite, secondary epidote, sericite and carbonates were generated.

In the quartz diorites and quartz monzodiorites, the mineral assemblages and textural relationships between different minerals are very similar to those observed in the dominant granodiorite, amphibole and plagioclase being more abundant whilst quartz and K-feldspars modal contents are lower than in the granodiorite.

The mineralogy of the layered rocks is similar to that of the Rio Maria granodiorite and intermediate rocks. The textural variations are directly related to the different layers of the rock. The darker layers display inequigranular texture and the cumulus material is formed by centimeter-sized euhedral pargasite to magnesium-hornblende crystals (Fig. 3e, f) with rims of magnesium-hornblende to actinolitic hornblende, partially replaced by biotite. The intercumulus material is mainly composed of quartz and intensely saussuritized plagioclase, with subordinate amphibole, biotite, and epidote. The accessory minerals are allanite, titanite, magnetite, and apatite. The gray layers display also an inequigranular texture. In these layers, the cumulus material is composed of comparatively smaller amphibole crystals whose replacement by biotite is more intense when compared to the darker layers. The intercumulus phases are similar to those observed in the darker layers.

For a more detailed study of mafic enclaves, portable drill core samples were collected in four different localities. The central part of the cores, had no apparent interaction with the granodiorite, and is laminated. Such cores have dioritic to quartz monzonitic composition (Fig. 4) (e.g., Käpyaho, 2006) and follow a monzonitic trend in the QAP plot (Fig. 4) (Lameyre & Bowden, 1982). The textures in the dioritic rocks are not distinct from those of intermediate Rio Maria rocks. In the monzodiorite to quartz monzonite, the presence of abundant poikilitical coarse K-feldspar crystals with inclusions of medium to fine-grained amphibole, is remarkable. The alkali-feldspar crystals are subeuhedral and display regular contacts with plagioclase. Textural evidence indicates that it crystallized in equilibrium with other minerals and does not correspond to entrained crystals of the enclosing granodiorite. These enclaves are rich in mafic minerals with $M \geq 40\%$ (Fig. 4). Amphibole is by far the most abundant mafic mineral, being followed by biotite, magmatic epidote, and the same accessory mineral assemblage found in the granodiorite.

The amphibole crystals are generally euhedral and show minute inclusions of opaque minerals. Quartz modal contents are low and their crystals are anhedral, filling the interstices between other minerals, suggesting its late crystallization. The contacts between the enclaves

and the granodiorite are sharp but indented in detail. Amphibole crystals are concentrated along the contact and the ratio plagioclase/K-feldspar is larger toward the enclave border zone.

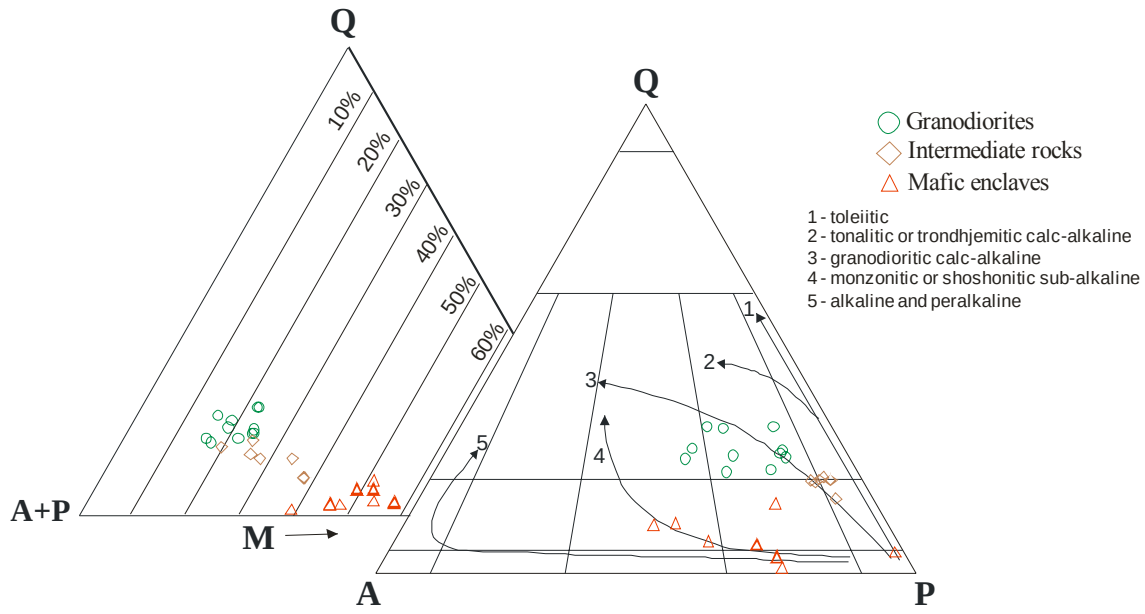

Fig. 4 - QAP and Q-(A+P)-M plots for the rocks of the Rio Maria suite (Bannach area). Data sources: Granodiorites and intermediate rocks (Oliveira, 2005); Mafic enclaves (This study).

4 – GEOCHEMISTRY

A detailed discussion about the geochemistry of the studied sanukitoid rocks is beyond the scope of the present paper. In the following we just provide an overview of the major geochemical characteristics of the Rio Maria sanukitoids, focusing on aspects relevant to petrological interpretations. In the case of layered rocks, which were previously interpreted as cumulate rocks (Oliveira *et al.*, 2009), it is clear that the analyzed samples do not correspond to real liquids and can provide information about the nature of original magmas only indirectly. As note above, the fact that the dominant granodiorite variety carries systematically mafic enclaves and variable amounts of mafic clots, suggests that mingling processes and different degrees of interaction between distinct magmas has occurred. This implies that the original magmatic composition of the enclaves and granodiorites could have been modified to some extent. However, as discussed below, the compositions of the four studied groups are similar in their broad aspects, which suggests that they all share similar petrogenetic mechanism of production and evolution. In other words, we assume that the principal magmatic geochemical

characteristics of the studied sanukitoid rocks are preserved enough so that their compositions can give clues about the nature and conditions of formation of their original magmas.

The four groups of sanukitoid rocks, i.e. layered rocks, mafic enclaves, intermediate rocks and granodiorites, have in common a typical sanukitoid signature. This is indicated by their metaluminous character, high Mg#, Cr and Ni contents, in addition to elevated contents in large ion lithophile elements (LILE), especially Ba and Sr (Table 2). Layered rocks and mafic enclaves have similar silica contents, which varyies from 50 to 57 wt.% (Table 2), showing perhaps a small compositional gap (Fig. 5a) with the intermediate rocks and granodiorites (respectively, 59 to 64 wt% and 63 to 67 wt%). The Al_2O_3 contents are similar in the enclaves, intermediate rocks and granodiorites, reaching the lowest values in the layered rocks which are

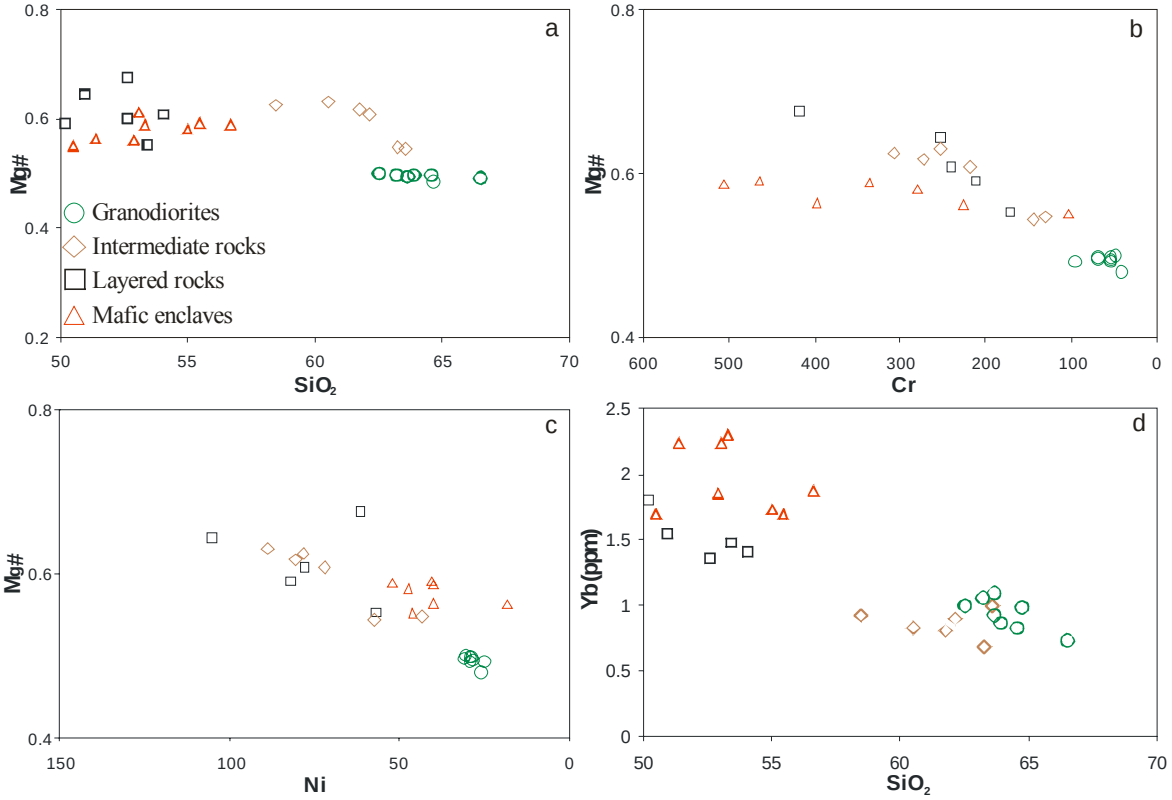

Fig. 5 - (a) Mg# vs. SiO_2; (b) Mg# vs. Cr; (c) Mg# vs. Ni; (d) Yb vs. SiO_2 diagrams for the different rocks of the Rio Maria suite (Bannach area).

impoverished in feldspars relative to the other members of the suite. All analyzed rocks display Al_2O_3 contents (Table 2) that are lower than those of typical calc-alkaline series of similar silica contents (Irvine & Baragar, 1971; Ringwood, 1975; Wilson, 1989). The Mg# values vary from 0.67 to 0.48, decreasing from the layered rocks to the granodiorites (Table 2). The Mg# of the

gray layers is sligthly lower Mg# than that of the dark one (Table 2). The Mg# in the enclaves is generally intermediate between those of layered and intermediate rocks and granodiorites (Table 2, Fig. 5a). The Cr contents are higher in the enclaves, and lower in the granodiorites, with layered and intermediate rocks displaying intermediate values between both aforementioned groups (Fig. 5b).

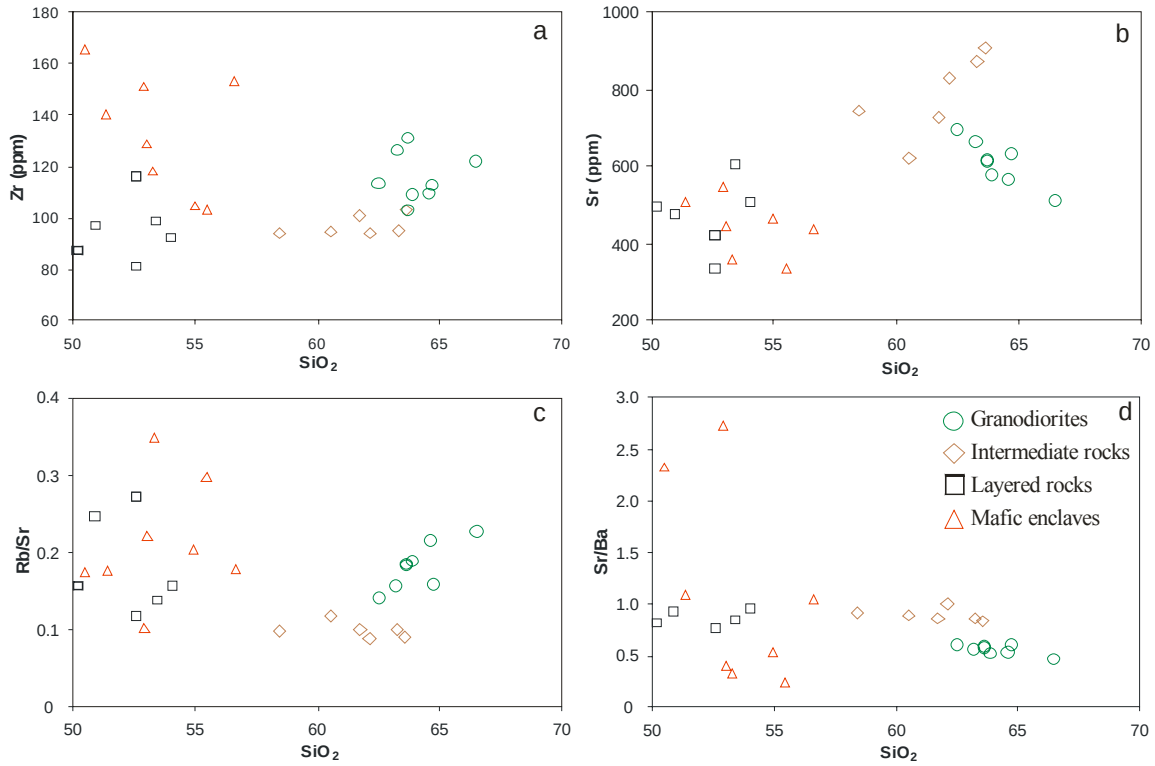

Fig. 6 - (a, b, c, d) Harker diagrams for the different rocks of the Rio Maria suite (Bannach area).

Ni content, in contrast, is higher in layered and intermediate rocks, decreasing in the enclaves and granodiorites (Fig. 5c). Yb is significantly higher in enclaves and layered rocks as compared to intermediate and granodiorites rocks (Fig. 5d). LILE and Zr are also good geochemical discriminants between different groups (Fig. 6, Table 2). The alkali contents in the studied rocks are high compared to typical calc-alkaline series. In the TAS diagram (Fig. 7, fields of Le Maitre *et al*., 2002), the intermediate rocks and granodiorite samples plot along the divide line between the oversaturated and saturated fields (the analyzed samples of layered rocks also show a similar behavior but since they do not correspond to magmatic liquids, they have not been plotted in this diagram). On the other hand, the enclaves plot dominantly in the saturated field of that diagram, in agreement with their affinity with the monzonitic series (Fig. 4. QAP). The K/Na ratios do not

Table 2
Chemical composition of the samples of the Rio Maria suite (Bannach area).

	Layered rocks						Mafic enclaves								Intermediate rocks						Granodiorites							
Facies	Dark Layer			Gray Layer			EBAD to EBAQMz								EBAQzD to EBAQzMD						EBAGD to EBAMzG							
Sample	MFR-07B	MFR-12B	ADR-1	MFR-07D	Cr-71	MFR-12A	MFR-27C	MD-02C	MD-03A	299	MD-02A	ADR-2	MD-02B	MD-03B	ADR-4A	ADR-4B	ADR-5	MFR-102	MFR-100D	ADR-7	MFR-114	MFR-27	MFR-111	MFR-29	ADR-3A	MFR-112	MFR-91A	MFR-80A
SiO_2 (wt.%)	50.92	52.60	54.04	50.14	52.60	53.41	50.51	51.38	52.89	53.03	53.3	54.98	55.46	56.64	58.47	60.51	61.75	62.15	63.29	63.61	62.52	63.23	63.66	63.66	63.9	64.58	64.72	66.49
TiO_2	0.73	0.56	0.63	0.97	0.70	0.78	0.88	0.72	0.69	0.72	0.69	0.61	0.55	0.85	0.47	0.44	0.43	0.39	0.38	0.37	0.46	0.49	0.42	0.45	0.43	0.42	0.39	0.33
Al_2O_3	12.11	10.91	13.02	13.08	13.21	14.76	16.19	13.77	15.63	13.56	12.29	14.34	13.09	13.28	14.02	14.03	13.96	14.5	14.97	14.94	15.23	14.82	14.87	14.84	14.82	14.65	14.98	14.55
Fe_2O_3	4.16	3.28	3.41	3.63	11.89	4.07	5.06	11.15	9.58	10.49	10.2	3.59	8.94	9.05	2.46	2.37	2.89	2.34	2.51	3.12	2.91	2.8	2.81	3,00	2.91	2.86	2.71	2.27
FeO	5.96	5.96	3.41	7.08	n.d.	4.83	4.46	n.d.	n.d.	n.d.	n.d.	4.14	n.d.	n.d.	3.94	3.43	2.44	2.56	1.96	1.41	1.97	1.89	1.64	1.48	1.65	1.47	1.49	1.32
MnO	0.15	0.15	0.13	0.15	0.15	0.13	0.13	0.2	0.17	0.18	0.19	0.14	0.17	0.16	0.09	0.09	0.07	0.07	0.06	0.06	0.07	0.06	0.06	0.06	0.06	0.06	0.06	0.05
MgO	9.94	10.51	7.37	8.48	9.17	5.98	5.65	7.38	6.28	8.39	7.43	5.82	6.61	6.61	5.81	5.37	4.62	4.11	2.89	2.86	2.61	2.49	2.31	2.31	2.39	2.28	2.06	1.85
CaO	8.21	9.3	8.15	8.81	8.55	7.88	7.61	8.36	7.66	7.79	7.42	6.73	6.24	6.52	5.88	4.73	4.84	4.65	4.18	4.03	4.4	4.36	3.99	4.17	4.02	3.77	4.08	3.02
Na_2O	2.49	2.06	2.86	2.60	2.36	2.99	4.06	3.53	4.72	2.87	2.31	3.86	2.59	3.83	3.77	4.04	3.98	4.21	4.36	4.4	4.3	4.21	4.19	4.09	4.05	4.04	4.29	4.13
K_2O	2.04	1.03	1.74	1.72	1.94	2.00	2.33	1.94	1.1	2.32	4.23	3.07	4.96	1.76	2.21	2.16	2.31	2.24	2.57	2.66	2.93	3.01	3.32	3.22	3.21	3.44	2.98	3.75
P_2O_5	0.22	0.15	0.17	0.17	0.24	0.23	0.45	0.37	0.33	0.25	0.31	0.27	0.29	0.31	0.17	0.18	0.16	0.14	0.15	0.13	0.17	0.15	0.15	0.14	0.14	0.15	0.12	0.14
LOI	2.10	2.50	2.30	2.00	n.d.	2.10	1.90	0.8	0.6	n.d.	1.2	1.6	0.6	0.6	1.9	1.9	1.9	2,00	2,00	1.8	1.6	1.8	1.9	1.9	1.8	1.5	1.5	1.4
Total	99.03	99.01	99.10	98.83	100.81	99.16	99.23	99.56	99.65	99.60	99.57	99.15	99.50	99.61	99.19	99.25	99.35	99.36	99.32	99.39	99.17	99.31	99.32	99.32	99.38	99.22	99.38	99.3
Ba (ppm)	511	442	527	608	n.d.	711	344	468	199	1145	1088	876	1382	417	812	701	847	830	1008	1090	1139	1175	1052	1022	1098	1064	1044	1089
Rb	118	39	80	77	115	84	140	89	56	98	125	94	101	77	73	72	72	74	87	82	98	103	113	112	109	122	101	116
Sr	477	335	507	494	422	604	800	508	544.8	445	357.7	463	338	436	745	618	724	828	872	905	692	661	615	611	576	567	632	512
Zr	97	81	92	87	116	99	165	140	151	129	118	105	103	153	94	94	101	94	95	103	113	126	103	131	109	110	113	122
Nb	5	4	5	5	5	5	7	8	7	11	11	11	7	7	6	5	6	5	6	7	8	9	8	8	7	11	9	10
Y	17	17	17	23	15	19	23	23	22	24	25	23	19	23	11	10	11	10	10	12	16	13	11	15	11	12	17	12
Ga	17	14	17	18	n.d.	20	25	19	20	n.d.	16	20	15	17	18	18	19	20	20	20	20	20	19	20	20	19	20	19
Th	8	6	6	6	n.d.	6	1	2	2	n.d.	2	5	2	3	3	2	5	5	6	5	7	7	7	8	5	11	8	12
Ni	105	61	80	82	n.d.	57	46	40	18	n.d.	40	47	40	52	79	89	81	72	43	57	31	29	28	29	31	29	26	25
Cr	253	417	239	212	n.d.	171	103	397	226	n.d.	506	281	465	335	308	253	274	219	130	144	48	68	55	96	68	55	41	55
La	33	24.3	25.4	31.8	n.d.	27.6	28.5	25,00	25.4	n.d.	22.4	29	18.4	30.8	23.7	23.3	25.1	25.2	42.2	33.8	37.3	36.9	33.7	34.3	20.0	40.7	53.5	48.0
Ce	62.8	43.7	55.2	67.2	n.d.	53.9	77.1	67.2	60.4	n.d.	64.8	72.1	50.2	71,00	51.1	50.3	51.4	47.6	68.3	58.6	72.8	71.9	64.1	64.1	45.7	70.8	72.2	64.2
Pr	6.47	5.28	5.69	6.97	n.d.	6.54	10.11	10.41	9.85	n.d.	10.43	9.42	7.99	10.41	5.35	5.35	5.3	5.35	7.37	7.35	7.19	7.57	6.32	6.53	4.94	7.04	8.51	6.81
Nd	25.1	20.9	24.5	28.9	n.d.	27.1	44	41.6	43.5	n.d.	43,00	40.4	32.8	41.8	21.4	21.4	19.3	20.8	26.1	29.2	27.2	27.8	22.9	24.7	21.7	25.6	31.6	23.9
Sm	4.80	4.10	4.5	6.1	n.d.	5.3	8.6	8.4	8.35	n.d.	8.61	7.5	6.62	7.91	3.6	3.4	3.3	3.6	4.1	4.3	4.4	4.9	3.7	4.3	3.7	3.9	4.5	3.4
Eu	1.29	1.14	1.33	1.69	n.d.	1.59	1.73	1.58	1.62	n.d.	1.75	1.52	1.27	1.59	1.02	0.95	0.98	0.99	1.05	1.23	1.25	1.35	1.06	1.14	1.05	1.07	1.3	0.95
Gd	4.04	3.59	3.64	5.06	n.d.	4.74	5.71	6.65	6.64	n.d.	6.92	5.8	5.4	6.7	2.78	2.49	2.58	2.42	2.82	3.19	3.47	3.56	2.9	3.2	2.63	2.71	3.37	2.43
Tb	0.6	0.51	0.58	0.82	n.d.	0.72	0.86	0.97	0.88	n.d.	0.96	0.98	0.74	0.88	0.45	0.37	0.37	0.4	0.35	0.48	0.56	0.53	0.42	0.47	0.41	0.4	0.52	0.36
Dy	2.82	2.79	2.89	3.9	n.d.	3.37	4.35	4.94	4.36	n.d.	4.66	4	3.83	4.5	2.25	1.84	1.98	1.75	1.67	2.2	2.41	2.19	1.92	2.19	1.86	1.9	2.31	1.56
Ho	0.54	0.53	0.6	0.77	n.d.	0.69	0.78	0.87	0.81	n.d.	0.87	0.74	0.71	0.8	0.38	0.34	0.33	0.34	0.31	0.42	0.48	0.42	0.34	0.42	0.41	0.4	0.49	0.32
Er	1.51	1.52	1.68	2.14	n.d.	1.82	2.05	2.41	2.14	n.d.	2.33	2.04	1.88	2.16	1.03	0.97	0.88	0.95	0.78	1.13	1.3	1.15	0.92	1.19	1.02	0.92	1.25	0.81
Tm	0.23	0.24	0.19	0.33	n.d.	0.26	0.29	0.37	0.32	n.d.	0.38	0.27	0.28	0.35	0.13	0.1	0.1	0.1	0.11	0.13	0.14	0.17	0.11	0.17	0.1	0.23	0.17	0.12
Yb	1.55	1.36	1.41	1.8	n.d.	1.48	1.7	2.24	1.85	n.d.	2.3	1.73	1.69	1.88	0.93	0.83	0.81	0.9	0.69	1,00	1,00	1.06	0.92	1.09	0.87	0.83	0.99	0.73
Lu	0.22	0.2	0.23	0.3	n.d.	0.25	0.25	0.32	0.28	n.d.	0.34	0.29	0.26	0.28	0.15	0.14	0.12	0.13	0.12	0.15	0.16	0.16	0.11	0.15	0.14	0.15	0.15	0.13
ΣREE	144.97	110.16	127.84	157.78	n.d.	135.36	186.03	172.96	166.4	n.d.	169.75	175.79	132.07	181.06	114.27	111.78	112.55	110.53	155.97	143.18	159.66	159.66	139.42	143.95	104.53	156.65	180.86	153.72
$(La/Yb)_n$	14.37	12.06	12.16	11.92	n.d.	12.59	11.32	7.53	9.27	n.d.	6.57	11.31	7.35	11.06	17.20	18.95	20.92	18.90	41.28	22.81	25.18	23.50	24.72	21.24	15.52	33.10	36.48	44.38
$(La/Sm)_n$	4.33	3.73	3.55	3.28	n.d.	3.28	2.09	1.87	1.92	n.d.	1.64	2.43	1.75	2.45	4.14	4.31	4.79	4.41	6.48	4.95	5.34	4.74	5.73	5.02	3.4	6.57	7.49	8.89
$(Dy/Yb)_n$	1.18	1.33	1.33	1.41	n.d.	1.48	1.66	1.43	1.53	n.d.	1.32	1.5	1.47	1.56	1.57	1.44	1.59	1.26	1.57	1.43	1.57	1.34	1.36	1.31	1.39	1.49	1.52	1.39
Eu/Eu*	0.9	0.91	1,0	0.93	n.d.	0.97	0.75	0.65	0.67	n.d.	0.69	0.7	0.65	0.67	0.99	1.00	1.03	1.03	0.94	1.02	0.98	0.99	0.99	0.94	1.03	1.01	1.02	1.01
Rb/Sr	0.25	0.12	0.16	0.16	0.27	0.14	0.17	0.18	0.10	0.22	0.35	0.20	0.30	0.18	0.1	0.12	0.1	0.09	0.1	0.09	0.14	0.16	0.18	0.18	0.19	0.22	0.16	0.23
Sr/Ba	0.93	0.76	0.96	0.81	n.d.	0.85	2.32	1.09	2.74	0.39	0.33	0.53	0.24	1.04	0.92	0.88	0.85	1.00	0.86	0.83	0.61	0.56	0.58	0.6	0.53	0.53	0.61	0.47
K/Na	0.54	0.33	0.40	0.44	0.54	0.44	0.38	0.36	0.15	0.53	1.20	0.52	1.26	0.30	0.39	0.35	0.38	0.35	0.39	0.40	0.45	0.47	0.52	0.52	0.52	0.56	0.46	0.60
$FeO_t/(FeO_t+MgO)$	0.49	0.46	0.47	0.55	0.54	0.59	0.61	0.58	0.58	0.53	0.55	0.56	0.55	0.55	0.52	0.51	0.52	0.53	0.59	0.60	0.64	0.64	0.64	0.64	0.64	0.64	0.66	0.65
Mg#	0.64	0.67	0.61	0.59	0.60	0.55	0.55	0.56	0.56	0.61	0.59	0.58	0.59	0.59	0.62	0.63	0.62	0.61	0.55	0.54	0.50	0.50	0.50	0.49	0.49	0.50	0.48	0.49

Data Source: Oliveira (2005). Chemical ratios: Mg# molecular ratio Mg/(Mg+Fe); K/Na molecular ratio. Eu/Eu* = EuN / (0.5 * (SmN + GdN). E = epidote; B = biotite; A = amphibole; Qz = quartz; D = diorite; MzD = monzodiorite; Mz = monzonite; GD = granodiorite; MzG = monzogranite.

show significant variations among the different groups, except for the quartz monzonitic enclaves which are enriched in K_2O with K/Na ratios > 1.

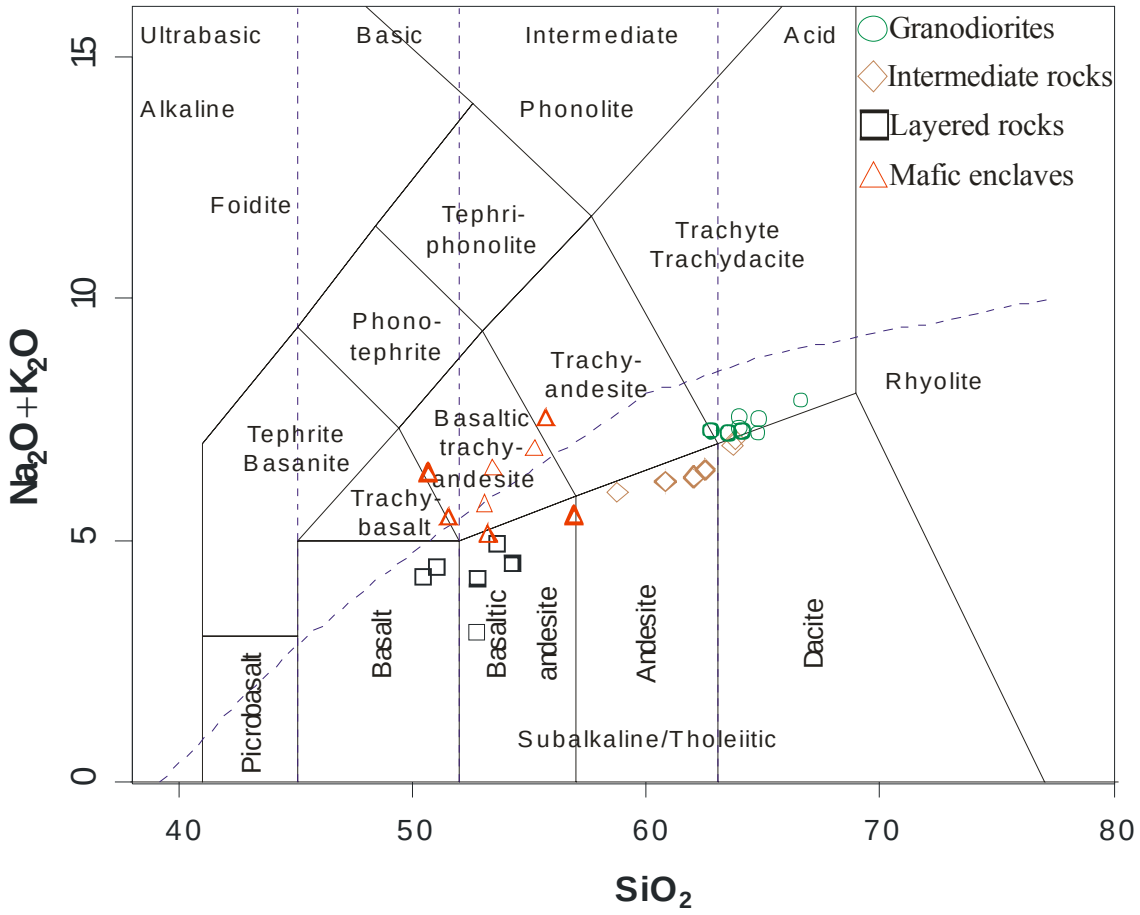

Fig. 7 - Total alkali-silica diagram (TAS) showing the composition of rocks of the Rio Maria suite (Bannach area). TAS diagram classification according to Le Bas *et al.* (1986).

The patterns of rare earth elements (REE) in the granodiorites and intermediate rocks are similar, with pronounced enrichment in light rare earth elements (LREE) and strong to moderate fractionation of heavy rare earth elements (HREE), associated with small or absent Eu anomaly. The patterns of rare earth elements (REE) in the layered rocks and enclaves show a less pronounced enrichment in LREE, and minor fractionation of HREE relative to the granodiorites and intermediate rocks [Table 2; $(La/Yb)_N$ ratios from 6.57 to 11.32, enclaves; 11.92 to 14.37, layered rocks; 17.20 to 41.28, intermediate rocks; 15.52 to 44.38, granodiorites], and show either

a small/absent (layered rocks) or marked negative europium anomaly (enclaves; Eu/Eu* from 0.65 to 0.75).

Despite these geochemical similarities, Oliveira *et al*. (2009) have shown that granodiorites and intermediate rocks must have followed two distinct trends during crystallization. The contrast in Mg#, Zr, Sr, Rb/Sr, Sr/Ba, in both groups of rocks (Fig. 5a, b, c and 6a, b, c, d) and the strong overlap of REE patterns between the intermediate rocks and the Rio Maria granodiorite (Fig. 8) do not favor the hypothesis that they were linked by fractional crystallization. Thus, Oliveira *et al*. (2009) concluded that granodiorites and intermediate rocks probably derived from two distinct magmas, both with sanukitoid affinity, possibly originated from different degrees of melting of a modified mantle source.

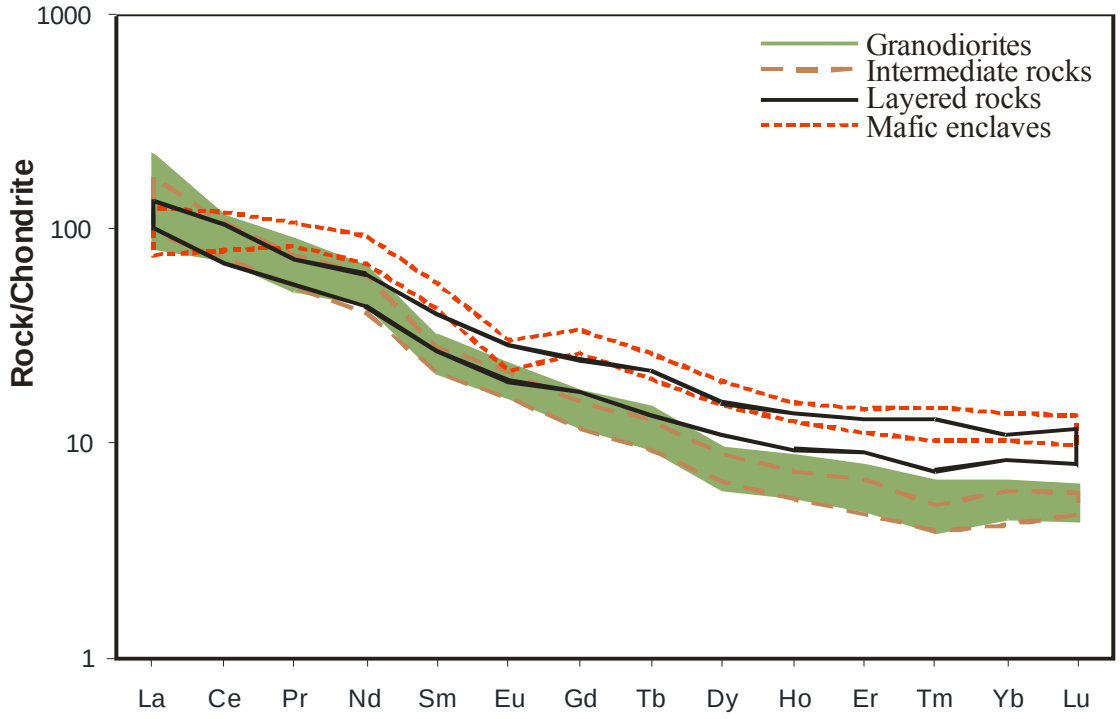

Fig. 8 - Chondrite-normalized REE patterns for the rocks of the Rio Maria suite of Bannach area (normalization values from Evensen *et al*., 1978).

5 - MAGNETIC SUSCEPTIBILITY AND Fe-Ti OXIDES

Bulk magnetic susceptibility values were measured in representative samples of granodiorites and intermediate rocks of the Rio Maria suite of Bannach area, using SI-1 flat and cylindrical coils in the magnetic petrology laboratory of UFPA. The granodiorite samples

display generally very low magnetic susceptibility values (MS < $1x10^{-3}$ in SI volume units; Dias *et al*., 2006; Nascimento, 2006) whilst the intermediate rocks has low to intermediate MS (mostly > $1x10^{-3}$ SI units). The layered rocks display MS values that, in most cases, overlap those of the intermediate rocks with the lowest MS values.

In the granodiorites, Fe-Ti oxide minerals are rare to absent, excepting a few samples in which 0.1 to 0.2 % magnetite + ilmenite + hematite modal contents were observed. In the intermediate rocks, on the other hand, opaque minerals modal contents vary from 0.1 to 1.0 %, and magnetite and hematite are common accessory phases, which is consistent with their higher MS values as compared to the granodiorites. In the layered rocks, opaque modal contents are variable but goethite is relatively abundant and magnetite is scarce, explaining the low MS values of these rocks.

The magnetic behavior of the studied sanukitoids is not uniform. The intermediate rocks can be classified as magnetite-series granitoids, according to the terminology of Ishihara (1977, 1981). However, assuming that the present iron-titanium oxide assemblage is representative of the magmatic stage of evolution, the granodiorite would be more akin to the ilmenite series of the same author (but see below). The magnetic behavior of the layered rocks is also ambiguous, but they approach more that of the intermediate rocks than the granodiorite.

6 – MINERALOGY

6.1 – Analytical methods

The compositions of amphibole, biotite and epidote minerals were determined by electron microprobe at the laboratory of the University at São Paulo, using a JEOL *superprobe* JXA-8600 microprobe using the following analytical conditions: 15 kV acceleration voltage, 20 nA sample current, 10 s total counting time.

6.2 – Amphibole chemistry

The amphibole was analyzed on one sample each of granodiorite, intermediate rock, mafic enclave, and on two samples of layered rocks (Table 3). According to the classification of Leake *et al*. (1997), the amphibole from the Rio Maria suite is an Mg-hornblende; subordinate pargasite and Mg-hastingsite occur in the layered rocks and mafic enclaves (Fig. 9). The amphibole rims are enriched in silica and impoverished in alumina relative to the cores,

displaying Mg-hornblende to actinolitic hornblende compositions, the later being found only in the intermediate rocks and in the cumulate crystals of layered rocks (Fig. 9).

Amphibole Fe/(Fe+Mg) ratios (Fe#) range from 0.25-0.43 in the different rocks of the Rio Maria suite (Table 3; Fig. 10), the lowest values being found in the amphibole cores of the cumulate crystals of the layered rocks (0.25-0.33; Fig. 10a, b). The Fe# of the amphibole core increases gradually from the intermediate rocks to the intercumulate layered rocks (respectively, 0.29-0.35 and 0.28-0.40). The highest Fe# values are found in the amphibole core of enclaves (0.37-0.43) and granodiorite (0.36-0.43; Fig. 10a, b). A similar pattern is observed in the amphibole rim

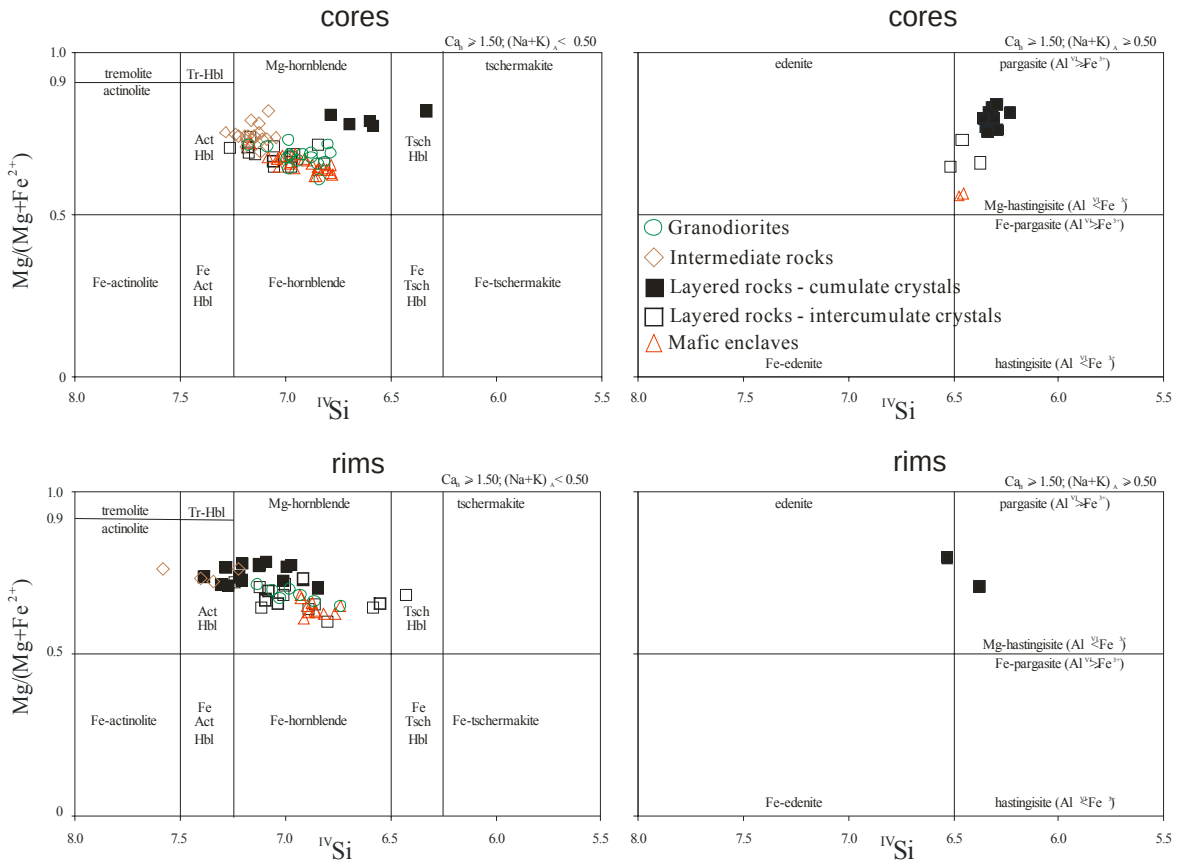

Fig. 9 – Classification diagrams of amphibole (Leake *et al.*, 1997) for samples of the different rocks of the Rio Maria suite (Bannach area).

compositions of the different studied rocks (Table 3; Fig. 10c, d).

The ^{IV}Al and ^{IV}Al + ^{VI}Al contents are very similar in the amphibole crystals of the Rio Maria suite, except for the amphibole cores of cumulate crystals of the layered rocks, which show higher ^{IV}Al and total Al contents (Table 3; Fig. 10a, c). The significant difference in ^{IV}Al

Table 3
Representative electron microprobe analyses of amphibole from the Rio Maria suite (Bannach area).

	Layered rocks								Mafic enclaves				Intermediate rocks				Granodiorites			
Sample	MFR-12B								MFR-27C				ADR-4B				ADR-3A			
Facies	Cumulate crystals				Intercumulate crystals				EBAD				EBAQzD				EBAGD			
	core	core	rim	rim	core	core	rim	rim	core	core	rim	rim	core	core	rim	rim	core	core	rim	rim
SiO_2 (wt.%)	43,359	43,462	49,884	50,349	48,997	49,440	47,834	49,941	47,012	47,555	47,609	47,767	48,356	49,088	49,839	50,549	47,501	47,923	48,602	49,367
TiO_2	1,592	1,274	0,522	0,395	0,538	0,392	0,533	0,421	1,063	0,986	1,170	1,024	0,469	0,454	0,518	0,162	0,918	0,462	0,554	1,030
Al_2O_3	11,685	11,862	5,736	5,245	5,887	5,858	6,963	5,349	6,980	6,683	7,048	6,501	5,964	5,619	4,942	4,741	7,362	7,227	6,581	5,968
FeO	10,417	10,314	11,219	11,727	13,015	12,919	13,218	12,395	15,372	15,187	15,349	15,768	13,852	13,453	13,537	12,496	14,920	15,012	15,429	13,118
MnO	0,131	0,140	0,186	0,247	0,227	0,234	0,223	0,238	0,348	0,310	0,343	0,332	0,281	0,274	0,329	0,267	0,346	0,348	0,351	0,349
MgO	14,910	14,961	15,592	15,232	14,306	14,651	14,139	15,066	12,993	12,943	13,053	13,353	13,900	14,573	14,780	15,109	12,578	13,006	13,342	14,423
CaO	12,611	12,482	13,046	13,075	12,635	12,847	12,513	12,843	12,229	12,420	12,209	12,355	12,435	12,069	11,811	12,678	12,269	12,383	12,376	12,234
Na_2O	1,771	1,551	0,646	0,582	0,929	0,775	0,873	0,688	1,091	0,833	0,918	0,930	0,879	0,915	0,711	0,636	0,940	0,741	1,002	0,960
K_2O	0,836	0,805	0,404	0,356	0,453	0,383	0,523	0,334	0,741	0,663	0,704	0,678	0,474	0,447	0,406	0,294	0,684	0,581	0,537	0,490
F	0,119	0,005	*	*	*	*	0,113	0,070	0,033	0,004	0,116	0,000	0,115	0,079	0,076	0,148	0,456	0,116	*	*
Cl	0,018	0,018	*	0,026	*	0,023	0,034	0,018	0,049	0,067	0,054	0,034	0,052	0,060	0,112	0,026	0,031	0,044	0,036	0,016
O-F-Cl	0,050	0,010	*	*	*	*	0,060	0,030	0,020	0,020	0,060	0,010	0,060	0,050	0,060	0,070	0,200	0,060	*	*
Total	97,450	96,870	*	*	*	*	96,970	97,360	97,910	97,650	98,570	98,740	96,780	97,030	97,060	97,110	98,010	97,840	*	*
Structural formulae as 13-CNK																				
Si	6,307	6,317	7,220	7,309	7,178	7,183	7,006	7,247	6,902	6,991	6,925	6,933	7,121	7,150	7,225	7,346	6,987	6,998	7,031	7,136
Al^{IV}	1,693	1,683	0,780	0,691	0,822	0,817	0,994	0,753	1,098	1,009	1,075	1,067	0,879	0,850	0,775	0,654	1,013	1,002	0,969	0,864
Fe^{3+}	0,450	0,582	0,166	0,101	0,195	0,257	0,396	0,251	0,459	0,368	0,492	0,569	0,355	0,529	0,651	0,279	0,285	0,466	0,479	0,340
Al^{VI}	0,309	0,348	0,198	0,206	0,194	0,185	0,207	0,161	0,108	0,148	0,132	0,044	0,155	0,114	0,068	0,157	0,262	0,241	0,153	0,152
Ti	0,174	0,139	0,057	0,043	0,059	0,043	0,059	0,046	0,117	0,109	0,128	0,112	0,052	0,050	0,056	0,018	0,102	0,051	0,060	0,112
Mg	3,233	3,242	3,364	3,297	3,124	3,173	3,087	3,259	2,844	2,837	2,830	2,889	3,052	3,164	3,194	3,273	2,758	2,831	2,877	3,108
Fe^{2+}	0,818	0,672	1,192	1,323	1,400	1,313	1,223	1,254	1,429	1,500	1,375	1,345	1,351	1,110	0,990	1,239	1,551	1,368	1,388	1,246
Mn	0,016	0,017	0,023	0,030	0,028	0,029	0,028	0,029	0,043	0,039	0,042	0,041	0,035	0,034	0,040	0,033	0,043	0,043	0,043	0,043
Ca	1,966	1,944	2,000	2,000	1,983	2,000	1,964	1,997	1,924	1,956	1,903	1,921	1,962	1,883	1,834	1,974	1,934	1,938	1,918	1,895
Na	0,034	0,056	0,000	0,000	0,017	0,000	0,036	0,003	0,076	0,044	0,097	0,079	0,038	0,117	0,166	0,026	0,066	0,062	0,082	0,105
ANa	0,465	0,381	0,181	0,164	0,247	0,218	0,212	0,190	0,234	0,194	0,162	0,183	0,213	0,142	0,034	0,153	0,202	0,147	0,199	0,164
AK	0,155	0,149	0,075	0,066	0,085	0,071	0,098	0,062	0,139	0,124	0,131	0,126	0,089	0,083	0,075	0,055	0,128	0,108	0,099	0,090
Sum A	0,620	0,530	0,279	0,264	0,332	0,289	0,309	0,252	0,373	0,318	0,292	0,309	0,302	0,225	0,109	0,208	0,330	0,256	0,299	0,254
Sum cat	15,620	15,530	15,279	15,264	15,332	15,289	15,309	15,252	15,373	15,318	15,292	15,309	15,302	15,225	15,109	15,208	15,330	15,256	15,299	15,254
Al_{total}	2,002	2,031	0,978	0,897	1,016	1,002	1,201	0,914	1,206	1,157	1,207	1,111	1,034	0,964	0,843	0,811	1,275	1,243	1,122	1,016
Fe/(Fe+Mg)	0,274	0,269	0,285	0,300	0,335	0,327	0,338	0,312	0,393	0,392	0,391	0,391	0,354	0,334	0,330	0,313	0,396	0,387	0,387	0,333

Total Fe reported as FeO. Key to abbreviations. *not determinated; E = epidote; B = biotite; A = amphibole; Qz = quartz; D = diorite; GD = granodiorite.

and total Al contents between the core and rim amphibole of the cumulate crystals is remarkable (Fig. 10a, c).

6.3 – Biotite chemistry

The dark mica from different rocks of Rio Maria suite is a magnesium-biotite (Table 4; Fig. 11a, Foster, 1960; Rieder *et al*., 1998), with Fe/(Fe+Mg) ratios (Fig. 11b) increasing from the intermediate rocks and intercumulate biotite crystals of layered rocks (0.36-0.38), toward the granodiorite (0.40-0.42) and mafic enclaves (0.42-0.46). Fe/(Fe+Mg) ratios in coexisting

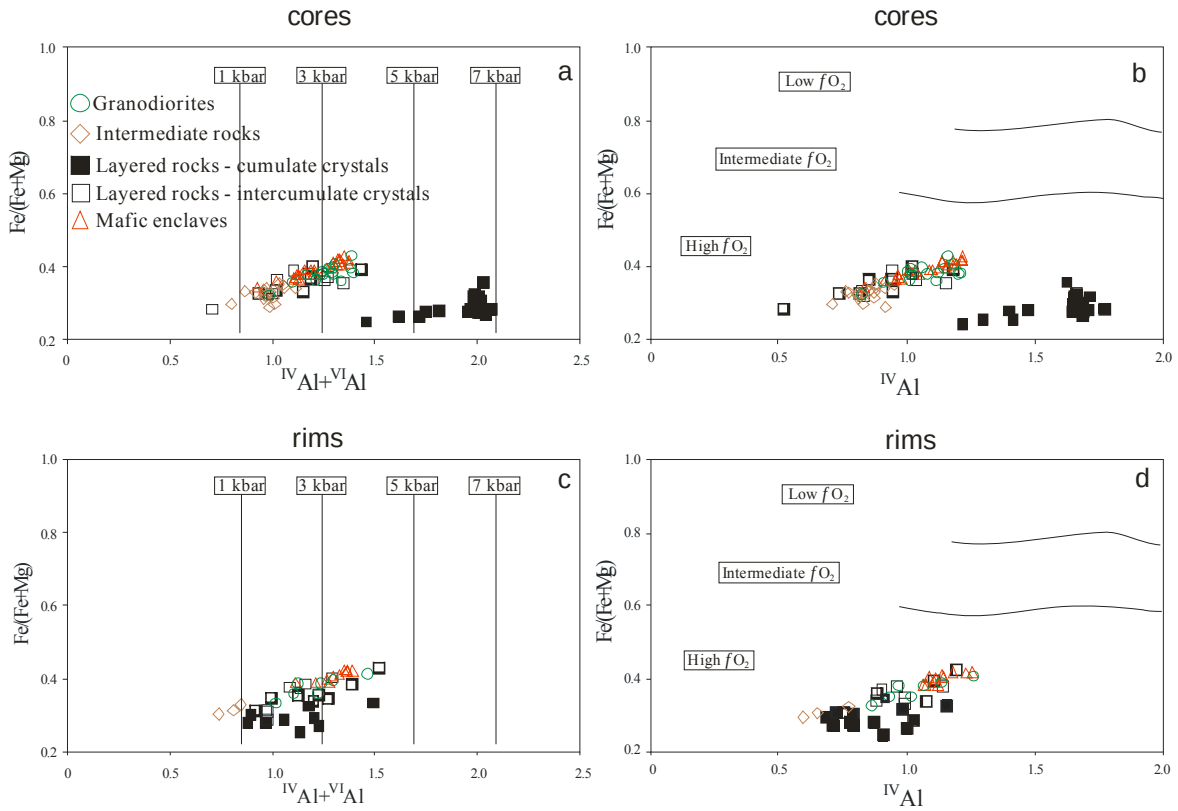

Fig. 10 - (a, c) amphibole Fe/(Fe+Mg) x Al_{tot} diagrams (Anderson & Smith, 1995) showing the possible crystallization pressures for amphibole of the Rio Maria suite; (b, d) amphibole Fe/(Fe+Mg) x ^{IV}Al diagrams (Anderson & Smith, 1995) showing the possible oxygen fugacity conditions during the crystallization of rocks of the Rio Maria suite (Bannach area).

hornblende and biotite are similar in the different studied rocks, except in the mafic enclaves, where biotite has Fe/(Fe+Mg) ratios higher than those of associated amphibole (Fig. 11b).

Table 4
Representative electron microprobe analyses of biotite from the Rio Maria suite (Bannach area).

	Layered rocks			Mafic enclaves			Intermediate rocks			Granodiorites		
Sample	MFR-12B			MFR-27C			ADR-4B			ADR-3A		
Facies	Intercumulus			EBAD			EBAQzD			EBAGD		
SiO_2 (wt.%)	37,213	37,753	37,820	37,308	37,322	37,648	37,330	37,384	37,878	37,400	37,534	37,759
TiO_2	1,034	1,119	1,170	1,317	1,164	1,212	0,722	0,395	0,477	1,285	1,028	1,250
Al_2O_3	15,533	16,017	15,947	15,277	15,666	15,809	16,075	16,001	16,159	15,720	15,091	14,979
FeO	14,560	15,128	13,866	18,216	18,241	18,220	15,134	14,841	14,623	16,714	16,309	15,689
MnO	0,206	0,169	0,147	0,164	0,226	0,224	0,208	0,186	0,165	0,210	0,220	0,200
MgO	14,051	13,814	13,657	12,636	12,720	12,766	14,205	14,886	14,590	12,959	13,654	13,395
CaO	0,059	0,022	0,000	0,018	0,037	0,004	0,006	0,000	0,000	0,000	0,051	0,011
Na_2O	0,009	0,053	0,041	0,069	0,108	0,117	0,029	0,108	0,122	0,177	0,075	0,109
K_2O	9,862	9,883	9,798	9,492	9,523	9,479	9,875	9,322	9,342	9,381	9,490	9,448
F	0,294	0,108	0,225	0,217	0,217	0,071	0,361	0,000	0,154	0,292	0,252	0,083
H_2O	3,857	3,948	3,891	3,895	3,896	3,966	3,826	4,000	3,926	3,859	3,878	3,960
Total	92,821	94,066	92,671	94,714	95,224	95,550	93,945	93,123	93,510	94,138	93,704	92,923
Structural formulae on the basis of 22 oxygens												
Si	5,721	5,717	5,780	5,702	5,674	5,685	5,683	5,693	5,738	5,708	5,748	5,798
Al^{IV}	2,279	2,283	2,220	2,298	2,326	2,315	2,317	2,307	2,262	2,292	2,252	2,202
Al^{VI}	0,535	0,576	0,652	0,453	0,481	0,499	0,568	0,565	0,622	0,535	0,472	0,508
Ti	0,120	0,127	0,134	0,151	0,133	0,138	0,083	0,045	0,054	0,147	0,118	0,144
Fe^{2+}	1,872	1,916	1,772	2,328	2,319	2,301	1,927	1,890	1,852	2,133	2,089	2,015
Mn	0,027	0,022	0,019	0,021	0,029	0,029	0,027	0,024	0,021	0,027	0,029	0,026
Mg	3,220	3,119	3,111	2,879	2,883	2,874	3,224	3,380	3,295	2,948	3,117	3,066
Na	0,003	0,016	0,012	0,020	0,032	0,034	0,009	0,032	0,036	0,052	0,022	0,032
K	1,934	1,909	1,910	1,851	1,847	1,826	1,918	1,811	1,805	1,826	1,854	1,851
F	0,143	0,052	0,109	0,105	0,910	0,034	0,174	0,000	0,074	0,015	0,013	0,004
Fe/(Fe+Mg)	0,368	0,381	0,363	0,447	0,446	0,445	0,374	0,359	0,360	0,420	0,401	0,397

Total Fe reported as FeO. Key to abbreviations. E = epidote; B = biotite; A = amphibole; Qz = quartz; D = diorite; GD = granodiorite.

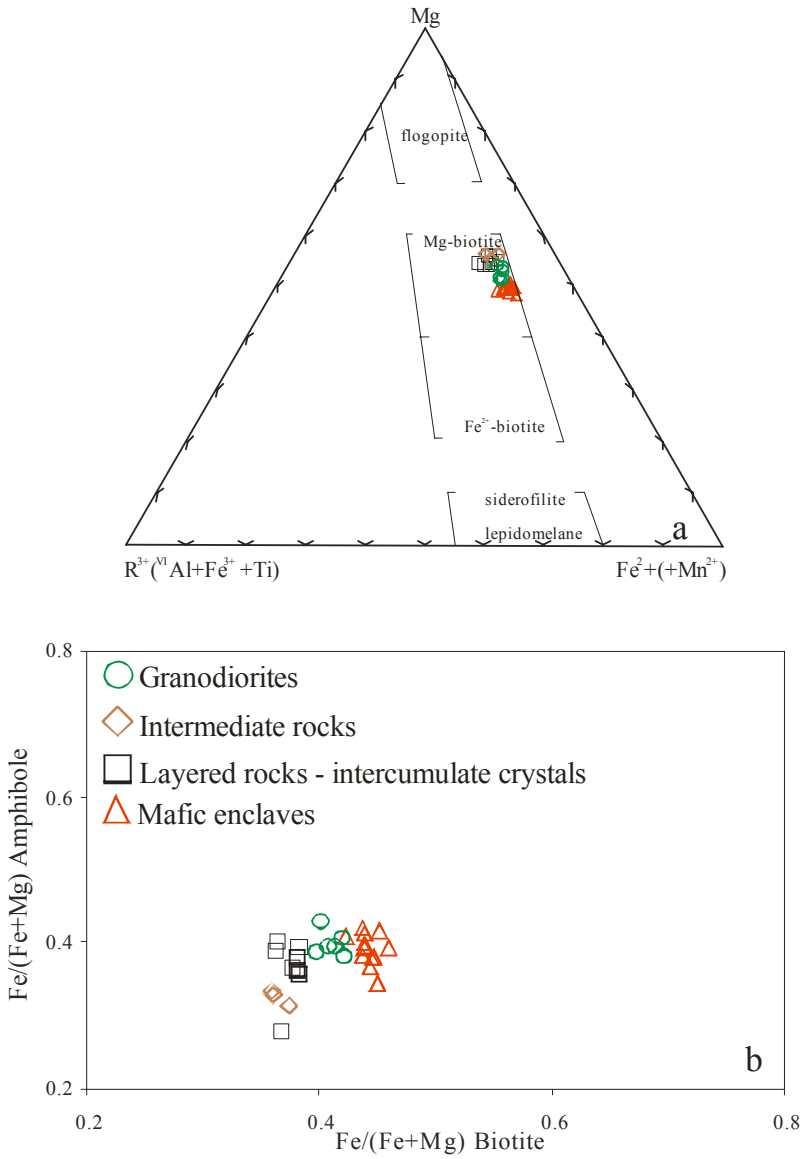

Fig. 11 (a) Mg-R^{3+}-Fe^{2+} Classification diagram (Foster, 1960) for micas of the different rocks of the Rio Maria suite; (b) amphibole Fe/(Fe+Mg) x biotite Fe/(Fe+Mg) comparative plot for amphiboles and biotites of the Rio Maria suite (Bannach area).

The Al contents show a narrow range in the biotite of the studied sanukitoid suite, varying from 15 to 16.3 wt % (Table 4). The biotite has also low TiO_2 contents (mostly below 1.4 wt. %), the lowest values being found in the intermediate rocks (0.39-0.72 wt. %).

6.4 – Epidote chemistry

Textural criteria described by Zen & Hammarstrom (1984) were used by Oliveira *et al*. (2009) to distinguish magmatic from secondary epidote in rocks of the Rio Maria suite. These criteria include the presence of allanite-rich core and chemical zoning in magmatic epidote, both features commonly observed in the rocks of Rio Maria suite (see above). In the present work, additional compositional criteria (Tulloch, 1979; Evans and Vance, 1987), based on the pistacite (Ps = molar [Fe^{3+}/ (Fe^{3+}+Al)]x100) and the TiO_2 wt. % content of epidote were also used to evaluate its magmatic vs. subsolidus origin. More than sixty microprobe analyses of epidote crystals interpreted as magmatic on textural grounds and a few comparative analyses on secondary epidote grains were performed. The core- and rim-composition of at least eight grains per group of rocks were determined (Table 5, Fig. 12).

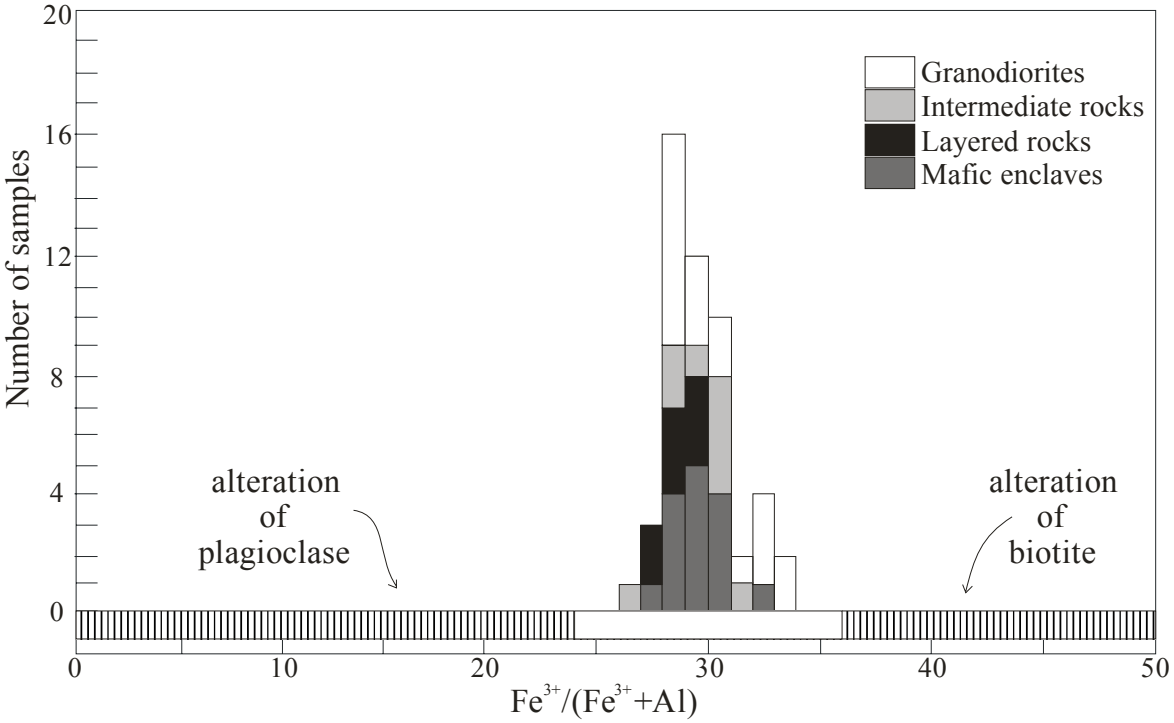

Fig. 12 - Histogram of mole percent (mol%) pistacite (Ps) in magmatic epidotes from different rocks of the Rio Maria suite (Bannach area). The compositional ranges of epidote from alteration of plagioclase and biotite are from Tulloch (1979).

Euhedral epidote crystals of the Rio Maria suite have < 0.2 wt.% TiO_2 (Table 5), whereas epidote crystals replacing biotite have > 0.6 wt.% TiO_2. These results are in agreement with a magmatic and a secondary origin, respectively (Evans and Vince, 1987). Tulloch (1979) and Vyhnal *et al*. (1991) reported pistacite contents between 25 and 29 (mol%) as typical of

Table 5
Representative electron microprobe analyses of epidote from the Rio Maria suite (Bannach area).

	Layered rocks						Mafic enclaves						Intermediate rocks						Granodiorites					
Sample	MFR-12B						MFR-27C						ADR-4B						ADR-3A					
Facies	Intercumulus						EBAD						EBAQzD						EBAGD					
	core	core	core	rim	rim	rim	core	core	core	rim	rim	rim	core	core	core	rim	rim	rim	core	core	core	rim	rim	rim
SiO_2 (wt.%)	37,464	37,206	37,082	37,655	37,721	37,280	37,374	37,704	37,398	37,585	37,489	37,767	37,483	36,958	37,376	37,481	37,078	37,383	37,217	36,952	36,181	36,994	37,115	36,392
TiO_2	0,147	0,010	0,098	0,069	0,039	0,015	0,078	0,000	0,069	0,108	0,064	0,064	0,000	0,039	0,123	0,054	0,000	0,113	0,010	0,074	0,108	0,000	0,088	0,020
Al_2O_3	22,477	22,491	22,018	22,735	22,759	22,865	22,127	22,324	21,738	22,386	22,428	22,330	21,792	21,891	21,429	22,828	22,546	22,118	22,835	22,233	21,131	22,779	22,609	21,460
Fe_2O_3	13,626	14,445	14,470	13,612	14,112	14,492	14,268	14,684	14,992	13,607	14,045	15,183	14,325	14,698	15,348	12,684	14,203	13,951	14,894	15,138	16,323	14,091	15,364	16,134
MgO	0,000	0,000	0,007	0,012	0,021	0,007	0,055	0,000	0,007	0,006	0,000	0,001	0,006	0,006	0,006	0,025	0,020	0,030	0,014	0,018	0,015	0,000	0,013	0,000
CaO	23,277	22,206	22,816	23,475	22,869	23,004	22,341	23,482	22,976	23,170	22,732	22,697	22,842	22,525	22,719	22,599	21,842	22,918	22,694	23,457	22,893	23,103	23,008	22,360
MnO	0,108	0,124	0,086	0,115	0,110	0,114	0,182	0,094	0,105	0,128	0,112	0,153	0,133	0,170	0,179	0,146	0,120	0,203	0,183	0,121	0,076	0,195	0,195	0,042
Total	97,099	96,482	96,577	97,673	97,631	97,777	96,425	98,288	97,285	96,990	96,870	98,195	96,581	96,287	97,180	95,817	95,809	96,716	97,847	97,993	96,727	97,162	98,392	96,408
Number of cations on the basis of 13 oxygens																								
Si	3,135	3,132	3,128	3,133	3,138	3,103	3,136	3,128	3,137	3,148	3,142	3,133	3,158	3,128	3,142	3,161	3,138	3,143	3,099	3,085	3,076	3,099	3,083	3,092
Ti	0,009	0,001	0,006	0,004	0,003	0,001	0,005	0,000	0,004	0,007	0,004	0,004	0,000	0,003	0,008	0,003	0,000	0,007	0,001	0,005	0,007	0,000	0,006	0,001
Al	2,217	2,231	2,189	2,230	2,231	2,243	2,188	2,183	2,149	2,210	2,216	2,183	2,164	2,184	2,123	2,269	2,249	2,191	2,241	2,188	2,117	2,249	2,213	2,149
Fe^{3+}	0,858	0,915	0,919	0,852	0,883	0,908	0,901	0,917	0,946	0,858	0,886	0,948	0,908	0,936	0,971	0,805	0,905	0,883	0,933	0,951	1,044	0,888	0,960	1,032
Mg	0,000	0,000	0,001	0,002	0,003	0,001	0,007	0,000	0,001	0,001	0,000	0,000	0,001	0,001	0,001	0,003	0,003	0,004	0,002	0,002	0,002	0,000	0,002	0,000
Ca	2,087	2,003	2,062	2,093	2,038	2,052	2,009	2,087	2,065	2,079	2,041	2,018	2,062	2,043	2,046	2,042	1,981	2,064	2,025	2,098	2,085	2,074	2,047	2,035
Mn	0,008	0,009	0,006	0,008	0,008	0,008	0,013	0,007	0,008	0,009	0,008	0,011	0,010	0,012	0,013	0,010	0,009	0,015	0,013	0,009	0,006	0,014	0,014	0,003
Ps	28	29	30	28	28	29	29	30	31	28	29	30	29	30	31	26	29	29	29	30	33	28	30	32

Total Fe reported as Fe_2O_3. Key to abbreviations. Ps = molar $[Fe^{3+}/(Fe^{3+}+Al)]x100$; E = epidote; B = biotite; A = amphibole; Qz = quartz; D = diorite; GD = granodiorite.

magmatic epidote. Tulloch (1979) also showed that epidote grains formed in the same rock by subsolidus alteration of plagioclase and biotite have Ps_{0-24} and Ps_{36-48}, respectively (Fig. 12). In addition, analyses of synthetic epidotes obtained by Liou (1973) indicate a pistacite content range of 25 to 35%. The mole percent Ps of magmatic epidote in the Rio Maria suite lies in a narrow range Ps_{26} - Ps_{33} (see Sial *et al*., 1999), with a slight core-to-rim variation of Al and Fe contents (Table 5). The pistacite contents of inferred magmatic epidote in the granodiorite range between 28 and 33. Similar values are found in the layered rocks (Ps_{28} to Ps_{30}), mafic enclaves (Ps_{28} to Ps_{31}), and intermediate rocks (Ps_{26} to Ps_{31}).

Hence, the chemical data obtained on epidote crystals of the different rocks of the Rio Maria suite and interpreted as magmatic on textural grounds, show that they have pistacite and TiO_2 contents within the range expected for magmatic epidote according to previous studies (Liou, 1973; Tulloch, 1979; Vyhnal *et al*., 1991; Sial *et al*., 1999)

7 – REVIEW OF EXPERIMENTAL STUDIES ON SIMILAR ROCKS

Naney (1983) performed experiments on a synthetic granodioritic composition with higher SiO_2, Al_2O_3, and CaO and lower Fe_2O_3 and MgO contents compared to the Rio Maria granodiorite. Naney (1983) emphasized the dependence of water content in the liquid for amphibole stability and described the occurrence of magmatic epidote as a near solidus phase at high pressure (800 MPa). More recently, Schmidt & Thompson (1996) performed experiments at high pressure (750 to 1800 MPa) and from 650 to 800°C, on a rock of granodioritic composition to estimate the magmatic stability field of epidote as a function of pressure,

Table 6
Chemical composition of the starting materials (wt %) of experimental studies on similar rocks and comparison with representative samples of Rio Maria suite (Bannach area).

	Synthetic Granodiorite[1]	Alpine Adamello Granodiorite[2]	Pinatubo, 1991[3]	Lyngdal granodiorite[4]		Layered rocks[5]	Mafic enclaves[5]	Intermediate rocks[5]	Granodiorites[5]
Sample	R5+10M	Au7	Tuff	98N50	98N06	MFR-12B	MFR-27C	ADR-4B	ADR-3A
SiO_2 (wt.%)	67.51	66.66	64.60	60.20	65.20	52.60	50.51	60.51	63.9
TiO_2	0.53	0.40	0.53	1.74	1.11	0.56	0.88	0.44	0.43
Al_2O_3	17.45	15.92	16.50	13.8	14.4	10.91	16.19	14.03	14.82
FeO_t	2.20	3.28	4.37	9.26	5.80	8.91	9.01	5.56	4.27
MnO	0.10	0.11	0.10	0.16	0.10	0.15	0.13	0.09	0.06
MgO	1.19	1.58	2.39	2.15	1.39	10.51	5.65	5.37	2.39
CaO	3.52	4.43	5.23	5.35	5.50	9.3	7.61	4.73	4.02
Na_2O	3.90	2.49	4.49	3.15	3.27	2.06	4.06	4.04	4.05
K_2O	3.99	2.63	1.54	2.88	3.15	1.03	2.33	2.16	3.21
P_2O_5	-	0.12	-	0.85	0.92	0.15	0.45	0.18	0.14

Data Source: [1] Naney (1983); [2] Schmidt and Thompson (1996); [3] Pallister et al. (1996) used in Scaillet and Evans (1999) and Prouteau and Scaillet (2003); [4] Bogaerts et al. (2006); [5] Oliveira et al. (2009).

temperature and oxygen fugacity. The used granodiorite has also higher SiO_2, Al_2O_3, and CaO and lower Fe_2O_3 and MgO contents relative to the Rio Maria granodiorite. Schmidt & Thompson (1996) demonstrated that oxidizing conditions enhances the magmatic stability field of epidote, implying that it remains stable at higher temperatures and lower pressures relative to previous estimates (Naney, 1983; Johnston & Wyllie, 1988; Van der Laan & Wyllie, 1992).

The samples selected for experimental studies of the Holocene Pinatubo dacite (Scaillet & Evans, 1999; Prouteau & Scaillet, 2003) and Proterozoic Lyngdal granodiorite (Bogaerts *et al*., 2006) have silica contents similar to those of the granodiorite and intermediate rocks of the Archean Rio Maria suite (Table 6). The Pinatubo dacite ressembles the Rio Maria granodiorite also in its TiO_2, FeO_t, MgO, and Na_2O contents, differing slightly by a higher Al_2O_3 and CaO and, more significantly, lower K_2O contents. In contrast, the Lyngdal granodiorites differ from the Rio Maria granodiorite and intermediate rocks by its higher the FeO/(FeO+MgO) ratios and TiO_2 and CaO contents.

Despite the aforementioned compositional differences between the Rio Maria sanukitoid rocks and those used in phase equilibrium studies, the latter will be employed in this paper in an effort to constrain the intensive parameters prevalent during the crystallization of the Rio Maria suite, keeping in mind the possible distortions of phase equilibria that may arise from minor compositional variations.

Scaillet & Evans (1999) performed crystallization experiments on a representative sample of a crystal-rich dacite with 65 wt. % SiO_2 ejected during the 15 june 1991 eruption of Mount Pinatubo, to estimate the pre-eruption conditions of that major volcanic event. The experiments were performed at ~220 MPa and between 760 and 900°C. The fO_2 was varied from NNO up to NNO + 2.7, but most of the experiments were carried out at NNO + 1 to NNO + 2. All experiments were fluid saturated and water activity (aH_2O) was varied by addition of CO_2 to the charges. Prouteau & Scaillet (2003) performed crystallization experiments on the same dacite rock used by Scaillet & Evans (1999), at temperatures varying between 750 and 1000°C, and fO_2 of NNO + 2 to NNO + 4.8, but exploring more specifically the effect of pressure on phase topology, by performing experiments at 400 MPa and 960 MPa, under variable water activity.

The phase diagram at 220 MPa of the Pinatubo dacite (Scaillet & Evans, 1999) indicates that orthopyroxene, plagioclase, and magnetite are the liquidus phases, crystallizing above

900°C for $H_2O \leq 5.5$ wt. %. At higher water contents, orthopyroxene is no more stable and hornblende becomes a near liquidus phase. Although hornblende and orthopyroxene stability fields partly overlap, experimental results indicate that their relative occurrence is controlled by a peritetic reaction (orthopyroxene + liquid → hornblende). A similar effect of water on amphibole and pyroxenes stability fields is reported in experimental studies performed on more silicic compositions (Naney, 1983; Dall'Agnol *et al*., 1999; Klimm *et al*., 2003). Phase equilibria performed by Costa *et al*. (2004) on a more potassium-rich dacite yielded results comparable to those obtained for the Pinatubo dacite, except for a slightly expanded field of biotite, in agreement with the K_2O-rich nature of the starting product.

The phase relations at 400 MPa (Prouteau & Scaillet, 2003) are similar to those established at 220 MPa with two important differences: (1) for $H_2O_{melt} < 7$ wt. %, the presence at the liquidus of clinopyroxene, besides plagioclase and orthopyroxene; (2) for $H_2O_{melt} > 7$ wt. %, amphibole becomes the liquidus silicate phase, crystallizing above 900°C and before plagioclase. At 960 MPa (Prouteau & Scaillet, 2003), the phase diagram shows again a similar topology relative to that at 400 MPa. Magnetite is the liquidus phase, followed by clinopyroxene, except for the most water-rich domain in the diagram ($H_2O_{melt} > 9$ wt. %), where amphibole replaces clinopyroxene. Amphibole is stable up to ~950°C for $H_2O_{melt} > 7$ wt % and its thermal stability decreases at lower H_2O_{melt}. Prouteau & Scaillet (2003) suggest that clinopyroxene displays a peritetic relationship with amphibole for water-rich compositions.

The comparison between 220, 400, and 960 MPa isobaric sections obtained at high fO_2 in the Pinatubo dacite thus shows that the main effect of increasing pressure is to destabilize orthopyroxene, which is not observed in the experiments at 960 MPa. Moreover, for melt water contents higher than ~7-9 wt % and pressures above 400 MPa amphibole becomes the liquidus silicate phase.

The Proterozoic Lyngdal granodiorite (950 Ma) of southern Norway belongs to a series of hornblende-biotite metaluminous ferroan granitoids and have many geochemical characteristics of rapakivi granitoids (Bogaerts *et al*., 2006). Bogaerts *et al*. (2006) performed crystallization experiments on two samples of granodiorites with 60 and 65 wt. % SiO_2 (Table 6). Experiments were performed at 400 MPa, from 775 to 1000°C, and at fO_2 of NNO to NNO + 1, under fluid-saturated conditions with variable H_2O-CO_2 ratios for each temperature. For both compositions, clinopyroxene is the liquidus silicate phase and the crystallization temperature for

amphibole is around 900°C but its stability field is restricted to water-rich compositions (H_2O_{melt} > 5 wt % to 6 wt %). The amphibole is never the liquidus silicate phase under any explored conditions.

8 – DISCUSSION: PARAMETERS OF CRYSTALLIZATION OF THE RIO MARIA SANUKITOID SUITE

The available data on the Rio Maria suite demonstrate that its major geochemical attributes better fit with those of the Pinatubo dacite, rather than with compositions used in other experimental studies (Table 6). The phase relations obtained in the experiments on the Pinatubo dacite, and more specifically those at pressures of 400 and 960 MPa (Prouteau & Scaillet, 2003), are generally consistent with the order of crystallization deduced for the Rio Maria suite on the basis of mineralogical and petrographic studies. In contrast, the experimental study at 400 MPa on the Lyngdal granodiorites indicate that clinopyroxene is the liquidus phase regardless of the melt water content, an observation difficult to reconcile with the total absence of this mineral in all Rio Maria rocks so far analysed. The Lyngdal phase equilibria appear thus less appropriate to deduce the crystallization conditions of Rio Maria magmas. Hence, in the following the experimental data on the Pinatubo dacite will be preferentially employed to constrain the intensive parameters prevailing during the crystallization of the Rio Maria suite. However, for the epidote, a mineral phase not identified in the Pinatubo experiments, other experimental studies will be also considered (Naney, 1983; Schmidt & Thompson, 1996).

Pressure

Hammarstron & Zen (1986) first suggested that total Al content of hornblende in intermediate calc-alkaline rocks varies linearly with crystallization pressure provided that the buffering assemblage consisting of quartz, K-feldspar, plagioclase, biotite, hornblende, titanite, and Fe-Ti oxide is present. Those authors proposed an empirical barometric equation based on total aluminum content in amphibole to infer the pressure during the final emplacement of granitoid plutons. A similar approach was presented by Hollister *et al*. (1987). This Al-in barometer has been calibrated by Johnson and Rutherford (1989), Thomas & Ernst (1990), and Schmidt (1992) using different T-H_2O conditions and starting materials. Anderson & Smith (1995) argued that these calibrations overestimate pressures for granitoid rocks with high

Fe/(Fe+Mg) ratios which possibly crystallized at low fO_2. They proposed an improved Al-in-hornblende barometer applicable only with the appropriate mineral assemblage and when the Fe/(Fe+Mg) ratios for hornblende are at least in the range 0.40-0.65, indicating high fO_2.

If we consider magmatic epidote in place of Fe-Ti oxide, the studied rocks show the full mineral assemblage required for the use of the Al-in-amphibole geobarometer (Hammarstron & Zen, 1986; Hollister *et al*., 1987). Besides, the Rio Maria sanukitoids display systematically low Fe/(Fe+Mg) ratios indicating their formation in oxidizing rather than reducing conditions. The presence of hornblende as a near liquidus phase and the absence of clinopyroxene and orthopyroxene in the rocks of Rio Maria suite suggest additionally that the magmas were relatively water-rich. Finally, the occurrence of magmatic epidote in the studied rocks is indicative of low CO_2 activity (Ghent *et al*., 1991). Hence, the calibrations of Schmidt (1992) and Anderson & Smith (1995) appear both suited for estimating the crystallization pressure of the Rio Maria suite.

The pressures calculated using these calibrations with rim compositions (Table 7) range from 100 to 300 MPa, increasing from the intermediate rocks to the mafic enclaves. Pressure estimates using core compositions gave similar results, except for the cumulate amphibole of the layered rocks which gives pressures varying from 420 to 745 MPa (Fig. 13a, b). The significance of the latter values is questionable because the cumulate amphibole crystals are not in equilibrium with associated minerals. Yet, the fact that the intercumulus amphibole of the layered rocks records pressures similar to those of the other Rio Maria sanukitoid suggest that the core amphibole of the cumulate formed at higher pressures, relative to the intercumulus amphibole which crystallized at the level of final emplacement at around 200 ± 100 MPa.

Table 7
Pressure estimates obtained by Al-in-hornblende barometry in this study.

	Layered rocks				Mafic enclaves		Intermediate rocks		Granodiorites	
Sample	MFR-12B				MFR-27C		ADR-4B		ADR-3A	
Facies	Cumulate crystals		Intercumulate crystals		EBAD		EBAQzD		EBAGD	
	core	rim	core	rim	core	rim	core	rim	core	rim
Anderson and Smith (1995) P (MPa)	420 to 745 MPa	120 to 300 MPa	150 to 405 MPa	140 to 450 MPa	130 to 340 MPa	220 to 350 MPa	80 to 215 Mpa	75 to 90 Mpa	110 to 290 MPa	130 to 320 MPa
Schmidt (1992) P (MPa)	400 to 680 MPa	115 to 280 MPa	145 to 380 MPa	135 to 420 MPa	140 to 355 MPa	230 to 360 MPa	90 to 230 Mpa	85 to 100 Mpa	170 to 360 MPa	180 to 400 MPa

Total Fe reported as FeO. Key to abbreviations. *not determinated; E = epidote; B = biotite; A = amphibole; Qz = quartz; D = diorite; GD = granodiorite.

Prouteau & Scaillet (2003) used the Al vs Na + K and Al vs Mg number diagrams based in amphibole composition to further refine their pressure estimates. As for Pinatubo, the application of such projections to Rio Maria magmas (Fig. 13a, b) suggests also two distinct

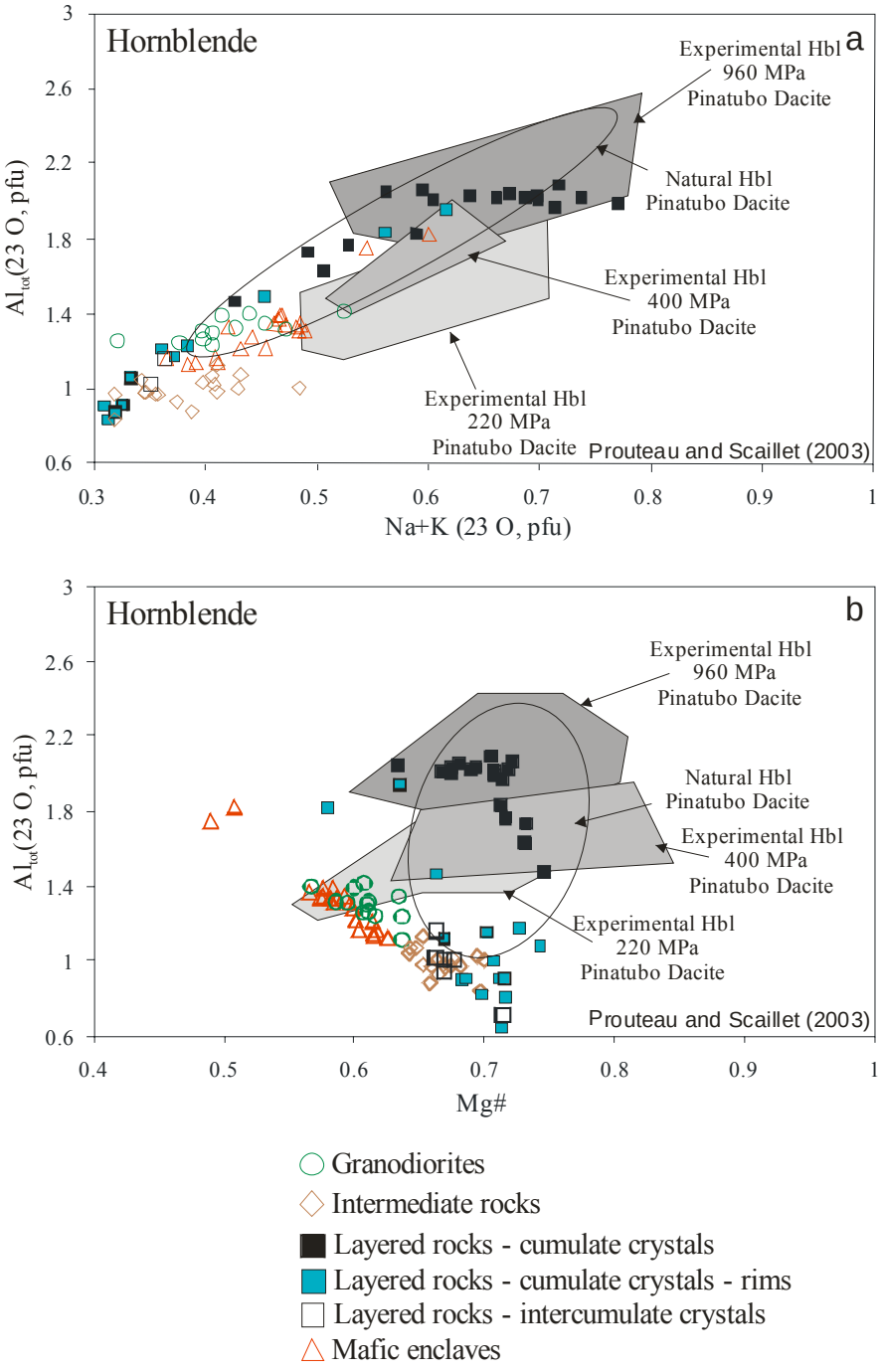

Fig. 13 – Amphiboles from different rocks of the Rio Maria suite (Bannach area), compared with amphiboles of the 1991 Pinatubo dacite (Bernard *et al.*, 1991, 1996) and experimental amphiboles produced in the dacite system at 220MPa (Scaillet & Evans, 1999), 400 and 960MPa (Prouteau & Scaillet, 2003). Fields by Prouteau & Scaillet (2003).

stages of evolution: a high pressure stage of crystallization (core composition of cumulate amphibole) consistent with experimental compositions of amphibole obtained at 960 MPa, eventually extending to 400 MPa; a low pressure stage of crystallization indicated by amphibole compositions (all other amphiboles) similar to those obtained in experiments at 220 MPa (Scaillet & Evans, 1999) and interpreted as related to the upper level emplacement of the magma in a shallow crustal chamber. The amphiboles of other varieties of rocks do not strictly overlap with the fields of experimental or natural Pinatubo amphibole, but their overall lower Al_{tot} contents are indicative of lower pressure of crystallization or re-equilibration at ~200 MPa.

Therefore, as proposed by Prouteau & Scaillet (2003) for the Pinatubo dacite, the mineralogical evidence points to crystallization of the Rio Maria sanukitoid involving at least two stages. A first high pressure stage, possibly around 700-1000 MPa, followed by a second crystallization stage at ca. 200 MPa, corresponding to the final emplacement of the Rio Maria magmas in upper crust. The occurrence of some amphibole compositions of cumulate crystals in the 400 MPa field can be interpreted as an evidence of partial re-equilibration of the amphiboles formed at higher pressures during magma ascent or to an intermediate level of magma transient arrest. The high pressure stage is thus preserved only in the cumulate amphibole. In the remainder rocks, any high pressure amphibole must have been entirely re-equilibrated at low pressure. This hypothesis is reinforced by the fact that the composition of thin rims of the cumulate crystals and of the core of the intercumulate amphibole are also similar to those of the amphibole of other varieties, suggesting that the cumulate amphibole was also affected to some extent by the re-equilibration process (Fig. 14), and that the intercumulate amphibole also re-equilibrated at low pressure.

H_2O contents and crystallization temperatures

The experimental data summarized above show clearly that, at any given pressure and oxygen fugacity, the crystallization sequence of magmas in general, and the stability of amphibole in particular, are both extremely dependent on the H_2O content of the melt (Naney, 1983; Schmidt & Thompson, 1996; Scaillet & Evans, 1999; Dall'Agnol *et al*., 1999; Prouteau & Scaillet, 2003; Klimm *et al*., 2003; Bogaerts *et al*., 2006).

Field and petrographic data of the Rio Maria suite strongly suggest an early crystallization of amphibole, in addition to the absence of orthopyroxene and clinopyroxene during magmatic cooling. Specifically, the euhedral character of amphibole crystals, its occurrence as inclusions in quartz and alkali-feldspar, its common association with plagioclase, the absence of relicts of pyroxenes in their crystals, the presence of amphibole as the only mafic

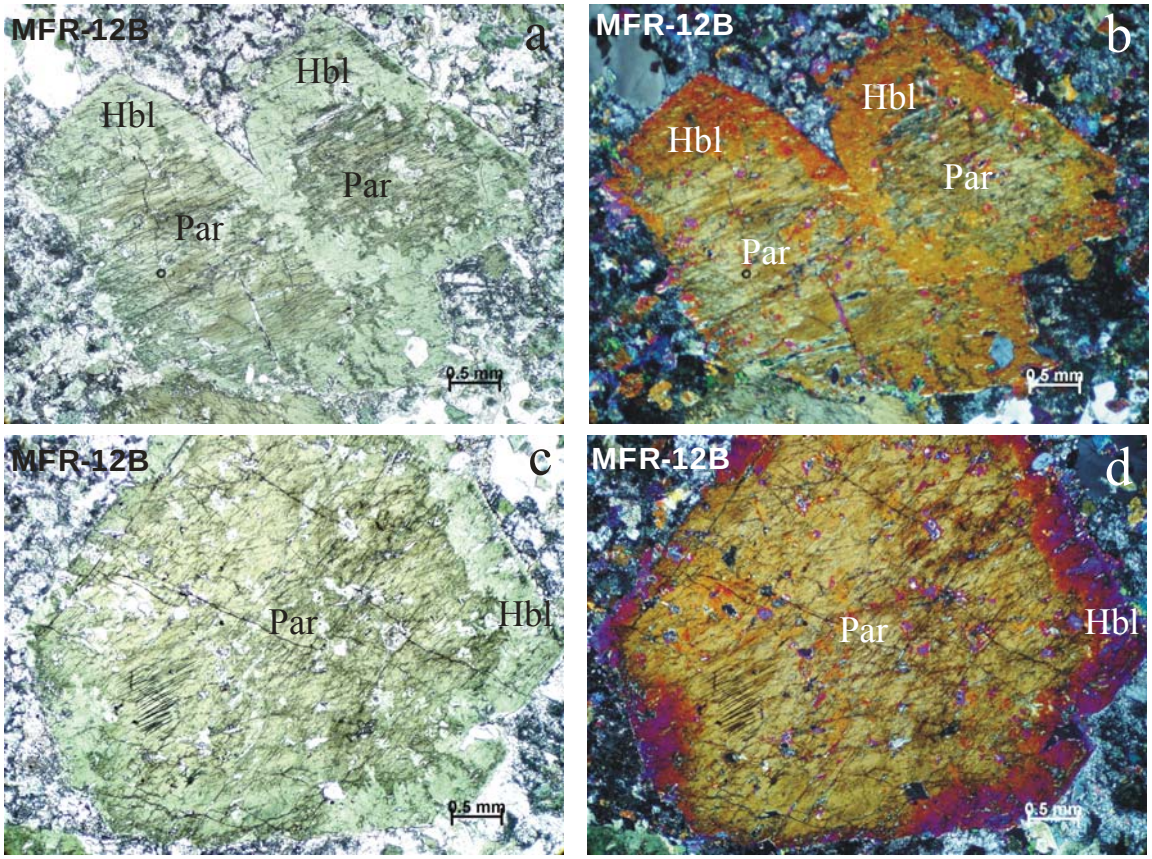

Fig. 14 – Photomicrographs of centimeter sized euhedral amphibole crystals from the layered rocks showing textures with re-equilibrium evidence in the thin border zones. Hbl – hornblende; Par – pargasite.

megacrystal in the layered rocks, where it is interpreted as a cumulate phase, are key observational features pointing toward a major role of amphibole during magma crystallization. That some, if not all, of these features are found in all four groups of studied rocks suggests that amphibole was a near liquidus phase in the whole suite. In contrast, the lack of both clinopyroxene and orthopyroxene suggests that either the stability field of these phases was not crossed during crystallization, or, if pyroxenes were stable at some early magmatic stage, that

these phases must have reacted out completely during cooling (see Naney, 1983; Dall'Agnol *et al*., 1999). Textural relationships indicate that plagioclase was also a liquidus phase, at least in the granodiorite and intermediate rocks.

The phase diagrams obtained on a synthetic granodiorite, at 800 MPa (Naney, 1983) and on the Pinatubo dacite, at 400 MPa and 960 MPa (Prouteau & Scaillet, 2003), indicate that H_2O contents of 5 wt. % at 400 MPa, or 7 to 9 wt. % at 960 MPa, are required for amphibole to be the liquidus silicate phase an prevent pyroxenes appearance. Therefore the widespread occurrence of amphibole in the the Rio Maria suite indicates that during the early stages of crystallization, the precursor magma had minimum dissolved H_2O contents higher than 5 wt%, and possibly over 9 wt%, depending on pressure. An additional indirect evidence of the high H_2O content of the Rio Maria sanukitoid magmas is the widespread pervasive subsolidus alteration that affected the studied rocks, responsible for the intense saussuritization of its plagioclase and other associated reactions. Lastly, the high modal abundance of amphibole throughout the whole suite is indicative also of high water pressure during magma crystallisation, possibly in excess of 7 wt%. It could be obviously argued that the original modal abundances in the whole rock series have been affected to some extent by cumulative processes during magma fractionation in the mid to upper crust. However, the feldspar to amphibole ratio in many Rio Maria rocks is similar to that obtained in experimental studies.

For instance, in the Pinatubo experiments, a characteristic Pl/Hbl wt% ratio of 2-3 is observed in the temperature range 850-780°C at 200 MPa (Scaillet & Evans, 1999), which is close to that of the preponderant granodiorite variety (Table 1). Similarly, this ratio in the more mafic enclaves hosted by the granodiorite is close to 0.8-1 (Table 1), which is again similar to the Pl/Hbl ratio obtained in hydrous arc basalt crystallization at ca 950°C-400 MPa (Pichavant *et al*., 2002). Therefore, if crystal sorting has occurred during Rio Maria magma evolution, the comparison with experimental constraints indicates that the cotectic mineral ratios of plutonic rocks were reasonably well preserved. Accepting that premise, it can be inferred that water rich conditions were possibly already prevailing in the original magma(s) parental to the suite, i.e. when magmas had still mafic-enriched composition. Owing to the generally incompatible behaviour of water in magmas, it can be anticipated that any fractionation process that has operated to produce the chemical array nowadays preserved across the Rio Maria pluton, likely

lead to an increase in the melt water content of the felsic derivatives relative to their parent magmas.

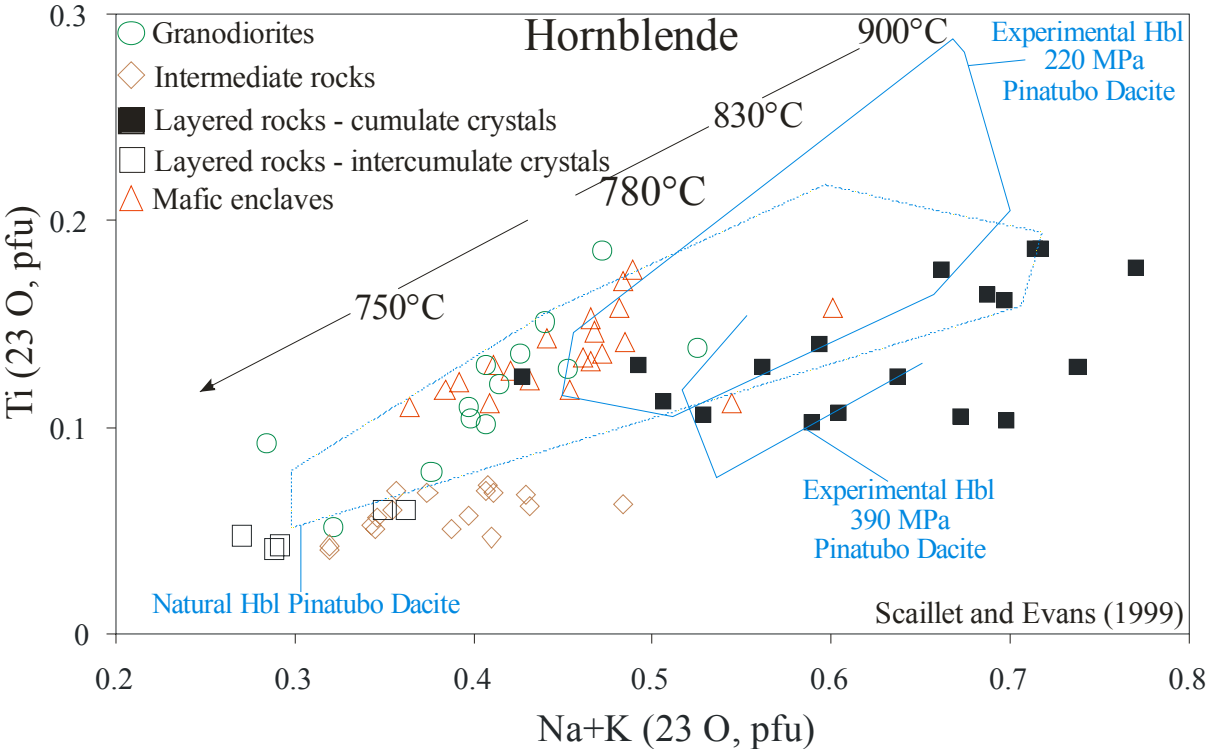

Fig. 15 - Comparison of hornblende from different rocks of the Rio Maria suite (Bannach area) and natural and experimental hornblende (at 220 MPa) from the Pinatubo dacite (Scaillet & Evans, 1999) in terms of Ti vs Na+K. The higher Na+K of the natural hornblende can be attributed to their higher crystallization temperature (Scaillet & Evans, 1999).

In the Pinatubo dacite experiments, at 400 MPa and > 7 wt.% H_2O, the crystallization of amphibole begins near the liquidus at ~950°C and at 960 MPa and > 9% wt. H_2O, around ~970°C (Prouteau and Scaillet, 2003). At 400 MPa, after a small decrease of temperature, the plagioclase crystallizes soon after the amphibole. At 960 MPa, plagioclase appears next to amphibole in the crystallization sequence, but a larger temperature decrease is needed before it begins to precipitate. Following Scaillet & Evans (1999), additional constraints on magma crystallization temperature can be gained by comparing experimental and natural compositions of amphiboles, using plots Ti vs Na+K, two components known to be sensitive to temperature. In such diagrams (Fig. 15), the compositions of the amphiboles from the different groups define a broad trend between 780 and 730°C, while those from layered rocks indicate a larger interval

temperature, from 900 to 760°C. Although these temperatures estimates are somehow dependent on pressure, for the time being, the experimental evidence suggests that the Rio Maria sanukitoid could have possibly begun to crystallize near 950°C, extending to temperatures of ~700°C near the solidus. The lowest temperatures possibly reflect re-equilibration of near liquidus amphibole as cooling proceeds, as well as continuous amphibole precipitation through the crystallization interval. This is consistent with the lower pressure of final emplacement of the Rio Maria rocks, compared to the pressure at which the magma has been produced, as discussed above.

An independent evaluation of the estimated crystallization temperatures is given by apatite saturation temperatures (Harrison & Watson, 1984). The resulting temperatures vary between 815 and 938 °C and 785 and 859 °C (Table 2) for intermediate and granodiorite rocks, respectively. These estimates overlap with the range of crystallization temperatures derived above. For the other varieties of studied rocks, the apatite saturation temperatures are significantly higher (1085 to 1525 °C for the enclaves; 1065 to 1265 °C for the layered rocks) possibly reflecting apatite accumulation. Zircon saturation temperatures (Watson & Harrison, 1983) are much lower than those indicated by apatite saturation temperatures (Table 2). In the cases of enclaves and layered rocks the calculated saturtaion temperatures encompass the subsolidus range (590 to 689 °C), while for the intermediate (676 to 716 °C) and granodiorite (715 to 740 °C) rocks the values approach the temperatures estimated for the solidus. The obtained zircon saturation temperatures are, however, difficult to reconcile with the petrographic evidence for early zircon crystallization and with the temperatures inferred from experimental data and apatite thermometry.

Oxygen fugacity

Several experimental studies have shown that, at fixed T, fO_2 exerts a dominant control on the Fe/(Fe+Mg) ratios of the mafic mineral silicates and whole rock (Anderson & Smith, 1995; Dall'Agnol *et al*., 1999; Scaillet & Evans, 1999; Martel *et al*., 1999; Pichavant *et al*., 2002; Prouteau & Scaillet, 2003; Bogaerts *et al*., 2006). Therefore, the composition of amphibole, biotite and magmatic epidote of the studied sanukitoid rocks can be used also to provide more precise constraints on redox conditions of the Rio Maria magmas.

The Fe/(Fe+Mg) ratios in natural amphiboles of layered rocks (0.25-0.43), intermediate rocks (0.25-0.35), mafic enclaves (0.34-0.43) and granodiorite (0.32-0.43) of the Rio Maria suite

are relatively low. In the layered rocks, Fe/(Fe+Mg) ratios are lower in the cumulate amphibole (0.25-0.33) than in the intercumulate one (0.28-0.43). The Fe/(Fe+Mg) ratios of amphibole increase from the cumulate and intermediate rocks toward the granodiorite and enclaves (Fig. 10), suggesting that the granodiorite and enclaves probably formed under slightly less oxidizing conditions relative to cumulate and intermediate rocks. Similarly, the compositional variation of the amphibole in the layered rocks suggests that the cumulate amphibole crystallized under more oxidizing conditions than that formed in the intercumulate portion. Aside from these minor inter-group variations, amphibole compositions suggest altogether that the Rio Maria magmas evolved under relatively oxidizing conditions, above NNO buffer (see below). This is also born out by the relatively low whole rock $FeO_t/(FeO_t+MgO)$ ratios of different rocks of Rio Maria suite (Table 2) which point to relatively oxidizing conditions as well (see Pichavant *et al*., 2002). For instance, the FeOtot/MgO ratio of Rio Maria granodiorite is within the range 1-2 (Table 2), which is similar to that of silicic liquids (60-64 wt% SiO_2) produced by hydrous basalt crystallization at 400 MPa at around NNO+2 (Pichavant *et al*., 2002).

Since the Rio Maria granodiorite and Pinatubo dacite share almost identical bulk rock Fe/Mg ratios (Table 6), the empirical relationships established between the Fe/Mg of amphibole and fO_2 for Pinatubo amphiboles by Scaillet & Evans (1999), and the data of Prouteau & Scaillet (2003) can be used to infer redox conditions of the Rio Maria granodiorite magma. This empirical calibration has been established at 780°C, which falls midway in the range inferred for Rio Maria suite (Fig. 15). It can be anticipated that the overall positive correlation between fO_2 and Fe/Mg ratio still holds true at other temperatures, being displaced toward higher (lower) Mg content when temperature increases (decreases). To a first approximation, application of such a relationships to rocks with lower Fe/Mg ratio than that of Pinatubo dacite (i.e. all Rio Maria suite except granodiorites) will likely retrieve maximum possible fO_2 for amphibole crystallization. The Fe/(Fe+Mg) ratios of experimental amphibole from Pinatubo dacite obtained at 400 MPa and 960 MPa and at an fO_2 NNO+2 to NNO+4.8 (Prouteau & Scaillet, 2003) vary between 0.15 and 0.30 and are partially coincident with those of intermediate rocks but generally lower than those of the enclaves and granodiorite of Rio Maria suite. The fact that Fe/(Fe+Mg) ratios as low as 0.15 are not found in Rio Maria amphibole suggests that the magmas evolved at fO_2 conditions less oxidized than NNO+2, even if amphiboles from both rocks partially overlap with each other. Application of the relationships of Scaillet & Evans (1999) to Rio Maria suite

thus indicates that the magmas parental to these rocks should have crystallized at relatively oxidizing conditions above the NNO buffer, yielding an overall range between NNO+0.5 to NNO+2.7 (Fig. 16). In detail, keeping in mind the caveats given above, amphibole in the cumulate and intermediate rocks seems to record relatively more oxidizing conditions (NNO+1.5 to NNO+ 2.7) relative to that of the granodiorite and mafic enclaves (NNO + 0.5 to NNO+ 1.4).

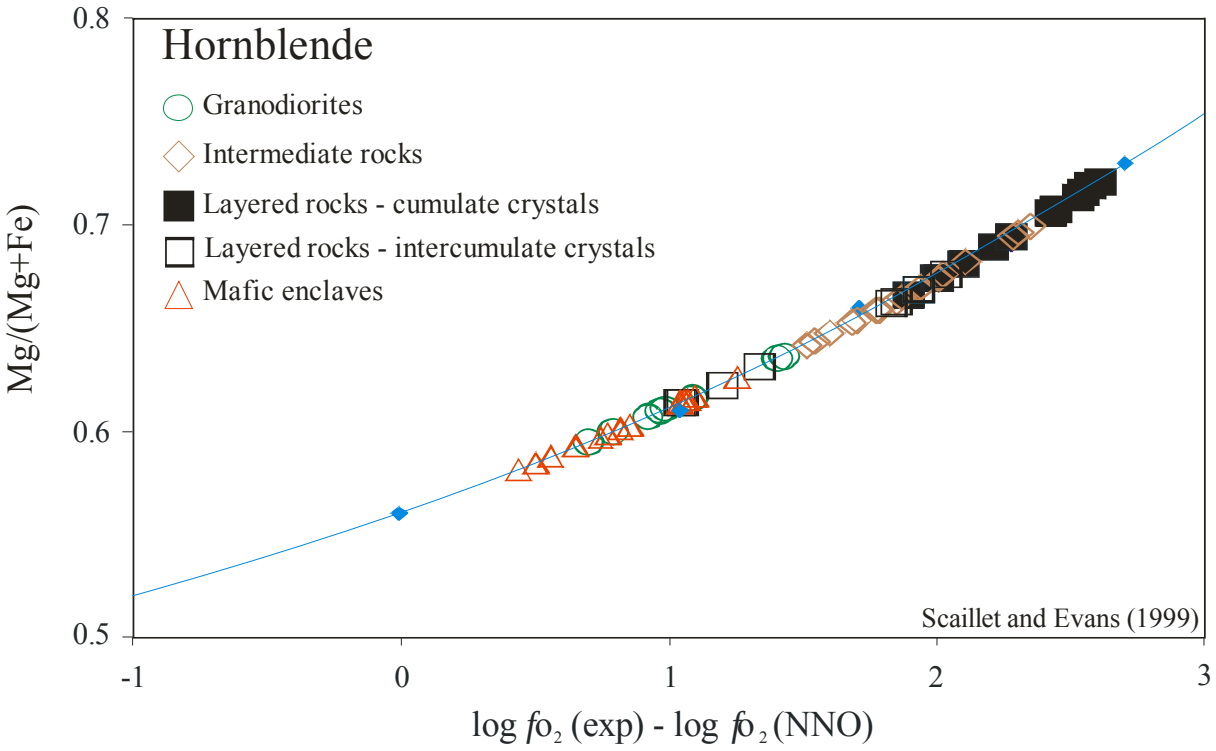

Fig. 16 - Estimative of oxygen fugacity conditions of the Rio Maria magmas, based in plot by Scaillet & Evans (1999). This plot evaluated the effect of fO_2 on the mg-number of experimental hornblende in S-free and S-bearing dacite at 780 °C and 220 MPa. The curve for hornblende in the S-free system is a second-order polynomial fit: $\Delta NNO = -20.206 + 51.56\ (\text{mg-number}) - 27.605\ (\text{mg-number})^2$ with a correlation coefficient $r^2 = 0.995$ (Scaillet & Evans, 1999).

The Fe/(Fe+Mg) ratios in natural biotite of Rio Maria suite are slightly higher than those of amphibole (see Tables 3, 4 and Fig. 11b) and, as for amphibole, point to relatively oxidizing conditions during the evolution of these rocks and to fO_2 conditions slightly lower than that inferred for the Pinatubo dacite (NNO+1.7, Scaillet & Evans, 1999). The lower fO_2 recorded by

biotite may arise from its greater propensity to re-equilibrate down temperature as compared to amphibole. Variations in biotite TiO_2 contents are significant and apparently related to the degree of oxidation of different magmas. This is suggested by the fact that the intermediate rocks have the lowest TiO_2 contents in biotite but also the lowest Fe/(Fe+Mg) ratios in biotite and amphibole. A similar behavior was observed in the Jamon granite and associated dikes: there an oxidized rhyolite porphyry displays at the same time the lowest Fe/(Fe+Mg) ratios in biotite and amphibole and the lowest TiO_2 content in biotite (Dall'Agnol *et al*., 1999). In contrast, the Mata Geral sanukitoid, which occurs south of Bannach area in the Rio Maria granite-greenstone terrane, displays the highest Fe/(Fe+Mg) ratios in biotite and amphibole of the Rio Maria sanukitoid, and the highest TiO_2 content in biotite (M. A. Oliveira, unpublished data).

As noted in previous sections, the studies of the Fe-Ti oxides and magnetic susceptibility (MS, Dias *et al*., 2006; Nascimento, 2006) of the Rio Maria suite of Bannach area furnished mostly low magnetic susceptibility values for those rocks. The magnetic susceptibility of granodiorites is usually low and magnetite is rare to absent. At first sight, this could be interpreted as a typical behavior of ilmenite series granitoids which crystallized under low fO_2 (Ishihara, 1977; 1981). However, this is in contradiction with the composition of mafic minerals found in those rocks, in particular the lack of ilmenite. A similar paradox was observed in epidote-bearing granites of North-east Brazil, Argentine, and Chile, which do not have magnetite as an accessory mineral, yet they also show evidence of crystallization under relatively oxidizing conditions (Sial *et al*., 1999). We thus conclude that, in the Rio Maria rocks, MS data and the nature and content of iron oxide minerals are not conclusive about the oxidation conditions of their magmas.

The presence of magmatic epidote and its chemical composition are also useful tools to estimate the redox conditions of Rio Maria magmas. As stressed already above, several studies have shown that the thermal stability of epidote increases with fO_2 (Holdaway, 1972; Liou, 1973; Schmidt & Thompson, 1996; Schmidt & Poli, 2004; Poli & Schmidt, 2004). In particular, Liou (1973) showed that the Fe^{3+} content of synthetic epidotes increases with fO_2. In the Rio Maria sanukitoids, the pistacite content of magmatic epidote crystals of the granodiorite varies between 28 and 33 mol%, whereas those of the intermediate rocks have somewhat lower values, between 26 and 31 mol%. In the experiments performed by Liou (1973), these ranges of

pistacite contents occur only between HM and NNO buffers, giving further support to high fO_2 prevailing during Rio Maria magmas crystallization (above NNO buffer).

The conclusion that the granodiorite magma crystallized at fO_2 above NNO contrasts with the fact that the resulting granodiorite is generally devoid of magnetite. However, in the rare granodiorite samples where magnetite is present, it is found as inclusions in amphibole, indicating that magnetite crystallized near the liquidus, along with amphibole and plagioclase. On the other hand, textural evidence suggests that epidote crystallized in equilibrium with biotite down to near-solidus conditions. These textural observations suggest therefore the operation of the following reaction (e.g., Schmidt & Thompson, 1996):

hornblende + (K-feldspar$_{melt}$) + plagioclase + magnetite + melt = epidote + biotite + (quartz$_{melt}$) + H_2O

The effectiveness of this reaction during the magmatic crystallization of the Rio Maria granodiorite is suggested by experimental studies showing that, for water-rich magmas (H_2O > 4 wt%) evolving under oxidizing conditions, early crystallizing hornblende will be replaced upon cooling by biotite- and titanite-bearing (Dall'Agnol *et al*., 1999) or biotite- and epidote-bearing (Naney, 1983) assemblages. Hence, the abundance of magmatic epidote in Rio Maria magmas probably originates from a peritectic reaction during cooling involving magnetite on the high temperature side.

9 – CONCLUSIONS AND PERSPECTIVES

Geological and mineralogical studies on the Rio Maria Archean sanukitoid rocks opposed to experimental results obtained in rocks or synthetic materials of similar compositions allowed us to make quantitative estimates of the parameters of crystallization of their magmas. These rocks were derived from cogenetic but not comagmatic magmas that should have evolved under similar conditions. We conclude that the Rio Maria magmas were water-rich, with > 7 wt. % estimated water contents, and evolved in oxidizing conditions above the condition of NNO buffer, probably in between NNO + 0.5 to NNO + 2.5. These conditions allowed the crystallization of amphibole as the liquidus phase and inhibited clinopyroxene and orthopyroxene. Those magmas should begin to crystallize at a temperature estimated at 950 °C, crystallizing essentially amphibole.

The magma ascent was rapid and the proportion liquid/crystals in the magma were high to explain the high level of emplacement of the Rio Maria suite and the limited deformational

structures observed on their rocks. After magma ascent to upper crustal levels, plagioclase begun to crystallize (cf. the evolution proposed for the Pinatubo dacite; Prouteau & Scaillet, 2003, their Fig. 12). At lower temperatures, a peritectic reaction involving amphibole + plagioclase + magnetite + ($K\text{-feldspar}_{melt}$) resulted in the presence of biotite and magmatic epidote. The stability of epidote in those conditions was ensured by the oxidized character of the Rio Maria magmas. Their final emplacement should have occurred at ca. 200 MPa and any early precipitated amphibole possibly re-equilibrated extensively at these conditions, except for the coarse amphibole crystals, such as that found in the cumulate rocks (Fig. 14). It is assumed in the proposed evolution scenario that the different magmas which have formed the Rio Maria sanukitoid evolved in similar conditions and ascended in the crust together or almost simultaneously, at short intervals of geological time.

The P-T-H_2O-fO_2 estimates reached above for the Rio Maria suite point therefore to oxidized and wet conditions for their precursor magmas, two features characteristic of present-day arc magmas, including those with a strong slab melt signature, such as Pinatubo. The immediate, and perhaps principal, implication is that Sanukitoid petrogenesis at Rio Maria is indeed compatible with a subduction zone geodynamic setting during the Archean in this area. It remains, however, to be demonstrated whether such arc attributes are specific to Rio Maria magmas or characterize Sanukitoid occurrences worldwide. The origin of the primary or primaries magmas of the Rio Maria sanukitoid rocks deserve complementary data and approaches and should be the focus of future studies.

ACKNOWLEDGEMENTS

F.G.C. Nascimento, S.B. Dias and M.A.C. da Costa are acknowledged for support in data about magnetic susceptibility and Fe-Ti oxides. N.V. Siqueira contributed in the Fe chemical analyses. S. R. F. Vlach, E. Ruberti, and M. Mansueto are acknowledged for support on electron microprobe analyses (Institute of Geosciences of São Paulo University). This research received financial support from CNPq (Roberto Dall'Agnol – Grants 0550739/2001-7, 476075/2003-3, 307469/2003-4; Marcelo Augusto de Oliveira – master and doctor scholarship), and Federal University of Pará (UFPA). This paper is a contribution to the Brazilian Institute of Amazonia Geosciences (INCT program – CNPq/MCT/FAPESPA – Process no 573733/2008-2).

REFERENCES

Althoff, F. J., Barbey, P. & Boullier, A. M. (2000). 2.8-3.0 Ga plutonism and deformation in the SE Amazonian craton: the Archean granitoids of Marajoara (Carajás Mineral province, Brazil). *Precambrian Research* **104**, 187-206.

Anderson, J.L. & Smith, D.R. (1995). The effects of temperature and fO_2 on the Al-in-hornblende barometer. *American Mineralogist* **80**, 549–559.

Bagai, Z., Armstrong, R. & Kampunzu, A.B. (2002). U–Pb single zircon geochronology of granitoids in the Vamba granite-greenstone terrane (NE Botswana): implications for the evolution of the Archaean Zimbabwe craton. *Precambrian Research* **118**, 149– 168.

Barros, E.M., Sardinha, A.S., Barbosa, J.P.O., Krimski, R. & Macambira, M.J.B. (2001). Pb-Pb and U-Pb zircon ages of Archean syntectonic granites of the Carajás Metallogenic Province, northern Brazil. In: Simposio Sudamericano de Geologia Isotopica, 3. Pucon, Chile. Sociedade Geologica de Chile. (CD ROM).

Bogaerts, M., Scaillet, B. & Auwera, J.V. (2006). Phase Equilibria of the Lyngdal granodiorite (Norway): Implications for the Origin of Metaluminous Ferroan Granitoids. *Journal of Petrology*, 2405-2431.

Clemens, J.D., Holloway, J.R. & White, A.J.R. (1986). Origin of A-type granite: experimental constraints. *American Mineralogist* **71**, 317-324.

Condie, K.C. (2005). TTGs and adakites: are they both slab melts?. *Lithos* **80**, 33-44.

Dall'Agnol, R., Oliveira, M.A., Almeida, J.A.C., Althoff, F.J., Leite, A.A.S., Oliveira, D.C. & Barros, C.E.M. (2006). Archean and Paleoproterozoic granitoids of the Carajás metallogenetic province, eastern Amazonian craton. In: Dall'Agnol, R., Rosa-Costa, L.T., Klein, E.L. (eds.). Symposium on Magmatism, Crustal Evolution, and Metallogenesis of the Amazonian Craton. Abstracts Volume and Field Trips Guide. Belém, PRONEX-UFPA/SBG-NO, 99-150.

Dall'agnol, R. & Oliveira, D. C. (2007). Oxidized, magnetite-series, rapakivi-type granites of Carajás, Brazil: implications for classification and petrogenesis of A-type granites. *Lithos* **93**, p 215-233.

Dall'agnol, R., Teixeira, N. P., Ramö, O. T., Moura, C. A. V., Macambira, M. J. B. & Oliveira, D. C. (2005). Petrogenesis of the Paleoproterozoic rapakivi A-type granites of the Archean Carajás metallogenic province, Brazil. *Lithos* **80**, 101-129.

Dall'agnol, R., Scaillet, B. & Pichavant, M. (1999). An experimental study of a Lower Proterozoic A-type granite from the eastern Amazonian craton, Brazil. *Journal of Petrology* **40 (11)**, 1673-1698.

Dias, S.B., Dall'agnol, R. & Oliveira, M. A. (2006). Estudo dos Minerais Óxidos de Fe e Ti do Granodiorito Rio Maria e Rochas Máficas e Intermediárias Associadas, Leste de Bannach, SE do Pará In: XLIII Congresso Brasileiro de Geologia, 2006, Aracaju. XLIII Congresso Brasileiro de Geologia. Brasília: SBG, 2006.

Duarte, K. D. (1992). Geologia e geoquímica do Granito Mata Surrão (SW de Rio Maria – Pa): um exemplo de granito "stricto sensu" Arqueano. Belém, Centro de Geociências, Universidade Federal do Pará, 217p. M.Sc. Thesis. Programa de Pós-Graduação em Geologia e Geoquímica, Centro de Geociências, UFPA (in Portuguese).

Evans, B.W. & Vance, J.A. (1987). Epidote phenocrysts in dacitic dikes, Boulder county, Colorado. *Contribution to Mineralogy and Petrolology* **96**, 178–185.

Foster M.D. (1960). Interpretation of the composition of trioctahedral micas. U. S. Geol. Surv., Prof. Paper, 354:1-49.

Ghent, E.D., Nicholls, J., Simony, P.S., Sevigny, J.H. & Stout, M.Z. (1991). Hornblende geobarometry of the Nelson Batholith, southeastern British Columbia: tectonic implications. *Canadian Journal of Earth Sciences* **2**, 1982–1991.

Halla, J. (2005). Late Archean high-Mg granitoids (sanukitoids) in the southern Karelian domain, eastern Finland: Pb and Nd isotopic constraints on crust_mantle interactions. *Lithos* **79**, 161– 178.

Hammarstrom, J.M. & Zen, E-an. (1986). Aluminum in hornblende: An empirical igneous geobarometer. *American Mineralogist* **71**, 1297-1313.1992. Petrological characteristics of magmatic epidote-bearing granites of the western cordillera of America (abs.). Transactions of the Royal Society of Edinburgh: Earth Sciences, 83, 490-491.

Holdaway, M.J. (1972). Thermal stability of AI-Fe-epidote as a function of fO_2, and Fe content. *Contributions to Mineralogy and Petrology* **37**, 307-340.

Hollister, L.S., Grissom, G.c., Peters, E.K., Stowell, H.H. & Sisson, V.B. (1987). Confirmation of the empirical correlation of Al in hornblende with pressure of solidification of calc-alkaline plutons. *American Mineralogist* **72**, 231-239.

Huhn, S. R. B., Santos, A. B. S., Amaral, A. F., Ledsham, E. J., Gouveia, J. L., Martins, L. B. P., Montalvão, R. M. G. & Costa,V. G. (1988). O terreno granito-greenstone da região de Rio Maria - Sul do Pará. In: Congresso Brasileiro de Geologia, 35., Belém. Anais do congresso Brasileiro de Geologia. Belém, SBG. v. 3, p. 1438-1453.

Irvine, T. N. & Baragar, W. R. A. (1971). A guide to the chemical classification of the common volcanic rocks. *Canadian Journal of the Earth Science* **8**: 523-547.

Ishihara, S. (1977). The magnetite-series and ilmenite-series granitic rocks. *Mining Geology* **27**, 293-305.

Ishihara, S. (1981). The granitoid series and mineralization. In: SKINNER, B. J. ed. *Economic Geology* 75th ann. Vol. 458-484.

Johnson, M.C. & Rutherford, M.J. (1989). Experimental calibration of the aluminum-in-hornblende geobarometer with application to Long Valley caldera (California) volcanic rocks. *Geology* **17**, 837-841.

Johnston, A. D. & Wyllie, P. J. (1988). Constraints on the origin of Archean trondhjemites based on phase relationships of Nûk gneiss with H_2O at 15 kbar. *Contribution to Mineralogy and Petrology* **100**, 35-46.

Kamber, B.S., Ewart, A., Collerson, K.D., Bruce, M.C. & McDonald, G.D. (2002). Fluid-mobile trace element constraints on the role of slab melting and implications for Archaean crustal growth models. *Contributions to Mineralogy and Petrology* **144**, 38–56.

Käpyaho, A. (2006). Whole-rock geochemistry of some tonalite and high Mg/Fe gabbro, diorite, and granodiorite plutons (sanukitoid suites) in the Kuhmo district, eastern Finland. *Bulletin of the Geological Society of Finland* **78**, 121–141.

Klimm, K., Holtz, F., Johannes, W. & King, P. L. (2003). Fractionation of metaluminous A-type granites: an experimental study of the Wangrah Suite, Lachlan Fold Belt. *Australia. Precambrian Research* **124**, 327-341.

Kovalenko, A.V., Clemens, J.D. & Savatenkov, V.M. (2005). Petrogenetic constraints for the genesis of Archaean sanukitoid suites:geochemistry and isotopic evidence from Karelia, Baltic Shield. *Lithos* **79**, 147– 160.

Lafon, J. M., Rodrigues, E. & Duarte, K. D. (1994). Le granite Mata Surrão: un magmatisme monzogranitique contemporain des associations tonalitiques-trondhjemitiques-

granodioritiques archéennes de la région de Rio Maria (Amazonie Orientale, Brésil). p. 642- 649.

Lameyre, J. & Bowden, P. (1982). Plutonic rock type series: discrimination of various granitoid series and related rocks. *Journal of Volcanology and Geothermal Research* **14**, 169-186.

Le Bas, M.J., Le Maitre, R.W., Streckeisen, A. & Zanettin, B. (1986). A classification of volcanic rocks based on the total alcalis-silica diagram. *Journal of Petrology* **27**, 745-750.

Le Maitre, R. W. (2002). A classification of igneous rocks and glossary of terms. 2nd Edition , London, 193 p.

Leake, B. E., Woolley, A. R. & Arps, C. E. S. (1997). Nomenclature of amphiboles: report of the subcommittee on amphiboles of the International Mineralogical Association, commission on new minerals and mineral names. *Canadian Mineralogist* **35**, 219–246.

Leite, A. A. S., Dall'agnol, R., Macambira, M. J. B. & Althoff, F. J. (2004). Geologia e geocronologia dos granitóides arqueanos da região de Xinguara (PA) e suas implicações na evolução do Terreno Granito-Greenstone de Rio Maria. *Revista Brasileira de Geociências* **34**, 447-458.

Leite, A. A. S. (2001). Geoquímica, petrogênese e evolução estrutural dos granitóides arqueanos da região de Xinguara, SE do Cráton Amazônico. Belém, Universidade Federal do Pará, Centro de Geociências. 330p. Doctor Thesis. Programa de Pós-Graduação em Geologia e Geoquímica, Centro de Geociências, UFPA (in Portuguese).

Liou, J.G. (1973). Synthesis and stability relations of epidote, $Ca_2Al_2FeSiO_3O_{12}$_OH.. *Journal of Petrology* **14**, 381–413.

Macambira, M. J. B. & Lancelot, J. (1996). Time constraints for the formation of the Archean Rio Maria crust, southeastern Amazonian Craton, Brazil. *International Geology Review* **38 (12)**, 1134-1142

Macambira, M. J. B. & Lafon, J. M. (1995). Geocronologia da Província Mineral de Carajás; Síntese dos dados e novos desafios. *Boletim do Museu Paraense Emílio Goeldi, série Ciências da Terra, Belém* 7, 263-287.

Machado, N., Lindenmayer, Z. G., Krogh, T. E. & Lindenmayer, D. (1991). U-Pb geochronology of Archean magmatism and basement reactivation in the Carajás area, Amazon shield, Brazil. *Precambrian Research* **49**, 329-354.

Martel, C., Pichavant, M., Holtz, F., Scaillet, B., Bourdier, J.-L. & Traineau, H. (1999). Effects of fO_2 and H_2O on andesite phase relations between 2 and 4 kbar. *Journal of Geophysical Research* **104**, 29453–29479.

Martin, H., Smithies, R.H., Rapp, R., Moyen J.-F. & Champion D. (2005). An overview of adakite, tonalite–trondhjemite–granodiorite (TTG), and sanukitoid: relationships and some implications for crustal evolution. *Lithos* **79**, 1–24.

Medeiros, H. (1987). Petrologia da porção leste do maciço granodiorítico Rio Maria, Sudeste do Pará. 166p. M.Sc. Thesis. Programa de Pós-Graduação em Geologia e Geoquímica, Centro de Geociências, UFPA (in Portuguese).

Moyen, J. F., Martin, H., Jayananda, M. & Auvray, B. (2003). Late-Archaean granites: a typology based on the Dharwar Craton (India). *Precambrian Research* 2375, 1-21.

Naney, M. T. (1983). Phase equilibria of rock-forming ferromagnesian silicates in granitic systems. *American Journal of Science* **283**, 993-1033.

Naney, M. T. & Swanson, S. E. (1980). The effect of Fe and Mg on crystallization in granitic systems: *American Mineralogist* **65**, 639-653.

Nascimento, F.G.C. (2006). Petrologia magnética das associações magmáticas arqueanas de Canaã dos Carajás-PA. Universidade Federal do Pará. 141p. M.Sc. Thesis. Programa de Pós-Graduação em Geologia e Geoquímica, Centro de Geociências, UFPA (in Portuguese).

Oliveira, M. A., Dall'Agnol, R., Althoff, F. J. & Leite, A.A.S. (2009). Mesoarchean sanukitoid rocks of the Rio Maria Granite-Greenstone Terrane, Amazonian craton, Brazil. *Journal of South American Earth Sciences* **27**, 146-160.

Oliveira, M. A., Dall'Agnol, R. & Althoff, F. J. (2006). Petrografia e Geoquímica do Granodiorito Rio Maria da região de Bannach e comparações com as demais ocorrências no terreno Granito-Greenstone de Rio Maria-Pará. *Revista Brasileira de Geociências* **36 (2)**, 313-326.

Oliveira, M. A. (2005). Geologia, Petrografia e Geoquímica do Granodiorito Sanukitóide Arqueano Rio Maria e Rochas Máficas Associadas, Leste de Bannach-PA. Universidade Federal do Pará. 141p. M.Sc. Thesis. Programa de Pós-Graduação em Geologia e Geoquímica, Centro de Geociências, UFPA (in Portuguese).

Pichavant, M., Martel, C., Bourdier, J.-L. & Scaillet, B. (2002). Physical conditions, structure and dynamics of a zoned magma chamber: Mt. Pele¤ e (Martinique, Lesser Antilles Arc). *Journal of Geophysical Research* **107**, doi:10.1029/2001JB000315.

Pichavant, M., Costa, F., Burgisser, A., Scaillet, B., Martel, C. & Poussineau, S. (2007). Equilibration Scales in Silicic to Intermediate Magmas-Implications for Experimental Studies. *Journal of Petrology* **48**, 1955-1972.

Pimentel, M. M. & Machado, N. (1994). Geocronologia U-Pb dos Terrenos granito-greenstone de Rio Maria, Pará. In: Congresso Brasileiro de Geologia, 38. Camboriú, 1988. Boletim de Resumos Expandidos. Camboriú, SBG. p. 390-391.

Poli, S., & Schmidt, M.W. (2004). Experimental subsolidus studies on epidote minerals. *Reviews in Mineralogy & Geochemistry* **56**, 171-195. Mineralogical Society of America.

Prouteau, G. & Scaillet, B. (2003). Experimental constraints on the origin of the 1991 Pinatubo dacite. *Journal of Petrology* **44**, 2203–2241.

Rapp, R.P., Shimizu, N., Norman, M.D. & Applegate, G.S. (1999). Reaction between slab-derived melts and peridotite in the mantle wedge: experimental constraints at 3.8 GPa. *Chemical Geology* **160**, 335– 356.

Rieder, M., Cavazzini, G., D'Yakonov, Y., Frank-Kameneteskii, V. A., Gottardi, G., Guggenheim, S., Koval, P., Mueller, G., Neiva, A. M. R., Radoslovich, E. M., Robert, J., Sassi, F. P., Takeda, H., Weiss, Z. & Wones, D. R. (1998). Nomenclature of Micas. *American Mineralogist* **83**,1366-1998.

Ringwood, A. E. (1975). Composition and Petrology of the earth's mantle. MacGraw-Hill Editor. 618p.

Scaillet, B. & Evans, B.W. (1999). The June 15, 1991, eruption of Mount Pinatubo: I. Phase equilibria and pre-eruption P-T-fO_2-fH_2O conditions of the dacite magma. *Journal of Petrology* **40**, 381-411.

Schmidt, M.W. & Poli, S. (2004). Magmatic Epidote. *Reviews in Mineralogy & Geochemistry* **56**, 399-430. Mineralogical Society of America.

Schmidt, M.W. & Thompson, A.B. (1996). Epidote in calc-alkaline magmas: an experimental study of stability, phase relationships, and the role of epidote in magmatic evolution. *American Mineralogist* **81**, 424–474.

Schmidt, M.W. (1992). Amphibole composition in tonalite as a function of pressure: An experimental calibration of the Al-in-hornblende-barometer. *Contributions to Mineralogy and Petrology* **110**, 304-310.

Sial, A.N., Toselli, A.J., Saavedra, J., Parada, M.A. & Ferreira, V.P. (1999). Emplacement, petrological and magnetic susceptibility characteristics of diverse magmatic epidote-bearing granitoid rocks in Brazil, Argentina and Chile. *Lithos* **46**, p. 367–392.

Smithies, R.H. & Champion, D.C. (2000). The Archaean high-Mg diorite suite: links to tonalite–trondhjemite–granodiorite magmatism and implications for early Archaean crustal growth. *Journal of Petrology* **41 (12)**, 1653– 1671.

Souza, Z.S., Potrel, H., Lafon, J.M., Althoff, F.J., Pimentel, M.M., Dall'agnol, R. & Oliveira, C.G. (2001). Nd, pb and sr isotopes of the identidade belt, na archaean greenstone belt of the rio maria region (carajas province, brazil): implications for the archaean geodynamic evolution of the amazonian craton. *Precambrian research* **109**, 293–315.

Souza, Z. S. & Dall'Agnol, R. (1995). Geochemistry of metavolcanic rocks in the Archean Greenstone Belt of Identidade, SE Pará, Brazil. *Anais da Academia Brasileira de Ciências* **67 (2)**, 217-233.

Souza, Z. S. (1994). Geologia e petrogênese do "Greenstone Belt" Identidade: implicações sobre a evolução geodinâmica do terreno granito-"greenstone" de Rio Maria, SE do Pará. v- 1 e 2, 624p. Doctor Thesis. Programa de Pós-Graduação em Geologia e Geoquímica, Centro de Geociências, UFPA (in Portuguese).

Stern, A. L. & Hanson, G. (1991). Archean high-Mg granodiorite: a derivate of light rare earth element-enriched monzodiorite of mantle origin. *Journal of Petrology* **32**, 201-238.

Stern, R.A., Hanson, G.N. & Shirey, S.B. (1989). Petrogenesis of mantle-derived, LILE-enriched Archean monzodiorites and trachyandesites (sanukitoids) in southwestern Superior Province. *Canadian Journal of Earth Sciences* **26**, 1688– 1712.

Stevenson, R., Henry, P. & Garie´py, C. (1999). Assimilation– fractional crystallization origin of Archaean sanukitoid suites: Western Superior Province, Canada. *Precambrian Research* **96**, 83– 99.

Tassinari, C.C.G., & Macambira, M.J.B. (2004). Evolução tectônica do Cráton Amazônico. In: Mantesso-Neto, V., Bartorelli, A., Carneiro, C. D. R., Brito Neves, B. B. de. (Org.).

Geologia do Continente Sul Americano: Evolução da obra de F.F.M. de Almeida. São Paulo: BECA, 471-486.

Taylor, S.R. & McLennan, S.M. (1985). The continental crust: Its composition and evolution. *Backwell Scientific*, Oxford, 321p.

Thomas, W.M. & Ernst, W.G. (1990). The aluminium content of hornblende in calc-alkaline granitic rocks: a mineralogic barometer calibrated experimentally to 12 kbar. In: Spencer, R.J., Shou, I-Ming (Eds.), Fluid Mineral Interactions: A Tribute to H.P. Eugster, vol. 2. *Geochemical Society*, 59–63. Special publication.

Tulloch, A. (1979). Secondary Ca–Al silicates as low-grade alteration products of granitoid biotite. *Contributions to Mineralogy and Petrology* **69**, 105–117.

Vyhnal, C.R., McSween, H.Y. Jr. & Speer, J.A. (1991). Hornblende chemistry in southern Appalachian granitoids: implications for aluminum hornblende thermobarometry and magmatic epidote stability. *American Mineralogist* **76**, 176–188.

Van der Laan, S.R. & Wyllie, P.J. (1992). Constraints on Archean trondhjemite genesis from hydrous crystallization experiments on NUk Gneiss at 10-17 kbar. *Journal of Geology* **100**, 57-68.

Wilson, M. (1989). Igneous petrogenesis. London, Academic Press. 466p.

Wyllie, P. J. (1984). Sources of granitoid magmas at convergent plate boundaries. *Physics of the Earth and Planetary Interiors* **35**, 12-18.

Zen, E. & Hammarstrom, J.M. (1984). Magmatic epidote and its petrologic significance. *Geology* **12**, 515–518.

CAPÍTULO – 4

PETROLOGY OF THE MESOARCHEAN RIO MARIA SUITE: IMPLICATIONS FOR THE GENESIS OF SANUKITOID ROCKS

Marcelo Augusto de Oliveira
Roberto Dall'Agnol
José de Arimatéia Costa de Almeida
Submetido: *LITHOS*

Dear Dr. Oliveira,

Your submission entitled "PETROLOGY OF THE MESOARCHEAN RIO MARIA SUITE: IMPLICATIONS FOR THE GENESIS OF SANUKITOID ROCKS" (Research Paper) has been received by Lithos.

Please note that submission of an article is understood to imply that the article is original and is not being considered for publication elsewhere. Submission also implies that all authors have approved the paper for release and are in agreement with its content.

You will be able to check on the progress of your paper by logging on to http://ees.elsevier.com/lithos/ as Author.

Your manuscript will be given a reference number in due course.

Thank you for submitting your work to this journal.

Kind regards,

Journal management
Lithos

PETROLOGY OF THE MESOARCHEAN RIO MARIA SUITE: IMPLICATIONS FOR THE GENESIS OF SANUKITOID ROCKS

Marcelo Augusto de Oliveira[1,2,*] (mao@ufpa.br), Roberto Dall'Agnol[1,2] (robdal@ufpa.br), José de Arimatéia Costa de Almeida[1,2] (ari@ufpa.br),

[1]Group of Research on Granite Petrology – Instituto de Geociências (IG) – Universidade Federal do Pará (UFPA). Caixa Postal 8608. 66075-900, Belém, Pará.

[2]Programa de Pós-Graduação em Geologia e Geoquímica (PPGG) – IG – UFPA

*Corresponding author. Tel.: +55 91 3201 7477; fax +55 91 3201 7474. E-mail address: mao@ufpa.br

ABSTRACT

Petrogenetic modeling is presented for 2.87 Ga Rio Maria sanukitoid suite of the eastern Amazonian craton, Brazil. The rocks of the Rio Maria suite include granodiorites, intermediate rocks, layered rocks and mafic enclaves, which have typical sanukitoid signature similar to those of the sanukitoid suites from others Archean terranes. In spite of their broad geochemical similarities, these rocks show some significant differences in their REE patterns and in the behavior of Rb, Ba, Sr, and Y. The granodiorites and intermediate rocks are not related by fractional crystallization and the internal evolution of intermediate rocks were leaded by fractionation of amphibole + biotite ± apatite, whereas granodiorites evolved by fractionation of plagioclase + amphibole ± biotite. The layered rocks should have been derived from the granodiorite magma by accumulation of 50% of amphibole (dark layer) and 30% of amphibole ± plagioclase accumulation (gray layer).

Modeling and geochemical data suggest that mafic enclave and granodiorite magmas were originated at different depths and should have mingled during their ascent and final emplacement and a limited interaction would explain the relatively uniform geochemical behavior of each rock variety and the distinct trends displayed by their rocks in different modal and geochemical diagrams. These contrasts between granodiorites and mafic enclaves are reflected in the behavior of the Sr and Y, which are generally seen as good indicators of the pressure of melt formation.

The behavior of these elements indicates that the geochemical and modal contrasts observed between the granodioritic and monzonitic sanukitoid series are a general feature of these rocks and their origin is strongly dependent of the pressure of magma generation and, as a consequence, that the nature of the series could indicate the approximate depth of formation of its magma.

The petrogenesis of the Rio Maria suite requires melting of a modified mantle extensively metasomatized by addition of about 30% TTG-like melt to generate the granodiorite (21% of melt) and intermediate magmas (24% of melt), and ~20% TTG-like melt in the case of mafic enclave magma (9% of melt). Our modeling results indicate that an active subduction tectonic setting was present in the Rio Maria terrane in between 2.98 to 2.92 Ga to generate the TTG magmas and the proposed metasomatism of the mantle by these magmas, before the melting process responsible for the origin of the sanukitoid magmas. A tectonothermal event at ~2.87 Ga, possibly related to a mantle plume, causing the partial melting of the metasomatized mantle and generating the Rio Maria sanukitoid magmas.

keywords: Amazonian craton; High-Mg granitoids; Sanukitoids; Petrogenesis; Modeling; Metasomatized mantle.

1 - INTRODUCTION

In several cratons, Meso to Late Archean times (<3.0 Ga) were characterized by intense magmatic activity. The TTG suites are the more voluminous rocks formed during these events, but the relevance of sanukitoid rocks and granites in these Archean terranes was also demonstrated (Stern et al., 1989; Sylvester, 1994; Moyen et al., 2003; Smithies et al., 2004). It is widely accepted that convergent plate margin processes played a role in the origin of TTG series (Martin, 1994, 1999; Kusky & Polat, 1999; Smithies et al., 2004; Martin et al., 2005). However, in the origin of sanukitoid suites, the role of slab melts and the link between TTG and sanukitoid is controversial. Sanukitoid rocks were now studied in various Archean terranes: Superior province of Canada (Shirey and Hanson, 1984, Stern et al. 1989), Fennoscandian shield (Lobach-Zhuchenko et al., 2005, Kovalenko et al., 2005, Halla, 2005), Dharwar craton (Moyen et al., 2003), Ukrainian shield (Artemenko et al., 2003), Pilbara craton (Smithies and Champion, 2000), and, more recently, in the eastern Amazonian craton (Althoff et al., 2000; Leite, 2001; Oliveira et

al., 2009; Oliveira et al., submitted). Nevertheless, they show paradoxical geochemical features, similar to both mantle- and crust-derived magmatic rocks, and their petrogenesis is not well constrained.

To explain the origin of sanukitoid magmas several processes have been tested. Stern et al. (1989) modeled contamination of basaltic or komatiitic magmas by a LILE-rich felsic crust. They concluded that interaction between mafic or ultramafic melts and crustal material cannot produce both the high Ni and Cr, and the high SiO_2 and LILE compositions of primitive sanukitoids. However, Pb isotopic data indicate a significant crustal influence in sanukitoid magma evolution (Halla, 2005). On the other hand, partial melting of mantle peridotite that had been previously metasomatized by TTG melts (Evans and Hanson, 1997; Smithies and Champion, 2000) or slab-melts that have assimilated peridotite during ascent through mantle wedge (Martin et al., 2005), have been considered as able to generate the typical features of sanukitoid series and are alternatives to explain the petrogenesis of these rocks (Rapp et al., 1999, 2007).

Smithies and Champion (2000) had shown that, in spite of the strong similarities between wedge-modified adakites and sanukitoids, the latter are late- to post-kinematic intrusions (Stern et al., 1989; Evans and Hanson, 1997) which in Archean cratons are not temporally associated with the voluminous TTG magmas commonly interpreted as slab derived. In this respect, the sanukitoid series tectonic setting differs markedly from that of wedge-modified adakite. Anyway, high-Mg suites are the only Archean felsic series that appears to be derived from the mantle, and an understanding of its petrogenesis, tectonic setting and possible relationship to the TTG series may clarify the processes involved in the Archean crustal evolution.

Typical sanukitoid rocks have been identified in the Rio Maria Granite-Greenstone terrane, southeast of Amazonian craton and form the ~2.87 Ga old Rio Maria suite (Oliveira et al., 2009; Oliveira et al., submitted). These rocks are post-kinematic intrusions into 2.98 to 2.90 Ga supracrustal sequences and TTG suites (Althoff et al., 2000). The sanukitoid series are temporarily associated with intrusions of leucogranodiorites and potassic leucogranites of calc-alkaline affinity and a direct link of their origin with contemporaneous subduction was previously suggested (Leite, 2001), but not demonstrated. All occurrences of the dominant granodiorites of

the sanukitoid Rio Maria suite contain high-K, mafic to intermediate enclaves, which share sanukitoid geochemical characteristics (Oliveira et al., 2009; Oliveira et al., submitted).

This paper presents extensive geochemical and Nd isotopic data on the granodiorites, intermediate rocks, layered rocks, and mafic enclaves from the Bannach area, which is representative of the Mesoarchean sanukitoid Rio Maria suite of the Amazonian craton. The aim of this paper is to explore geochemical data with modeling techniques to discuss the magma sources and magmatic evolution of the studied sanukitoid rocks and to contribute to clarify the role of convergent plate margin processes and mantle metasomatism in the evolution of sanukitoid series.

2 – GEOLOGIC SETTING

The Rio Maria sanukitoid suite is exposed in the Carajás province (Machado et al., 1991; Macambira and Lafon, 1995; Rämö et al., 2002; Dall'Agnol et al., 2006; Vasquez et al., 2008) which is the largest Archean tectonic province of the Amazonian craton. The Carajás province is included into the Central Amazonian province, eastern part of the Amazonian craton (Tassinari and Macambira, 2004), and comprises mostly Archean rocks intruded by Paleoproterozoic anorogenic granites (Dall'Agnol et al., 2005). To the west, it is limited by a terrane dominated by Proterozoic granitoids and Uatumã volcanic-pyroclastic assemblages; to the east, by the Neoproterozoic Araguaia belt, whose evolution is associated with the Brasiliano (Pan-African) cycle that did not significantly affect the Amazonian craton; and to the north and south, respectively, by the Maroni-Itacaiúnas province and Santana do Araguaia domain (Vasquez et al., 2008), both formed during the 2.2–2.1 Ga Trans-Amazonian event.

The Carajás province is divided into the Rio Maria granite-greenstone terrane (3.0 to 2.86 Ga) (Macambira and Lafon, 1995; Dall'Agnol et al., 2006; Vasquez et al., 2008), and the rift-related Carajás basin (2.76 to 2.55) (Machado et al., 1991; Macambira and Lafon, 1995; Barros et al., 2001), located, respectively, in the southern and northern parts of the province. The studied sanukitoid rocks are situated in the Rio Maria granite-greenstone terrane (Fig. 1b) which consists of greenstone belts and Archean granitoids covered by sediments of the Rio Fresco group, probably also of Archean age, and intruded by Paleoproterozoic A-type granites of the Jamon suite (Dall'Agnol et al., 2005).

In the Rio Maria granite-greenstone terrane (Fig. 1b), the greenstone-belts (Andorinhas supergroup) are composed mostly of komatiites and tholeiitic basalts (2.98 – 2.90 Ga; Hunh et

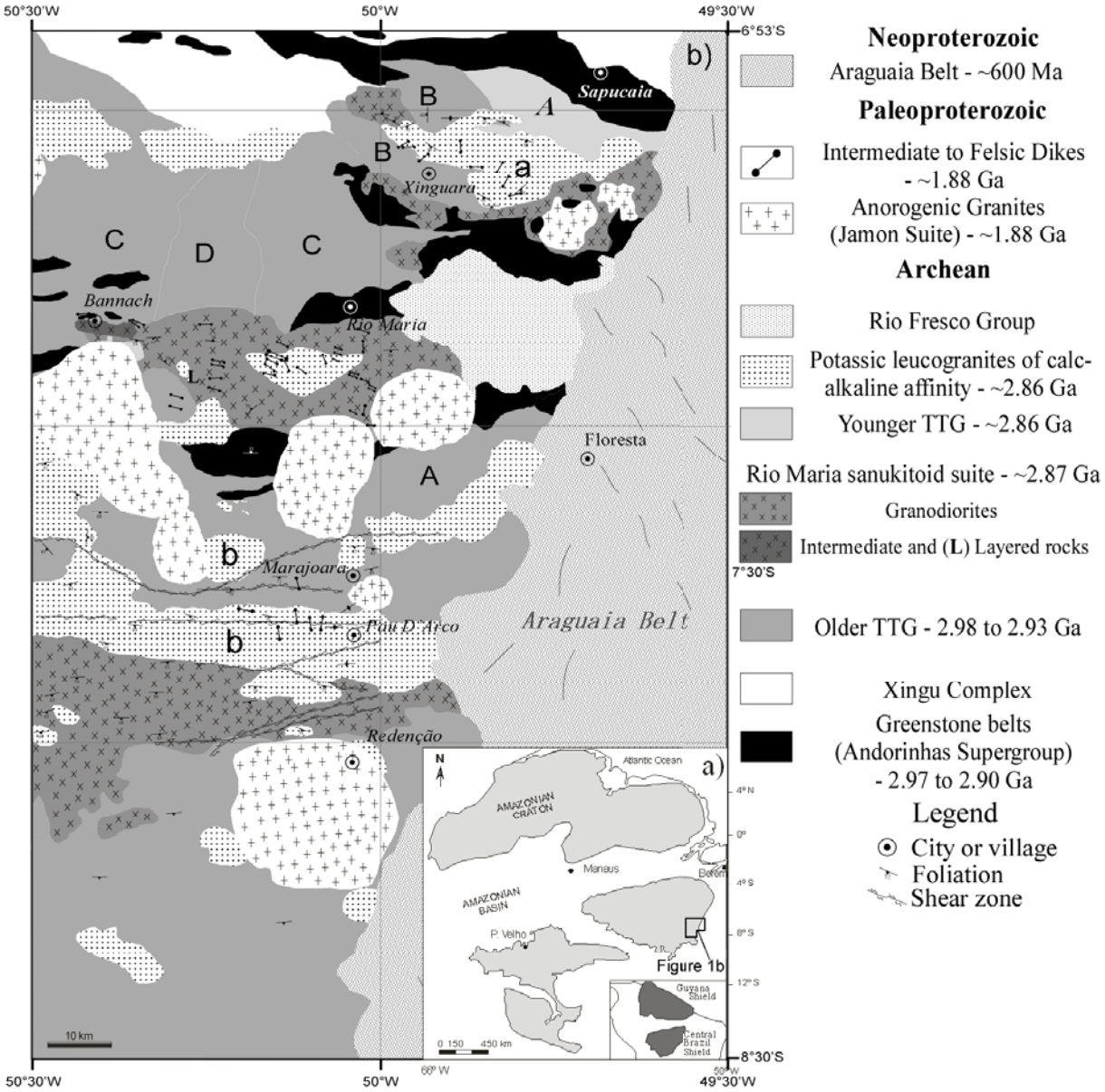

Fig. 1 - (a) Location of the studied area in the Amazonian craton; (b) Geological map of the Rio Maria granite-greenstone terrane (modified from Leite, 2001). A) Arco Verde tonalite; B) Caracol tonalitic complex; C) Mogno trondhjemite; D) Mariazinha trondhjemite. *A*) Água Fria trondjemite. a) Xinguara granite; b) Mata Surrão granite.

al., 1988; Souza et al., 2001). The Archean granitoids have ages between 2.98 and 2.86 Ga and four principal groups have been distinguished (modified from Dall'Agnol et al., 2006): (1) An older tonalitic-trondhjemitic series (TTG) represented by the Arco Verde, Caracol and Mariazinha tonalites and the Mogno trondhjemite (~2.98 to 2.92 Ga; Althoff et al., 2000; Leite et al., 2004; Almeida et al., submitted; Guimarães et al., submitted); (2) The 2.87 Ga Rio Maria sanukitoid suite formed by the different occurrences of the Rio Maria granodiorite and associated rocks (Medeiros, 1987; Macambira and Lancelot, 1996; Althoff et al., 2000; Leite et al., 2004; Oliveira et al., 2009; Oliveira et al., submitted); (3) A younger TTG series represented by the Água Fria trondhjemite (2.86 Ga; Huhn et al., 1988; Pimentel and Machado, 1994; Leite et al., 2004); and (4) 2.87 to 2.86 Ga Xinguara, Mata Surrão, and similar potassic leucogranites of calc-alkaline affinity (Lafon et al., 1994; Leite et al., 2004). The last shearing deformational event identified in this terrane occurred at around 2.87 Ga (Althoff et al., 2000; Souza et al., 2001; Leite, 2001) and, after it, the terrane remained stable until the emplacement of 1.88 Ga A-type granites.

3 – THE RIO MARIA SUITE

3.1 – Geologic and geochronologic aspects

In the Rio Maria Granite-Greenstone terrane, the sanukitoid rocks are intrusive in the greenstone sequences (Andorinhas supergroup; Souza et al., 2001), Arco Verde, Caracol and Mariazinha tonalites (Althoff et al., 2000; Leite, 2001; Guimarães et al., submitted) and are intruded by the Água Fria trondhjemite (younger TTG series; Leite et al., 2004), the Archean Xinguara granite (Leite et al., 2004), and the Paleoproterozoic granites of the Jamon suite (Dall'Agnol et al., 2005).

The Bannach area was selected for this study because it contains the largest expositions of mafic and intermediate rocks associated and cogenetic with the Rio Maria granodiorite (Oliveira et al., 2009). The dominant variety of rock in the Rio Maria sanukitoid suite is an epidote-biotite-hornblende granodiorite. In the Bannach area, the associated intermediate and mafic rocks occur in two domains. In the main domain, located near Bannach, it is exposed a stock composed mostly of quartz diorites and quartz monzodiorites; in the second domain, situated along the road

between Rio Maria and Bannach, an occurrence of layered rocks was described (Fig. 2). More detailed information about these rocks, as well as about the mafic enclaves and their relationships with host granodiorites, is provided by Oliveira et al. (2009, submitted).

Zircon dating by the Pb-evaporation method (Kober, 1986) was conduced at the Laboratório de Geologia Isotópica (Pará-Iso) of the Universidade Federal do Pará, Belém, using the double-filament array. Isotopic ratios were measured in a FINNIGAN MAT 262 mass spectrometer and data were acquired in the dynamic mode using the ion-counting system of the instrument. For each step of evaporation, a step age is calculated from the average of the $^{207}Pb/^{206}Pb$ ratios. When different steps yield similar ages, all are included in the calculation of the crystal age. If distinct crystals furnish similar mean ages, then a mean age is calculated for the sample. Crystals or steps showing lower ages probably reflect Pb loss after crystallization and are not included in sample age calculation. Common Pb corrections were made according to Stacey and Kramers (1975) and only blocks with $^{206}Pb/^{204}Pb$ ratios higher than 2500 were used for age calculations. $^{207}Pb/^{206}Pb$ ratios were corrected for mass fractionation by a factor of 0.12% per a.m.u, given by repeated analysis of the NBS-982 standard, and analytical uncertainties are given at the 2σ level.

Representative samples of the Rio Maria granodiorite, from its different areas of occurrence, yielded remarkably uniform U-Pb and Pb-Pb evaporation zircon ages (~2.87 Ga; Table 1). The only intermediate rock dated so far came from a restrict occurrence near Xinguara and gave an age of 2878 ± 4 Ma (Pb-Pb evaporation zircon; Dall'Agnol et al., 1999). For this reason, zircons extracted from the sample MFR-102, an epidote-biotite-hornblende quartz diorite (Oliveira et al., 2009) representative of the intermediate rocks of Bannach (Fig. 2) were dated by the Pb evaporation method. Zircons are generally prismatic, yellowish, and translucent. Some fractures and zoning are present. Six measured zircons (Table 2, Fig. 3) indicated an age of 2860 ± 2 Ma (2σ). This age is considered as the emplacement age of the intermediate rocks and indicates that these rocks are a little younger than the dominant granodiorites.

3.2 – Petrography

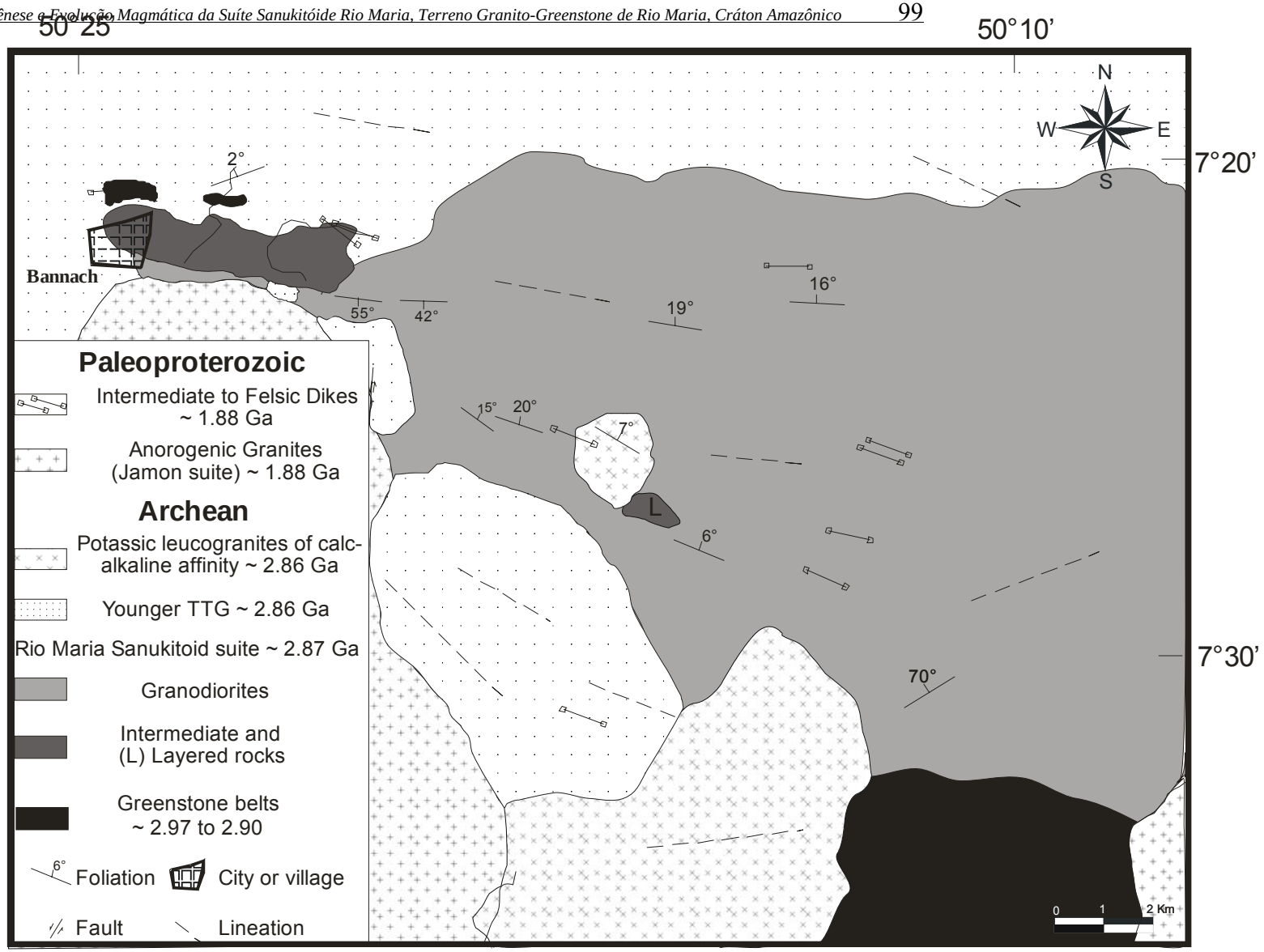

Fig. 2 - Geological map of Bannach area.

Table 1 - Geochronology of the Rio Maria granodiorite and intermediate rocks.

Area	Rock	Method	Analized material	Age
Rio Maria	Granodiorite	U-Pb	Zircon	2874 + 9/-10 Ma (1)
Rio Maria	Granodiorite	U-Pb	Zircon,Titanite	2872 ± 5 Ma (2)
Xinguara	Quartz-diorite	Pb-Pb	Zircon	2878 ± 4 Ma (3)
Serra do Inajá	Granodiorite	Pb-Pb	Zircon	2879 ± 4 Ma (4)
Serra do Inajá	Granodiorite	Pb-Pb	Zircon	2877 ± 6 Ma (4)
Serra do Inajá	Granodiorite	Pb-Pb	Zircon	2888 ± 8 Ma (5)
Serra do Inajá	Granodiorite	Pb-Pb	Zircon	2880 ± 4 Ma (5)
Serra do Inajá	Granodiorite	Pb-Pb	Zircon	2875 ± 7 Ma (5)

Data Source: (1) Macambira (1992), (2) Pimentel and Machado (1994), (3) Dall'Agnol et al. (1999), (4) Rolando and Macambira (2002), (5) Rolando and Macambira (2003).

The general petrographic aspects of the Rio Maria suite from the Bannach area have been discussed by Oliveira et al. (2009, submitted). In that area, the suite is composed of four principal groups of rocks: granodiorites, intermediate rocks, layered rocks and mafic enclaves. All facies of the Rio Maria suite present a strongly saussuritized plagioclase and contain amphibole ± biotite ± magmatic epidote as their principal mafic minerals. M' values (total modal content of mafic minerals in percentage) vary between 10 to 25 in the granodiorites, 20 to 40 in the intermediate rocks, and are ≥ 40 in the mafic enclaves (Fig. 4). The assemblage of accessory minerals includes apatite, magnetite, titanite, allanite, and zircon, which is absent only in the layered rocks.

Table 2
Pb isotopic data from single-grain zircon evaporation of the intermediate rock of the Rio Maria suite.

Zircon	Temperature (°C)	Number of ratios	$^{204}Pb/^{206}Pb$	2\	$^{208}Pb/^{206}Pb$	2\	$(^{207}Pb/^{206}Pb)_c$	2\	Age (Ma) step	2\	Age (Ma) Crystal	2\
Grain #1	1450	8/8	0,000037	0,000028	0,13679	0,00119	0,20378	0,00216	2857	17		
	1500	38/38	0,000124	0,000035	0,15471	0,0018	0,20424	0,00087	2861	7	2860	6
Grain #3	1500	36/36	0,000092	0,000011	0,14323	0,00061	0,20367	0,00082	2856	7	2856	7
Grain #4	1500	34/34	0,000157	0,000007	0,14089	0,00154	0,20385	0,00078	2858	6	2858	6
Grain #5	1500	14/22	0,000144	0,000002	0,14213	0,0007	0,20439	0,00047	2862	4	2862	4
Grain #6	1500	8/8	0,000026	0,000002	0,10736	0,01091	0,20478	0,00149	2865	12	2865	12
Grain #15	1500	26/34	0,000173	0,000039	0,15473	0,00158	0,20421	0,00085	2861	7	2861	7

$_c$ $^{207}Pb/^{206}Pb$ corrected for common Pb.

The dominant variety is an epidote-biotite-hornblende granodiorite which display equigranular, medium or coarse even-grained texture. The associated intermediate rocks are quartz diorites and quartz monzodiorites with equigranular, medium- to fine-grained texture. In the quartz diorites and quartz monzodiorites, the mineral assemblages and textural relationships

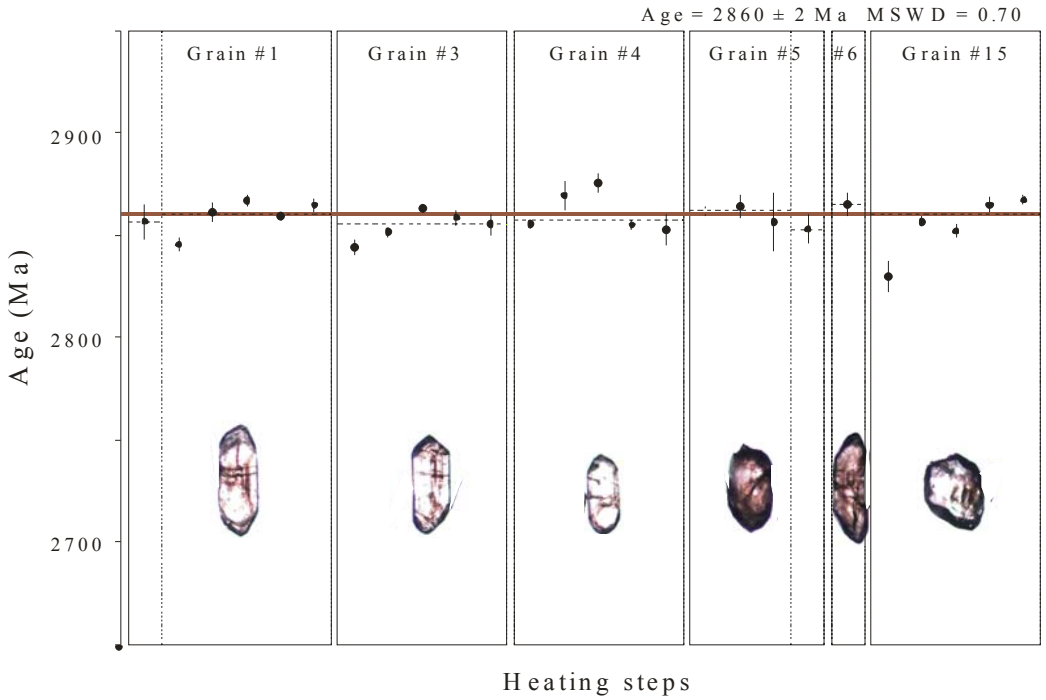

Fig. 3 - $^{207}Pbr^{206}Pb$ single zircon Pb evaporation age of the intermediate rock of the Rio Maria suite.

between different minerals are very similar to those observed in the dominant granodiorite, but amphibole and plagioclase are more abundant and quartz and K-feldspars modal contents are lower than in the granodiorite and these minerals begin to crystallize later.

The mineralogy of the layered rocks is similar to that of the Rio Maria granodiorite and intermediate rocks. The textural variations are directly related to the different layers of the rock (dark and gray layers, reflecting variation in modal content of mafic phases). The cumulus material is formed by centimeter sized euhedral pargasite to magnesium-hornblende crystals while the intercumulus material is mainly composed of intensely saussuritized plagioclase, with subordinate quartz, amphibole, biotite, and epidote. The accessory minerals are allanite, titanite, magnetite, and apatite.

The mafic enclaves have dioritic to quartz monzonitic compositions (Oliveira et al., submitted) and follow a monzonitic trend in the QAP plot (Lameyre and Bowden, 1982), whereas the granodiorites and intermediate rocks follow a granodioritic trend. In the enclaves, the mineral assemblage is very similar to those found in the other rocks of the suite, but, considering their low modal contents of quartz, the enclaves have relatively higher modal alkali feldspar (Fig. 4).

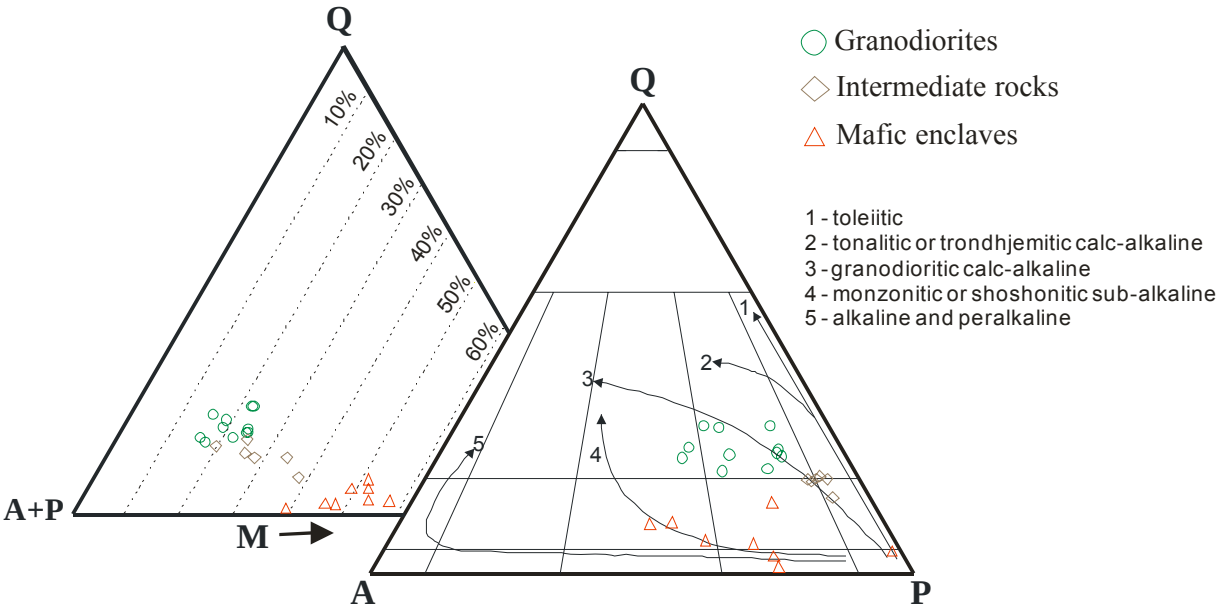

Fig. 4 - QAP and Q-(A+P)-M plots for the rocks of the Rio Maria suite. Data sources: Granodiorites and intermediate rocks (Oliveira, 2005); Mafic enclaves (Oliveira et al., submitted).

In the enclave samples, peculiar textural aspects as the presence of coarse poikilitical K-feldspar crystals including medium to fine grained euhedral amphibole are remarkable. In the epidote-biotite-hornblende granodiorite (Oliveira et al., 2006, 2009, submitted), the crystallization sequence of the minerals is: (a) apatite, zircon, magnetite, and allanite were the first to crystallize; (b) they were followed by magnesium hornblende and plagioclase that are also near liquidus phases; (c) biotite began to crystallize after hornblende and plagioclase and displays regular contacts with euhedral epidote suggesting equilibrium between it and the mica, implying that both have crystallized in a similar temperature interval; (d) quartz forms subhedral to anhedral medium-grained crystals and should initiate its crystallization probably after biotite; (e) K-feldspars is a later phase forming anhedral, sometimes poikilitical crystals, including quartz, plagioclase and euhedral amphibole; (f) at the subsolidus stage, chlorite, secondary epidote, sericite and carbonates were generated.

3.3 – Geochemistry

3.3.1 – General aspects

Chemical analyses of representative samples of the Rio Maria suite are given in Table 3. Major and trace elements were analyzed by ICP–ES and ICP–MS, respectively, at the Acme Analytical Laboratories Ltd. in Canada. All rocks of the suite are metaluminous and follow the calc-alkaline series trend in some diagrams (Fig. 5).

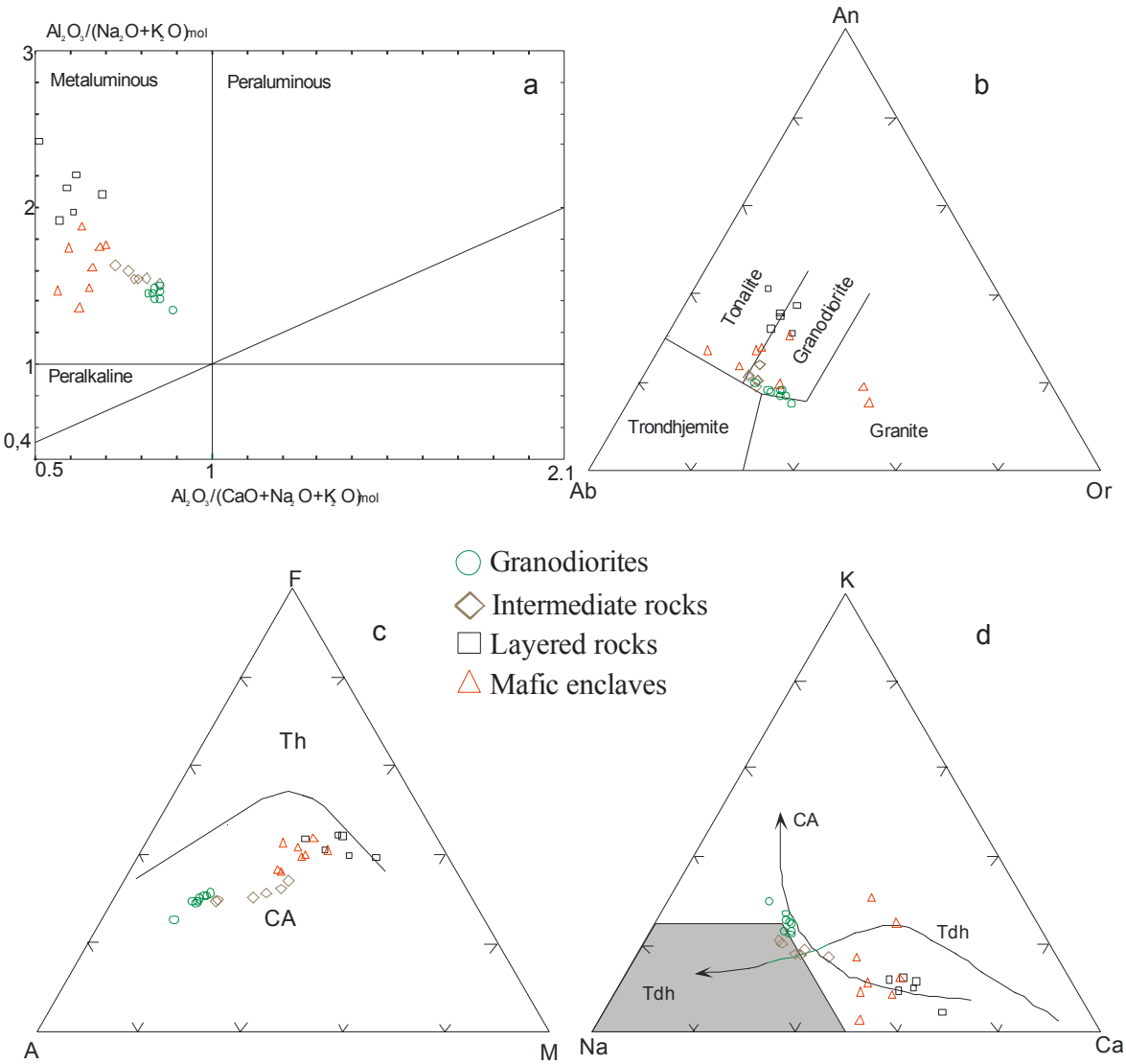

Fig. 5 - Diagrams showing the distribution of samples of the Rio Maria suite (a) Rocks from Rio Maria suite plot in the metaluminous field of the $[Al_2O_3/(CaO+Na_2O+K_2O)]$mol vs. $[Al_2O_3/(K_2O+Na_2O)]_{mol}$ diagram (Shand, 1950); (b) Ab-An-Or normative diagram. Fields from Barker (1979); (c) AFM diagram (Irvine and Baragar, 1971). CA=calc-alkaline, Th=tholeiitic; (d) K-Na-Ca plots. Trends for calc-alkaline (CA) and trondhjemite (Tdh) series as defined by Nockolds and Allen (1953) and Barker and Arth (1976).

Table 3
Chemical composition of the samples of the Rio Maria suite (Bannach area).

	Layered rocks						Mafic enclaves								Intermediate rocks						Granodiorites							
Facies	Dark Layer			Gray Layer			EBAD to EBAQMz								EBAQzD to EBAQzMD						EBAGD to EBAMzG							
Sample	MFR-07B	MFR-12B	ADR-	MFR-	Cr-71	MFR-12A	MFR-27C	MD-02C	MD-03A	299	MD-02A	ADR-2	MD-02B	MD-03B	ADR-4A	ADR-4B	ADR-5	MFR-102	MFR-100D	ADR-7	MFR-114	MFR-27	MFR-111	MFR-29	ADR-3A	MFR-112	MFR-91A	MFR-80A
SiO_2 (wt.%)	50.92	52.60	54.04	50.14	52.60	53.41	50.51	51.38	52.89	53.03	53.3	54.98	55.46	56.64	58.47	60.51	61.75	62.15	63.29	63.61	62.52	63.23	63.66	63.66	63.9	64.58	64.72	66.49
TiO_2	0.73	0.56	0.63	0.97	0.70	0.78	0.88	0.72	0.69	0.72	0.69	0.61	0.55	0.85	0.47	0.44	0.43	0.39	0.38	0.37	0.46	0.49	0.42	0.45	0.43	0.42	0.39	0.33
Al_2O_3	12.11	10.91	13.02	13.08	13.21	14.76	16.19	13.77	15.63	13.56	12.29	14.34	13.09	13.28	14.02	14.03	13.96	14.5	14.97	14.94	15.23	14.82	14.87	14.84	14.82	14.65	14.98	14.55
Fe_2O_3	4.16	3.28	3.41	3.63	11.89	4.07	5.06	11.15	9.58	10.49	10.2	3.59	8.94	9.05	2.46	2.37	2.89	2.34	2.51	3.12	2.91	2.8	2.81	3,00	2.91	2.86	2.71	2.27
FeO	5.96	5.96	3.41	7.08	n.d.	4.83	4.46	n.d.	n.d.	n.d.	n.d.	4.14	n.d.	n.d.	3.94	3.43	2.44	2.56	1.96	1.41	1.97	1.89	1.64	1.48	1.65	1.47	1.49	1.32
MnO	0.15	0.15	0.13	0.15	0.15	0.13	0.13	0.2	0.17	0.18	0.19	0.14	0.17	0.16	0.09	0.09	0.07	0.07	0.06	0.06	0.07	0.06	0.06	0.06	0.06	0.06	0.06	0.05
MgO	9.94	10.51	7.37	8.48	9.17	5.98	5.65	7.38	6.28	8.39	7.43	5.82	6.61	6.61	5.81	5.37	4.62	4.11	2.89	2.86	2.61	2.49	2.31	2.31	2.39	2.28	2.06	1.85
CaO	8.21	9.3	8.15	8.81	8.55	7.88	7.61	8.36	7.66	7.79	7.42	6.73	6.24	6.52	5.88	4.73	4.84	4.65	4.18	4.03	4.4	4.36	3.99	4.17	4.02	3.77	4.08	3.02
Na_2O	2.49	2.06	2.86	2.60	2.36	2.99	4.06	3.53	4.72	2.87	2.31	3.86	2.59	3.83	3.77	4.04	3.98	4.21	4.36	4.4	4.3	4.21	4.19	4.09	4.05	4.04	4.29	4.13
K_2O	2.04	1.03	1.74	1.72	1.94	2.00	2.33	1.94	1.1	2.32	4.23	3.07	4.96	1.76	2.21	2.16	2.31	2.24	2.57	2.66	2.93	3.01	3.32	3.22	3.21	3.44	2.98	3.75
P_2O_5	0.22	0.15	0.17	0.17	0.24	0.23	0.45	0.37	0.33	0.25	0.31	0.27	0.29	0.31	0.17	0.18	0.16	0.14	0.15	0.13	0.17	0.15	0.15	0.14	0.14	0.15	0.12	0.14
LOI	2.10	2.50	2.30	2.00	n.d.	2.10	1.90	0.8	0.6	n.d.	1.2	1.6	0.6	0.6	1.9	1.9	1.9	2,00	2,00	1.8	1.6	1.8	1.9	1.9	1.8	1.5	1.5	1.4
Total	99.03	99.01	99.10	98.83	100.81	99.16	99.23	99.56	99.65	99.60	99.57	99.15	99.50	99.61	99.19	99.25	99.35	99.36	99.32	99.39	99.17	99.31	99.32	99.32	99.38	99.22	99.38	99.3
Ba (ppm)	511	442	527	608	n.d.	711	344	468	199	1145	1088	876	1382	417	812	701	847	830	1008	1090	1139	1175	1052	1022	1098	1064	1044	1089
Rb	118	39	80	77	115	84	140	89	56	98	125	94	101	77	73	72	72	74	87	82	98	103	113	112	109	122	101	116
Sr	477	335	507	494	422	604	800	508	544.8	445	357.7	463	338	436	745	618	724	828	872	905	692	661	615	611	576	567	632	512
Zr	97	81	92	87	116	99	165	140	151	129	118	105	103	153	94	94	101	94	95	103	113	126	103	131	109	110	113	122
Nb	5	4	5	5	5	5	7	8	7	11	11	11	7	7	6	5	6	5	6	7	8	9	8	8	7	11	9	10
Y	17	17	17	23	15	19	23	23	22	24	25	23	19	23	11	10	11	10	10	12	16	13	11	15	11	12	17	12
Ga	17	14	17	18	n.d.	20	25	19	20	n.d.	16	20	15	17	18	18	19	20	20	20	20	20	19	20	20	19	20	19
Th	8	6	6	6	n.d.	6	1	2	2	n.d.	2	5	2	3	3	2	5	5	6	5	7	7	7	8	5	11	8	12
Ni	105	61	80	82	n.d.	57	46	40	18	n.d.	40	47	40	52	79	89	81	72	43	57	31	29	28	29	31	29	26	25
Cr	253	417	239	212	n.d.	171	103	397	226	n.d.	506	281	465	335	308	253	274	219	130	144	48	68	55	96	68	55	41	55
La	33	24.3	25.4	31.8	n.d.	27.6	28.5	25,00	25.4	n.d.	22.4	29	18.4	30.8	23.7	23.3	25.1	25.2	42.2	33.8	37.3	36.9	33.7	34.3	20.0	40.7	53.5	48.0
Ce	62.8	43.7	55.2	67.2	n.d.	53.9	77.1	67.2	60.4	n.d.	64.8	72.1	50.2	71,00	51.1	50.3	51.4	47.6	68.3	58.6	72.8	71.9	64.1	64.1	45.7	70.8	72.2	64.2
Pr	6.47	5.28	5.69	6.97	n.d.	6.54	10.11	10.41	9.85	n.d.	10.43	9.42	7.99	10.41	5.35	5.35	5.3	5.35	7.37	7.35	7.19	7.57	6.32	6.53	4.94	7.04	8.51	6.81
Nd	25.1	20.9	24.5	28.9	n.d.	27.1	44	41.6	43.5	n.d.	43,00	40.4	32.8	41.8	21.4	21.4	19.3	20.8	26.1	29.2	27.2	27.8	22.9	24.7	21.7	25.6	31.6	23.9
Sm	4.80	4.10	4.5	6.1	n.d.	5.3	8.6	8.4	8.35	n.d.	8.61	7.5	6.62	7.91	3.6	3.4	3.3	3.6	4.1	4.3	4.4	4.9	3.7	4.3	3.7	3.9	4.5	3.4
Eu	1.29	1.14	1.33	1.69	n.d.	1.59	1.73	1.58	1.62	n.d.	1.75	1.52	1.27	1.59	1.02	0.95	0.98	0.99	1.05	1.23	1.25	1.35	1.06	1.14	1.05	1.07	1.3	0.95
Gd	4.04	3.59	3.64	5.06	n.d.	4.74	5.71	6.65	6.64	n.d.	6.92	5.8	5.4	6.7	2.78	2.49	2.58	2.42	2.82	3.19	3.47	3.56	2.9	3.2	2.63	2.71	3.37	2.43
Tb	0.6	0.51	0.58	0.82	n.d.	0.72	0.86	0.97	0.88	n.d.	0.96	0.98	0.74	0.88	0.45	0.37	0.37	0.4	0.35	0.48	0.56	0.53	0.42	0.47	0.41	0.4	0.52	0.36
Dy	2.82	2.79	2.89	3.9	n.d.	3.37	4.35	4.94	4.36	n.d.	4.66	4	3.83	4.5	2.25	1.84	1.98	1.75	1.67	2.2	2.41	2.19	1.92	2.19	1.86	1.9	2.31	1.56
Ho	0.54	0.53	0.6	0.77	n.d.	0.69	0.78	0.87	0.81	n.d.	0.87	0.74	0.71	0.8	0.38	0.34	0.33	0.34	0.31	0.42	0.48	0.42	0.34	0.42	0.41	0.4	0.49	0.32
Er	1.51	1.52	1.68	2.14	n.d.	1.82	2.05	2.41	2.14	n.d.	2.33	2.04	1.88	2.16	1.03	0.97	0.88	0.95	0.78	1.13	1.3	1.15	0.92	1.19	1.02	0.92	1.25	0.81
Tm	0.23	0.24	0.19	0.33	n.d.	0.26	0.29	0.37	0.32	n.d.	0.38	0.27	0.28	0.35	0.13	0.1	0.1	0.1	0.11	0.13	0.14	0.17	0.11	0.17	0.1	0.23	0.17	0.12
Yb	1.55	1.36	1.41	1.8	n.d.	1.48	1.7	2.24	1.85	n.d.	2.3	1.73	1.69	1.88	0.93	0.83	0.81	0.9	0.69	1,00	1,00	1.06	0.92	1.09	0.87	0.83	0.99	0.73
Lu	0.22	0.2	0.23	0.3	n.d.	0.25	0.25	0.32	0.28	n.d.	0.34	0.29	0.26	0.28	0.15	0.14	0.12	0.13	0.12	0.15	0.16	0.16	0.11	0.15	0.14	0.15	0.15	0.13
ΣREE	144.97	110.16	127.84	157.78	n.d.	135.36	186.03	172.96	166.4	n.d.	169.75	1/3.7 / 0	132.07	181.06	114.27	111.78	112.55	110.53	155.97	143.18	159.66	159.66	139.42	143.95	104.53	156.65	180.86	153.72
$(La/Yb)_n$	14.37	12.06	12.16	11.92	n.d.	12.59	11.32	7.53	9.27	n.d.	6.57	11.31	7.35	11.06	17.20	18.95	20.92	18.90	41.28	22.81	25.18	23.50	24.72	21.24	15.52	33.10	36.48	44.38
$(La/Sm)_n$	4.33	3.73	3.55	3.28	n.d.	3.28	2.09	1.87	1.92	n.d.	1.64	2.43	1.75	2.45	4.14	4.31	4.79	4.41	6.48	4.95	5.34	4.74	5.73	5.02	3.4	6.57	7.49	8.89
$(Dy/Yb)_n$	1.18	1.33	1.33	1.41	n.d.	1.48	1.66	1.43	1.53	n.d.	1.32	1.5	1.47	1.56	1.57	1.44	1.59	1.26	1.57	1.43	1.57	1.34	1.36	1.31	1.39	1.49	1.52	1.39
Eu/Eu*	0.9	0.91	1,0	0.93	n.d.	0.97	0.75	0.65	0.67	n.d.	0.69	0.7	0.65	0.67	0.99	1.00	1.03	1.03	0.94	1.02	0.98	0.99	0.99	0.94	1.03	1.01	1.02	1.01
Rb/Sr	0.25	0.12	0.16	0.16	0.27	0.14	0.17	0.18	0.10	0.22	0.35	0.20	0.30	0.18	0.1	0.12	0.1	0.09	0.1	0.09	0.14	0.16	0.18	0.18	0.19	0.22	0.16	0.23
Sr/Ba	0.93	0.76	0.96	0.81	n.d.	0.85	2.32	1.09	2.74	0.39	0.33	0.53	0.24	1.04	0.92	0.88	0.85	1.00	0.86	0.83	0.61	0.56	0.58	0.6	0.53	0.53	0.61	0.47
K/Na	0.54	0.33	0.40	0.44	0.54	0.44	0.38	0.36	0.15	0.53	1.20	0.52	1.26	0.30	0.39	0.35	0.38	0.35	0.39	0.40	0.45	0.47	0.52	0.52	0.52	0.56	0.46	0.60
$FeO_t/(FeO_t+MgO)$	0.49	0.46	0.47	0.55	0.54	0.59	0.61	0.58	0.58	0.53	0.55	0.56	0.55	0.55	0.52	0.51	0.52	0.53	0.59	0.60	0.64	0.64	0.64	0.64	0.64	0.64	0.66	0.65
Mg#	0.64	0.67	0.61	0.59	0.60	0.55	0.55	0.56	0.56	0.61	0.59	0.58	0.59	0.59	0.62	0.63	0.62	0.61	0.55	0.54	0.50	0.50	0.50	0.49	0.49	0.50	0.48	0.49

Data Source: Oliveira (2005). Chemical ratios: Mg# molecular ratio Mg/(Mg+Fe); K/Na molecular ratio. Eu/Eu* = EuN / (0.5 * (SmN + GdN). E = epidote; B = biotite; A = amphibole; Qz = quartz; D = diorite; MzD = monzodiorite; Mz = monzonite; GD = granodiorite; MzG = monzogranite.

The layered rocks, mafic enclaves, intermediate rocks, and granodiorites have in common a typical sanukitoid signature indicated by their metaluminous character, and high Mg#, Cr, and Ni, conjugate with elevated contents of large ion lithophile elements (LILE), especially Ba and Sr (Oliveira et al., 2009, submitted). Layered rocks and mafic enclaves have similar silica contents varying from 50.14 to 56.64 wt.% (Table 3), showing an important compositional gap (Fig. 6) with the intermediate rocks and granodiorites (respectively, 58.47 to 63.61 and 62.52 to 66.49 wt.% of silica).

The alkali contents in the studied rocks are high compared to typical calc-alkaline series. In the TAS diagram (Fig. 6; fields for volcanic rocks of Le Maitre et al., 2002, are shown for comparison), the intermediate rocks and granodiorite samples plot along the divide between the oversaturated and saturated domains. On the other hand, the enclaves plot dominantly in the saturated field of that diagram, consistently with their affinity with the monzonitic series (Fig. 4). In the case of layered rocks, which were previously interpreted as cumulate rocks (Oliveira et al., submitted), it is clear that the analyzed samples do not correspond to real liquids. However, their chemical compositions can provide indirect information about the nature of original magmas and are shown also for comparison with those of the other varieties of rocks.

Al_2O_3 contents are similar in the enclaves, intermediate rocks and granodiorites, attaining the lowest values in the layered rocks which are impoverished in alkali feldspar compared to the other mentioned groups. All analyzed rocks display Al_2O_3 contents (Table 3) that are lower than those found in rocks of similar silica contents of typical calc-alkaline series (Irvine and Baragar, 1971; Ringwood, 1975; Wilson, 1989). Mg# values vary from 0.67 to 0.48, decreasing from the layered rocks to the granodiorites. There are clear contrasts in Mg# in the dark and gray layers of the layered rocks, with the gray layers showing comparatively lower Mg# (Table 3). The Mg# in the enclaves is generally intermediate between those of layered and intermediate rocks and granodiorites (Fig. 7c). K/Na ratios do not show accentuated variation in the different groups (Table 3), except for the quartz monzonitic enclaves which are enriched in K_2O compared to dominant rocks and display K/Na ratios > 1.

3.3.2 – The behavior of trace elements

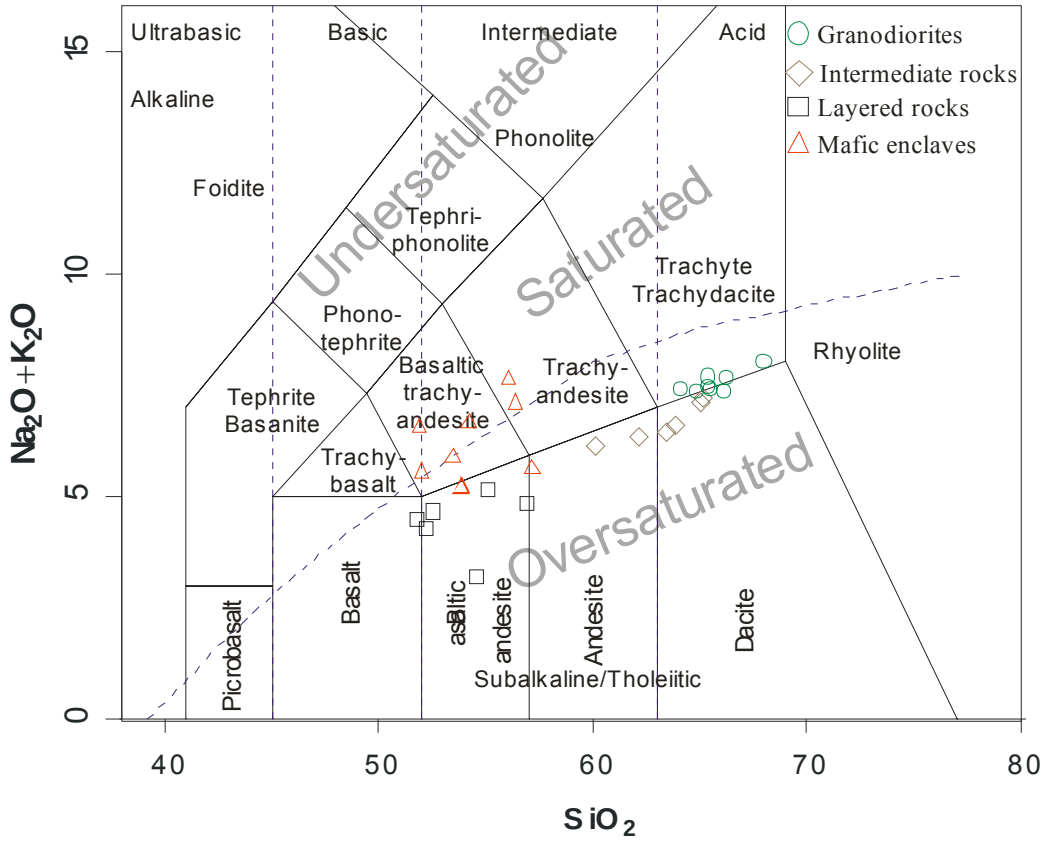

Fig. 6 - The total alkali-silica diagram (TAS) showing the composition of rocks of the Rio Maria suite. TAS diagram classification according to Le Bas *et al*. (1986).

Besides quartz, the most abundant minerals in the rocks of the Rio Maria suite are amphibole, biotite, plagioclase, and alkali feldspar. Petrographic aspects, as well as the different ranges of silica of the studied rocks and other geochemical parameters, indicate that plagioclase had an important role in the magmatic evolution of these rocks. The influence of amphibole, principal mafic mineral of the Rio Maria suite, and that of biotite will also be discussed. The trace elements are useful in estimating the extent of fractionation of these minerals and whether magmatic evolution was controlled dominantly by fractional crystallization, partial melting or more complex processes (Hanson, 1978, 1989; Rämö, 1991; Rollinson, 1993; Dall'Agnol et al., 1999; Rapp et al., 1999; Martin et al., 2005).

Rb, Sr, and Ba

Rb behaves incompatibly in all varieties of the studied rocks (Table 3, Fig. 7a). In the granodiorites and mafic enclaves, the increase of Rb along magmatic differentiation is more accentuated, compared to the intermediate rocks. Sr behavior is contrasting in these rocks, being compatible in the granodiorites and mafic enclaves and incompatible in the intermediate rocks. Ba is clearly incompatible in the intermediate rocks and mafic enclaves and show limited variation in the granodiorites. Rb and Sr show positive correlation in the intermediate rocks, and negative correlation in the granodiorites and mafic enclaves; Sr and Ba display positive correlation in the intermediate rocks and negative in the mafic enclaves and granodiorites (Fig. 7a, b). In the Rb/Sr vs. Sr/Ba plot (Fig. 7c), it is observed a negative correlation between these ratios in the granodiorites, with an important increase in the Rb/Sr ratio parallel to increasing silica, while the Sr/Ba ratio remains almost constant. In the mafic enclaves, the correlation is also negative but, in this case, it is the Sr/Ba ratio that shows a larger variation. Finally, in the intermediate rocks, Rb/Sr and Sr/Ba ratios do not show significant variations.

Rb vs. Sr, Sr vs. Ba, and Rb/Sr vs. Sr/Ba plots (Fig. 7a, b, c) show that granodiorites, intermediate rocks, and mafic enclaves display geochemical trend distinct in all these diagrams. If these rocks evolved by fractional crystallization, it indicates that they derive from distinct liquids or that their differentiation was controlled by different phases or both and implies that they could not be derived from a same magma. Admitting an evolution by fractional crystallization of each variety of rock, the trends shown by the granodiorites and mafic enclaves can be explained by simultaneous fractionation of plagioclase and amphibole. This hypothesis is consistent with the significant decrease of Sr and increase of Rb and Ba from the low silica to the more silica-rich samples (Table 3; Fig. 7a, b). Moreover, the mentioned diagrams show that these two varieties derived from two entirely distinct liquids and the proportions of fractionated amphibole and plagioclase also differ. The trends defined by the intermediate rocks indicate fractionation of amphibole and biotite, reflected in the important increase of Sr and Ba and small variation in Rb along differentiation.

Sr and Y

Sr and Y contents in Archean rocks are extremely dependent of, respectively, plagioclase and garnet behavior during magma genesis and differentiation. Sr concentrations in melts

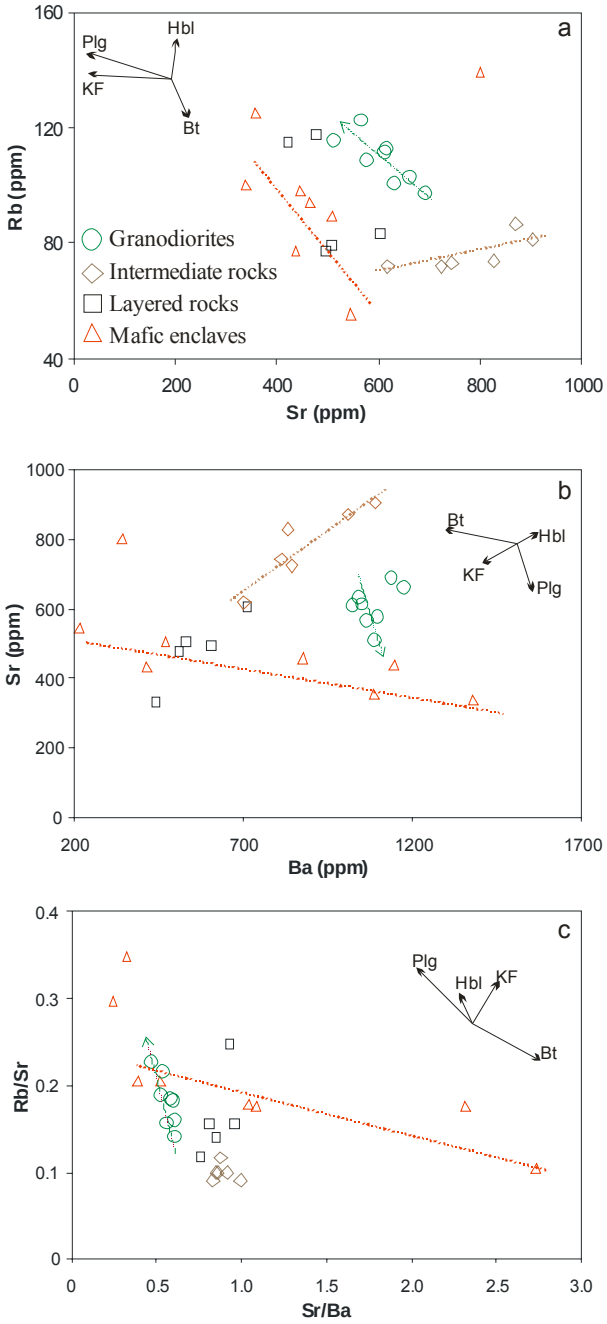

Fig. 7 – (a) Rb *vs.* Sr; (b) Sr *vs.* Ba; (c) Rb/Sr *vs.* Sr/Ba plots for rocks from the Rio Maria suite (Bannach area). The vectors indicate the influence of fractionation of plagioclase (Plg), potassium feldspar (KF), hornblende (Hbl) and biotite (Bt) in the composition of the residual liquids. The arrows show possible trends during fractional crystallization into of granodiorites, intermediate rocks and mafic enclaves.

increase sharply above plagioclase domain of stability (Zamora, 2000; Martin et al., 2005). Y behavior is geochemically similar to that of Yb, and low Y contents in the melt are also generally seen as indicative of presence of significant amounts of garnet in the residue. Consequently, Sr/Y ratio behavior is similar to that of the La/Yb ratio during melting events that produce garnet and consume plagioclase (Moyen and Stevens, 2006). In addition, because of the strong influence of pressure conditions in plagioclase and garnet stability, Sr/Y ratios are a good pressure indicator, high-pressure melts being Sr-richer and Y-poorer than low-pressures ones.

The studied intermediate rocks have the highest Sr/Y ratios and the lowest Y contents (Table 3; Fig. 8a), possibly reflecting a more abundant garnet content and an absence or restrict influence of plagioclase in the residue of its magma (as suggested by modelling; see below). On the contrary, the mafic enclaves show the highest Y contents and the lowest Sr/Y ratios values, indicating an important change in the residual assemblage in relation to the intermediate rocks with inversed roles of garnet and plagioclase, suggesting a comparatively lower pressure of partial melting for the mafic enclave magma. The Sr/Y and Y of the granodiorite analyzed samples are in between those of intermediate rocks and mafic enclaves, suggesting magma formation in moderate pressure conditions.

Cr and Ni

Mantle peridotites have Cr/Ni around 1.5 (Taylor and McLennan, 1985; McDonough and Sun, 1995) and its possible metasomatism by TTG melts should not significantly modify their Cr/Ni ratio because the $Cr_{peridotite}/Cr_{TTG}$ and $Ni_{peridotite}/Ni_{TTG}$ are very high (10 and 20, respectively). Consequently, the Cr/Ni ratio of the magmas derived from metasomatized mantle is strongly dependent of the residual assemblage of mantle melting (Martin et al., 2005). Several possible residual phases of mantle melting have $Kd_{(Cr/Ni)}^{min/liq}$ greater than one (orthopyroxene=2.5; garnet=4.4; pargasite=4; Rollinson, 1993) but their effect is buffered by olivine ($Kd_{(Cr/Ni)}^{min/liq}$~0.1; Rollinson, 1993). The range of Cr/Ni ratios vary from 1.5 to 3.0 in the granodiorites and between 2.5 and 4 in the intermediate rocks. In the mafic enclaves Cr/Ni ratios attain the highest values (~12; Fig. 8b, c). These values point to contrasts in residual assemblage, between the mafic enclaves, in one hand, and intermediate rocks and granodiorites, in the other

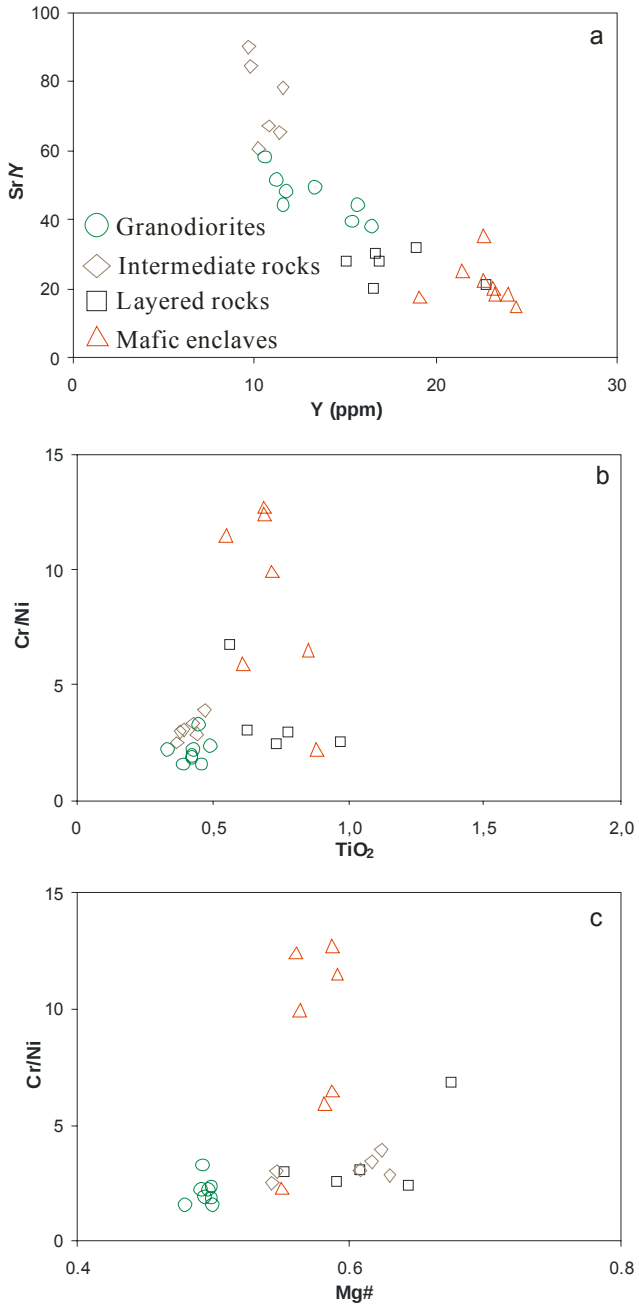

Fig. 8 – (a) Sr/Y *vs.* Y; (b) Cr/Ni *vs.* TiO_2; (c) Cr/Ni *vs.* Mg# plots for rocks from the Rio Maria suite (Bannach area).

hand, and suggest minor content of mineral phases with $Kd_{(Cr/Ni)}^{min/liq} > 1$ in the mafic enclaves magma residue compared to that of other varieties.

Rare earth elements

Granodiorites and intermediate rocks have similar patterns (Fig. 8) of rare earth elements (REE), with pronounced enrichment in light rare earth elements (LREE) and strong to moderate fractionation of heavy rare earth elements (HREE) (La/Yb_N ratios of 15.52 to 44.38, granodiorites; 17.20 to 41.28, intermediate rocks), associated with small or absent Eu anomaly (Eu/Eu* from 0.94 to 1.03, in both granodiorites and intermediate rocks; Table 3). The patterns of REE in the layered rocks and mafic enclaves show a less pronounced enrichment in LREE, and minor fractionation of HREE compared to granodiorites and intermediate rocks, reflected in the their lower La/Yb_N ratios (6.57 to 11.32, enclaves; 11.92 to 14.37, layered rocks). This feature is associated with a small or absent (layered rocks; Eu/Eu* from 0.90 to 1.00) or important negative europium anomaly (mafic enclaves; Eu/Eu* from 0.65 to 0.75).

The similarities in the REE patterns of granodiorites and intermediate rocks could be seen as evidence that these rocks were linked by fractional crystallization process. However, the lack of significant variation in the Eu/Eu* ratio from the intermediate rocks to the granodiorites and the geochemical behavior of these rocks in other geochemical diagrams (Figs. 7 and 8) do not give support to the mentioned hypothesis. A possible alternative is to consider that these varieties were derived from at least two distinct magmas, both with sanukitoid affinity, but originated from different degrees of melting of a modified mantle source (Oliveira et al., 2009). Anyway, this and other hypotheses should be tested by geochemical modeling.

Granodiorites and intermediate rocks show REE patterns with a concave shape of the HREE branch (Fig. 9), suggesting that amphibole was probably an important fractionating phase. This aspect is not observed in the REE patterns of the layered rocks and, associated with the minor fractionation of HREE in those rocks compared with the granodiorites and intermediate rocks, it suggests that the process of amphibole accumulation was determinant in the REE signature of these rocks (Oliveira et al., submitted). Mafic enclave REE patterns, besides their higher contents of HREE and important negative europium anomaly, display a convex shape of the LREE branch pattern. These aspects and geochemical evidence shown above indicate that the

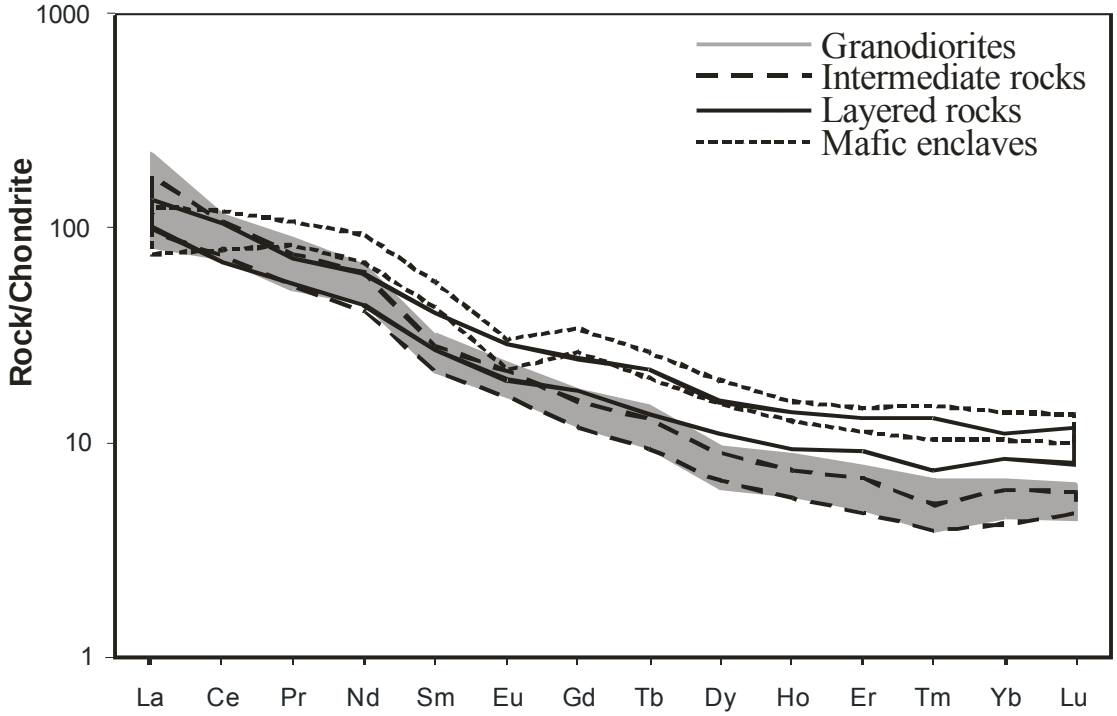

Fig. 9 - Chondrite-normalized REE patterns for the rocks of the Rio Maria suite of Bannach area (normalization values from Evensen et al., 1978).

mafic enclaves and the other varieties of rocks of the studied sanukitoid suite are not comagmatic and that, in the former, plagioclase was a more important residual or fractionating phase than garnet during partial melting or fractional crystallization processes.

3.4 – Nd isotopes

Nd isotope data in four samples of granodiorites and one sample of intermediate rock of the Rio Maria suite are available (Leite, 2001; Souza et al., 2001; Rämö et al., 2002; Dall'Agnol et al., 2006). The analyzed rocks show quite uniform positive ε_{Nd} values, varying from 0.2 to 1.2 and depleted-mantle T_{DM} ages (DePaolo, 1981) ranging from 2.92 to 3.01 Ga, just a little older than their crystallization age of 2.87 Ga. The data are from Rämö et al. (2002) and are listed in Table 3 and they are also shown in a ε_{Nd} vs. age diagram in Figure 10.

Table 4
Sm-Nd isotopic data for the granodiorites and intermediate rocks of Rio Maria suite.

Sample#	*Rock type*	*Sm (ppm)*	*Nd (ppm)*	$^{147}Sm/^{144}Nd$	$^{143}Nd/^{144}Nd$	ε_{Nd}	T_{DM} *(Ma)*
Granodiorites (2872 ± 5 Ma)							
AL-141	Biotite-hornblende-granodiorite	7.39	46.99	0.095	0.510772 ± 12	1.2	2923
AL-166	Hornblende-biotite-granodiorite	4.44	26.20	0.1024	0.510911 ± 9	1.1	2929
F-66	Biotite-hornblende-granodiorite	3.78	20.87	0.1094	0.510998 ± 10	0.2	3003
HRM-284	Hornblende-biotite-granodiorite	3.06	18.60	0.0993	0.510834 ± 9	0.8	2953
Intermediate rock (2878 ± 4 Ma)							
Z-509B	Biotite-hornblende-quartz-diorite	5.89	29.26	0.1216	0.511235±15	0.4	3010

Data source: Rämö et al. (2002).

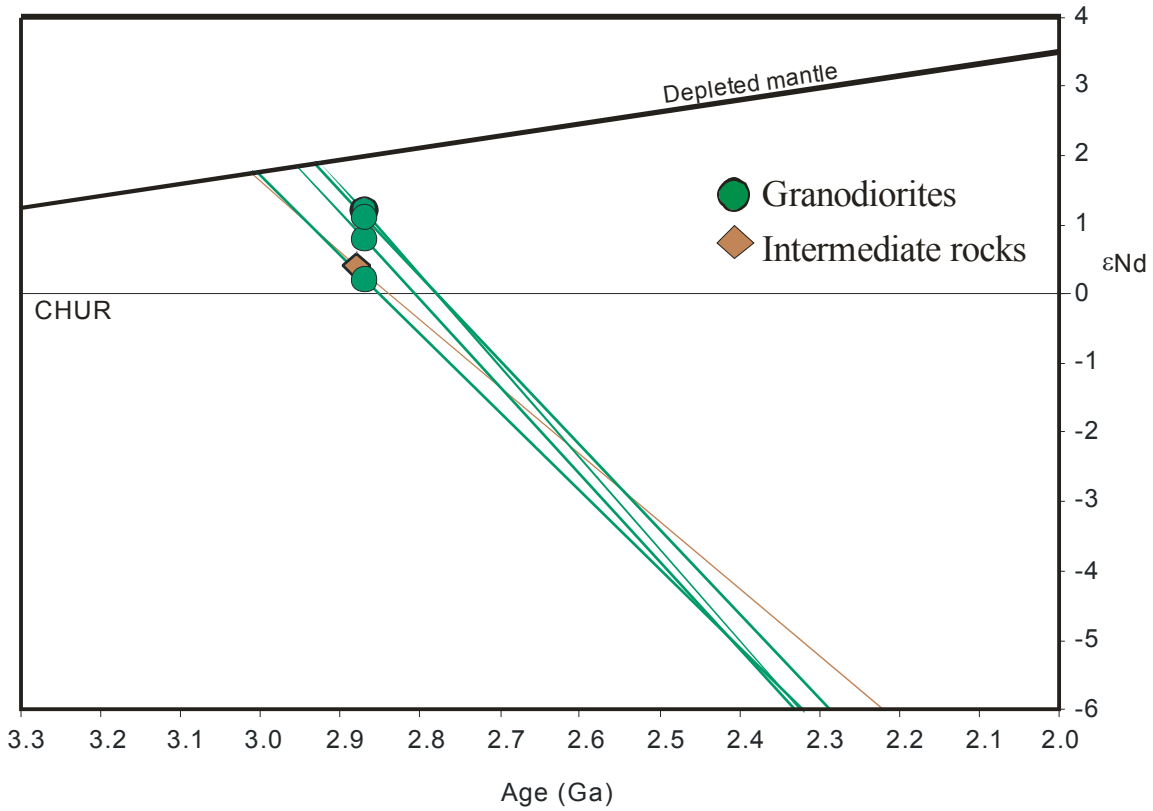

Fig. 10 - ε_{Nd} values *vs.* age diagram showing the neodymium isotopic composition of granodiorites, intermediate rocks and mafic enclaves from Rio Maria suite from Rio Maria granite-greenstone terrane (Rämö et al., 2002). Also shown is the evolution of depleted mantle (DePaolo, 1981), undifferentiated Earth (Chondritic Uniform Reservoir—CHUR; DePaolo and Wasserburg, 1976) and Post-Archaean average Australian Shale (PAAS; Nance and Taylor, 1976).

3.5 – Geochemical modeling and petrogenesis

The most primitive sanukitoid magmas must derive from a source able to account for the LILE-rich, HFSE-depleted nature of the rocks (e.g., Shirey and Hanson, 1984; Stern, 1989; Smithies and Champion, 2000). Geochemical modeling showed that contamination of basaltic or komatiitic magmas by a typical Archean felsic crust cannot produce both the high Ni and Cr, and the high SiO_2 and LILE compositions of sanukitoids (Stern et al., 1989; Smithies and Champion, 2000). Processes such as partial melting of mantle peridotite that had been previously metasomatized by TTG melts (Evans and Hanson, 1997; Smithies and Champion, 2000) or slab-melts that have assimilated peridotite during ascent through mantle wedge (Martin et al., 2005) are able to generate the mentioned features and alternatives to explain the petrogenesis of sanukitoid series (Rapp et al., 1999, 2007).

Geochemical data presented above demonstrate that granodiorites, intermediate rocks, mafic enclaves, and layered rocks of Bannach area all have in common sanukitoid characteristics. However, a preliminary evaluation of trace element data indicates that the three former varieties are cogenetic but not comagmatic rocks (this paper; cf. also Oliveira et al., 2009, submitted). Nevertheless, a possible relationship between these rocks by fractional crystallization was also evaluated by modeling. The hypothesis of a magmatic link between the layered rocks and granodiorites or intermediate rocks was also tested. Additionally, it was evaluated if different degrees of metasomatism of a mantle source or of assimilation of peridotite by slab-melts could explain the contrasting geochemical aspects of the studied rocks. Finally, the effect of variable degrees of partial melting of the source in the primitive magma composition was considered.

Thus, we have tested quantitatively fractional crystallization, assimilation and partial melting models in order to establish constraints for the petrogenesis of the Rio Maria sanukitoid suite. The nature of the magma source of these rocks, including the possible influence of processes of mantle metasomatism or assimilation of peridotite by slab-melts, was also investigated. This was done using major elements, as well as selected trace elements, including REE.

3.5.1 – Methodology of modeling

We performed mass balance calculations for the major elements using the program GENESIS (Teixeira, 2005). The model is calculated by adjusting the relative proportions of fractionating or residual minerals from the initial melt or source, respectively, to reproduce the composition of the expected melt. The quality of the model is evaluated using the sum of the squared residuals ($\sum R^2$), and the model is consistent if $\sum R^2 < 1$. For trace elements modeling, Excel tables created by Sergio C. Valente (Universidade Federal Rural do Rio de Janeiro, Brazil) were employed. The mineral/liquid partition coeficients (K_d) used in the modeling are available from the first named author upon request. Most of them are from Rollinson (1993).

The compositions of the initial liquids of intermediate rocks, granodiorites and mafic enclaves are not precisely known and need to be estimated. In the case of intermediate rocks and granodiorites, the samples with the lowest silica contents of each group were assumed as representatives of the initial liquids (ADR-4A and MFR-114, respectively; Table 3), though some comparisons with other samples have been made. In the case of the mafic enclaves, the sample with the lowest silica content is not assumed as representative and the next sample in the range of silica was used (MD-02C; Table 3).

The compositions of the fractionating amphibole and biotite were taken from selected representative analyses (Oliveira et al., submitted) of these minerals found in intermediate rocks, granodiorites, mafic enclaves, and layered rocks of the Rio Maria suite (Table 5). The compositions of plagioclase, potassium feldspar, apatite and zircon are those corresponding to magmatic compositions found in Archean granitoids (Martin, 1985). In our partial melting and assimilation modeling, the compositions of residual mineral phases tested include those given by Nixon et al. (1981), Rapp et al. (1999), and Moyen et al. (2001) (see more details below).

3.5.2 – Fractional crystallization modeling

We have examined: (1) whether the intermediate rocks and granodiorites could be related by fractional crystallization and, (2) if each group evolved internally by that process. Besides, we have evaluated a possible magmatic link between layered rocks and granodiorites or intermediate rocks by accumulation processes. A derivation of intermediate rocks and granodiorite from the mafic enclave magma by fractional crystallization was also tested but results were not acceptable

Table 5
Major elements compositions of minerals used for the major element modeling of crystallization and acumulation processes related to the rocks from Rio Maria suite (Bannach area).

	Layered rocks		Mafic enclaves		Intermediate rocks		Granodiorites	
Mineral	Amphibole	Biotite	Amphibole	Biotite	Amphibole	Biotite	Amphibole	Biotite
SiO_2 (wt.%)	43,359	37,753	47,012	37,322	48,356	37,384	47,501	37,534
TiO_2	1,592	1,119	1,063	1,164	0,469	0,395	0,918	1,028
Al_2O_3	11,685	16,017	6,980	15,666	5,964	16,001	7,362	15,091
FeO	10,417	15,128	15,372	18,241	13,852	14,841	14,920	16,309
MnO	0,131	0,169	0,348	0,226	0,281	0,186	0,346	0,220
MgO	14,910	13,814	12,993	12,720	13,900	14,886	12,578	13,654
CaO	12,611	0,022	12,229	0,037	12,435	0,000	12,269	0,051
Na_2O	1,771	0,053	1,091	0,108	0,879	0,108	0,940	0,075
K_2O	0,836	9,883	0,741	9,523	0,474	9,322	0,684	9,490
Total	97,312	93,958	97,829	95,007	96,610	93,123	97,518	93,452

Data Source: Oliveira et al. (Submitted). Total Fe reported as FeO.

($\sum R^2 > 10$). A similar conclusion was also suggested by geochemical evidence and, for this reason, that hypothesis was discarded.

In the fractional crystallization modeling between intermediate rocks and granodiorites, the sample ADR-4B (Table 3) of the former was assumed as the parent and the sample MFR-114 (Table 3) of the latter as the daughter. The best models were obtained fractionating (1) amphibole + biotite, and (2) + plagioclase. However, even in these cases, the sums of the squared residuals are relatively high ($\sum R^2 > 2$, Table 6) and both fractionates give a bad fit for the REE (Figs. 11a, c). Other important trace elements, especially Ba, Y, Nb, and Zr (Fig. 11b, d), decrease with fractionation, on the opposite sense of the increasing trend observed in the analyzed samples of intermediate rocks and granodiorite. Hence, for the derivation of the granodiorite magma from that of intermediate rocks, it is concluded that an acceptable model was not obtained. This reinforces the hypothesis that these rocks are not comagmatic.

To test if internal variation in the group of intermediate rocks was compatible with fractional crystallization, the sample ADR-4A was used as parent and sample MFR-102 as daughter. Two major element models fractionating amphibole + biotite ± apatite (Table 6) gave consistent results and were selected for trace element modeling. The lowest sums of the squared residuals ($\sum R^2 = 0.773$, model 1, Table 6) occur when apatite is also fractionated, and in this case, the fractionating phases, composed of 73% of amphibole, 22% of biotite, and 5% of apatite, represent 17% of the original liquid. For rare earth elements and additional trace elements, the two models gave a good fit (Fig. 12a, b, c, d).

In the case of granodiorites, the sample MFR-114 was used as parent and MFR-80A as daughter. Two major element models, both showing $\sum R^2 < 1$ and plagioclase and amphibole as major fractionating phases (~55% and 38 to 45%, respectively; Table 5), were selected for trace element modeling. In one of these models, biotite was also included as fractionating phase (7%; model 1, Table 6). In these models, the fractionating assemblages correspond to 25% of the original liquid, and both fractionate gave a good fit for the REE (Fig. 13a, c) and the other evaluated trace elements (Fig. 13b, d).

Assuming a cumulate origin for the layered rocks (Oliveira et al., submitted), we tested whether these rocks could be derived from the parental liquids of the granodiorites or intermediate rocks. For the granodiorites and intermediate rocks, the samples with the lowest

Table 6
Modelling major element compositions. fractionated and accumulated mineral assemblages for differetiation of the Rio Maria suite (Bannach area).

Varieties	Intermediate to Granodiorite			Intermediate rocks			Granodiorites			Intermediate rock to Layered rock				Granodiorite to Layered rock	
Sample/Model	MFR-114	1	2	MFR-102	1	2	MFR-80A	1	2	MFR-12B	MFR-12A	Dark layer	Gray layer	Dark layer	Gray layer
SiO_2 (wt.%)	62.52	62.78	62.80	62.15	61.98	61.69	66.49	66.48	66.37	52.60	53.41	50.40	51.87	52.49	53.32
TiO_2	0.46	0.44	0.44	0.39	0.47	0.46	0.33	0.48	0.49	0.56	0.78	0.69	0.85	0.59	0.80
Al_2O_3	15.23	15.29	15.27	14.5	14.98	15.05	14.55	14.53	14.62	10.91	14.76	11.97	14.97	11.20	14.79
Fe_2O_3	5.10	4.70	4.72	5.73	5.16	4.91	3.74	4.05	4.11	9.90	9.44	8.9	9.03	9.81	9.40
MgO	2.61	3.63	3.64	4.11	4.08	3.83	1.85	1.61	1.65	10.51	5.98	12.5	7.24	10.61	5.99
CaO	4.40	3.79	3.77	4.65	5,00	5.27	3.02	2.89	2.65	9.30	7.88	12.1	9.78	9.22	7.98
Na_2O	4.30	4.57	4.56	4.21	4.42	4.45	4.13	4.43	4.41	2.06	2.99	1.20	2,00	1.90	2.79
K_2O	2.93	2.38	2.39	2.24	1.96	1.99	3.75	3.56	3.75	1.03	2.00	0.45	2.45	0.99	1.98
P_2O_5	0.17	0.28	0.27	0.14	0.12	0.16	0.14	0.13	0.13	0.15	0.23	0.20	0.25	0.16	0.24
Plagioclase	-	-	2.40	-	-	-	-	54.40	55.40	-	-	-	10.27	-	10.27
Amphibole	-	89.10	87.30	-	73.20	67.26	-	38.40	44.60	-	-	100.00	89.73	100.00	89.73
Biotite	-	10.90	10.30	-	21.80	32.74	-	7.20	-	-	-	-	-	-	-
Apatite	-	-	-	-	5.00	-	-	-	-	-	-	-	-	-	-
$\sum R^2$	-	2.04	2.04	-	0.77	1.21	-	0.33	0.45	-	-	14.53	12.25	0.43	0.14
% Crystallisation	-	15.00	15.00	-	17.00	19.00	-	25.00	25.00	-	-	-	-	-	-
% Accumulation	-	-	-	-	-	-	-	-	-	-	-	50.00	30.00	50.00	30.00

Total Fe reported as Fe_2O_3.

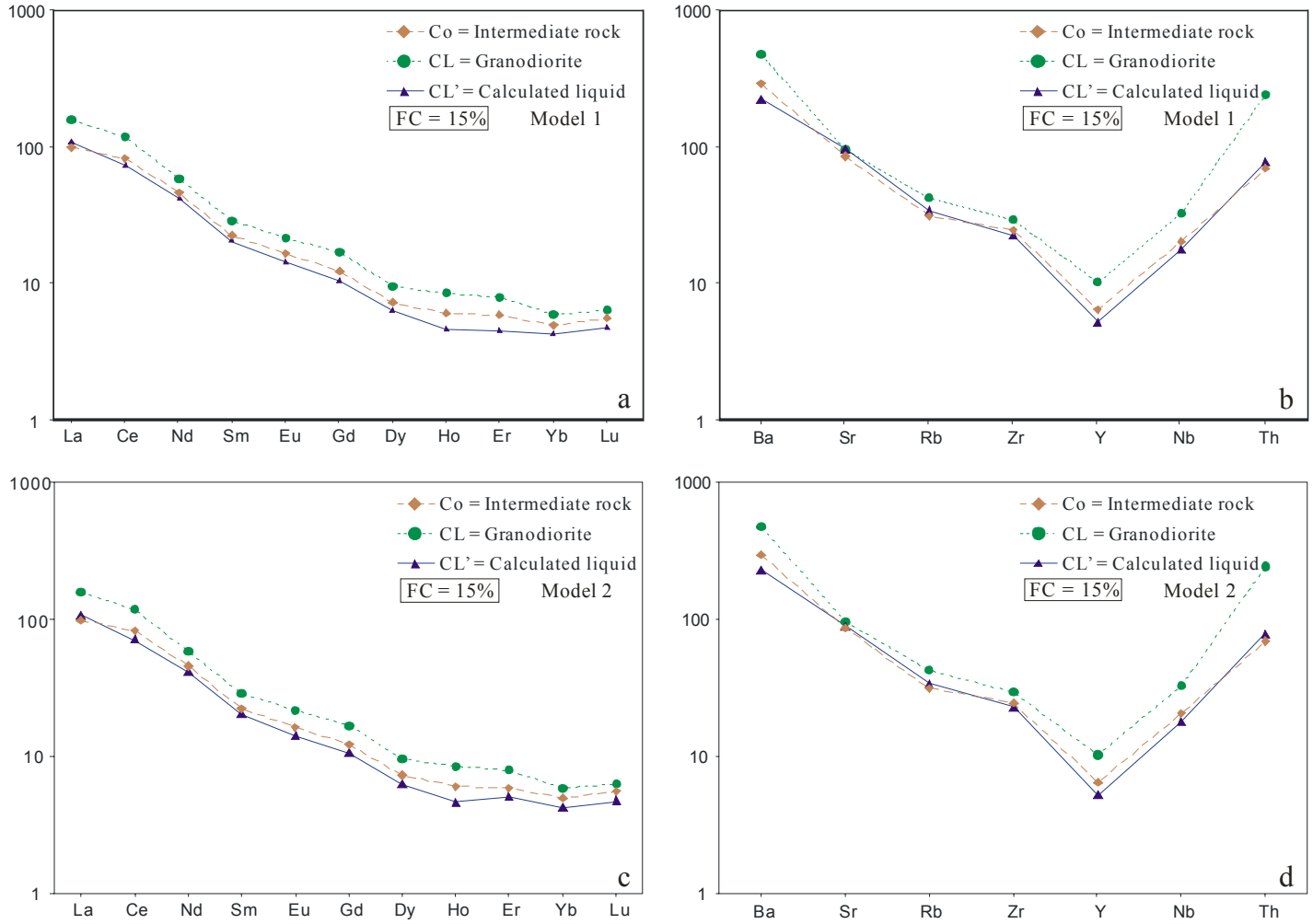

Fig. 11 – Fractional crystallization (FC) modeling from the intermediate rocks (parent) to granodiorites (daughter). (a, c) REE patterns; (b, d) Trace elements plots; (a, b) model 1; (c, d) model 2; FC is percentage of crystallization.

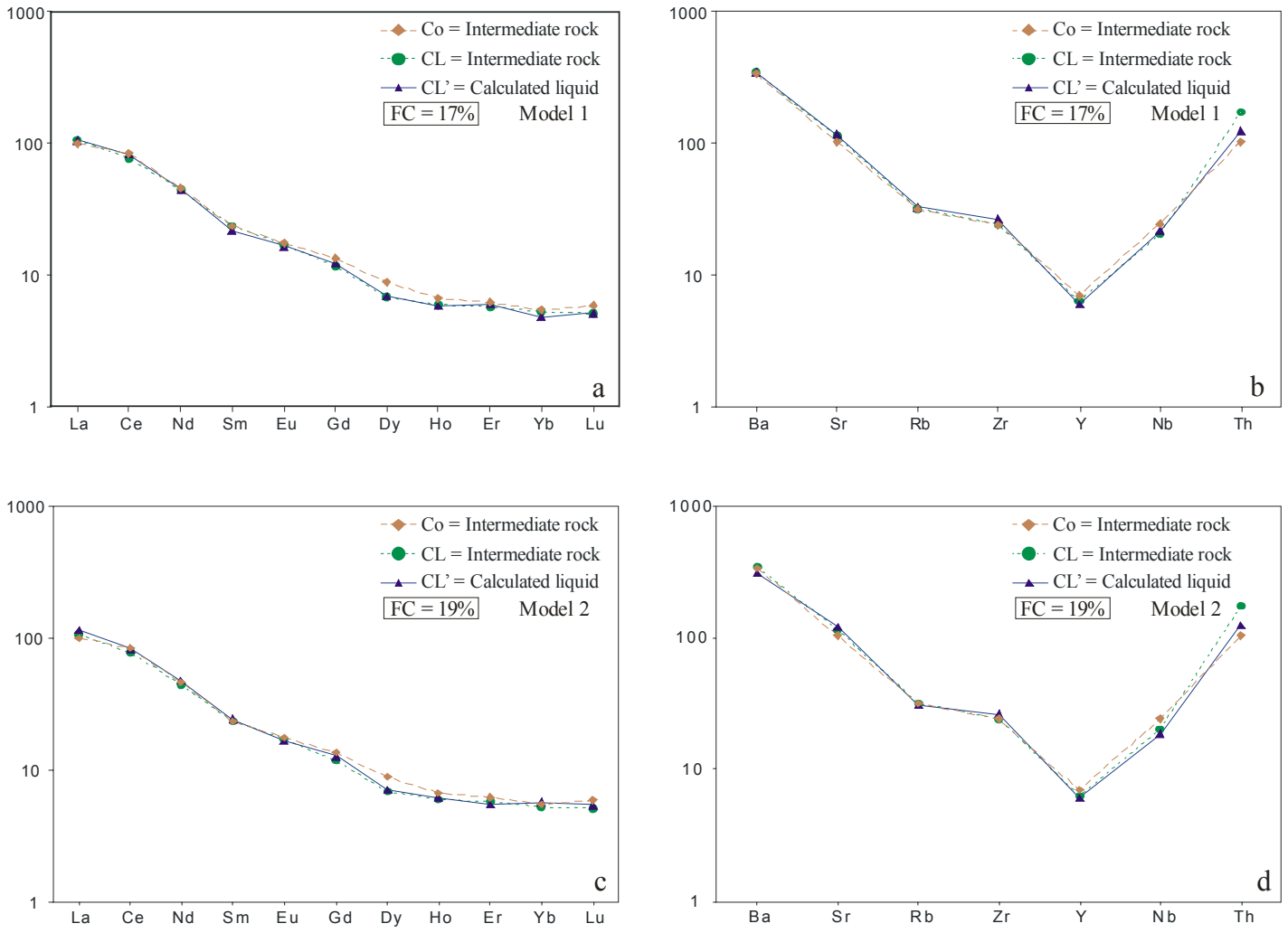

Fig. 12 – Fractional crystallization (FC) modeling into of intermediate rocks. (a, c) REE patterns; (b, d) Trace elements plots; (a, b, c, d) Sample ADR-4A to sample MFR-102, models 1 and 2; FC is percentage of crystallization.

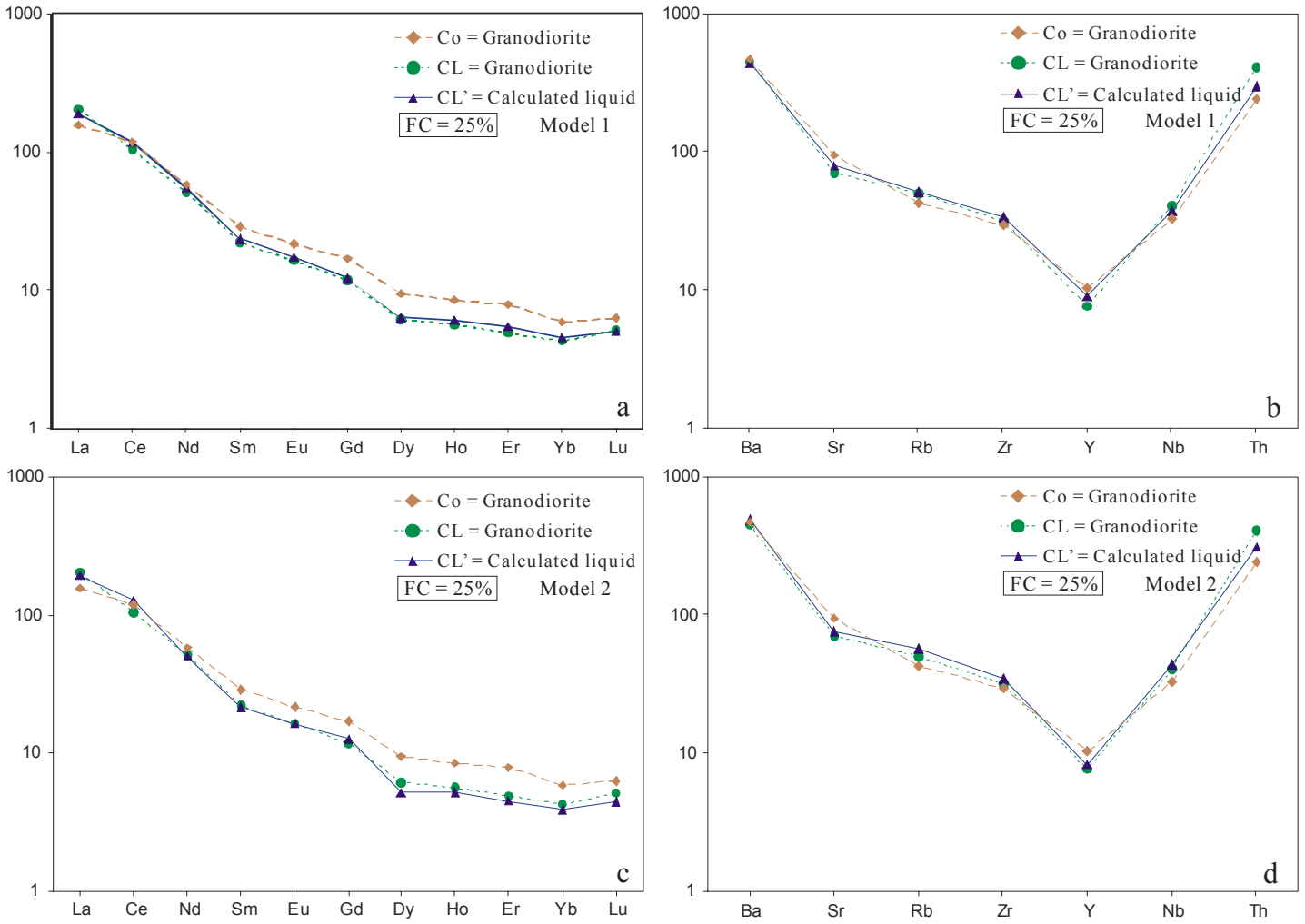

Fig. 13 – Fractional crystallization (FC) modeling into of granodiorites. (a, c, e, g) REE patterns; (b, d, f, h) Trace elements plots; (a, b, c, d) Sample MFR-114 to sample MFR-27A, models 1 and 2; (e, f, g, h) Sample MFR-114 to MFR-80A, models 3 and 4; FC is percentage of crystallization.

silica contents were assumed as representative of the initial liquid from which the layered rocks could have derived. We have examined whether the initial liquid was able to generate the dark (sample MFR-12B) and gray (sample MFR-12A) layers, which compose these rock, by accumulation of amphibole, mainly. Assuming the intermediate composition as initial liquid, trace element models give poor fits for REE and other trace elements between calculated liquid compositions and that of the layered rocks (Figs. 14a, b, c, d), On the other hand, when we have tested the granodiorite magma as initial liquid, in the major element models, best fits ($\sum R^2 < 1$, Table 6) were obtained with the composition of both, dark and gray layers. According to the major and trace element models, the accumulation of 30% and 50 % of amphibole ± plagioclase from the initial liquid would be able to generate, respectively, the gray and dark layers (Table 6). These models gave an excellent fit for REE and other trace elements (Fig. 15a, b, c, d).

3.5.3 – Protoliths of the Rio Maria suite

Geochemical and isotopic characteristics of the Rio Maria suite suggest that both mantle and subduction-related components must play an important role in the petrogenesis of these rocks (Oliveira et al. 2009). In addition, the P-T-H_2O-fO_2 estimate for the Rio Maria suite (Oliveira et al., submitted) point to oxidized and wet conditions for their precursor magmas, two typical features of present-day arc magmas, including those with a strong slab melt signature, such as Pinatubo (Scaillet and Evans, 1999; Prouteau and Scaillet, 2003). The principal implication is that the characteristics of the Rio Maria Sanukitoid are compatible with a subduction zone geodynamic setting during the Archean in that area. In other Archean terranes containing high-Mg suites, a similar tectonic setting has also been admitted (Superior Province of Canada, Stern and Hanson, 1991; Pilbara, Smithies and Champions, 2000; Karelian, Kovalenko et al., 2005, Halla, 2005).

Two principal petrogenetic models involving an important slab component have been proposed for sanukitoid genesis. In the two-stage model, it is admitted that sanukitoids are produced by melting of a mantle source that has been extensively metasomatised by assimilation of slab melts (Smithies and Champion, 2000; Kovalenko et al., 2005). In the single-stage model, it is proposed that a slab melt rising through peridotite mantle is able to assimilate olivine, resulting in a "hybridized slab melt" which chemical characteristics are very similar to

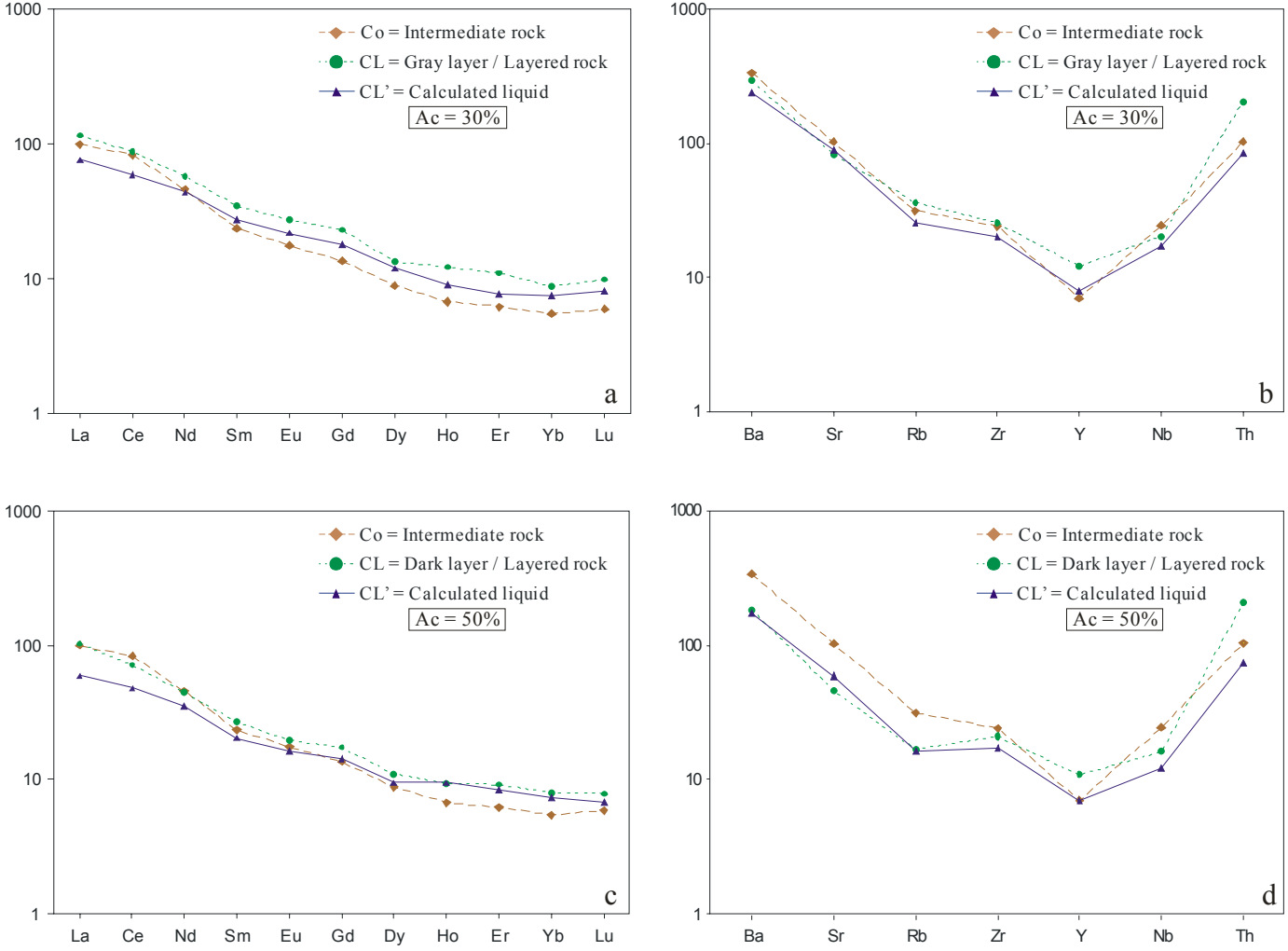

Fig. 14 – Accumulation process (Ac) modeling of the layered rocks from intermediate magma of the Rio Maria suite. (a, c) REE patterns; (b, d) Trace elements plots; (a, b) Gray layer, model 1; (c, d) Dark layer, model 2; Ac is percentage of accumulation.

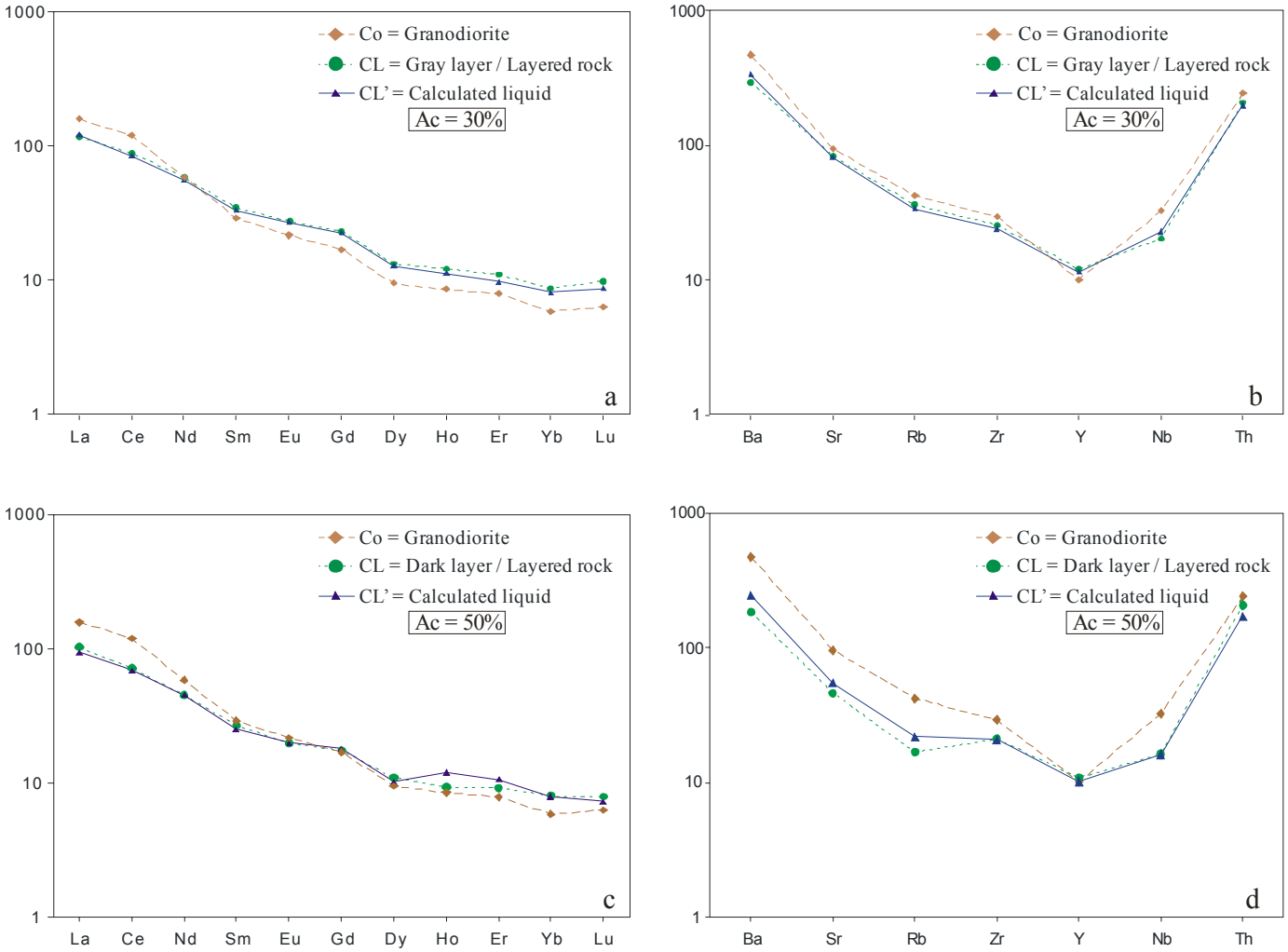

Fig. 15 – Accumulation process (Ac) modeling of the layered rocks from granodiorite magma of the Rio Maria suite. (a, c) REE patterns; (b, d) Trace elements plots; (a, b) Gray layer, model 1; (c, d) Dark layer, model 2; Ac is percentage of accumulation.

sanukitoids (Rapp et al., 1999). We have tested these possibilities using geochemical modeling and the results are presented and discussed below.

Rapp et al. (1999), Scaillet and Prouteau (2001) and Prouteau et al. (2001) have shown that the "effective" slab melt:peridotite ratio and the nature of the metasomatizing agent play a important role in the genesis of metasomatized mantle derived magmas. According to experiments performed by Rapp et al. (1999), that ratio could even determine the nature of process. When the slab melt:peridotite ratio is approximately 3:1, the reaction product is a Mg-rich, high-SiO_2, hybridized melt. However, when the slab melt:peridotite is nearly 1:1, the slab-derived TTG-like melt is fully consumed in metasomatic reactions that produce alkali-rich amphibole, pyrope-rich garnet, and both low-Mg# and high-Mg# orthopyroxene. Prouteau et al. (2001) suggested that mantle metasomatism by slab melt is a more common and ten times more efficient process than metasomatism by hydrous fluids.

Anyway, the compositions of metasomatised mantle or hybridized slab melts able to originate the Rio Maria suite magmas are not precisely known, being necessary to estimate the compositions of the pristine slab-melt and peridotite mantle involved in the metasomatism or assimilation process. We tested two peridotite compositions representative of both depleted and primitive mantle, corresponding, respectively, to harzburgite and spinel lherzolite (Table 7) used by Rapp et al. (1999) in their slab melting and peridotite assimilation experiments. The initial results of modeling using depleted mantle compositions are not shown here, however they have indicated that the Ca and Al-poor, and Ni-rich harzburgite composition (Table 7) modified by metasomatism or assimilation processes is not able to generate the Rio Maria suite magmas. Thus, a primitive mantle composition corresponding to spinel lherzolite (Table 7) was used in modeling.

Independent of the adopted model (single or two-stage), the magma source of the Rio Maria sanukitoid suite should apparently result from the interaction between a TTG slab-melt and a primitive mantle. For an effective interaction between the TTG melt and the mantle, a subduction tectonic setting is required. Prouteau et al. (2001) demonstrated that hydrous basalt partial melting experiments yield trondhjemitic melts, while dehydration melting of unaltered basalt leads to more granitic liquids. Furthermore, Scaillet and Prouteau (2001) showed that slab melts are silicic and strongly sodic (trondhjemitic). Based in these previous works, we have

Table 7
Chemical compositions of starting materials for metasomatism of mantle

	Peridotite mantle		Slab melt
Oxide	Harzburgite[1]	Spinel lherzolite[2]	Mogno trondhjemite[3]
SiO_2 (wt.%)	44.48	44.59	69.79
TiO_2	0.00	0.16	0.35
Al_2O_3	0.69	3.59	15.63
Fe_2O_3	8.26	9.00	2.76
MnO	0.12	0.12	0.03
MgO	43.85	39.22	0.95
CaO	0.91	3.44	3.18
Na_2O	0.31	0.30	4.46
K_2O	0.04	0.02	1.74
P_2O_5	-	-	0.09
LOI	0.00	0.00	0.90
Total	97.95	99.43	99.88
Ba (ppm)	3.20	4.10	584
Rb	0.04	0.06	58
Sr	142	11.5	667
Zr	0.16	6.3	135
Nb	0.04	0.15	3.9
Y	0.09	4.70	4.30
Th	0.005	0.004	8.40
Ni	2752	1866	7.30
Cr	2903	3083	10
La	0.022	0.064	27.00
Ce	0.049	0.410	48.10
Pr	0.006	0.110	5.50
Nd	0.029	0.800	19.20
Sm	0.007	0.380	2.36
Eu	0.002	0.152	0.55
Gd	0.008	0.660	1.72
Tb	0.0015	0.122	0.20
Dy	0.009	0.860	1.01
Ho	0.003	0.190	0.13
Er	0.011	0.620	0.39
Yb	0.024	0.620	0.30
Lu	0.005	0.098	0.06

Data Source: [1]Harzburgite xenolith, Valvoyam Volcanic Field, N. Kamchatka Arc (Kepezhinskas et al., 1995); [2]Spinel lherzolite xenolith, Kilborne Hole, NM, USA (Takahashi, 1986); [3]2.96 Ga Mogno trondhjemite, Rio Maria granite-greenstone terrane (Sample FMR-95; Guimarães et al., submitted; Almeida et al., submitted).

assumed that the slab-melts involved in the mantle assimilation or metasomatism had trondhjemitic instead of tonalitic compositions. Thus, we have tested in the geochemical modeling as possible slab melt-derived TTG, only representative trondhjemitic samples of the Mogno trondhjemite (~2,96 Ga; Almeida et al., submitted), Arco Verde tonalite (2,98-2,94 Ga; Macambira, 1992; Rolando and Macambira, 2003; Almeida et al., 2008) and Caracol tonalitic

complex (2,95-2,92 Ga; Leite et al., 2004) of the Rio Maria granite-greenstone terrane. The best fits were obtained using a sample of the Mogno trondhjemite (Table 7).

Modeling of different degrees of assimilation (5 to 50% of mantle component) of peridotite mantle by slab melts showed that this process is not able to generate LILE and REE concentrations equivalent to those found in the rocks of the Rio Maria suite. On the other hand, the results of modeling of partial melting of metasomatized mantle by slab melt were more consistent and will be discussed in the following.

Granodiorites

To test the hypothesis mentioned above, the granodiorite sample MFR-114, adopted as representative of the initial liquid of this rock type in previous modeling, was also assumed as the liquid resulting of partial melting of the modified mantle source.

The metasomatized mantle source required to produce the granodiorite liquid by partial melting was obtained by mixing ~30% TTG into the spinel lherzolite mantle. The pertinent modified mantle whole rock composition is shown in Table 8. However, the compositions of the mineral phases that were present in this mantle at the time of melting are not known. Thus, three mineral compositions were tested: (1) from peridotite xenoliths from South African kimberlites (Nixon et al., 1981); (2) formed during metasomatic reaction between a slab melt and a peridotite (Rapp et al., 1999), and; (3) the incomplete metasomatic assemblage of Moyen et al. (2001).

Incongruent melting modeling using mineral phases from Rapp et al. (1999) and with olivine and orthopyroxene in the residue gave inconsistent results ($\sum R^2 \geq 15$). Similar inconsistencies were obtained in calculations using the mineral compositions of Moyen et al. (2001) and the same mineral phases in the residual assemblage ($\sum R^2 \geq 17$). These results indicate that our assumed modified mantle with the mineral phase compositions used by Rapp et al. (1999) and Moyen et al. (2001) is probably not able to generate the initial liquids of Rio Maria suite by partial melting processes. On the other hand, our mass balance calculations using the mineral phases of peridotite xenoliths from South African kimberlites gave excellent results ($\sum R^2 < 1$). The best fit model ($\sum R^2 = 0.129$, Table 9) was achieved with a proportion melt:residue of 21 to 79%, the latter consisting of olivine (23%), orthopyroxene (56%), amphibole (14%), and garnet (7%). These same proportions of melt and of residual mineral phases were tested in the trace elements modeling. The resulting model gave an excellent fit for REE and other trace

Table 8
Chemical compositions of metasomatized mantle used in the protolith modeling of the rocks of Rio Maria suite.

	Metasomatized mantle		
Oxide	20% TTG-like melt	30% TTG-like melt	40% TTG-like melt
SiO_2 (wt.%)	50.03	52.75	55.47
TiO_2	0.17	0.17	0.18
Al_2O_3	5.81	6.92	8.03
Fe_2O_3	7.62	6.93	6.25
MnO	0.10	0.09	0.08
MgO	31.47	27.59	23.71
CaO	3.35	3.31	3.27
Na_2O	1.20	1.65	2.10
K_2O	0.27	0.40	0.53
P_2O_5	0.02	0.03	0.04
Total	100.04	99.84	99.66
Ba (ppm)	120	178	236
Rb	12	17	23
Sr	143	208	274
Y	5	5	5
Zr	32	45	58
Nb	1	1	2
Th	2	3	3
Ni	1494	1308	1123
Cr	2470	2164	1858
La	5.45	8.14	10.84
Ce	9.95	14.72	19.49
Pr	1.19	1.73	2.27
Nd	4.48	6.32	8.16
Sm	0.78	0.97	1.17
Eu	0.23	0.27	0.31
Gd	0.87	0.98	1.08
Tb	0.14	0.15	0.15
Dy	0.89	0.91	0.92
Ho	0.18	0.17	0.17
Er	0.57	0.55	0.53
Tm	0.06	0.06	0.06
Yb	0.45	0.43	0.41
Lu	0.09	0.09	0.08

elements (Fig. 16a, b) between the calculated initial liquid, generated from incongruent melting, and the assumed primitive granodiorite magma.

Mass balance calculations including plagioclase as an additional residual phase also gave good fits for major elements ($\sum R^2 = 0.029$), but the trace element modeling indicated that this is a not acceptable model, because of the poor fit for REE and, specially, Ba and Sr, when compared with the assumed granodiorite primitive liquid.

Table 9
Mass-balance models for metasomatized mantle melting.

Oxide	Granodiorite (Sample MFR-114)	Metasomatized mantle by 30% TTG-like melt	Proportions of melt and residual minerals
SiO_2 (wt.%)	62.52	52.75	
TiO_2	0.46	0.17	Olivine = 0.23
Al_2O_3	15.23	6.92	Orthopyroxene = 0.56
Fe_2O_3	5,10	6.93	Garnet = 0.07
MnO	0.07	0.09	Amphibole = 0.14
MgO	2.61	27.59	
CaO	4.40	3.31	Sum of the squared residuals = 0.129
Na_2O	4.30	1.65	
K_2O	2.93	0.40	
P_2O_5	0.17	0.03	Melt fraction = 21%
	Intermediate rock (Sample ADR-4A)	Metasomatized mantle by 30% TTG-like melt	Proportions of melt and residual minerals
SiO_2 (wt.%)	58.47	52.75	
TiO_2	0.47	0.17	Olivine = 0.20
Al_2O_3	14.02	6.92	Orthopyroxene = 0.60
Fe_2O_3	6,84	6.93	Garnet = 0.12
MnO	0.09	0.09	Amphibole = 0.08
MgO	5.81	27.59	
CaO	5.88	3.31	Sum of the squared residuals = 0.345
Na_2O	3.77	1.65	
K_2O	2.21	0.40	
P_2O_5	0.17	0.03	Melt fraction = 24%
	Mafic enclave (Sample MD-02C)	Metasomatized mantle by 20% TTG-like melt	Proportions of melt and residual minerals
SiO_2 (wt.%)	51.38	50.03	
TiO_2	0.72	0.17	Olivine = 0.38
Al_2O_3	13.77	5.81	Orthopyroxene = 0.43
Fe_2O_3	11,15	7.62	Plagioclase = 0.14
MnO	0,20	0.10	Amphibole = 0.05
MgO	7.38	31.47	
CaO	8.36	3.35	Sum of the squared residuals = 0.024
Na_2O	3.53	1.20	
K_2O	1.94	0.27	
P_2O_5	0.37	0.02	Melt fraction = 9%

Intermediate rocks

Based on geochemical and petrographical data, Oliveira et al. (2009) suggested that intermediate rocks and granodiorites were generated from different degrees of melting of a similar source. Thus, we have tested this hypothesis in mass balance calculations and trace element modeling. For that a metasomatized mantle source (~30% TTG melt into spinel lherzolite mantle) and residual phases identical to those employed in the discussion of the origin of the granodiorite liquid were considered. The assumed primitive intermediate liquid should correspond in composition to the ADR-4A sample (Table 9).

An excellent fit ($\sum R^2 = 0.345$; Table 9) was obtained with a small increase in the melt proportion (24% melt, compared to 21 % in the case of the granodiorite liquid). In the residue, the proportions of orthopyroxene (60 vs. 56%) and garnet (12 vs. 7%) increased, and those of

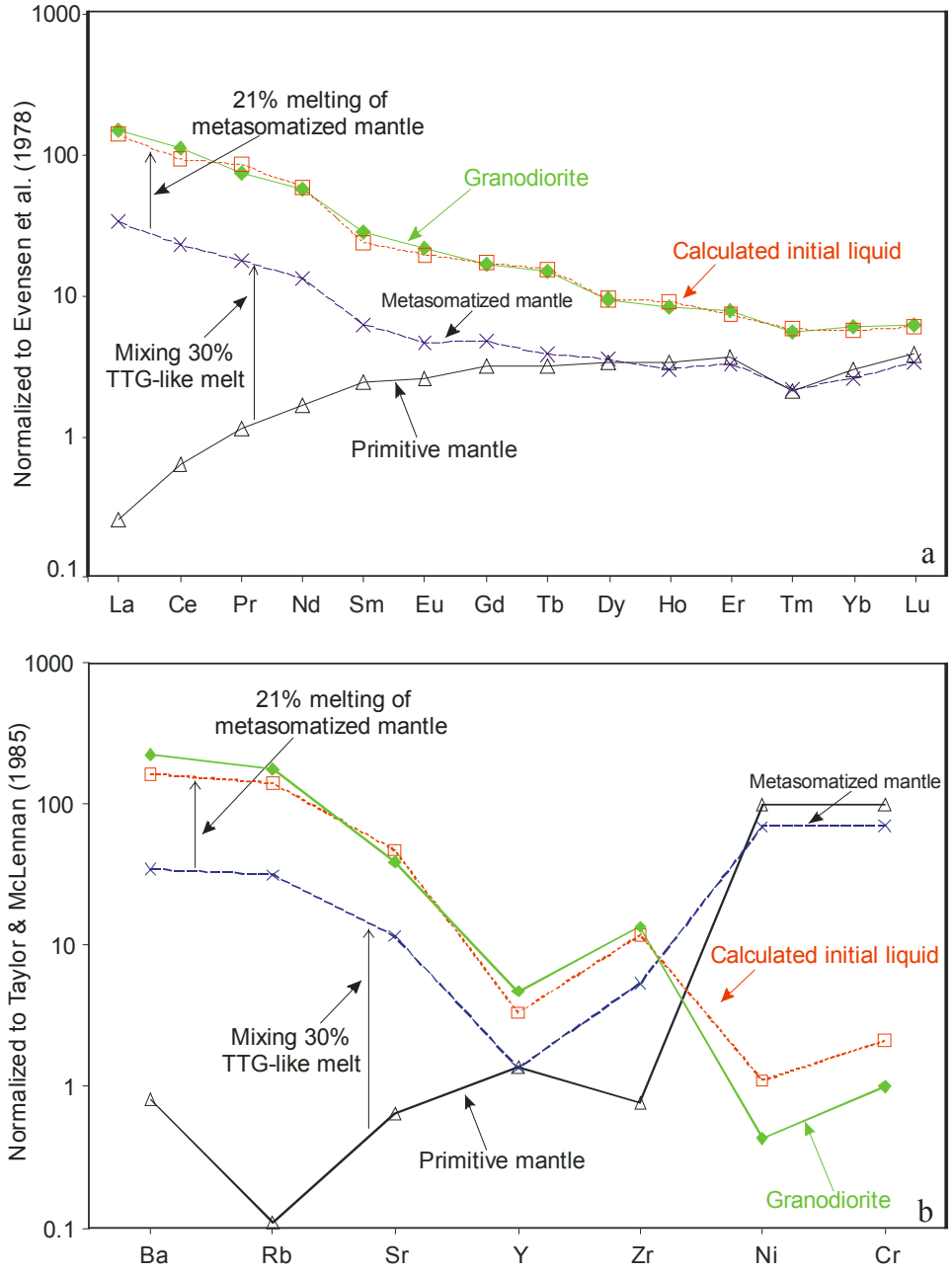

Fig. 16 – (a) REE patterns; (b) Other trace elements. Comparison of the REE and other trace elements of the assumed primitive granodiorite magma composition with calculated liquids modeled by mixing 30% TTG melt in the peridotite mantle, following by 21% partial melting. The primitive and modified mantle compositions are shown in Tables 7, 8 and 9. The melt proportions of metasomatized mantle suitable to generate intermediate magma and residual phase proportions are given in Table 9.

olivine (20 vs. 23) and amphibole (8 vs. 14%) decreased when compared to which was observed in the case of the granodiorite liquid (Table 9). The REE pattern of the calculated primitive intermediate liquid (Fig. 17a) is consistent with the assumed intermediate magma composition, being slightly more impoverished in LHREE compared to the granodiorite one. This model also gave a good fit for the other trace elements considered (Fig. 17b).

Mafic Enclaves

Despite their typical sanukitoid signature, the mafic enclaves show geochemical and petrographical peculiarities which should reflect differences in the origin of these rocks in relation to those of the granodiorite and intermediate rocks. To verify this premise, mass balance calculations involving the partial melting of a metasomatized mantle (with 30% of added TTG melt, identical as in the case of granodiorite and intermediate rocks) to produce an initial liquid similar to the assumed mafic enclave composition (sample MD-02C) were done. The resulting model shows that for 21% melt and 79% residue, containing olivine, orthopyroxene and plagioclase as residual phases, a good fit was obtained for major elements ($\sum R^2 = 0.363$). However, for trace elements, and especially for the REE which are lower in the calculated liquid than in the mafic enclaves, the model gave a poor fit. Based in these results, we decided to examine the possibility of a different composition of the metasomatized mantle source.

Assuming a mantle that was modified only by 20% TTG melt, major element modelling showed that 9% of partial melting of that mantle, leaving a residue comprising olivine (38%), orthopyroxene (43%), amphibole (5%), and plagioclase (14%), was able to generate an initial liquid composition compatible with that of the assumed primitive mafic enclave liquid ($\sum R^2 = 0.024$). Mass balance calculations indicated also a good fit ($\sum R^2 = 0.074$) in the case of a model involving 11% of melting of the same source mentioned above, but without amphibole as residual phase. Trace element modeling gave good fits for REE and other trace elements, for both models. However, the model with amphibole as residual phase gave the best fit for the HREE, mainly Nd, Eu, Tb, and Ho, and was taken as representative of the melting process (Fig. 18a, b).

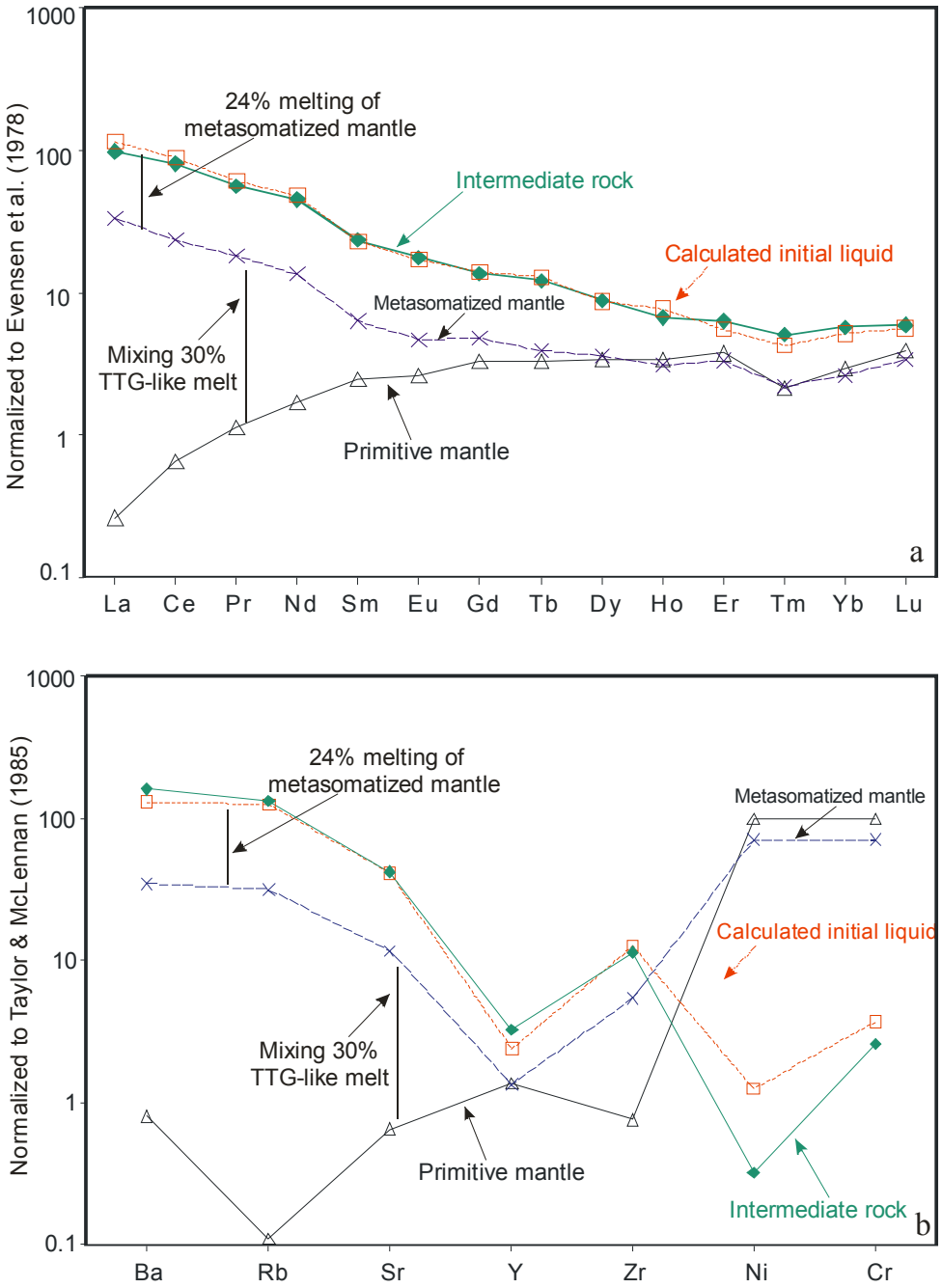

Fig. 17 – (a) REE patterns; (b) Other trace elements. Comparison of the REE and other trace elements of the assumed primitive intermediate magma composition with calculated liquids modeled by mixing 30% TTG melt in the peridotite mantle, following by 24% partial melting. The primitive and modified mantle compositions are shown in Tables 7, 8 and 9. The melt proportions of metasomatized mantle suitable to generate intermediate magma and residual phase proportions are given in Table 9.

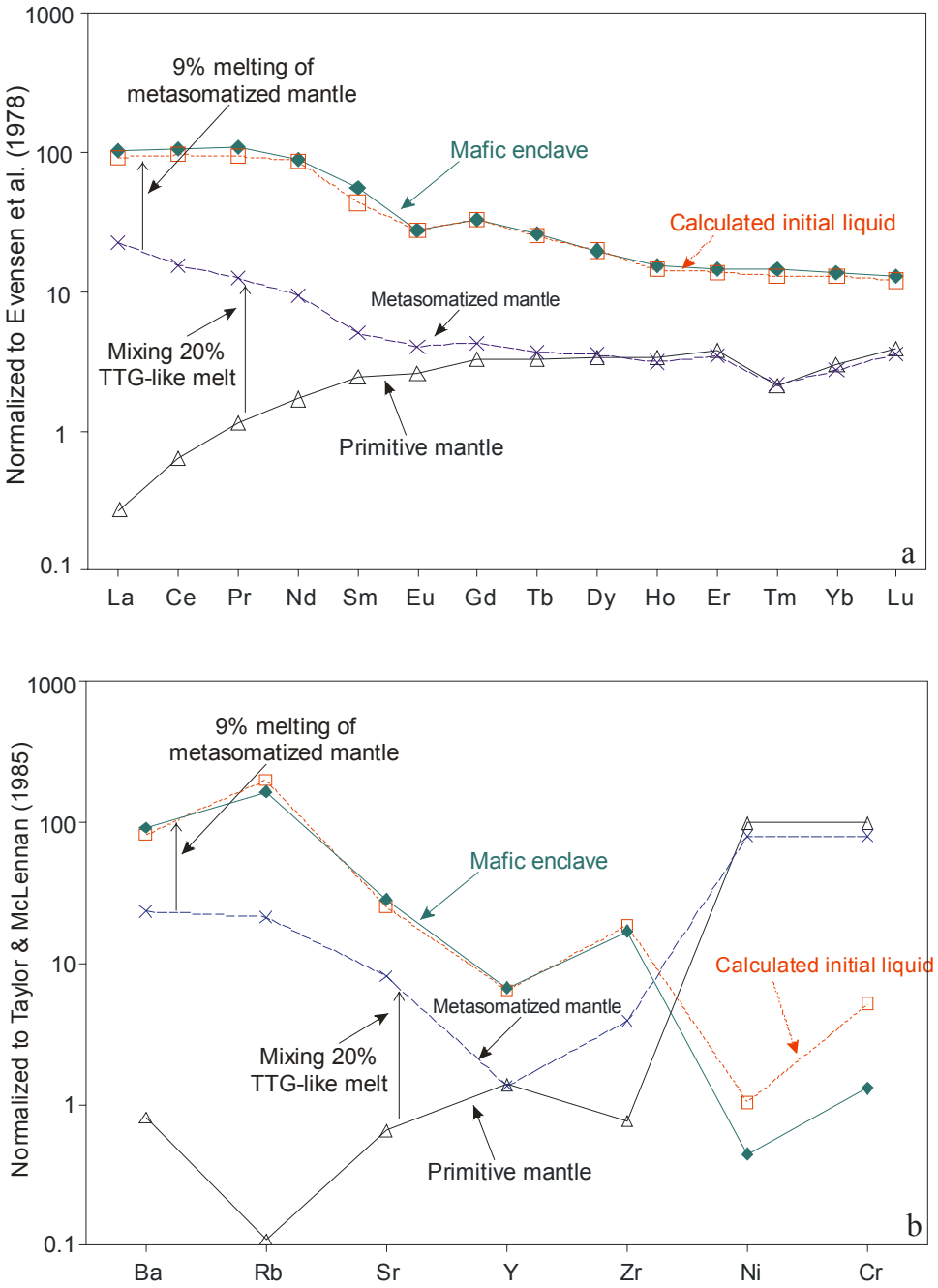

Fig. 18 – (a) REE patterns; (b) Other trace elements. Comparison of the REE and other trace elements of the assumed primitive mafic enclave magma composition with calculated liquids modeled by mixing 20% TTG melt in the peridotite mantle, following by 9% partial melting. The primitive and modified mantle compositions are shown in Tables 7, 8 and 9. The melt proportions of metasomatized mantle suitable to generate intermediate magma and residual phase proportions are given in Table 9.

4 – DISCUSSION

4.1 - Genesis of sanukitoid magmas in Rio Maria

Geochemical data demonstrated that granodiorites, intermediate rocks, layered rocks and mafic enclave have sanukitoid signature. Petrogenetic modeling indicates that the granodiorites and intermediate rocks are not related by fractional crystallization. The internal evolution of intermediate rocks were leaded by fractionation of amphibole + biotite ± apatite, whereas granodiorites evolved by fractionation of plagioclase + amphibole ± biotite. According to modeling, the dark layer of the layered rocks should have been derived from the granodiorite magma by accumulation of 50% of amphibole; the gray layer would result of 30% of amphibole ± plagioclase accumulation. Geochemical data and modal compositions indicated that a link between mafic enclaves and granodiorites or intermediate rocks by fractional crystallization is not consistent.

The petrogenesis of the Rio Maria suite requires melting of a modified mantle source. Modeling suggests that the mantle source of the Rio Maria sanukitoid was extensively metasomatized by addition of about 30% TTG-like melt to generate the granodiorite and intermediate magmas, and ~20% TTG-like melt in the case of mafic enclave magma. The partial melting processes that originated the granodiorite (21% of melt) and intermediate magma (24% of melt) produced a residual assemblage formed by olivine, orthopyroxene, amphibole, and garnet. In the case of mafic enclave, the degree of melting is more limited (9%) and the residual assemblage shows a relevant change: garnet by plagioclase. This fact suggests that the magma of the mafic enclaves was originated at lower pressure compared to that of granodiorite and intermediate rocks. The lowest Sr/Y ratios, highest Y contents, and moderate negative Eu anomaly of the mafic enclaves, are consistent with the presence of plagioclase as a residual phase and reinforce the results of modeling.

The adopted model implies the existence of an enriched mantle beneath Rio Maria granite-greenstone terrane at approximately 2.87 Ga. The mantle enrichment could be caused by fluids liberated from a mantle plume (Jayananda et al., 2000) or from a subducted slab (Martin et al., 2005). However, our modeling suggests that a mantle modified by fluids will not have the adequate composition to generate the Rio Maria sanukitoid magmas. It indicates also, as the most

likely hypothesis, that the Rio Maria mantle was previously enriched by TTG melts related to earlier subduction events (Shirey and Hanson, 1984; Stern, 1989; Stern and Hanson, 1991; Rapp et al., 1999; Smithies and Champion, 2000; Kovalenko et al., 2005).

The TTG series of Rio Maria were originally subdivided in older TTG series (2.98 to 2.92 Ga) and younger TTG series (~2.87 Ga) (Althoff et al., 2000; Leite et al., 2004; Dall'Agnol et al., 2006). However, recent geological and geochronological data (Almeida et al., submitted; Guimarães et al., submitted) have demonstrated that almost all TTG units were formed in between 2.98 and 2.92 Ga (Arco Verde tonalite, Caracol tonalitic complex, Mogno trondhjemite, Mariazinha tonalite). The younger TTG units are, at present, limited to the Água Fria trondhjemite (ca. 2.86 Ga; Leite et al., 2004), a TTG unit exposed in a small area to the north of Xinguara (Fig. 1). The 2.87 Ga Rio Maria suite occurs in different areas of the Rio Maria granite-greenstone terrane and, like sanukitoids elsewhere in the world, its rocks are 110 to 50 Myr. younger when compared with the largely dominant TTG magmatism of that terrane (Leite et al., 2004; Almeida et al., submitted).

Althoff et al. (2000) admitted that strong external forces associated with plate convergence were operative between 2.96 and 2.90 Ga in the Rio Maria terrane. Leite et al. (2001) also suggested that the evolution of the terrane at ca. 2.87 Ga was subduction-related. Our modeling results indicate that an active subduction tectonic setting was present in the terrane in between 2.98 to 2.92 Ga to explain the extensive formation of TTG magmas and the proposed metasomatism of the mantle by these magmas, before the melting process responsible for the origin of the sanukitoid magmas. In summary, the adopted model implies: (1) an extensive generation of TTG magmas, at least in part derived from the partial melting of a mafic slab in a subduction setting; (2) the interaction of these TTG magmas with the mantle, resulting a metasomatized mantle with significant TTG component (20 to 30% in volume); (3) a tectonothermal event at ~2.87 Ga, possibly related to a mantle plume, causing the partial melting of the metasomatized mantle and generating the Rio Maria sanukitoid magmas; (4) the nature of the magmas will depend of the degree of melting and of the depth (pressure) in which the melting process occur; (5) the magmas ascended to the crust and evolved by fractional crystallization; (6) the magmas were emplaced at relatively shallow crustal levels, possibly forming laccoliths or sheet-like plutons (Souza et al., 1992).

Available Sm-Nd isotope data on the Rio Maria sanukitoid suite are limited to five samples (four granodiorites and one intermediate rock; Table 4). All samples gave ε_{Nd} (t=2.87 Ga) varying between 0.2 and 1.2 and T_{DM} model ages of 2923 to 3010 Ma, suggesting a juvenile character for the suite and absence of imprint of a preexistent crust (Rämö et al., 2002). The Rio Maria suite has high LREE contents and low $^{147}Sm/^{144}Nd$ ratios (Table 4) and this feature, in sanukitoids, is commonly interpreted as the result of enrichment of their mantle source region simultaneously with or immediately before to magma genesis (Kovalenko et al., 2005).

4.2 – The role of pressure variation in the characteristics of sanukitoid series

The sanukitoid suites described in different Archean terranes consist of rocks that follow two distinct trends in modal Q-A-P diagrams: the dominant series vary from diorite and quartz diorite to the more abundant granodiorite, evolving along a granodioritic calc-alkaline trend (Fig. 4; Lameyre and Bowden, 1982). However, there is also a subordinate series that is composed of monzodiorites, quartz monzodiorites, monzonites, and quartz monzonites, which follow a monzonitic trend. The latter series is represented in the Rio Maria terrane by the mafic enclaves (Fig. 4). Rocks representative of both series are commonly described in the Archean sanukitoid suites (Smities and Champion, 2000; Moyen et al., 2003; Halla, 2005; Lobatch-Zuchenko et al., 2005; Kapyaho, 2006; Heilimo et al., 2007). The contrast between both series is also evident in geochemical data, at least in the case of the Rio Maria suite as discussed above. The observed differences suggest that these series cannot be derived from a same magma by fractional crystallization and should be a consequence of the processes responsible for the origin of the magmas of each series. Our modeling indicated that the partial melting processes which generated the primitive magmas of the studied rocks produced different residual assemblages. In the case of the granodiorite and intermediate rock magmas, garnet was a residual phase, whereas in the mafic enclave magma, garnet was absent and plagioclase was a residual phase. It was deduced that the mafic enclave magma was generated in the plagioclase stability domain and consequently at lower pressures, whereas the granodiorite and intermediate magmas were formed at comparatively higher pressures. This implies that the contrast in pressure in which it happened

the partial melting of the metasomatized mantle is determinant in the differences in modal and geochemical composition between both granodioritic and monzonitic sanukitoid series.

To test our working hypothesis, we have selected chemical compositions of rocks which we have assumed as representative of both series from sanukitoid suites of different Archean terranes. Considering that Sr, Y, and, Sr/Y ratios are generally seen as good indicators of the pressure of melt formation (Defant and Drummond, 1990; Drummond and Defant, 1990), we decided to evaluate the geochemical behavior of the mentioned elements in classical sanukitoid suites and to establish comparisons with that of Rio Maria. In the Sr/Y vs. Y plot (Fig. 19), monzonites and quartz monzonites from Karelian craton (Lobach-Zuchenko et al., 2005) and monzonites from Dharwar craton (Moyen et al., 2003) have low Sr/Y ratios and high Y contents, similar to those of the mafic enclaves of the Rio Maria suite. In contrast, granodiorites, quartz diorites and diorites of different sanukitoid intrusions from eastern Finland (Arola suite, Käpyaho, 2006; Lieksa granodiorite, Halla, 2005; Kaapinsalmi tonalite, Heilimo et al., 2007) and Pilbara craton (Smithies and Champion, 2000) have high to moderate Sr/Y ratios and low Y contents, and are concentrate in the diagram in the same domain of the granodiorite and intermediate rocks of the Rio Maria suite (Fig. 19). This approach indicates that the contrasts observed between the granodioritic and monzonitic sanukitoid series are a general feature of these rocks. Our data suggest also that the origin of these series is strongly dependent of the pressure of magma generation and, as a consequence, that the nature of the series could indicate the approximate depth of formation of its magma. If correct, this implies that the two fields shown in Figure 19 are indicative not only of the nature of sanukitoid series but also of their pressure of formation. The field labeled A corresponds to rocks of the monzonitic series which are supposed to be derived of relatively low pressure magmas and the field B includes rocks of the granodioritic series which magmas were formed at higher pressures.

4.3 – The relationship between mafic enclaves and granodiorite magma

In all occurrences of the Rio Maria suite, abundant and regularly distributed centimetric-sized mafic enclaves are systematically included in the host granodiorites (Oliveira et al., submitted). Modeling and geochemical data suggest that mafic and granodiorite magmas were

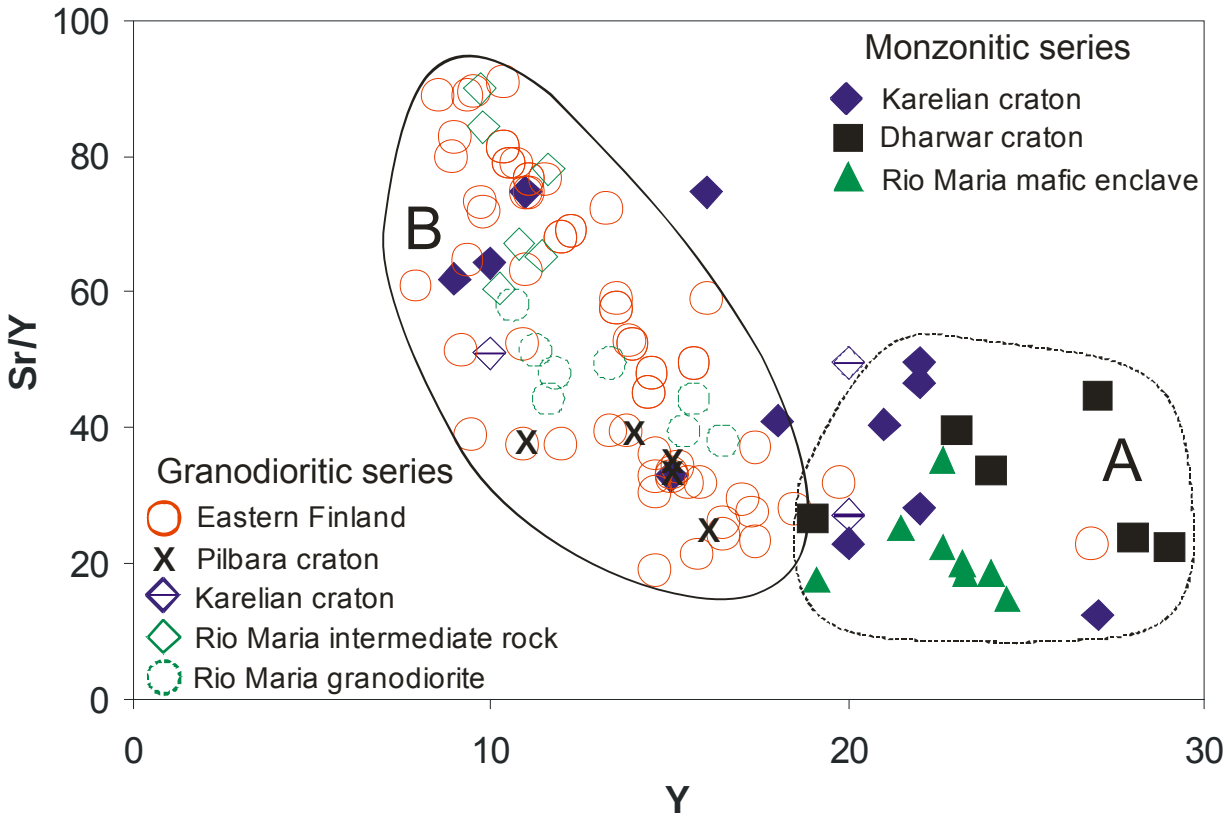

Fig. 19 - Sr/Y *vs.* Y plot for rocks from the Rio Maria suite (Bannach area) and from sanukitoid suites of the Eastern Finland (Halla, 2005; Käpyaho, 2006; Heilimo et al., 2007), Karelian craton (Lobach-Zhuchenko et al., 2005) and Dharwar craton (Moyen et al., 2001, 2003). Fields A – monzonitic sanukitoid series, and B – granodioritic sanukitoid series.

originated at different depths, the granodiorite magma being generated at higher pressure compared to that of the mafic enclave magma. Field relationships show evidence of limited interaction between the enclaves and the granodiorite, both rocks displaying a same finite strain pattern. Field and petrographic aspects suggest a low viscosity contrast between enclaves and the Rio Maria granodiorite and indicated that the two magmas coexisted when both were still partly molten (Althoff et al., 2000; Leite, 2001; Oliveira et al., submitted). Thus, it was deduced that the granodiorite and mafic enclave magmas should mingled during their ascent and final emplacement. Only a limited interaction between both magmas should have occurred to justify

the relatively uniform geochemical behavior of each rock variety and the distinct trends displayed by their rocks in different modal and geochemical diagrams (Figs. 4, 6, 7).

According to our modeling data, the sanukitoid granodiorite magma resulted of 21% of partial melting of the metasomatized mantle at a pressure > 1000 MPa, whereas the enclave magma was generated at a pressure ≤ 1000 MPa and resulted from a comparatively lower degree of partial melting (9%). It can be inferred that the enclave magma was at a higher lithospheric level and should have lower volume compared to the granodiorite one. We can thus admit that the granodiorite magma ascended due to viscosity and gravity instabilities, attained the level of enclave magma formation, interacted with that magma and both pursuit the ascension to the upper crust. The lower volume of mafic magma causes its disruption in bubbles included and dispersed in the granodiorite magma. Both magmas are in partially molten state and initiate their interaction. However, the relatively rapid ascent of the magmas prevents intense re-equilibration and their essential primitive features are well preserved.

5 – SUMMARY AND CONCLUSIONS

The 2.87 Ga Rio Maria suite consists of Archean sanukitoid rocks of the Rio Maria granite-greenstone terrane and intrudes greenstone belts and TTG series. These rocks occur in different areas of the terrane and, particularly, in the Bannach area is composed of four principal groups of rocks: granodiorites, intermediate rocks, layered rocks and mafic enclaves. Geochemical data demonstrated that these rocks have sanukitoid signature and are not related by fractional crystallization.

Petrogenetic modeling, indicates that the internal evolution of intermediate magma were leaded by fractionation of amphibole + biotite ± apatite, whereas granodiorites evolved by fractionation of plagioclase + amphibole ± biotite. Layered rocks have been derived from the granodiorite magma by accumulation of 50% of amphibole, in the case of dark layer, and the gray layer would result of 30% of amphibole ± plagioclase accumulation. Geochemical data and modal compositions indicated that mafic enclaves (monzonitic series) and granodiorites or intermediate rocks (granodioritic series) follow two distinct trends in modal Q-A-P diagrams and a link by fractional crystallization is not consistent.

According to modeling, the petrogenesis of the Rio Maria suite requires melting of a modified mantle source that was extensively metasomatized by addition of about 30% TTG melt to generate the granodiorite (21% of melt) and intermediate magmas (24% of melt) and ~20% TTG melt in the case of mafic enclave magma (9% of melt). In the case of the granodiorite and intermediate rock magmas, garnet was a residual phase, whereas in the mafic enclave magma, garnet was absent and plagioclase was a residual phase. The lowest Sr/Y ratios, highest Y contents, and moderate negative Eu anomaly of the mafic enclaves, are consistent with the presence of plagioclase as a residual phase and reinforce the results of modeling. This implies that the contrast in pressure in which it happened the partial melting of the metasomatized mantle is determinant in the differences in modal and geochemical composition between both granodioritic (granodiorites and intermediate rocks) and monzonitic (mafic enclaves) sanukitoid series.

Granodiorite and mafic enclave magmas were generated by partial melting of the metasomatized mantle at a pressure > 1000 MPa and ≤ 1000 MPa, respectively, The granodiorite magma ascended due to viscosity and gravity instabilities, attained the level of enclave magma formation, interacted with that magma and both pursuit the ascension to the upper crust. The lower volume of mafic magma causes its disruption in bubbles included and dispersed in the granodiorite magma. Both magmas are in partially molten state and initiate their interaction. However, the relatively rapid ascent of the magmas prevents intense re-equilibration and their essential primitive features are well preserved.

In summary, the adopted model to the generation of the rocks of the rio Maria suite implies: (1) an extensive generation of TTG magmas, at least in part derived from the partial melting of a mafic slab in a subduction setting; (2) the interaction of these TTG magmas with the mantle, resulting a metasomatized mantle with significant TTG component (20 to 30% in volume); (3) a tectonothermal event at ~2.87 Ga, possibly related to a mantle plume, causing the partial melting of the metasomatized mantle and generating the Rio Maria sanukitoid magmas; (4) the nature of the magmas will depend of the degree of melting and of the depth (pressure) in which the melting process occur; (5) the magmas ascended to the crust and evolved by fractional crystallization; (6) the magmas were emplaced at relatively shallow crustal levels, possibly forming laccoliths or sheet-like plutons (Souza et al., 1992).

ACKNOWLEDGEMENTS

O. T. Rämö, J. Halla, and E. Heilimo are acknowledged for opportunity to M.A.O, R.D., and J.A.C.A., participate in the field trip in Eastern Finland terrane. S. Valente is acknowledged for support in the Modeling. This research received financial support from CNPq (Roberto Dall'Agnol – Grants 0550739/2001-7, 476075/2003-3, 307469/2003-4; Marcelo Augusto de Oliveira – master and doctor scholarship; José de Arimatéia Costa de Almeida– master and doctor scholarship), and Federal University of Pará (UFPA). This paper is a contribution to the Brazilian Institute of Amazonia Geosciences (INCT program – CNPq/MCT/FAPESPA – Process no 573733/2008-2).

REFERENCES

Almeida, J.A.C., Dall'Agnol, R., Oliveira, M.A., Macambira, M.J.B., Pimentel, M.M., Leite, A.A.S., submitted. Zircon geochronology and geochemistry of the TTG suites of the Rio Maria granite-greenstone terrane: Implications for growth of Archean crust of Carajás Province, Brazil. Precambrian Research.

Almeida, J.A.C., Oliveira, M.A., Dall'Agnol, R., Althoff, F.J., Borges, R.M.K., 2008. Relatório de Mapeamento Geológico na escala 1:100.000 da Folha Marajoara (SB-22-Z-C V). Programa GeoBrasil, CPRM – Serviço Geológico do Brasil. 147p.

Althoff, F.J., Barbey, P., Boullier, A.M., 2000. 2.8-3.0 Ga plutonism and deformation in the SE Amazonian craton: the Archean granitoids of Marajoara (Carajás Mineral province, Brazil). Precambrian Research, 104, 187-206.

Artemenko, G.V., Lobach-Zhuchenko, S.B., Krylov, I.N., Orsa, V.I., 2003. Archean high-Mg granitoids (sanukitoids) in the J. Halla / Lithos 176 79 (2005) 161–178 Ukrainian Shield and its comparison with rocks of TTG suite. Abstracts of the Contributions of the EGS-AGU-EUG Joint Assembly, Nice, France, 06_11 April 2003, Geophysical Research Abstracts vol. 5. European Geophysical Society.

Barker, F., 1979. Trondhjemites: definition, environment and hypotheses of origin. In: Barker, F. (Ed.) Trondhjemites, dacites and related rocks. Amsterdam, Elsevier. p. 1-12.

Barker, F., Arth, J.G., 1976. Generation of trondhjemitic-tonalitic liquids and Archaean bimodal trondhjemite-basalt suites. Geology, 4: 596-600.

Barros, E.M., Sardinha, A.S., Barbosa, J.P.O., Krimski, R., Macambira, M.J.B., 2001. Pb-Pb and U-Pb zircon ages of Archean syntectonic granites of the Carajás Metallogenic Province, northern Brazil. In: Simposio Sudamericano de Geologia Isotopica, 3. Pucon, Chile. Sociedade Geologica de Chile. (CD ROM).

Dall'Agnol, R., Oliveira, M.A., Almeida, J.A.C., Althoff, F.J., Leite, A.A.S., Oliveira, D.C., Barros, C.E.M., 2006. Archean and Paleoproterozoic granitoids of the Carajás metallogenetic province, eastern Amazonian craton. In: Dall'Agnol, R., Rosa-Costa, L.T., Klein, E.L. (eds.). Symposium on Magmatism, Crustal Evolution, and Metallogenesis of the Amazonian Craton. Abstracts Volume and Field Trips Guide. Belém, PRONEX-UFPA/SBG-NO, 99-150.

Dall'agnol, R., Teixeira, N.P., Ramö, O.T., Moura, C.A.V., Macambira, M.J.B., Oliveira, D. C. 2005. Petrogenesis of the Paleoproterozoic rapakivi A-type granites of the Archean Carajás metallogenic province, Brazil. Lithos, 80: 101-129.

Dall'agnol, R., Ramö, O.T., Magalhães, M.S., Macambira, M.J.B., 1999. Petrology of the anorogenic, oxidised Jamon and Musa granites, Amazonian Craton: implications for the genesis of Proterozoic, A-type Granites. Lithos. 46: 431-462.

DePaolo, D.J., 1981. Neodymium isotopes in the Colorado Front Range and crust-mantle evolution in the Proterozoic. Nature 291, 193–196.

Defant, M.J., Drummond, M.S., 1990. Derivation of some modern arc magmas by melting of young subducted lithosphere. Nature 347, 662– 665.

Drummond, M.S., Defant, M.J., 1990. A model for trondhjemite–tonalite–dacite genesis and crustal growth via slab melting: Archaean to modern comparisons. J. Geophys. Res. 95, 21503– 21521.

Evans, O.C., Hanson, G.N., 1997. Late- to post-kinematic Archean granitoids of the S.W. Superior Province: derivation through direct mantle melting. In: de Wit, M.J., Ashwal, L.D. (Eds.), Greenstone Belts. Oxford Univ. Press, Oxford, pp. 280–295.

Evensen, N.M.; Hamilton, P.T.; O'Nions, R.K., 1978. Rare earth abundances in chondritic meteorites. Geochemical of Cosmochemical Acta, 39: 55.64.

Guimarães, F.V.G., Dall'Agnol, R., Almeida, J.A.C., Oliveira, M.A., submitted. Caracterização geológica, petrográfica e geoquímica do trondhjemito Mogno e tonalito Mariazinha, Terreno granito-greenstone de Rio Maria – Pará. Revista Brasileira de Geociências.

Halla, J. 2005. Late Archean high-Mg granitoids (sanukitoids) in the southern Karelian domain, eastern Finland: Pb and Nd isotopic constraints on crust_mantle interactions. Lithos, 79: 161–178.

Hanson, G.N., 1978. The application of trace elements to the petrogenesis of igneous rocks of granitic composition. Earth Planetary Sciences Letters, 38, 26–43.

Hanson, G.N., 1989. An approach to trace element modeling using a simple igneous system as an example. In: Lipin, B.R., McKay, G.A. _Eds.., Geochemistry and mineralogy of rare earth elements, Reviews in Mineralogy 21, 79–97.

Heilimo, E., Mikkola, P., Halla, J., 2007. Age and petrology of the Kaapinsalmi sanukitoid intrusion in Suomussalmi, Eastern Finland. Bulletin of the Geological Society of Finland, 79, p. 117–125.

Huhn, S.R.B., Santos, A.B.S., Amaral, A.F., Ledsham, E.J., Gouveia, J.L., Martins, L.B.P., Montalvão, R.M.G., Costa, V.G., 1988. O terreno granito-greenstone da região de Rio Maria - Sul do Pará. In: Congresso Brasileiro de Geologia, 35., Belém. Anais do congresso Brasileiro de Geologia. Belém, SBG. v. 3, p. 1438-1453.

Irvine, T.N., Baragar, W.R.A. 1971. A guide to the chemical classification of the common volcanic rocks. Canadian Journal of the Earth Science, 8: 523-547.

Käpyaho, A., 2006. Whole-rock geochemistry of some tonalite and high Mg/Fe gabbro, diorite, and granodiorite plutons (sanukitoid suite) in the Kuhmo district, Eastern Finland. Bulletin of the Geological Society of Finland 78, 121–141.

Kepezhinskas, P.K., Defant, M.J., Drummond, M.S., 1995. Na metasomatism in the island-arc mantle by slab melt–peridotite interaction: evidence from mantle xenoliths in the North Kamchatkan Arc. J. Petrol. 36, 1505–1527.

Kovalenko, A.V., Clemens, J.D., Savatenkov, V.M., 2005. Petrogenetic constraints for the genesis of Archaean sanukitoid suites:geochemistry and isotopic evidence from Karelia, Baltic Shield. Lithos 79, 147– 160.

Kober, B., 1986. Whole-grain evaporation for $^{207}Pb/^{206}Pb$-age-investigations on single zircons using a double-filament source. Contributions to Mineralogy and Petrology 93, 482–490.

Kusky, T.M., Polat, A., 1999. Growth of granite---greenstone terranes at convergent margins, and stabilization of Archaean cratons. Tectonophysics 305, 45---73.

Lafon, J.M., Rodrigues, E., Duarte, K.D., 1994. Le granite Mata Surrão: un magmatisme monzogranitique contemporain des associations tonalitiques-trondhjemitiques-granodioritiques archéennes de la région de Rio Maria (Amazonie Orientale, Brésil). p. 642-649.

Lameyre, J., Bowden, P., 1982. Plutonic rock type series: discrimination of various granitoid series and related rocks. Journal of Volcanology and Geothermal Research 14, 169-186.

Le Bas, M.J., Le Maitre, R.W., Streckeisen, A., Zanettin, B. 1986. A classification of volcanic rocks based on the total alcalis-silica diagram. Journal of Petrology 27, 745-750.

Le Maitre, R. W., 2002. A classification of igneous rocks and glossary of terms. 2nd Edition , London, 193 p.

Leite, A. A. S., Dall'agnol, R., Macambira, M. J. B., Althoff, F. J., 2004. Geologia e geocronologia dos granitóides arqueanos da região de Xinguara (PA) e suas implicações na evolução do Terreno Granito-Greenstone de Rio Maria. Revista Brasileira de Geociências. 34, 447-458.

Leite, A. A. S., 2001. Geoquímica, petrogênese e evolução estrutural dos granitóides arqueanos da região de Xinguara, SE do Cráton Amazônico. Belém, Universidade Federal do Pará, Centro de Geociências. 330p. Doctor Thesis. Programa de Pós-Graduação em Geologia e Geoquímica, Centro de Geociências, UFPA (in Portuguese).

Lobach-Zhuchenko, S.B., Rollinson, H., Chekulaev, V.P., Arestova, N.A., Kovalenko, A.V., Ivanikov, V.V., Guseva, N.S., Sergeev, S.A., Matukov, D.I., Jarvis, K.E., 2005. The Archaean sanukitoid series of the Baltic shield—geological setting, geochemical characteristics and implications for their origin. Lithos. 79, 107– 128.

Macambira, M. J. B., 1992. Chronologie U/Pb, Rb/Sr, K/Ar et croissance de la croûte continentale dans L'Amazonie du sud-est; exemple de la région de Rio Maria, Province de Carajas, Brésil. *Doctor Thesis.* Montpellier, Université Montpellier II-France. 212 p. (In French).

Macambira, M. J. B., Lancelot, J., 1996. Time constraints for the formation of the Archean Rio Maria crust, southeastern Amazonian Craton, Brazil. International Geology Review, 38 (12): 1134-1142.

Macambira, M. J. B., Lafon, J. M., 1995. Geocronologia da Província Mineral de Carajás; Síntese dos dados e novos desafios. Boletim do Museu Paraense Emílio Goeldi, série Ciências da Terra, Belém, (7): 263-287.

Machado, N., Lindenmayer, Z. G., Krogh, T. E., Lindenmayer, D. 1991. U-Pb geochronology of Archean magmatism and basement reactivation in the Carajás area, Amazon shield, Brazil. Precambrian Research, 49: 329-354.

Martin, H., Smithies, R.H., Rapp, R., Moyen J.-F., Champion D., 2005. An overview of adakite, tonalite–trondhjemite–granodiorite (TTG), and sanukitoid: relationships and some implications for crustal evolution. Lithos 79, 1–24.

Martin, H., 1999. The adakitic magmas: modern analogues of Archaean granitoids. Lithos 46 (3), 411– 429.

Martin, H., 1985. Nature, origine et e´volution dO_ un segment de crouˆ te continentale archéenne: contraintes chimiques et isotopiques. Exemple de la Finlande orientale. Mem.CAESS no. 1. Rennes, France. 324 pp.

Martin, H. 1994. The Archean grey gneisses and the genesis of continental crust. In: Condie, K. C. (ed.) Archean Crustal Evolution. Amsterdam: Elsevier, pp. 205---259.

Medeiros, H., 1987. Petrologia da porção leste do maciço granodiorítico Rio Maria, Sudeste do Pará. 166p. *M.Sc. Thesis*. Programa de Pós-Graduação em Geologia e Geoquímica, Centro de Geociências, UFPA (in Portuguese).

Moyen, J. F., Martin, H., Jayananda, M., Auvray, B., 2003. Late-Archaean granites: a typology based on the Dharwar Craton (India). Precambrian Research, 2375: 1-21.

Moyen, J.-F., Martin, H., Jayananda, M., 2001. Multi-element geochemical modelling of crust–mantle interactions during late- Archaean crustal growth: the Closepet granite (South India). Precambrian Research, 112, 87– 105.

Moyen, J.-F., Stevens, G., 2006. Experimental constraints on TTG petrogenesis: implications for Archean Geodynamics. In: Benn, K., Mareschal, J.-C., Condie, K.C. (Eds), Archean

Geodynamics and Environments. Geophysical Monograph 164. American Geophysical Union, Washington, DC.

Nixon, P.H., Rogers, N.W., Gibson, I.L., Grey, A., 1981. Depleted and fertile mantle xenoliths from Southern African kimberlites. Annu. Rev. Earth. Planet. Sci. 9, 285–309.

Nockolds, S.R., Allen, R., 1953. The geochemistry of some igneous rocks series. Geochimica et Cosmochimica Acta, 4: 105-142.

Oliveira, M.A., Dall'Agnol, R., Althoff, F. J., Leite, A.A.S., 2009. Mesoarchean sanukitoid rocks of the Rio Maria Granite-Greenstone Terrane, Amazonian craton, Brazil. Journal of South American Earth Sciences 27, 146-160.

Oliveira, M.A., Dall'Agnol, R., Scaillet, B., submitted. Petrological constraints on crystallization conditions of MesoArchean Sanukitoid Rocks, southeastern Amazonian craton, Brazil. Journal of Petrology.

Oliveira, M.A., Dall'Agnol, R., Althoff, F.J., 2006. Petrografia e Geoquímica do Granodiorito Rio Maria da região de Bannach e comparações com as demais ocorrências no terreno Granito-*Greenstone* de Rio Maria-Pará. Revista Brasileira de Geociências. 36 (2), 313-326.

Oliveira, M. A., 2005. Geologia, Petrografia e Geoquímica do Granodiorito Sanukitóide Arqueano Rio Maria e Rochas Máficas Associadas, Leste de Bannach-PA. Universidade Federal do Pará. 141p. M.Sc. Thesis. Programa de Pós-Graduação em Geologia e Geoquímica, Centro de Geociências, UFPA (in Portuguese).

Pimentel, M.M., Machado, N., 1994. Geocronologia U-Pb dos Terrenos granito-greenstone de Rio Maria, Pará. In: Congresso Brasileiro de Geologia, 38. Camboriú, 1988. Boletim de Resumos Expandidos. Camboriú, SBG. p. 390-391.

Prouteau, G., Scaillet, B., Pichavant, M., Maury, R.C., 2001. Evidence of mantle metasomatism by hydrous silicic melts derived from subducted oceanic crust. Nature 410, 197-200.

Prouteau, G., Scaillet, B., 2003. Experimental constraints on the origin of the 1991 Pinatubo dacite. Journal of Petrology 44, 2203–2241.

Rämö, O.T., Dall'Agnol, R., Macambira, M.J.B., Leite, A.A.S., de Oliveira, D.C., 2002. 1.88 Ga oxidized A-type granites of the Rio Maria region, eastern Amazonian craton, Brazil: positively anorogenic! Journal of Geology 110, 603– 610.

Rämö, O.T., 1991. Petrogenesis of the Proterozoic rapakivi granites and related basic rocks of southeastern Fennoscandia: Nd and Pb isotopic and general geochemical constraints. Geol. Surv. Finland Bull., 355, 161 pp.

Rapp, R.P., Shimizu, N., Norman, M.D., Applegate, G.S., 1999. Reaction between slab-derived melts and peridotite in the mantle wedge: experimental constraints at 3.8 GPa. Chemical Geology, 160, 335– 356.

Ringwood, A. E., 1975. Composition and Petrology os the earth's mantle. MacGraw-Hill Editor. 618p.

Rolando, A.P. and Macambira, M.J.B., 2003. Archean crust formation in Inajá range area, SSE of Amazonian Craton, Brazil, basead on zircon ages and Nd isotopes. In: South American Symposium on Isotope Geology, 4, Salvador. Expanded Abstracts. Salvador: CD-ROM.

Rolando, A.P., Macambira, M.J.B., 2002. Geocronologia dos granitóides arqueanos da região da Serra do Inajá, novas evidências sobre a formação da crosta continental no sudeste do Cráton Amazônico, SSE Pará. In: Congresso Brasileiro de Geologia, 41**.** Anais do Congresso Brasileiro de Geologia. João Pessoa, 2002. SBG. p. 525.

Rollinson, H., 1993. Using Geochemical Data. Longman, London 352 pp.

Scaillet, B., Evans, B.W., 1999. The June 15, 1991, eruption of Mount Pinatubo: I. Phase equilibria and pre-eruption P-T-fO_2-fH_2O conditions of the dacite magma. Journal of Petrology 40, 381-411.

Scaillet, B., Prouteau, G., 2001. Oceanic slab melting and mantle metasomatism. Science progress, 84 (4), 335-354.

Shand, S.J., 1950. Eruptive rocks their genesis, composition, classification e their relation to ore deposit. 4ed., London, 488p.

Shirey, S.B., Hanson, G.N., 1984. Mantle-derived Archean monzodiorites and trachyandesites. Nature. 310: 222-224.

Smithies, R.H., Champion, D.C., Sun, S-S., 2004. Evidence for Early LREE-enriched Mantle Source Regions: Diverse Magmas from the c. 3_0Ga Mallina Basin, Pilbara Craton, NW Australia. Journal of petrology 45 (8) 1515-1537.

Smithies, R.H., Champion, D.C., 2000. The Archaean high-Mg diorite suite: links to tonalite–trondhjemite–granodiorite magmatism and implications for early Archaean crustal growth. Journal of Petrology. 41 (12), 1653– 1671.

Souza, Z.S., Potrel, H., Lafon, J.M., Althoff, F.J., Pimentel, M.M., Dall'agnol, R., Oliveira, C.G., 2001. Nd, pb and sr isotopes of the identidade belt, na archaean greenstone belt of the rio maria region (carajas province, brazil): implications for the archaean geodynamic evolution of the amazonian craton. Precambrian research, 109 (2001) 293–315.

Souza, Z.S., Luiz, J.G., Cruz, J.C.R., Paiva, R.N., 1992. Geometria de greenstone belts arqueanos da região de Rio Maria (Sudeste do Pará, Brasil), a partir de interpretação gravimétrica. Revista Brasileira de Geociências, 22 (2), p 198-203.

Stacey, J.S., Kramers, J.D., 1975. Approximation of terrestrial lead isotope evolution by a two-stage model. Earth and Planetary Science Letters 26, 207–221.

Stern, A. L., Hanson, G., 1991. Archean high-Mg granodiorite: a derivate of light rare earth element-enriched monzodiorite of mantle origin. Journal of Petrology, 32: 201-238.

Stern, R.A., Hanson, G.N., Shirey, S.B., 1989. Petrogenesis of mantle-derived, LILE-enriched Archean monzodiorites and trachyandesites (sanukitoids) in southwestern Superior Province. Canadian Journal of Earth Sciences 26, 1688– 1712.

Sylvester, P.J., 1994. Archean granite plutons. In: Condie, K. C. (ed.) Developments in precambrian geology 11. Archean crustal evolution. Amsterdam, Elsevier. p. 261-314.

Tassinari, C. C. G., Macambira, M. J. B., 2004. Evolução tectônica do Cráton Amazônico. In: Mantesso-Neto, V., Bartorelli, A., Carneiro, C. D. R., Brito Neves, B. B. de. (Org.). Geologia do Continente Sul Americano: Evolução da obra de F.F.M. de Almeida. São Paulo: BECA, 2004, v., p. 471-486.

Takahashi, E., 1986. Melting of a dry peridotite KLB-1 up to 14 GPa: implications on the origin of peridotitic upper mantle. J. Geophys. Res. 91, 9367–9382.

Taylor, S.R., McLennan, S.M., 1985. The continental crust: Its composition and evolution. Backwell Scientific, Oxford, 321p.

Teixeira, L.R., 2005. GENESIS 4.0 - Software de Modelamento Geoquímico.

Vasquez, M.L., Sousa, C.S., Carvalho, J.M.A., 2008. Geologia e Recursos Minerias do Estado do Pará.

Wilson, M., 1989. Igneous petrogenesis. London, Academic Press. 466p.

Zamora, D., 2000. Fusion de la croûte océanique subductée: approche expérimentale et géochimique. Université Thesis Université Blaise Pascal, Clermont-Ferrand, 314 pp.

CAPÍTULO – 5

DISCUSSÕES E CONCLUSÕES FINAIS

DISCUSSÕES E CONCLUSÕES FINAIS

Rochas da Suíte Sanukitóide Rio Maria ocorrem em diferentes áreas do Terreno Granito-*Greenstone* de Rio Maria, sudeste do Cráton Amazônico, e forneceram idades em torno de 2,87 Ga. Essas rochas são dominantemente epidoto-bitotita-hornblenda granodioritos, com a presença marcante de enclaves máficos. Entretanto, exposições significativas de rochas intermediárias e rochas acamadadas foram recentemente descritas na área de Bannach. As rochas da Suíte Rio Maria apresentam assinatura geoquímica típica de séries sanukitóides descritas em outros terrenos arqueanos no mundo e admite-se que os granodioritos, rochas intermediárias, rochas acamadadas e enclaves máficos correspondem a uma série sanukitóide expandida formada em 2,87 Ga. Nas diferentes áreas de ocorrência os granodioritos apresentam composições químicas que, apesar de bastante similares, mostram algumas significativas diferenças que sugerem que a unidade anteriormente denominada Granodiorito Rio Maria, trata-se realmente de uma suíte de rochas, predominantemente granodioríticas, que derivaram a partir de magmas similares, com assinatura sanukitóide, porém distintos.

Composições modais e dados geoquímicos indicam que enclaves máficos (séries monzoníticas) e granodioritos ou rochas intermediárias (séries granodioríticas) seguem *trends* distintos em diagramas Q-A-P e em diagramas de variação para elementos-traço, demonstrando que estas rochas não estão relacionadas por processos de cristalização fracionada. Testes de modelamento geoquímico realizados neste trabalho reforçam essa idéia e indicam que a evolução interna das rochas intermediárias foi comandada pelo fracionamento de anfibólio + biotita ± apatita, enquanto que os granodioritos evoluíram pelo fracionamento de plagioclásio + anfibólio ± biotita. Aspectos de campo aliados as características petrográficas e geoquímicas indicam que as rochas acamadadas foram geradas, possivelmente, por processos envolvendo acúmulo de cristais. De acordo com o modelamento, essas rochas podem ter sido derivadas a partir do magma granodiorítico pelo acúmulo de 50% de anfibólio, no caso das camadas mais ricas em cristais cúmulus, e 30% de anfibólio ± plagioclásio, no caso dos níveis cinza, mais ricos em material intercúmulus.

Os testes de balanço de massa e modelamento de elementos-traço sugerem que a geração dos magmas Rio Maria requer a fusão de uma fonte mantélica metassomatizada pela adição de líquidos TTGs derivados de uma crosta oceânica subductada. Os magmas granodiorítico e intermediário seriam gerados a partir de uma fonte metassomatizada pela adição de ~30% de

líquido TTG, porém com diferentes graus de fusão, respectivamente 21% e 24%. No caso dos enclaves máficos a fusão de 9% de uma fonte mantélica metassomatizada por ~20% de líquido TTG seria adequada para formar o magma primitivo dessas rochas. As fusões que originaram os magmas granodiorítico e intermediário produziriam um resíduo a base de ortopiroxênio, olivina, anfibólio e granada, enquanto que as fases residuais quando da geração do magma do enclave máfico seriam as mesmas, porém com plagioclásio ao invés de granada.

A tendência monzonítica e saturada em sílica dos enclaves máficos, ao contrário daquela granodiorítica e supersaturada em sílica dos granodioritos e rochas intermediárias, deve ser resultado da presença do plagioclásio como fase residual na fusão que gerou o magma dos enclaves. Os conteúdos mais elevados de Y, bem como as mais baixas razões Sr/Y e moderadas anomalias negativas de Eu dos enclaves máficos comparadas às dos granodioritos e rochas intermediárias, são consistentes com características de magmas gerados no domínio de estabilidade do plagioclásio. Isto implica que o contraste nas condições de pressão da fusão parcial do manto metassomatizado é determinante para as diferenças observadas nas composições modais e químicas entre as séries granodioríticas (granodioritos e rochas intermediárias) e monzoníticas (enclaves máficos). Para explicar as relações entre os granodioritos e enclaves máficos, baseado nos dados petrográficos, químicos e de modelamento, admite-se que os magmas granodiorítico e máfico foram gerados pela fusão parcial do manto metassomatizado a pressões > 1000 MPa e ≤ 1000 MPa, respectively. O magma granodiorítico ascenderia devido às diferenças de viscosidade e gravidade, atingiria o nível de geração do magma do enclave máfico, ocorrendo à interação entre ambos que ascenderiam para a crosta superior. O menor volume de magma máfico causaria sua dispersão no magma granodiorítico em forma de "bolhas". Ambos os magmas estariam parcialmente cristalizados e iniciariam a interação. Entretanto, a relativamente rápida ascensão dos magmas impediria seus intensos reequilíbrios preservando suas características originais.

Em síntese, o modelo adotado para a geração dos magmas da Suíte Rio Maria implica: (1) em uma intensa geração de magmas TTGs, ao menos em parte derivados da fusão parcial da crosta oceânica em um ambiente de subducção; (2) a interação desses magmas TTGs com o manto, resultando em um manto metassomatizado por um importante componente TTG (20 a 30% em volume); (3) um evento tectonotermal em ~2,87 Ga, possivelmente relacionado a pluma do manto, causando a fusão parcial do manto metassomatizado e gerando os magmas

sanukitóides Rio Maria; (4) a natureza dos magmas dependeria do grau de metassomatismo, do grau de fusão e da profundidade na qual esse processo ocorreu; (5) os magmas ascenderam para a crosta e evoluíram por cristalização fracionada; (6) os magmas foram colocados em níveis crustais relativamente rasos formando lacólitos ou plútons pouco espessos.

Baseado em estudos geológicos e mineralógicos admite-se que esses magmas foram ricos em água, com conteúdos estimados em mais do que 7%, e evoluíram sob condições oxidantes acima do tampão NNO, provavelmente entre NNO + 0,5 a NNO + 2,5. Essas condições favoreceram a cristalização do anfibólio como fase do *liquidus* e inibem a cristalização de ortopiroxênio e clinopiroxênio. Os magmas Rio Maria devem ter iniciado suas cristalizações a uma temperatura estimada de 950° C, cristalizando essencialmente anfibólio. Os magmas ascenderam rapidamente com alta proporção líquido/cristal para explicar as colocações em níveis crustais rasos. Após ascenderem para níveis mais rasos, o plagioclásio iniciou a cristalização. Em mais baixas temperaturas, uma reação peritética envolvendo anfibólio + plagioclásio + magnetita + (K-feldspato$_{melt}$) resultou na presença de biotita e epidoto magmático. A estabilidade do epidoto nessas condições foi aumentada pelo caráter oxidante dos magmas. A final da colocação desses magmas deve ter ocorrido sob uma pressão de ~200 MPa e qualquer anfibólio cristalizado precocemente, reequilibrou sob essas condições, exceto os cristais grossos das rochas acamadadas, os quais tem origem cumulática.

No cenário proposto, os diferentes magmas que formaram as rochas da Suíte Rio Maria evoluíram sob condições oxidantes e ascenderam juntos ou quase simultaneamente, através da crosta, em um curto intervalo de tempo geológico. As condições de pressão, temperatura, conteúdo de água e condição de oxidação, indicam condições oxidantes e ricas em água para os magmas Rio Maria, duas feições características de magmas com importante participação de um componente derivado da crosta oceânica em zona de subducção. Este fato reafirma a origem admitida para os magmas da Suíte Maria, a partir da fusão parcial de um manto previamente metassomatizado por líquidos TTGs.

REFERÊNCIAS

ALMEIDA, J.A.C.; OLIVEIRA, M.A.; DALL'AGNOL, R.; ALTHOFF, F. J.; BORGES, R.M.K. 2008. Relatório de mapeamento geológico na escala 1:100.000 da Folha Marajoara (sb-22-z-c v). Programa Geobrasil, CPRM – Serviço Geológico do Brasil. 147p.

ALMEIDA, J.A.C.; DALL'AGNOL, R.; OLIVEIRA, M.A.; MACAMBIRA, M.J.B.; PIMENTEL, M.M.; LEITE, A.A.S. submitted. Zircon geochronology and geochemistry of the TTG suites of the Rio Maria granite-greenstone terrane: Implications for growth of Archean crust of Carajás Province, Brazil. *Precambrian Research*.

ALTHOFF, F.J. 1996. Etude pétrologique et structurale des granitoïdes de Marajoara (Pará, Brésil): leur rôle dans l'évolution archéenne du craton Amazonien (2,7-3,2 Ga). Université Henri Poincaré, Nancy I – France. 296p. Tese de Doutorado

ALTHOFF, F.J.; BARBEY, P.; MACAMBIRA, M.J.B.; SCHELLER, T.; LETERRIER, J.; DALL'AGNOL, R.; LAFON, J.M. 1998. La croissance du craton sud-amazonien (région de Rio Maria, Brésil). In: RÉUNION DES SCIENCES DE LA TERRE. *Resumés*. Brest, Societé Géologique de France, p. 62.

ALTHOFF, F.J.; BARBEY, P.; BOULLIER, A.M. 2000. 2.8-3.0 Ga plutonism and deformation in the SE Amazonian craton: the Archean granitoids of Marajoara (Carajás Mineral province, Brazil). *Precambrian Research*, **104**, 187-206.

AVELAR, V.G. 1996. Geocronologia Pb-Pb por evaporação em monocristal de zircão, do magmatismo da região de Tucumã, SE do Estado do Pará, Amazônia Oriental. Belém, Universidade Federal do Pará. CG. 199 p. Dissertação de Mestrado

AVELAR, V.G.; LAFON, J.M.; CORREIO Jr.F.C.; MACAMBIRA, E.M.B. 1999. O magmatismo arqueano da região de Tucumã-Província Mineral de Carajás: novos resultados geocronológicos. *Revista Brasileira de Geociências*. **29**(2), 454-460.

BAGAI, Z.; ARMSTRONG, R.; KAMPUNZU, A.B. 2002. U–Pb single zircon geochronology of granitoids in the Vamba granitegreenstone terrane (NE Botswana): implications for the evolution of the Archaean Zimbabwe craton. *Precambrian Research*, **118**, 149– 168.

BARROS, E.M.; SARDINHA, A.S.; BARBOSA, J.P.O.; KRIMSKI, R. & MACAMBIRA, M.J.B. 2001. Pb-Pb and U-Pb zircon ages of Archean syntectonic granites of the Carajás Metallogenic Province, northern Brazil. *In*: Simposio Sudamericano de Geologia Isotopica, 3. Pucon, Chile. Sociedade Geologica de Chile. (CD ROM).

BIBIKOVA, E.V.; PETROVA, A.; CLAESSON, S. 2005. The temporal evolution of sanukitóides in the karelian craton, baltic shield: an ion microprobe u-th-pb isotopic study of zircons. *Lithos.* **79** (2005) 129 – 145.

CONDIE, K.C. & HUNTER, D.R. 1976. Trace elements geochemistry of Archean granitic rocks from Barberton region, South Africa. *Earth and Planetary Science Letters*. **29**, 389-400.

CORDEIRO, A.A.C. 1982. Geologia preliminar da região de Andorinhas. In: Simpósio de Geologia da Amazônia, 1, Belém, 1982. *Anais do Simpósio de Geologia da Amazônia.* SBG, v-1, p. 45-49.

COSTA, J.B.S.; ARAÚJO, O.J.B.; SANTOS, A.; JORGE JOÃO, X. S.; MACAMBIRA, M.J.B.; LAFON, J.M. 1995. A província mineral de Carajás: aspectos tectono-estruturais, estratigráficos e geocronológicos. *Boletim do Museu Paraense Emílio Goeldi*, série Ciências da Terra, **7**:199-235.

DALL'AGNOL, R.; OLIVEIRA, D. C. 2007. Oxidized, magnetite-series, rapakivi-type granites of Carajás, Brazil: implications for classification and petrogenesis of A-type granites. *Lithos*. **93**, p 215-233.

DALL'AGNOL, R.; TEIXEIRA, N.P.; RÄMO, O.T.; MOURA, C.A.V.; MACAMBIRA, M.J.B.; OLIVEIRA, D.C. 2005. Petrogenesis of the Paleoproterozoic rapakivi A-type granites of the Archean Carajás metallogenic province, Brazil. *Lithos*, **80**: 101-129.

DALL'AGNOL, R.; OLIVEIRA, M.A.; ALMEIDA, J.A.C.; ALTHOFF, F.J.; LEITE, A.A.S.; OLIVEIRA, D.C.; BARROS, C.E.M. 2006. Archean and paleoproterozoic granitoids of the Carajás Metallogenetic Province, eastern Amazonian craton. *IN*: DALL'AGNOL, R., ROSA-COSTA, L.T., KLEIN, E.L. (EDS.). Symposium on magmatism, crustal evolution, and metallogenesis of the Amazonian craton. Abstracts volume and field trips guide. BELÉM, PRONEX-UFPA/SBG-NO, 99-150.

DALL'AGNOL, R.; SCAILLET, B.; PICHAVANT, M. 1999a. Evolution of A-type granite magmas*:* an experimental study of the Lower Proterozoic Jamon Granite, eastern Amazonian craton, Brazil. *Journal of Petrology*. **40** (11): 1673-1698.

DALL'AGNOL, R. ; RAMÖ, O.T.; MAGALHÃES, M.S.; MACAMBIRA, M.J.B. 1999b. Petrology of the anorogenic, oxidised Jamon and Musa granites, Amazonian Craton: implications for the genesis of Proterozoic, A-type Granites. *Lithos*. **46**: 431-462.

DALL'AGNOL, R.; SOUZA, Z.S.; ALTHOFF, F.J.; BARROS, C.E.M.; LEITE, A.A.S.; JORGE JOÃO, X.S. 1997a. General aspects of the granitogenesis of the Carajás metallogenic province. In: INTERNATIONAL. SYMPOSIUM ON GRANITES AND ASSOCIATED MINERALIZATIONS, 2. Salvador. *Excursions Guide.* Salvador: Superitendência de Geologia e Recursos Minerais-SGRM. p.135-161.

DALL'AGNOL, R.; VIEIRA, E.A.P.; SÁ, C.A.S.; MEDEIROS, H.; GASTAL, M.C.P.; TEIXEIRA, N.P. 1986. Estado atual do conhecimento sobre as rochas granitóides da porção sul da Amazônia Oriental. *Revista Brasileira de Geociências*. **16**: 11-23.

DIDIER, J.; BARBARIN, B. 1991. Enclaves and Granite Petrology. Elsevier Amsterdam, 621pp.

DOCEGEO. 1988. Revisão litoestratigráfica da Província Mineral de Carajás. In: Congresso Brasileiro de Geologia, 35. Belém, 1988. *Anais do Congresso Brasileiro de Geologia*. Belém, SBG. p. 11-54.

GUIMARÃES, F.V.G.; DALL'AGNOL, R.; ALMEIDA, J.A.C.; OLIVEIRA, M.A. submitted. Caracterização geológica, petrográfica e geoquímica do trondhjemito Mogno e tonalito Mariazinha, Terreno granito-greenstone de Rio Maria – Pará. *Revista Brasileira de Geociências*.

HALLA, J. 2005. Late Archean high-Mg granitoids (sanukitoids) in the southern Karelian domain, eastern Finland: Pb and Nd isotopic constraints on crust_mantle interactions. *Lithos*, **79**: 161– 178.

HUHN, S.R.B.; SANTOS, A.B.S.; AMARAL, A.F.; LEDSHAM, E.J.; GOUVEIA, J.L.; MARTINS, L.B.P.; MONTALVÃO, R.M.G.; COSTA, V.G. 1988. O terreno granito-greenstone da região de Rio Maria - Sul do Pará. In: Congresso Brasileiro de Geologia, 35., Belém. *Anais do congresso Brasileiro de Geologia*. Belém, SBG. v. 3, p. 1438-1453.

KOVALENKO, A.V.; CLEMENS, J.D.; SAVATENKOV, V.M. 2005. Petrogenetic constraints for the genesis of Archaean sanukitoid suites:geochemistry and isotopic evidence from Karelia, Baltic Shield. *Lithos.* **79**, 147– 160.

LAFON, J.M. & SCHELLER, T. 1994. Geocronologia Pb/Pb em zircão do Granodiorito Cumaru, Serra dos Gradaús, PA. In: Simpósio de Geologia da Amazônia, 4, Belém, 1994. *Boletim de Resumos Expandidos*. Belém, SBG/NO, p. 321-323.

LAFON, J.M.; RODRIGUES, E.; DUARTE, K.D. 1994. Le granite Mata Surrão: un magmatisme monzogranitique contemporain des associations tonalitiques-trondhjemitiques-

granodioritiques archéennes de la région de Rio Maria (Amazonie Orientale, Brésil). p. 642-649.

LEITE, A.A.S. 2001. Geoquímica, petrogênese e evolução estrutural dos granitóides arqueanos da região de Xinguara, SE do Cráton Amazônico. Belém, Universidade Federal do Pará, Centro de Geociências. 330p. Tese de Doutorado

LEITE, A.A.S.; DALL'AGNOL, R.; MACAMBIRA, M.J.B.; ALTHOFF, F.J. 2004. Geologia e geocronologia dos granitóides arqueanos da região de Xinguara (PA) e suas implicações na evolução do Terreno Granito-Greenstone de Rio Maria. *Revista Brasileira de Geociências*. **34**, 447-458.

LOBACH-ZHUCHENKO, S.B.; CHEKULAEV, V.P.; IVANIKOV, V.V.; KOVALENKO, A.V.; BOGOMOLOV, E.S. 2000. Late archaean high-mg and subalkaline granitoids and lamprophyres as indicators of gold mineralization in karelia (baltic shield) russia. IN: LOBACH-ZHUCHENKO, S.B., CHEKULAEV, V.P., ARESTOVA, N.A., LEVSKII, L.K., KOVALENKO, A.V., 2000B. ARCHEAN TERRANES IN KARELIA: geological and isotopic-geochemical evidence. *Geotectonics*. **34**, 452– 466.

LOBACH-ZHUCHENKO, S.B.; ROLLINSON, H.; CHEKULAEV, V.P.; ARESTOVA, N.A.; KOVALENKO, A.V.; IVANIKOV, V.V.; GUSEVA, N.S.; SERGEEV, S.A.; MATUKOV, D.I.; JARVIS, K.E.. 2005. The archaean sanukitoid series of the baltic shield—geological setting, geochemical characteristics and implications for their origin. *Lithos*. **79**, 107– 128.

MACAMBIRA, M.J.B. 1992. Chronologie U/Pb, Rb/Sr, K/Ar et croissance de la croûte continentale dans L'Amazonie du sud-est; exemple de la région de Rio Maria, Province de Carajas, Brésil. Montpellier, Université Montpellier II-France. 212 p. Tese de Doutorado

MACAMBIRA, M.J.B.; COSTA, J.B.S.; ALTHOFF, F.J.; LAFON, J.M.; MELO, J.C.V.; SANTOS, A. 2000. New geochronological data for the Rio Maria TTG terrane; implications for the time contraints of the crustal formation of the Carajás province, Brazil. In: INTERNATIONAL GEOLOGICAL CONGRESS, 31st, Rio de Janeiro, *Abstract*, Rio de Janeiro, CD-ROM. SBG.

MACAMBIRA, M.J.B. & LAFON, J.M. 1995. Geocronologia da Província Mineral de Carajás; Síntese dos dados e novos desafios. *Boletim do Museu Paraense Emílio Goeldi*, série Ciências da Terra, Belém, (7): 263-287.

MACAMBIRA, M.J.B. & LANCELOT, J. 1996. História arqueana da região de Rio Maria, SE do Estado do Pará, registrada em zircões detríticos de "*greenstone belts*" e de cobertura plataformal. In: SIMPÓSIO DE GEOLOGIA DA AMAZÔNIA, 3, Belém. *Anais do Simpósio de Geologia da Amazônia.* SBG. p. 59-69.

MACHADO, N., LINDENMAYER, Z.G., KROGH, T.E. & LINDENMAYER, D. 1991. U-Pb geochronology of Archean magmatism and basement reactivation in the Carajás area, Amazon shield, Brazil. *Precambrian Research.* **49**, 329-354.

MEDEIROS, H. 1987. Petrologia da porção leste do maciço granodiorítico Rio Maria, Sudeste do Pará. 166p. Belém, UFPA. Centro de Geociências. 116p. Dissertação de Mestrado

MEDEIROS, H.; DALL'AGNOL, R. 1988. Petrologia da porção leste do Batólito Granodiorítico Rio Maria, sudeste do Pará. *In*: CONGRESSO BRASILEIRO DE GEOLOGIA, 35, Belém. *Anais de Congresso Brasileiro de Geologia*. SBG. v 3, p.1488-1499.

MOYEN, J.F. ; MARTIN, H.; JAYANANDA, M.; AUVRAY, B. 2003. Late-Archaean granites: a typology based on the Dharwar Craton (India). *Precambrian Research*. **23**, 75: 1-21.

MOYEN, J.-F.; MARTIN, H.; JAYANANDA, M. 2001. Multi-element geochemical modelling of crust–mantle interactions during late- Archaean crustal growth: the Closepet granite (South India). *Precambrian Research.* **112**, 87– 105.

MOYEN, J.F.; MARTIN, H.; JAYANANDA, M. 1997. Origine du granite fini-Archéen de Closepet (Inde du Sud): apports de la modélisation géochimique du comportemént des elements en traces. C. R. Acad. Sci. Paris 325, 659-664.

OLIVEIRA, M.A.; DALL'AGNOL, R.; ALTHOFF, F.J.; LEITE, A.A.S. 2009. Mesoarchean sanukitoid rocks of the Rio Maria Granite-Greenstone Terrane, Amazonian craton, Brazil. *Journal of South American Earth Sciences.* 27, 146-160.

OLIVEIRA, M.A.; DALL'AGNOL, R.; SCAILLET, B. submitted a. Petrological constraints on crystallization conditions of MesoArchean Sanukitoid Rocks, southeastern Amazonian craton, Brazil. *Journal of Petrology*.

OLIVEIRA, M.A.; DALL'AGNOL, R.; ALMEIDA J.A.C. submitted b. Petrology of the Mesoarchean Rio Maria Suite: Implications for the genesis of Sanukitoid Rocks. *Litho.*

OLIVEIRA, M.A.; DALL'AGNOL, R.; ALTHOFF, F.J. 2006. Petrografia e Geoquímica do Granodiorito Rio Maria da região de Bannach e comparações com as demais ocorrências no

terreno Granito-*Greenstone* de Rio Maria-Pará. *Revista Brasileira de Geociências*. **36** (2), 313-326.

OLIVEIRA, M.A. 2005. Geologia, Petrografia e Geoquímica do Granodiorito Sanukitóide Arqueano Rio Maria e Rochas Máficas Associadas, Leste de Bannach-PA. Universidade Federal do Pará. 149p. Dissertação de Mestrado

PIMENTEL, M.M.; MACHADO, N. 1994. Geocronologia U-Pb dos Terrenos granito-greenstone de Rio Maria, Pará. In: CONGRESSO BRASILEIRO DE GEOLOGIA, 38. Camboriú, 1988. *Boletim de Resumos Expandidos*. Camboriú, SBG. p. 390-391.

RAPP, R.P.; SHIMIZU, N.; NORMAN, M.D. & APPLEGATE, G.S. (1999). Reaction between slab-derived melts and peridotite in the mantle wedge: experimental constraints at 3.8 gpa. *Chemical geology*. **160**, 335– 356.

ROLANDO, A.P.; MACAMBIRA, M.J.B. 2002. Geocronologia dos granitóides arqueanos da região da Serra do Inajá, novas evidências sobre a formação da crosta continental no sudeste do Cráton Amazônico, SSE Pará. In: Congresso Brasileiro de Geologia, 41**.** *Anais do Congresso Brasileiro de Geologia*. João Pessoa, 2002. SBG. p. 525.

ROLANDO, A.P.; MACAMBIRA, M.J.B. 2003. Archean crust formation in Inajá range area, SSE of Amazonian Craton, Brazil, basead on zircon ages and Nd isotopes. *In*: South American Symposium on Isotope Geology, 4, Salvador. *Expanded Abstracts*. Salvador: CD-ROM.

SHIREY, S.B.; HANSON, G.N. 1984. Mantle-derived Archean monzodiorites e trachyandesites. *Nature*. 310: 222-224.

SMITHIES, R.H.; CHAMPION, D.C.; CASSIDY, K.F.; 2003. Formation of Earth's early Archaean continental crust. *Precambrian Research.* **127** (1–3), 89– 101.

SMITHIES, R.H.; CHAMPION, D.C.; SUN, S-S. 2004. Evidence for Early LREE-enriched Mantle Source Regions: Diverse Magmas from the c. 3_0Ga Mallina Basin, Pilbara Craton, NW Australia. *Journal of petrology.* **45** (8) 1515-1537.

SMITHIES R.H.; CHAMPION, D.C.; 1999a. Archaean high-Mg diorite (sanukitoide) suite, Pilbara Craton, Western Australia: petrogenesis and links to tonalite-trondhjemite-granodiorite and alkaline magmatism. *Journal of Petrology*. **41**: 1653-1671.

SMITHIES, R.H., CHAMPION, D.C., 2000. The Archaean high-Mg diorite suite: links to tonalite–trondhjemite–granodiorite magmatism and implications for early Archaean crustal growth. *Journal of Petrology*. **41** (12), 1653– 1671.

SOUZA, Z.S. 1994. Geologia e petrogênese do "Greenstone Belt" Identidade: implicações sobre a evolução geodinâmica do terreno granito-*greenstone de Rio Maria, SE do Pará*. Universidade Federal do Pará. v- 1 e 2, 624p. Tese de Doutorado

STERN, A.L. & HANSON, G. 1991. Archean high-Mg granodiorite: a derivate of light rare earth element-enriched monzodiorite of mantle origin. *Journal of Petrology*, **32**: 201-238.

STERN, A.L.; HANSON, G.; SHIREY, S.B. 1989. Petrogenesis of mantle-derived, LILE-enriched Archean monzodiorites and trachyandesites (sanukitoids) in southwestern Superior Province. *Canadian Journal of Eath Sciences*, **26**: 1688-1712.

STEVENSON, R.; HENRY, P.; GARIÉPY, C. 1999. Assimilation-fractional crystallization origin of Archaean sanukitoid suites: Western Superior Province, Canadá. *Precambrian Research*. **96**: 83-99.

SYLVESTER, P.J. 1994. Archean granite plutons. In: Condie, K. C. (ed.) Developments in precambrian geology 11. Archean crustal evolution. Amsterdam, Elsevier. p. 261-314.

TASSINARI, C.C.G.; MACAMBIRA, M.J.B., 2004. Evolução tectônica do Cráton Amazônico. In: Mantesso-Neto, V., Bartorelli, A., Carneiro, C. D. R., Brito Neves, B. B. de. (Org.). Geologia do Continente Sul Americano: Evolução da obra de F.F.M. de Almeida. São Paulo: BECA, 2004, v., p. 471-486.

TAYLOR, S.R. & MCLENNAN, S.M. 198). The continental crust: Its composition and evolution. Backwell Scientific, Oxford, 321p.

TEIXEIRA, N.P.; BETTENCOURT, J.S.; MOURA, C.A.V.; DALL'AGNOL, R.; MACAMBIRA, E.M.B. 2002. Archean crustal sources for Paleoproterozoic tin- ineralized granites in the Caraja´s province, SSE Para´, Brazil: Pb–Pb geochronology and Nd isotope geochemistry. *Precambrian Research.* **119**, 257– 275.

VASQUEZ, M.L.; SOUSA, C.S.; CARVALHO, J.M.A. 2008. Geologia e Recursos Minerais do Estado do Pará.

Livros Grátis

(http://www.livrosgratis.com.br)

Milhares de Livros para Download:

Baixar livros de Literatura
Baixar livros de Literatura de Cordel
Baixar livros de Literatura Infantil
Baixar livros de Matemática
Baixar livros de Medicina
Baixar livros de Medicina Veterinária
Baixar livros de Meio Ambiente
Baixar livros de Meteorologia
Baixar Monografias e TCC
Baixar livros Multidisciplinar
Baixar livros de Música
Baixar livros de Psicologia
Baixar livros de Química
Baixar livros de Saúde Coletiva
Baixar livros de Serviço Social
Baixar livros de Sociologia
Baixar livros de Teologia
Baixar livros de Trabalho
Baixar livros de Turismo